AD NUMBER

AD877464

LIMITATION CHANGES

TO:

Approved for public release; distribution is unlimited.

FROM:

Distribution authorized to U.S. Gov't. agencies and their contractors; Critical Technology; AUG 1970. Other requests shall be referred to U.S. Army Aviation Materiel Laboratories, Fort Eustis, VA 23604. This document contains export-controlled technical data.

AUTHORITY

USAAMRDL ltr, 30 jul 1971

USAAVLABS TECHNICAL REPORT 70-39

STUDY OF A LIGHTWEIGHT INTEGRAL REGENERATIVE GAS TURBINE FOR HIGH PERFORMANCE

By

Colin F. McDonald

August 1970

U. S. ARMY AVIATION MATERIEL LABORATORIES
FORT EUSTIS, VIRGINIA

CONTRACT DAAJ02-69-C-0087
THE GARRETT CORPORATION
AiRESEARCH MANUFACTURING COMPANY
LOS ANGELES, CALIFORNIA

BLANK PAGES
IN THIS
DOCUMENT
WERE NOT
FILMED

DISCLAIMERS

The findings in this report are not to be construed as an official Department of the Army position unless so designated by other authorized documents.

When Government drawings, specifications, or other data are used for any purpose other than in connection with a definitely related Government procurement operation, the United States Government thereby incurs no responsibility nor any obligation whatsoever; and the fact that the Government may have formulated, furnished, or in any way supplied the said drawings, specifications, or other data is not to be regarded by implication or otherwise as in any manner licensing the holder or any other person or corporation, or conveying any rights or permission, to manufacture, use, or sell any patented invention that may in any way be related thereto.

DISPOSITION INSTRUCTIONS

Destroy this report when no longer needed. Do not return it to the originator.

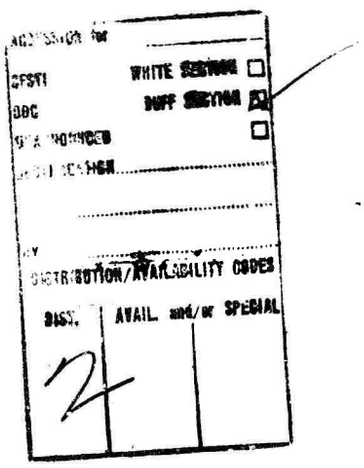

DEPARTMENT OF THE ARMY
HEADQUARTERS US ARMY AVIATION MATERIEL LABORATORIES
FORT EUSTIS, VIRGINIA 23604

The objectives of this contractual effort were to generate parametric data for the design of integrally regenerated engines and to arrive at optimum parametric values for two configurations of engines.

This report was prepared by the AiResearch Manufacturing Company of the Garrett Corporation under the terms of Contract DAAJ02-69-C-0087. It presents the variations in regenerative engine specific fuel consumption, horsepower, weight, volume, and cost with recuperator effectiveness and pressure drop as parameters. Basic engine component and cycle data were fixed for the purposes of this study.

This study has shown that the economic justification for a regenerative engine is strongly dependent upon the mission length and profile to be supported by the aircraft engine. It has also been shown that regenerative engines can be rugged and maintainable with proper integration of the recuperator into the engine system.

The U. S. Army project engineer for this study was Mr. Robert A. Langworthy. This report has been reviewed by technical personnel of this Command, and the conclusions contained herein are concurred in by this Command.

Task 1G162203D14417
Contract DAAJ02-69-C-0087
USAAVLABS Technical Report 70-39
August 1970

STUDY OF A LIGHTWEIGHT INTEGRAL REGENERATIVE GAS TURBINE FOR HIGH PERFORMANCE

Final Report

AiResearch Report
70-6179

By
Colin F. McDonald

Prepared by
The Garrett Corporation
AiResearch Manufacturing Company
Los Angeles, California

for
U.S. ARMY AVIATION MATERIEL LABORATORIES
FORT EUSTIS, VIRGINIA

ABSTRACT

This report describes the results of a 9-month study of a lightweight integral regenerative gas turbine for high performance.

Two well-integrated engine concepts have been designed by utilizing an annular recuperator of tubular construction wrapped around the turbomachinery to give compact, lightweight engine packages. In both designs, the recuperator is considered to be prime structure and acts as the structural backbone of the engine assembly. Utilizing such an arrangement, the recuperator and turbomachinery being concentric, minimizes any distortion, temperature differentials, and pressure losses, and by having all the ducts integral with the engine structure, contributes to a lower overall engine cost.

Ease of routine inspection and maintenance for the two engines, which were designed with the minimum of mechanical complexity, is emphasized by the fact that with a single tool, the engine assembly can be split into the three basic modules, namely, the gas generator power section, the power turbine section and the recuperator, in a few minutes.

For the cycle conditions, with an airflow of 5 lb/sec, pressure ratio of 9:1, and a turbine inlet temperature of 2300°F, a family of lightweight engine designs has been established over a range of recuperator effectiveness from 0.40 to 0.80 and a range of pressure loss from 4 percent to 10 percent. At the extreme end of the ranges of variables, an engine design is concluded with a specific fuel consumption of 0.333 lb/hp hr, the corresponding specific power being 194.70 hp/lb/sec. This performance is achieved within an engine envelope of 23.18 in. diameter by 33.0 in. length; the specific weight of the unit is 49.66 lb/lb/sec.

In the analysis, a reference engine design was established with a recuperator effectiveness and pressure loss of 0.65 and 6 percent respectively. With an SFC and specific power of 0.365 and 192.54 respectively, the specific weight of the lightest design was 34.72, this corresponding to a power-to-weight ratio of 5.55. This performance is achieved within an engine envelope of 19.04 in. diameter by 28.5 in. length and at an estimated cost of $42.9/horsepower.

To provide a direct comparison in the analytical studies, a nonrecuperative engine was designed using the same cycle conditions. With an SFC and specific power of 0.466 and 204.4 respectively, the specific weight of the engine was 23.35, this corresponding to a power-to-weight ratio of 8.75. This performance is achieved within an engine envelope of 14.0 in. diameter by 28.55 in. length and at an estimated cost of $33.24/horsepower.

TABLE OF CONTENTS

LIST OF ILLUSTRATIONS

TABLE OF CONTENTS (continued)

LIST OF ILLUSTRATIONS (Continued)

LIST OF ILLUSTRATIONS (Continued)

LIST OF ILLUSTRATIONS (Continued)

LIST OF ILLUSTRATIONS (Continued)

LIST OF TABLES

LIST OF TABLES (Continued)

LIST OF SYMBOLS

A	heat transfer surface area ft^2
C	material ductility constant
C_p	specific heat at constant pressure, Btu/lb ^0F
A'_{CR}	local velocity of sound, ft/sec
AIT	air inside tubes
d	tube diameter, in.
D	tube bundle diameter, in.
DMP	dimple
E	material elastic modulus, $lb/in.^2$
EOT	exhaust outside tubes
f	frequency
g	acceleration due to gravity, ft/sec^2
G	mass flow velocity, lb/sec ft^2
GGT	gas generator turbine
h	heat transfer coefficient, Btu/ft^2 hr ^0F
hA	thermal conductance, Btu/hr ^0F
hr	hour
hp	horsepower
$H_{ad_{tot}}$	compressor adiabatic compression head, ft
Hz	frequency, cycles/sec
I	moment of inertia
IB	in-line tube bundle
IFT	in-line finned-tube bundle

LIST OF SYMBOLS (Continued)

L	tube length, in.
LHV	fuel lower heating value, Btu/lb
M	bending moment
N	number of tubes (as noted)
N	number of cycles (as noted)
N'	rotating speed, rpm
N'_S	compressor specific speed $\frac{N'(Q_1)^{1/2}}{(H_{ad_{tot}})^{3/4}}$
P	fin pitch
P	pressure, lb/in.^{2}
PLNTD	plain tube diameter
PLNWS	plain tube with strip
PT	power turbine
R	radius
Q'	compressor inlet volume flow, ft^3/sec
S	tube dimple pitch, in.
SB	staggered tube bundle
SFC	specific fuel consumption, lb/hr hp
Sp hp	specific power, hp/lb/sec
SFT	staggered finned-tube bundle
t	tube wall thickness, in.
T	temperature, ^{0}F, ^{0}R
TDF	temperature distribution factor
U	blade tip speed, ft/sec

LIST OF SYMBOLS (Continued)

V	volume, ft^3
V_x	absolute axial velocity, ft/sec
W	flow rate lb/sec
W_T	tube weight, lb
X_T	transverse tube pitch
X_L	longitudinal tube pitch
Z	section modulus
$	dollar
δ	dimple depth (as noted)
δ	fin thickness, in. (as noted)
δ	ratio of compressor inlet pressure to standard sea level pressure (as noted)
Δ	denotes difference
ϵ	recuperator effectiveness
ϵ_p	plastic strain
η_p	compressor polytropic efficiency
η_S	compressor stage adiabatic efficiency
θ	ratio of compressor inlet temperature to standard sea level temperature
μ	tube mass per unit length, $lb\text{-}sec^2/in.^2$
ρ, γ	density, $lb/in.^3$, lb/ft^3
σ	stress, $lb/in.^2$
Ψ	dimple parameter (DMP)
$(\Delta P/P) \times 100$	recuperator pressure loss percent

LIST OF SYMBOLS (Continued)

SUBSCRIPTS

a	air side
B	blade
all	allowable
c	cooling air
D	disc
F	fuel
g	gas side
I	inside
ID	inside diameter
max	maximum
min	minimum
O	outisde
OD	outside diameter
ov	overall
P	polytropic
L	leakage
S	stage
R	rotor
T	total
ult	ultimate
Y	yield

INTRODUCTION

Application of recuperation to the small gas turbine can provide a significant improvement in Army aircraft range capability and in fuel logistics. Recuperators are attractive from standpoints of both increased range per load of fuel and potentially lower overall costs resulting from fuel savings.

To date, very few recuperative gas turbines have been utilized for aircraft or helicopter propulsion. In most cases, the engines evaluated have been existing gas turbines which were modified to accommodate a recuperator. While these engines, with essentially bolt-on recuperators, have performed satisfactorily and have demonstrated the structural integrity of the heat exchanger, they do not represent optimum designs from the standpoints of maximum performance and minimum weight.

In this study, analytical and design approaches have been made to arrive at a truly integrated engine design, not merely arrangements in which the recuperator was added to the turbomachinery. Various compressor, turbine, combustor, and recuperator arrangements were evaluated and assessed on the basis of degree of integration. One of the principal goals was to establish a lightweight, compact engine unit.

The engine cycle conditions were fixed; namely, a mass flow rate of 5.0 lb/sec, a turbine inlet temperature of 2300°F, and a compressor pressure ratio of 9:1. All of the component efficiencies were defined, with the exception of recuperator effectiveness and pressure loss, which were considered as variables in the study. The study was aimed at selecting two engine configurations, one for external installation on the aircraft or helicopter and the other for internal installation. Various flow configurations were evaluated as a part of the study aimed at identifying the optimum unit for each type of installation. Engine configurations having minimum weight and cost were selected, and a sensitivity study was carried out to show how small changes in any one of the basic parameters affect the complete system. For each type of installation, optimum recuperators are identified for maximum net weight savings at given mission times.

U. S. Army Aviation Materiel Laboratories initiated a 9-month program to evaluate lightweight integrated recuperator concepts for small high performance aircraft gas turbines. This document is part of the final report of that program.

The program was organized into five work tasks as outlined below:

Task 1 - Engine Performance and Design Data

Task 2 - Configuration Study

Task 3 - Recuperator Parametric Study

Task 4 - System Comparison and Evaluations

Task 5 - Sensitivity Study of Optimum Systems

Each work task is described in a separate section of this report. The results and the program conclusions are presented in the last two sections of this report.

ENGINE PERFORMANCE AND DESIGN DATA

CYCLE DETAILS

The basic engine design point parameters are outlined in Table I; in addition, a series of parameters necessary for establishing the size and performance of the turbomachinery components is outlined in Table II. This data was used in a computer program written for gas turbine engine cycle analysis and component evaluation.

TABLE I. ENGINE DESIGN POINT CYCLE DATA

Engine airflow, lb/sec	5
Compressor pressure ratio	9:1
Compressor efficiency, percent	82
Combustor efficiency, percent	99
Combustor pressure drop, percent	3
Turbine inlet temperature, ^{0}F	2300
Gas generator turbine efficiency, percent	86
Power turbine efficiency, percent	90
Cooling air, first nozzle, percent	1.5
Cooling air, first blade, percent	1.5
Cooling air, second nozzle, percent	0.5
Fixed geometry	

PERFORMANCE DATA

A study was carried out to estimate the performance of the recuperative engine as a function of the two basic heat exchanger parameters, namely, effectiveness and pressure loss. In Figure 1, the curves show specific fuel consumption (SFC) and engine specific power (sp hp) as a function of recuperator effectiveness and pressure loss. Recuperator effectiveness (ε)

TABLE II. ADDITIONAL DATA USED IN ENGINE CYCLE ANALYSIS

Inlet duct loss ($\Delta P/P$)	0
Interstage turbine diffuser loss, percent	3
Leakage (at compressor discharge pressure) W_L percent	1.5
LHV of fuel, Btu/lb	18,400
Accessory power, hp	6.0
Gas generator mechanical efficiency, percent	98
Recuperator leakage	0
*Range of recuperator effectiveness	0.40 to 0.90
**Range of recuperator pressure loss $\left(\frac{\Delta P}{P}\right)$, percent	2 to 10
Recuperator pressure loss split $(\Delta P/P)_{gas}/(\Delta P/P)_{air}$	1.5
Total cooling airflow W_C, percent	3.5
Compressor discharge mass flow, lb/sec	5.0
Recuperator inlet flow (cold side), lb/sec $5.0 - (1.5\% W_L + 3.5\% W_C)$	4.75
Gas generator turbine inlet flow, lb/sec $4.75 + (2\% W_{fuel})$	4.85
Power turbine inlet flow, lb/sec $4.85 + (3\% W_C$ reentered)	5.0
Recuperator inlet flow (hot side), lb/sec	5.0

*Recuperator effectiveness ϵ defined as $\epsilon = \dfrac{(W.C_p)_{air}\,(T_{out} - T_{in\,air})}{(W.C_p)_{min}\,(T_{in\,gas} - T_{in\,air})}$

where W = mass flow rate
Cp = specific heat
T = total temperature

**Recuperator overall pressure loss ($\Delta P/P$) defined as

$$(\Delta P/P) = \left(\frac{\Delta P_{air}}{P_{air\ in}}\right) + \left(\frac{\Delta P_{gas}}{P_{gas\ in}}\right)$$

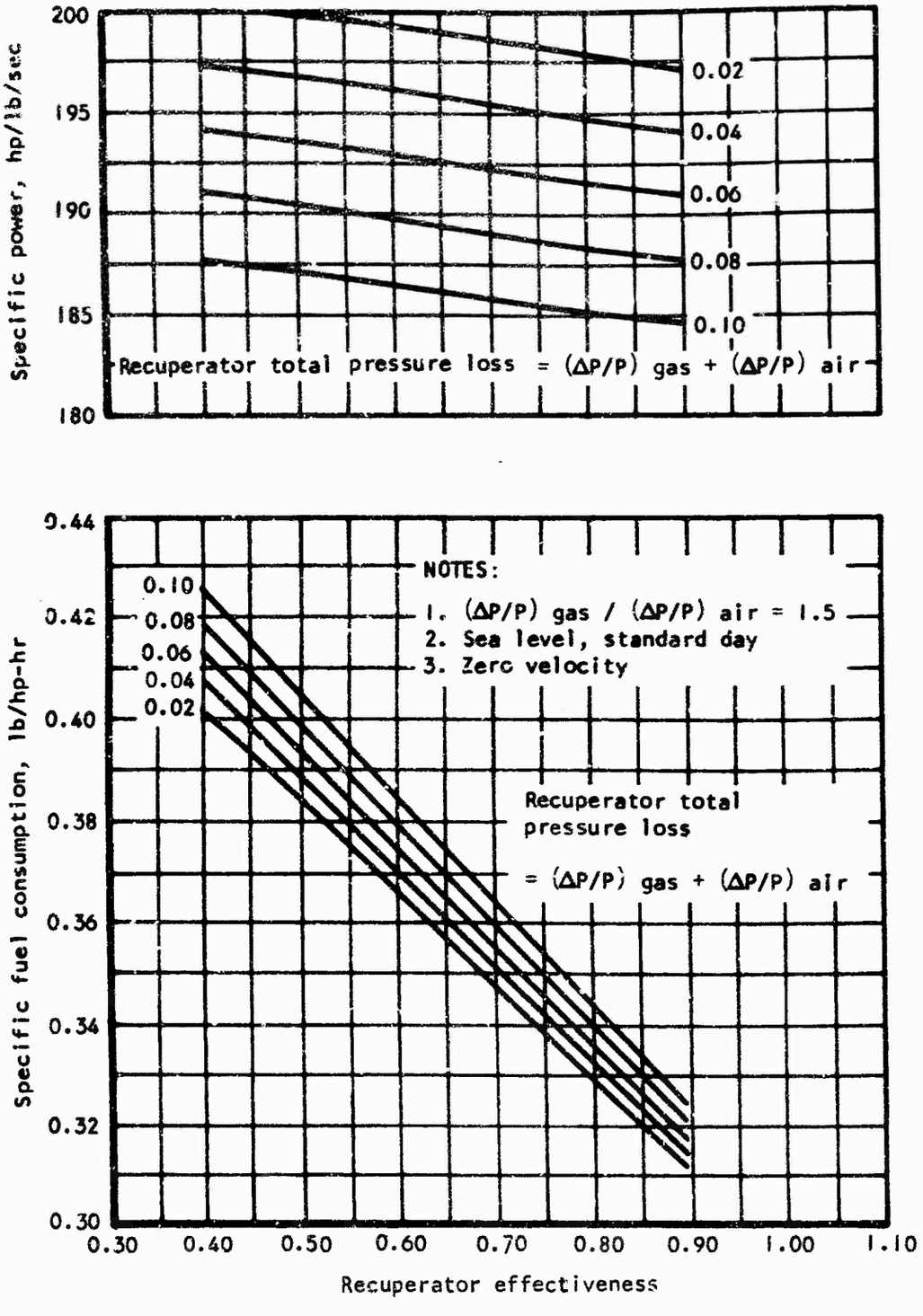

Figure 1. Effect of Recuperator on Specific Fuel Consumption and Specific Power.

is varied from 0.40 to 0.90, and pressure loss ($\Delta P/P$) is varied from 2 to 10 percent. The curves are drawn for standard day, sea level conditions, with zero aircraft velocity.

To compare performance, weight, and cost between a nonrecuperative and a recuperative engine, a further analysis was considered. Using the same cycle conditions and component efficiencies, a performance estimate of a nonrecuperative engine was carried out. Although a direct comparison of performance, weight, and cost between nonrecuperative and recuperative engines is being made, in actual practice the optimum nonrecuperative engine might have been at a much higher pressure ratio than the 9:1 given for the recuperative engine. To enable layouts to be made of the recuperative engine, a cycle point corresponding to intermediate values of effectiveness and pressure loss was selected. Considering mean values of effectiveness and pressure loss from the range given in Table II, a design with an effectiveness and pressure loss of 0.65 and 6 percent, respectively, was selected and sized so that conceptual design layouts of the recuperative and nonrecuperative engines could be made. Throughout the study, this engine design point has been referred to as the reference recuperative engine. From the performance analysis, a direct comparison between the reference recuperative engine and the nonrecuperative engine is given below.

	Specific Power (hp/lb/sec)	Power (hp)	SFC (hp/lb/hr)
Reference recuperative engine	192.54	962.7	0.365
Nonrecuperative engine	205.66	1028.3	0.464

Values of temperature and pressure throughout the cycle, together with salient component loadings, for the recuperated and nonrecuperated engines are given in Tables III and IV, respectively.

COMPRESSOR DESIGN

During the preliminary phase of this program, when the compressor type was being evaluated, advantage was taken of the findings from a small axial-centrifugal compressor matching program being carried out at AiResearch (Reference 1). This, together with other work in the industry, indicated that an axial-centrifugal compressor would provide high efficiency and would be well suited for an engine having the design point at the maximum power rating. The axial-centrifugal compressor configuration gives a short package envelope, and can be produced at a relatively low cost.

TABLE III. RECUPERATIVE ENGINE DATA

	Inlet Pressure (psia)	Inter-stage Pressure (psia)	Exit Pressure (psia)	Inlet Temperature (^{o}F)	Inter-stage Temperature (^{o}F)	Exit Temperature (^{o}F)
Compressor	14.69		132.26	59		601.5
Recuperator	131.95		129.09	601.5		1075.8
Burner	129.09		125.22	1075.8		2300
GGT	125.22		49.02	2300		1816.04
Diffuser	49.02		47.55	1816.04		1805.1
First-stage PT	47.55	47.01	27.33	1805.1	1805.1	1541.1
Second-stage PT	27.33	27.02	15.88	1541.1	1541.1	1331.7*
Diffuser	15.88		15.24*	1331.7*		1331.7*
Recuperator	15.24*		14.69	1331.7*		908.5*

	Gas Generator Turbine	Power Turbine
rpm	57,000	40,000
Blade stress σ_B) 1st, lb/sq in.	47,557	36,388
Blade stress σ_B) 2nd, lb/sq in.		44,442
Disc stress σ_D) 1st, lb/sq in.	60,000	55,036
Disc stress σ_D) 2nd, lb/sq in.		55,031
Rotor weight W_R) 1st, lb	4.914	5.907
Rotor weight W_R) 2nd, lb		5.828
Rotor weight W_T, lb	4.914	11.735
V_x/A'_{cr}) Exit	0.425	0.346

*Values based on reference engine conditions (ϵ = 0.65, $\Delta P/P$ = 6 percent)

TABLE IV. NONRECUPERATIVE ENGINE DATA

	Inlet Pressure (psia)	Inter-stage Pressure (psia)	Exit Pressure (psia)	Inlet Temperature (°F)	Inter-stage Temperature (°F)	Exit Temperature (°F)
Compressor	14.69		132.26	59		601.5
Burner	132.26		128.30	601.5		2300
GGT	128.30		50.24	2300		1816
Diffuser	50.24		49.16	1816		1814.5
First-stage PT	49.16	48.57	27.29	1814.5	1814.5	1506.7
Second-stage PT	27.29	26.96	15.15	1506.7	1506.7	1266.5
Diffuser	15.15		14.69	1266.5		1266.5

	Gas Generator Turbine	Power Turbine
rpm	57,000	40,000
Blade stress σ_B) 1st, lb/sq in.	46,877	37,203
Blade stress σ_B) 2nd, lb/sq in.		46,116
Disc stress σ_D) 1st, lb/sq in.	60,042	55,000
Disc stress σ_D) 2nd, lb/sq in.		55,054
Rotor weight W_R) 1st, lb	4.805	6.396
Rotor weight W_R) 2nd, lb		6.244
Rotor weight W_T, lb	4.805	12.640
V_x/A'_{cr}) Exit	0.423	0.357

Overall design performance estimates were made based on current in-house and industry technology and on advanced technology projections considered to be achievable within a 3-year development program. Component performance was estimated using existing test data and advanced technology projections for single-stage axial compressors as shown in Figures 2 and 3. The axial compressor performance was taken from the state-of-the-art curve shown in Figure 3. The aerothermodynamic analysis showed that the required performance could be realized with pressure ratios of 1.5 and 6.0 for the axial and centrifugal compressor stages, respectively.

The specific speed, N'_S, of the centrifugal compressor is in the order of 50, and for this value the projected curve on Figure 2 shows a polytropic efficiency of 86.5 percent. This is approximately one percentage point higher than that shown for existing compressors and is equivalent to an adiabatic efficiency of 81.6 percent at a pressure ratio of 6.0. The adiabatic efficiency of the axial stage is 90.5 percent, and combining the two-stage efficiencies yields an overall compressor efficiency of 82 percent.

TURBINE DESIGN

For a recuperative engine design of minimum volume and weight, it is desirable to establish a design in which the exit Mach number from the last turbine stage is as low as possible in order to minimize exit diffuser length and turning losses in the turbine to recuperator ducts. Although the design value of total-to-total power turbine efficiency of 90 percent may be attained in a single stage, the above mentioned condition could not be satisfied. For example, related studies involving similar engine types indicate a three percentage point penalty in total-to-static efficiency for a one-stage turbine compared to a two-stage turbine. The corresponding reduction in duct exit Mach number was 31 percent. For these reasons, a two-stage power turbine was selected for the recuperative engine design.

With a turbine inlet temperature of 2300°F, the relatively small amount of cooling air specified in the contractual agreement for the turbine components suggests the use of a highly sophisticated cooling scheme in combination with advanced materials which would allow metal temperature in excess of 1800°F. Using present materials and convective cooling techniques, it has been estimated that coolant flow would have to be increased by nearly a factor of 3 in order to realize a 1000-hr life from the critical rotating components. It is believed that within the projected time period to a preflight rating test for the subject engine, a material or materials will be developed which will allow use of uncooled stators for the desired operating temperature, or at least will allow a considerable reduction in the amount of cooling air required. If the stator coolant requirements are reduced enough, convective cooling techniques could provide the required cooling for the rotor blades with use of the specified total cooling airflow rate. If stator materials, such as silicon nitride and alloys of columbium, to allow vane temperature to exceed 1800°F are not available, then no significant reduction in stator cooling requirements would necessitate using transpiration cooling techniques for some, or possibly all, of the cooled components.

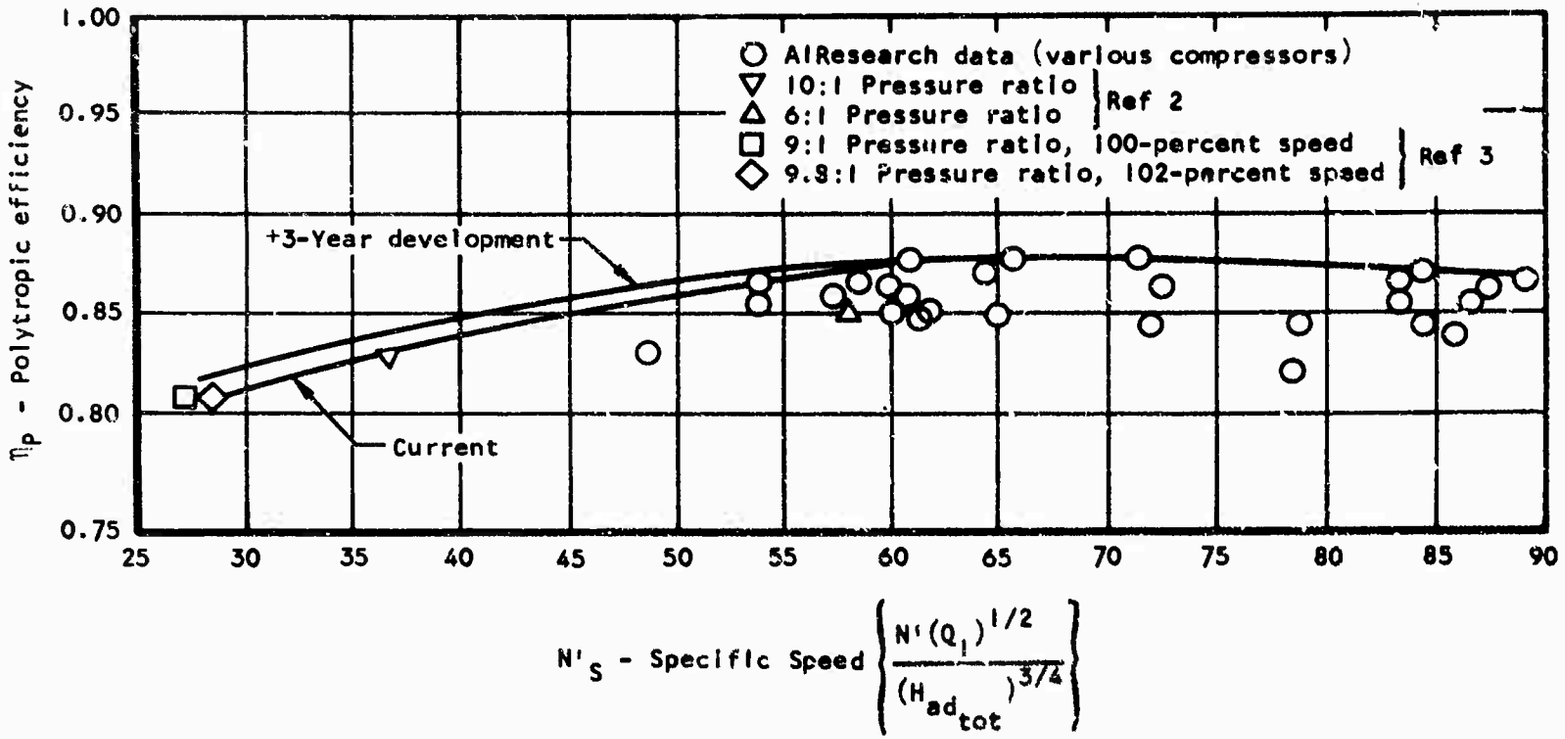

Figure 2. Single-Stage Centrifugal Compressor Polytropic Efficiency Estimates.

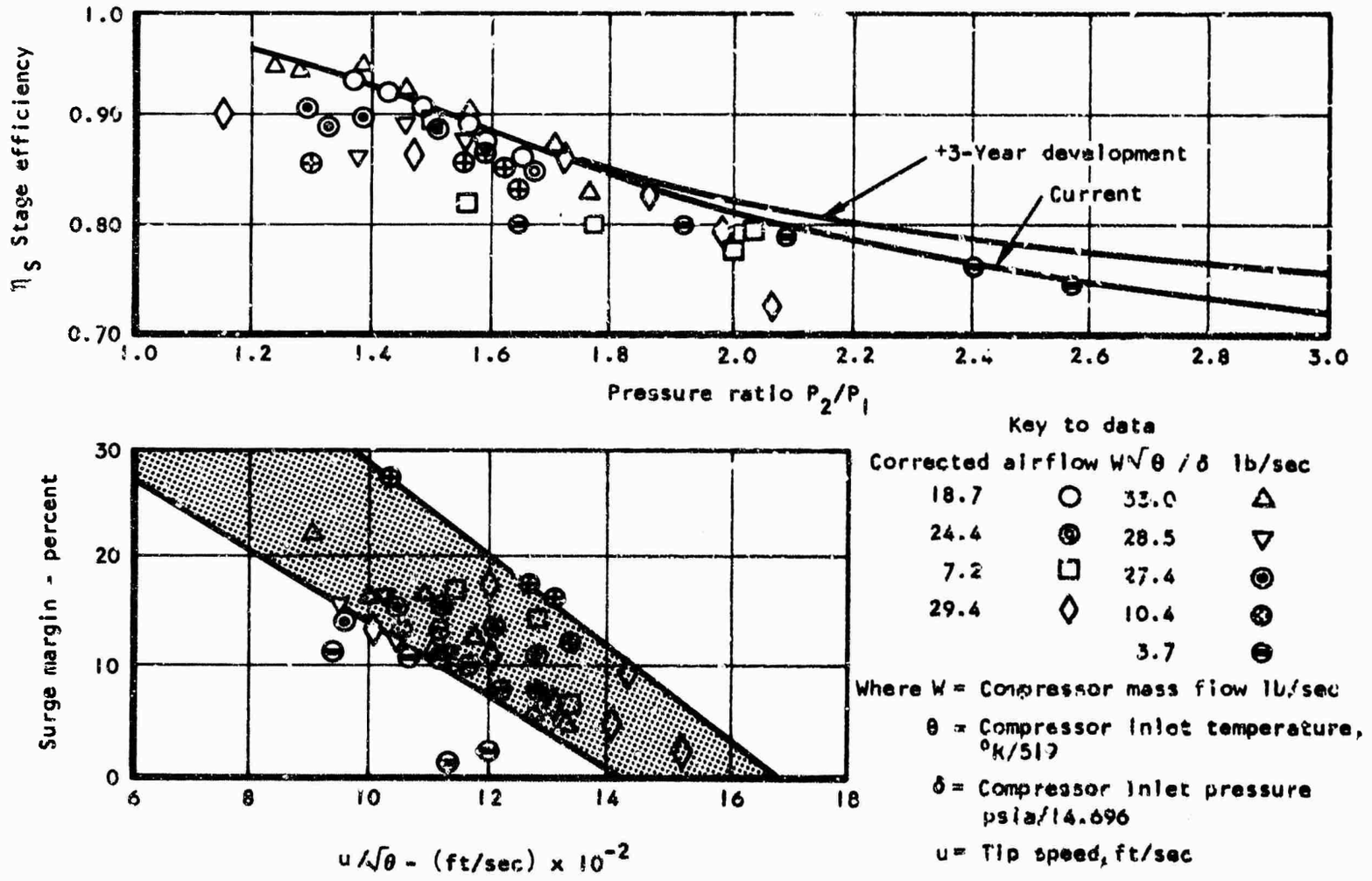

Figure 3. Single-Stage Axial Compressor Efficiency Estimates.

The turbine flow-path sizing and stage work, etc., were based upon use of the specified coolant flow rates and stage efficiencies. However, because of the uncertainty of the effects of transpiration cooling on the aerodynamic characteristics of the turbine stages, the effect of losses due to cooling was not considered in the estimation of the turbine efficiency.

The calculated total-to-total efficiency of the gas generator turbine, with an assumed 0.015-in. radial clearance, was 89.5 percent neglecting aerodynamic losses due to cooling. This value is 3.5 percentage points higher than the design value; therefore, it is felt that a sophisticated cooling technique and/or use of advanced materials would allow a developed axial gas generator turbine to operate with a total-to-total efficiency of 86 percent.

Since a two-stage turbine was selected, the aerodynamic design of the power turbine is more conservative than that for the gas generator turbine. Operating with a 0.015-in. radial clearance, the turbine is estimated to have a total-to-total efficiency of 90.5 percent (again neglecting aerodynamic losses due to cooling). The two-stage design has a relatively low exit Mach number (0.346), and thus it permits use of an exit diffuser having an effective length of only 3.5 in. Since the coolant flow rate is relatively low for this turbine (0.5 percent for the first-stage stator), it is felt that no significant problems would be encountered in developing the turbine to operate at the specified efficiency of 90.0 percent including cooling losses.

The efficiency estimation for this turbine was based upon counterrotating the power turbine in order to keep the power turbine first-stage stator turning losses low (since the gas generator turbine runs with 25 to 30 deg of counterswirl at the design point) If counterrotation was not provided, a small additional stage loss would be incurred.

COMBUSTOR DESIGN

In advanced regenerative engines having high compressor pressure ratios and high turbine inlet temperature, flame tube cooling becomes increasingly difficult. One partial solution to this problem is to reduce the surface area of the sheet metal to be cooled. Reduction of area is accomplished by shortening the combustor as much as possible. For this design the end result of shortening, traded off against pressure losses and efficiency effects, was a reduced volume combustor which fits conveniently into the cavity formed between the back face of the centrifugal compressor diffuser and the recuperator gas side duct. Although the combustor is relatively small, it is still conservative on pressure loss (which is set by the diffuser exit dynamic head) and should have starting capability up to 33,000-ft altitude.

In typical gas turbine engines, most of the heat input to the flame tube is from radiation, and 60 percent of the flame tube cooling is by external-forced convection (which effectively controls the allowable pressure loss). By utilizing a vaporizing, forced recirculation-type combustor which operates with a blue flame, radiation is reduced significantly and flame tube heating is thereby reduced. Additionally, as discussed above, the sheet metal surface was minimized in order to conserve cooling air. The net effect is that flame tube cooling is not considered to be a significant problem in this combustor design.

Attainment of an adequate temperature distribution factor, TDF, is considered to be the prime development problem with this combustor, where TDF is defined as

$$TDF = \frac{T_{max} - T_{av}}{T_{av} - T_{in.}}$$

HEAT EXCHANGER DESIGN

Since a complete section in this report is written specifically on the heat exchanger, this section merely outlines overall goals. The fixed boundary recuperator (as opposed to the rotary regenerator and liquid-coupled regenerator) was chosen because of its simplicity, high reliability, and zero leakage, and because much test and fabrication experience has been accumulated by AiResearch over the last few years. The matrix must be designed so that high heat transfer performance is achieved under severe limitations of pressure drop, weight, volume, and cost. The recuperator must be integrated with the engine with careful attention given to efficient diffusion of the air and gas streams, and good flow distribution. Material selection and mechanical design of the recuperator must be compatible with required service life under severe operating conditions of vibration, high temperature, and operation in a corrosive hot gas atmosphere.

MECHANICAL AND STRUCTURAL CONSIDERATIONS

The recuperator shown in the reference engine in Figure 4 is an annular design wrapped around the turbomachinery; with this arrangement, the recuperator is considered to be prime engine structure, thus giving a fully integrated, lightweight, compact engine package. With the recuperator being fully integrated with the turbomachinery, the need for additional ducting to take the air and gas to and from the heat exchanger is eliminated. The recuperator as shown is a lightweight tubular design of brazed and welded construction.

This engine design concept divides the components into two basic modules. The gas generator assembly, including all accessories, comprises one module. The other module integrates the power turbine and recuperator. Separation of these modules is accomplished by removal of bolts from one flange, which is located in a plane just aft of the centrifugal compressor. The two rotating assemblies are essentially isolated from each other. The only

internal mechanical connection is through a piston-ring seal between the gas-generator turbine shroud and the interstage diffuser duct. Thus, movement of the turbine shrouds relative to the blades, due to thermal gradients, should be minimized since the shrouds are cantilevered only a short distance from their respective turbine housings, and movement of structural members is not transmitted from component to component.

The primary load path, through which the power turbine bearing housing is supported, originates at the flange, passes through the outer plenum, and through three struts to the housing. The three struts pass through the turbine-to-recuperator duct and through the exhaust annulus. The entire assembly of outer shell, struts, turbine-to-recuperator duct, exhaust annulus, recuperator core, and bearing housing shell is formed as an integral unit by brazing and welding. With the same tool used for separating the basic engine modules, this entire recuperator assembly can be quickly removed from the power turbine section by the removal of bolts in one flange only. Considerable stability is afforded by this recuperator structure, and large excursions of the power turbine bearing housing due to thermal gradients are not expected. With the flow paths chosen, the outer shell of the assembly operates at the lowest temperature, and it is expected that growth of the recuperator due to temperature would be toward the front of the engine. Seals at the forward end of the recuperator which provide continuity of flow path between the two basic modules offer compliance to allow for this growth.

The power turbine stators and interstage diffuser are supported by members from a flange which is carried off the inner diameter of the turbine-to-recuperator duct.

The output shaft was located at the rear of the engine to obtain a simplified shafting and bearing system. By minimizing the shaft dynamics problem and, as noted above, by isolating each rotating assembly, it is expected that turbine tip clearance may be reduced to a minimum and thus provide increased turbine efficiency.

Accessories are driven from the front end of the gas generator shaft. Starter, fuel control, fuel pump, and oil pump are all sized to operate at 30,000 rpm. A considerable reduction in weight both in the accessories and in the accessory drive components is realized by allowing this relatively high rotative speed.

No final reduction gearbox has been shown on any of the designs considered in this report, and a power turbine shaft output rotational speed of 40,000 rpm is assumed.

MATERIALS

The gas generator turbine design was based upon use of Waspaloy for the disc material and MAR-M246 for the blade material, with an electron beam weld providing the attachment.

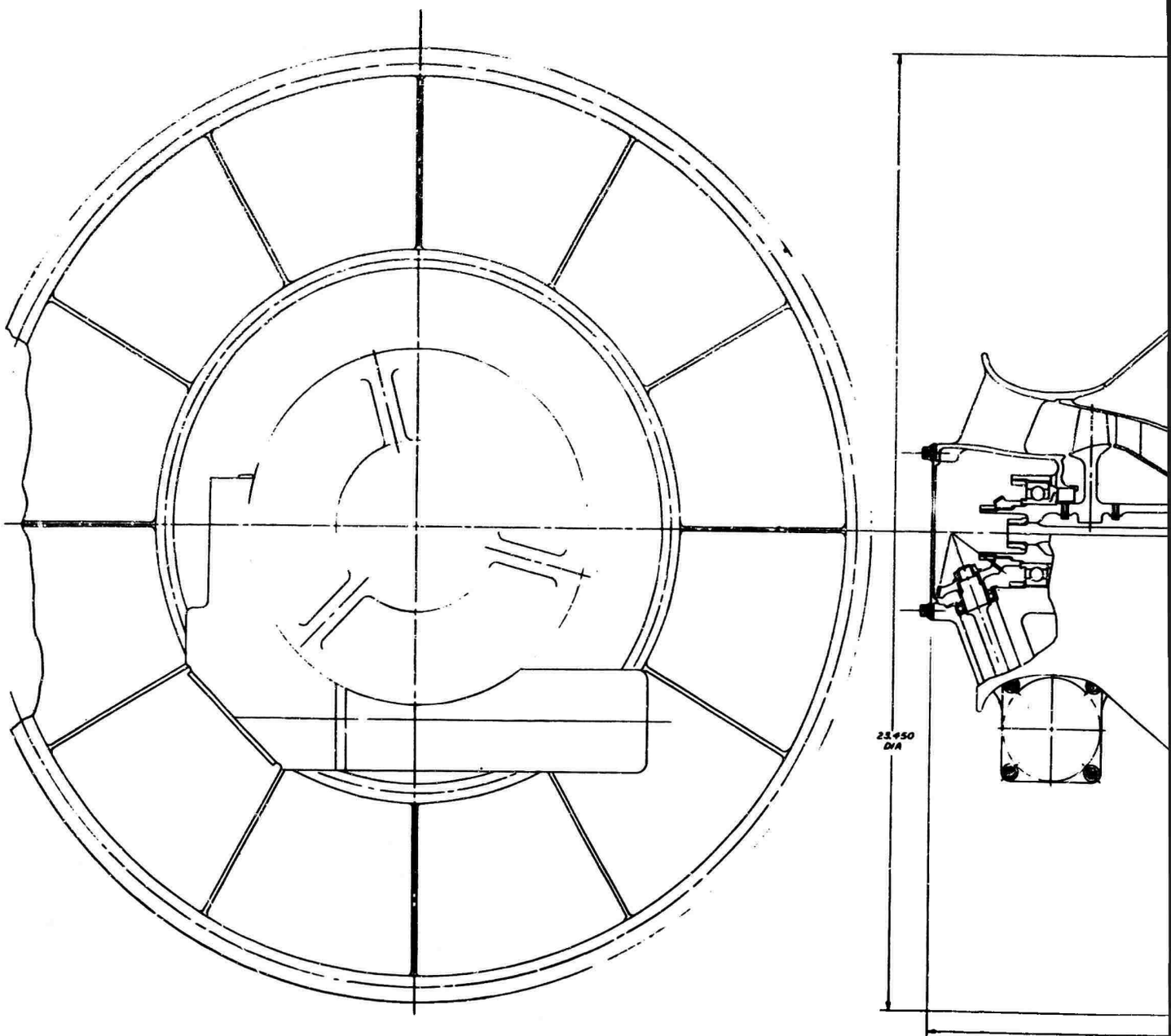

Figure 4. Reference Recuperative Engine Configuration A-1.

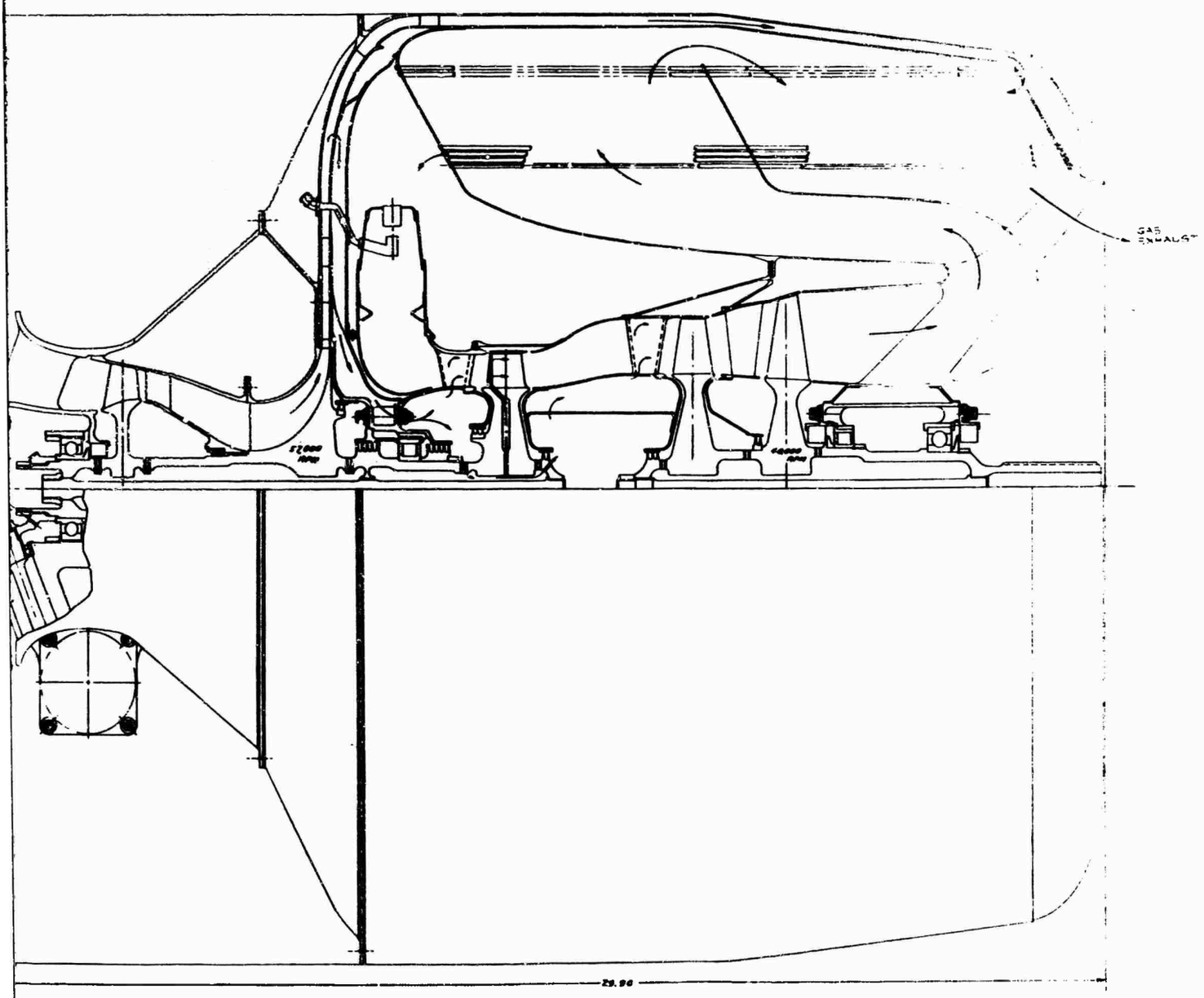
GAS
EXHAUST

An alternate material combination which could be considered is AF2-1DA for the disk and IN591 for the blades. The material AF2-1DA is extremely difficult to weld without the generation of cracks. Therefore, for this material combination, the design would probably require use of a fir tree attachment and might require some modifications to the blade design to accommodate the attachment.

If the gas generator turbine stator is assumed to have a cooling scheme which will maintain a vane metal temperature of 1800°F with the specified coolant flow and inlet gas temperatures, one of the following superalloys could be used for vane materials: IN738, MAR-M432 or MAR-M509. Stator material candidates that would allow the vane temperature to exceed 1800°F are silicon nitride and alloys of columbium. For the time period being considered, it is expected that these materials will be developed sufficiently to be used for this application.

The above discussion applied equally to the first-state stator in the power turbine. For the second-stage power turbine stator and both power turbine rotors, the gas temperature is low enough to permit use of typical currently used superalloys. For this study, it was assumed that the rotors were integrally cast of IN100. The second-stage stator could be cast of INCO 713C.

Presently available alloys considered for use as combustor liner materials include Hastelloy X and Haynes 188. It is believed that alloys of columbium or silicon nitride could be utilized for advanced designs.

For the compressor, the following materials are recommended:

Axial (blade and disc) titanium alloy 6Al-4V

Centrifugal (blades and disc) titanium alloy 6Al-2Sn-4Zr-2Mo

In the recuperator analysis a range of high temperature materials were evaluated, including 347 stainless steel, Hastelloy X, Incoloy 800, Inconel 625, and N-155.

NONRECUPERATED ENGINE DESIGN

To compare recuperative and nonrecuperative engines in the sensitivity study, a design of a nonrecuperative engine using the same cycle conditions was carried out. Details of the nonrecuperated engine are shown in Figure 5. The major design considerations upon which this configuration was based are outlined below:

1. The axial plus radial compressor configuration provides the required design efficiency in a short package envelope and at a relatively low cost.

2. The reverse-flow annular burner is utilized to reduce overall length. No penalty in diameter is incurred since the burner OD is within the package envelope dictated by the compressor diffuser.

3. A single-stage turbine having relatively high loading is utilized for the gas generator turbine. This design provides the design efficiency specified and, as studies of highly loaded stages have shown, has the design potential of a reduced relative gas temperature and, hence, lower metal temperature and reduced coolant flow rates.

4. A two-stage power turbine was selected to provide the design point efficiency and a low-leaving Mach number.

The nonrecuperative engine is also of modular construction. There is no mechanical connection between the gas generator and power turbine rotating assemblies, and these two major subassemblies can be separated by the removal of bolts from one flange, which is located in a plane directly in line with the power turbine first-stage rotor.

A

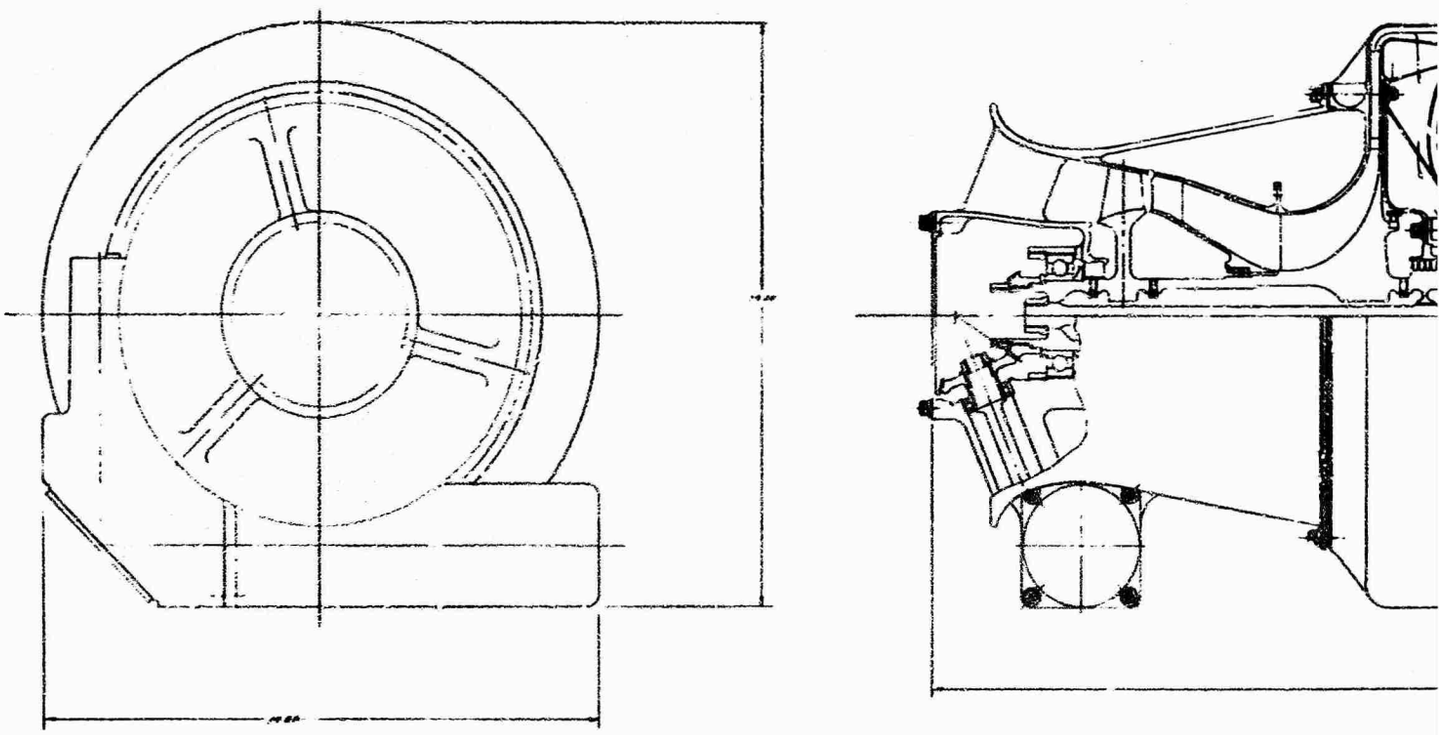

Figure 5. Nonrecuperative Engine Design.

B

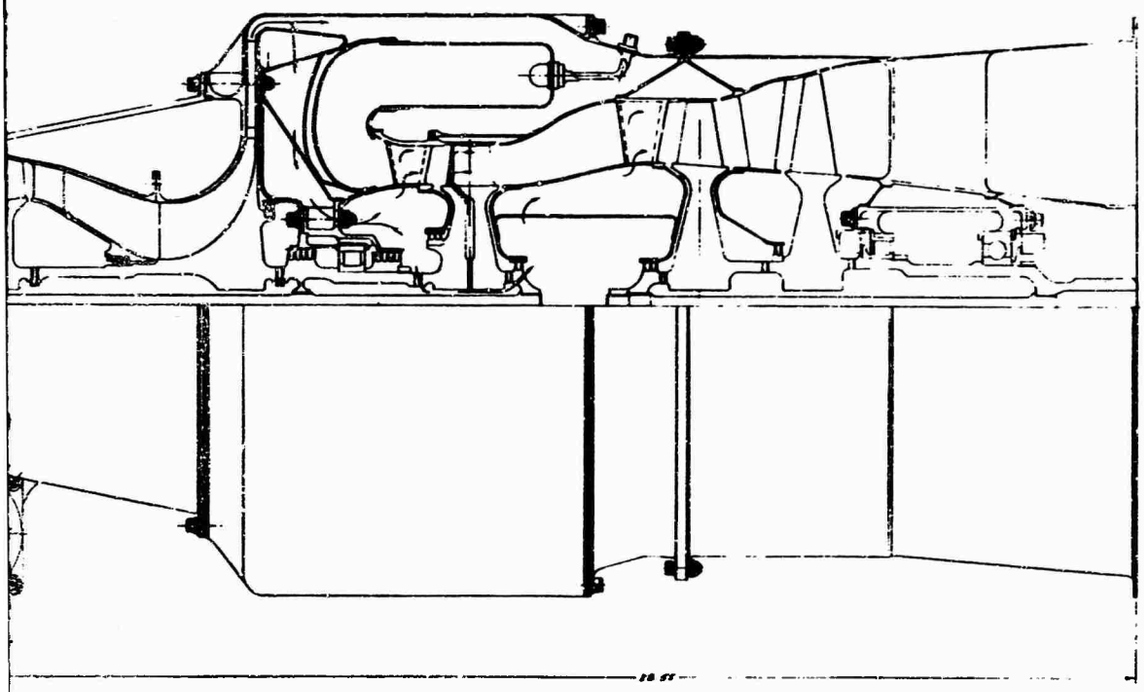

			LAYOUT	
			DESIGN STUDY	
			GE1 TURBINE ENGINE	
			(UNCLASSIFIED)	

CONFIGURATION STUDY

DEFINITION OF FULLY INTEGRATED CONCEPT

For industrial application, some gas turbines are designed for dual operation as recuperative or nonrecuperative engines. Provisioning this feature in the design usually necessitates some compromise in performance, mechanical integrity, and cost, because neither of the variants represent truly optimum designs. To date, very few recuperative gas turbines have been utilized for aircraft or helicopter propulsion. In most cases, the engines evaluated have been existing gas turbines which were modified to accommodate an exhaust heat exchanger. While these engines, with essentially bolt-on recuperators, have performed satisfactorily and have demonstrated the structural integrity of the heat exchanger, they do not represent optimum designs from the standpoints of maximum performance and minimum weight.

In this study, analytical and design approaches have been made to arrive at a truly integrated engine design, not merely arrangements in which the recuperator was added to the turbomachinery. In the sizing of the turbomachinery components, several gas flow paths were evaluated and assessed on the basis of degree of integration with the recuperator to form an integral package. In most of the designs, the recuperator is considered to be prime structure and forms the structural backbone of the engine assembly.

Flow configurations for two types of engine installation were evaluated. In the first installation, the engine assembly is mounted externally, and in the second, the engine assembly is internally installed within the vehicle structure. The various arrangements shown are conceptual designs only and are drawn to show the gas flow paths and how the recuperator is integrated with the turbomachinery. In the conceptual designs shown, features such as the gearbox, primary seals, bearings, detailed component interfaces, and exhaust ducts have not been included. These mechanical aspects associated with a truly integrated engine arrangement will be shown later in layouts of the selected configurations for each type of installation.

From the turbomachinery aerodynamic and thermodynamic studies, it was found that to achieve the 9:1 compressor pressure ratio at an efficiency of 82 percent, a single axial and radial stage could be utilized. This arrangement gives a short axial flow length, and air delivery ducts to the recuperator can be integrated with the engine structure by virtue of the air exiting from the compressor in a radial direction. To realize the gas generator and power turbine efficiencies of 86 percent and 90 percent respectively, axial stages are required; one stage is necessary for the gas generator turbine and two stages are necessary for the power turbine. For the combustor, straight through flow, reverse-flow annular, radial annular, and a centrally located conical arrangement were examined. With the basic turbomachinery aerothermodynamic ground rules establishing the number of stages, etc., a series of conceptual designs is outlined in which consideration is given to packaging of the recuperator and rotating components to give a compact engine unit.

DESIGN CONCEPTS FOR EXTERNAL ENGINE INSTALLATION (A)

The conceptual designs shown in Figures 6 through 21 illustrate the gas flow paths envisioned for an integral unit; the actual recuperator surface geometries for the selected configurations will be evaluated in the parametric study for a wide range of operating conditions. With this type of installation, where the engine assembly itself is exposed to external view, configurations have been considered in which the recuperator and as much of the associated high temperature ducting as possible are effectively hidden from view.

Configuration A-1 shown in Figure 6 is a two-pass cross-counterflow design with the high pressure compressor discharge air flowing single pass inside the tubes and the low pressure turbine exhaust gas flowing two pass across the bundle. As for most of the designs shown, plate-fin or finned-tube surface geometries could also be utilized. The recuperator is effectively shrouded by the compressor discharge annulus. The recuperator is considered to be prime engine structure, and this results in a fully integrated, lightweight, compact engine package. With the recuperator being fully integrated with the turbomachinery, the need for additional ducting to take the air and gas to and from the heat exchanger is eliminated. The exhaust gas leaves the engine-recuperator structure in an axial direction through an annulus at the rear of the engine. The turbomachinery layout is conventional, with the power turbine drive shaft at the rear (hot end) of the engine. The gas-generator and power turbine drive shaft assemblies are not mechanically connected, and the engine can be quickly split into the two basic power modules by removing the bolts from one flange only.

Configuration A-2 shown in Figure 7 is a three-pass cross-counterflow design in which the air flows single pass inside the tubes and the gas flows three pass across the bundle. To have an effectively shrouded recuperator with this flow configuration, it is necessary to exhaust the gas radially from the recuperator by means of a series of radial ports formed through the outer air annulus. Locally in the gas exit area, the recuperator matrix would be partially exposed. The recuperator is regarded as prime engine structure, and this results in a light, compact engine package.

Configuration A-3 shown in Figure 8 is a multipass variant of configuration A-1 for designs requiring a high level of effectiveness. The multipassing on the low pressure gas side implies that the surface geometry compactness would have to be fairly low to satisfy the low gas side pressure loss requirement. The recuperator again is assumed to be prime engine structure. The exhaust gas leaves the engine in an axial direction through an annulus at the rear of the package.

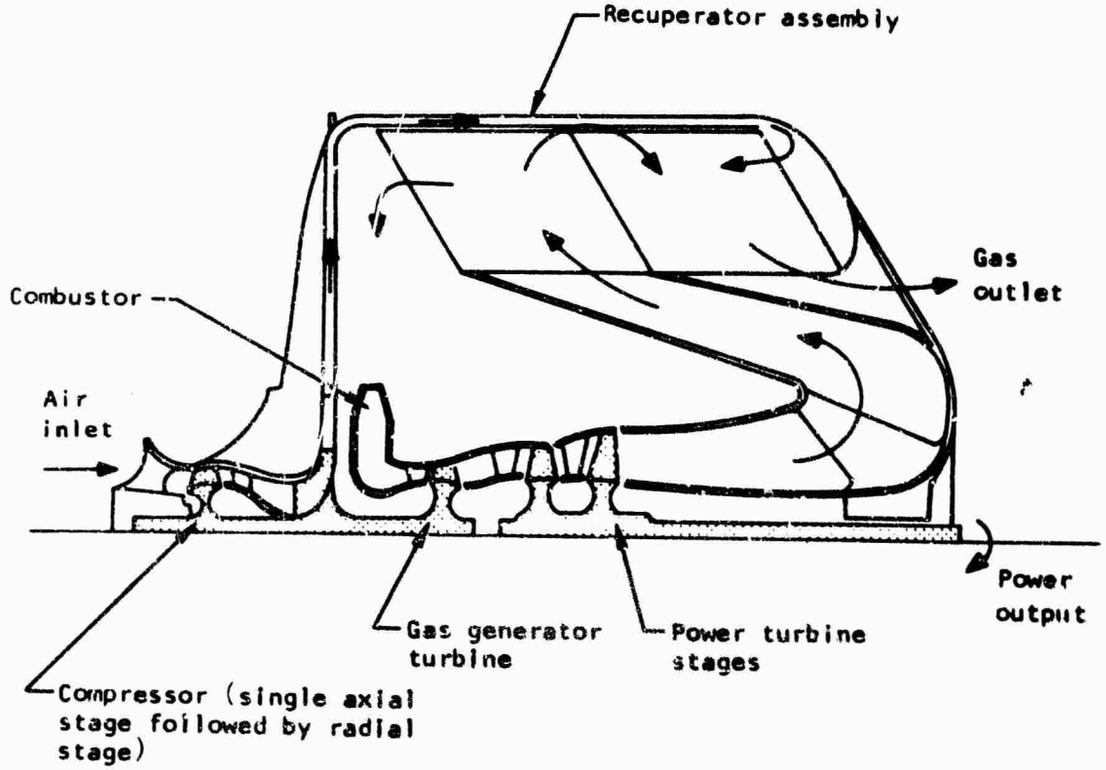

Figure 6. Engine Configurstion A-1.

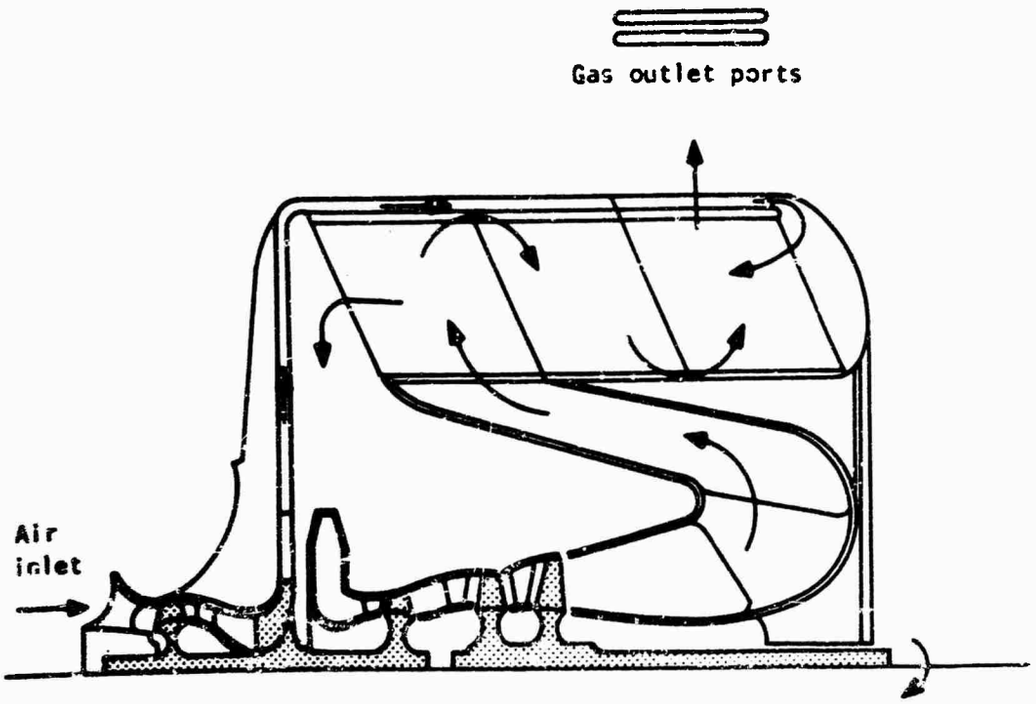

Figure 7. Engine Configuration A-2.

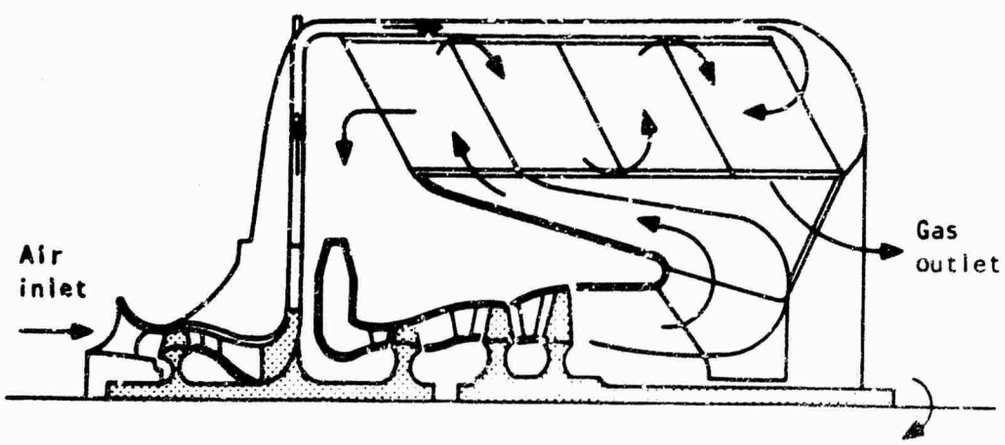

Figure 8. Engine Configuration A-3.

Configuration A-4 shown in Figure 9 is a two-pass cross-counterflow design with the high pressure air flowing two pass inside the tubes and the gas flowing single pass across the bundle. The recuperator is considered to be prime structure, but additional ducting is required as shown to give a design in which the recuperator is effectively hidden from view. The exhaust gas leaves the engine in an axial direction through an annulus at the rear of the package.

Configurations A-5 and A-6 shown in Figures 10 and 11 respectively are both counterflow plate-fin variants. With such a flow configuration, end sections are necessary to direct the air and gas to and from the pure counterflow portion of the heat exchanger. The conceptual designs show typical mitered headering arrangements that can be utilized in a plate-fin unit. The plate-fin variants could be either of modular construction, in which a series of elements would be circumferentially positioned around the turbomachinery, or a full annular core, in which the matrix would be fabricated as one assembly. In either case, the recuperator assembly could be considered as prime structure. In both configurations, the exhaust gas leaves the engine in an axial direction from the rear of the package.

Configuration A-7 shown in Figure 12 is a two-pass cross-counterflow design with the high pressure compressor discharge air flowing single pass across the bundle and the low pressure turbine exhaust gas flowing two pass inside the tubes. This flow pattern could also be realized with plate-fin or finned-tube surface geometries. The recuperator is again assumed to be prime engine structure giving an integral engine unit. The exhaust gas leaves the engine-recuperator structure in an axial direction from the rear of the engine.

Configuration A-8 shown in Figure 13 is an arrangement in which both fluids are multipassed. As drawn, the high pressure air flows three pass outside the tubes and the low pressure gas flows two pass inside the tubes to give three-pass cross-counter-parallel-flow arrangement. With this design, the core could also be constructed from plate-fin or finned-tube surface geometries. Multipassing on both sides of the unit necessitates the use of low compactness surfaces to satisfy the low pressure loss requirements, and this results in a heat exchanger core weight and volume penalty. The exhaust gas leaves the engine in an axial direction from the rear of the engine.

Configuration A-9 shown in Figure 14 is a pure counterflow tubular design in which the high pressure air flows inside the tubes. The low pressure gas flows in an axial direction outside the tubes. This design would probably have a large volume and weight because of the poor heat transfer coefficient associated with the axial gas flow outside the tubes.

Configuration A-10 shown in Figure 15 is a parallel-flow tubular design in which the high pressure air flows inside the tubes. The low pressure gas flows in an axial direction and leaves the core radially in a series of ports formed in the air delivery annulus. Thermodynamically, the

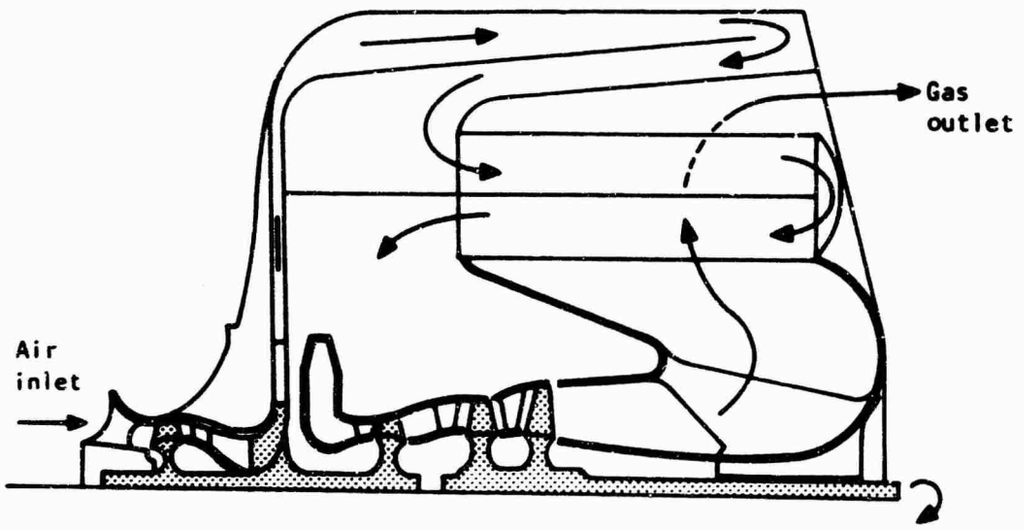

Figure 9. Engine Configuration A-4.

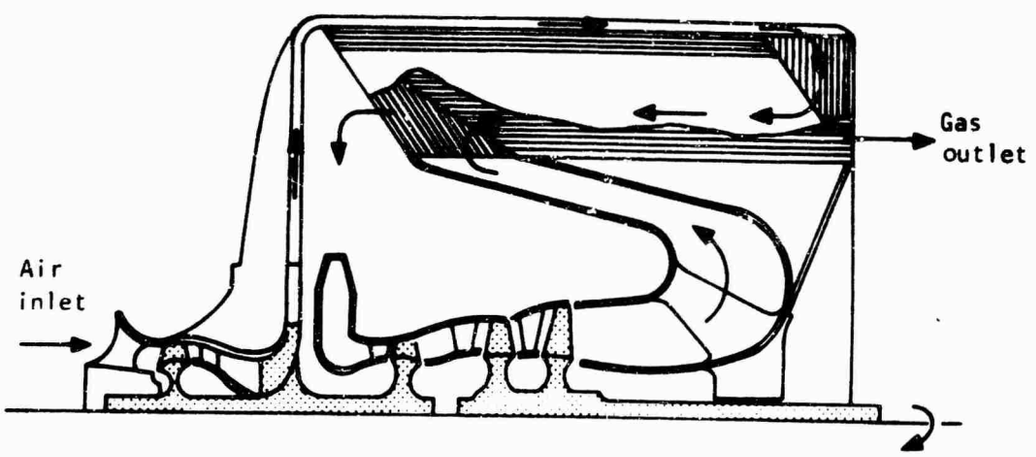

Figure 10. Engine Configuration A-5.

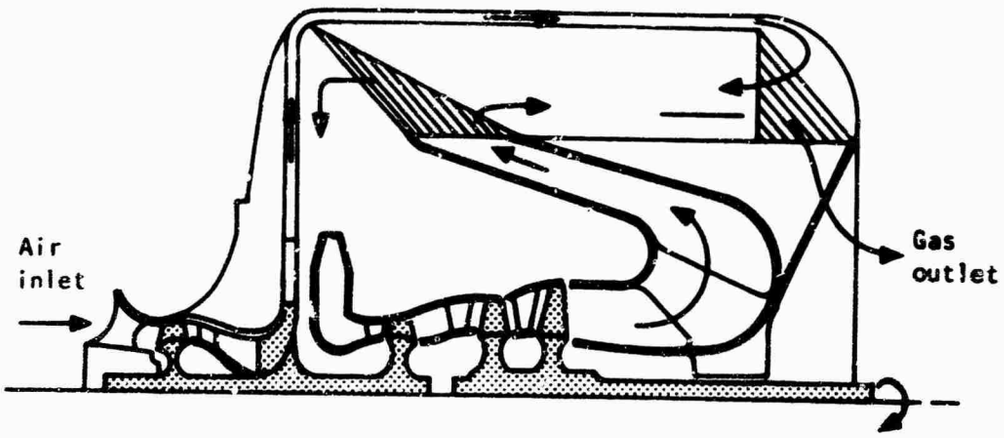

Figure 11. Engine Configuration A-6.

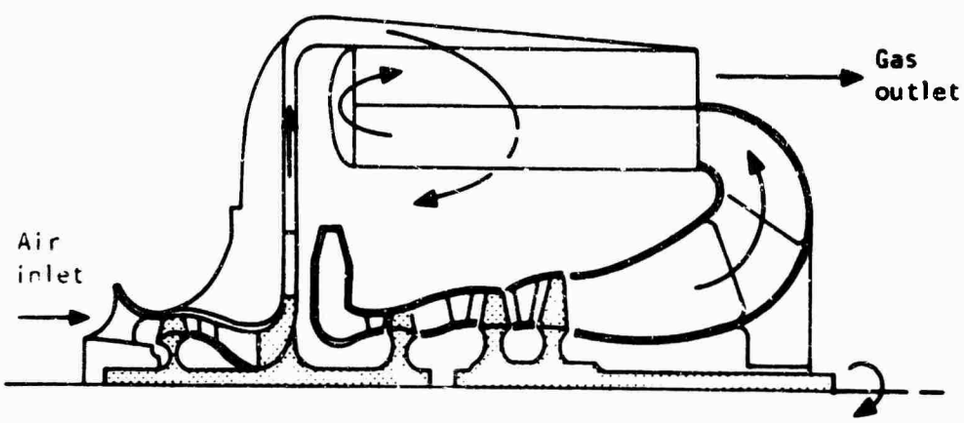

Figure 12. Engine Configuration A-7.

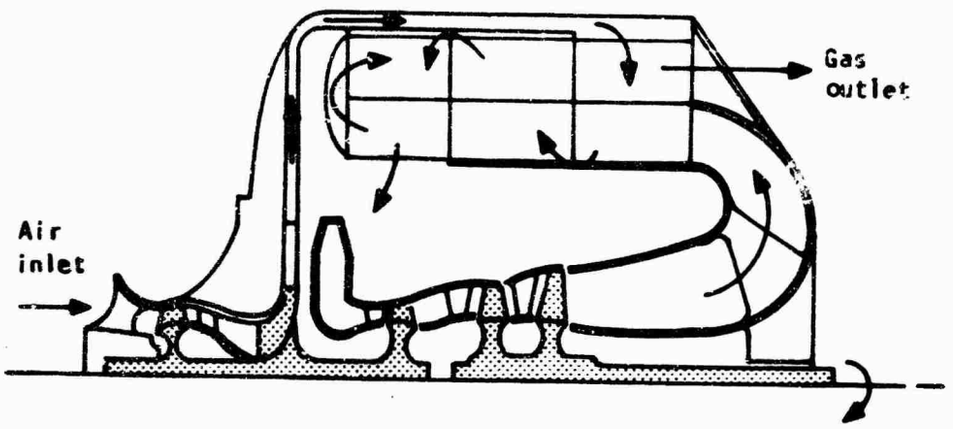

Figure 13. Engine Configuration A-8.

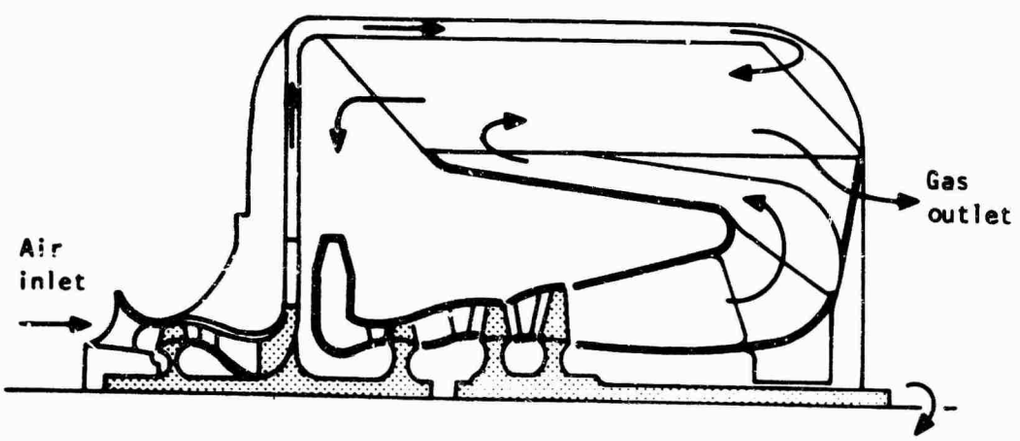

Figure 14. Engine Configuration A-9.

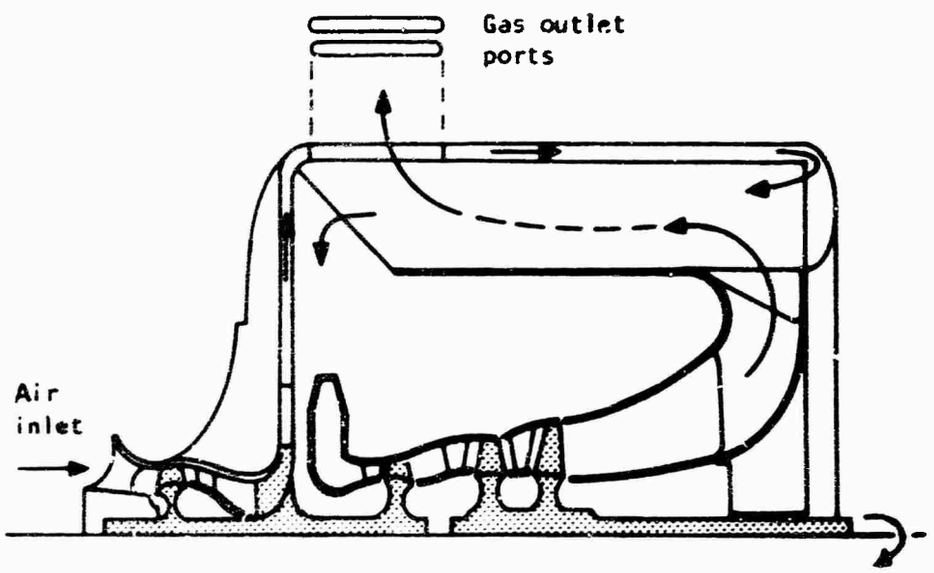

Figure 15. Engine Configuration A-10.

flow path is poor, since with a capacity rate ratio close to unity, the maximum attainable effectiveness for parallel flow is only 50 percent.

Configuration A-11 shown in Figure 16 is a two-pass cross-counterflow design in which the recuperator is mounted on the back of the engine. The high pressure air, which is delivered to the recuperator through a long annulus, flows two pass outside the tubes. The low pressure gas flows straight through the tubes and exits in an axial direction. In this design, the recuperator is added to the turbomachinery rather than being fully integrated at the design stage.

Configuration A-12 shown in Figure 17 is a counterflow plate-fin variant of A-11 and is drawn to show the end section arrangement necessary to duct the air and gas to and from the pure counterflow portion of the heat exchanger.

Configuration A-13 shown in Figure 18 is a two-pass cross-counterflow design with the recuperator located at the rear of the engine. The air flows single pass inside the tubes and the gas flows two pass outside the bundle. The gas flows from the recuperator in a radial inward direction, and some ducting is necessary to turn the exhaust gas in an axial direction.

Configuration A-14 shown in Figure 19 is a variation of the previous design with three passes on the air side and two passes on the gas side. Like Configuration A-8, multipassing on both sides of the heat exchanger results in a unit of increased volume and weight, because of the necessary utilization of low compactness surfaces to satisfy the low pressure loss requirements.

Configuration A-15 shown in Figure 20 is a three-pass cross-counterflow design with the high pressure air flowing three pass across the bundle and the low pressure gas flowing single pass inside the tubes. This design is integrated with a modified turbomachinery arrangement in which the number of compressor and turbine stages remains the same, but a rear mounted combustor is utilized. With this arrangement, the power turbine is interposed between the compressor and the gas-generator turbine; thus, the output shaft centerline must be offset from the centerline of the rotating assembly. This could be accomplished as shown by incorporating a reduction gear in the drive, and this necessitates taking the output shaft through the compressor diffuser passage.

Configuration A-16 shown in Figure 21 is a three-pass cross-counterflow design with the high pressure air flowing single pass across the bundle and the low pressure gas flowing three pass inside the tubes. As in the former arrangement, the gas exhausts from the recuperator in an axial direction.

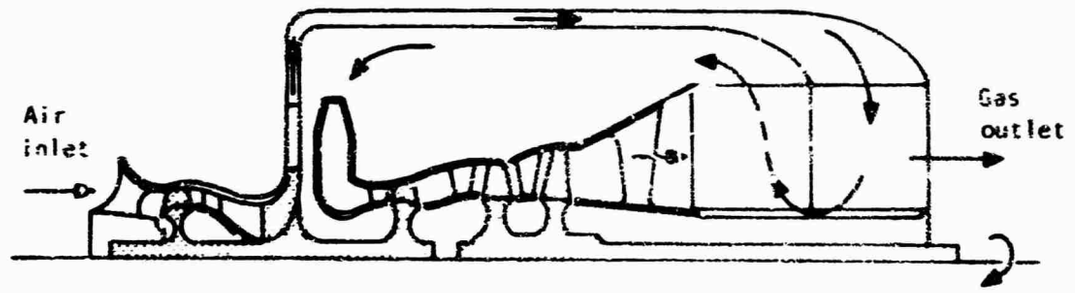

Figure 16. Engine Configuration A-11.

Figure 17. Engine Configuration A-12

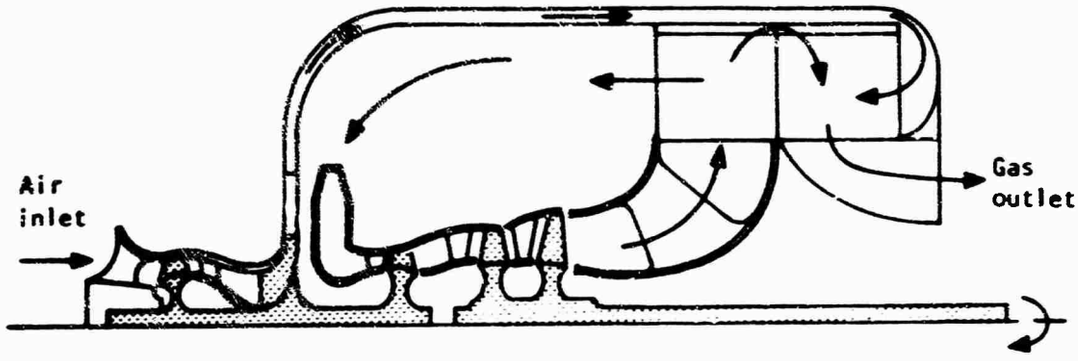

Figure 18. Engine Configuration A-13.

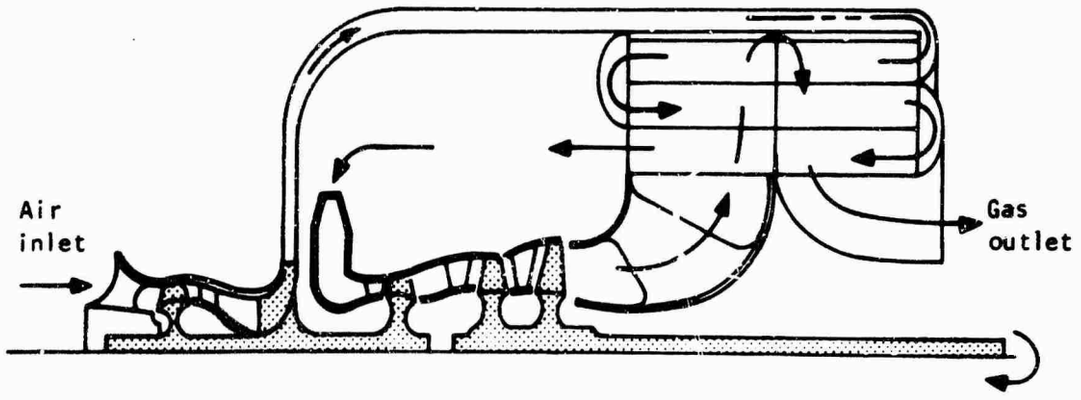

Figure 19. Engine Configuration A-14.

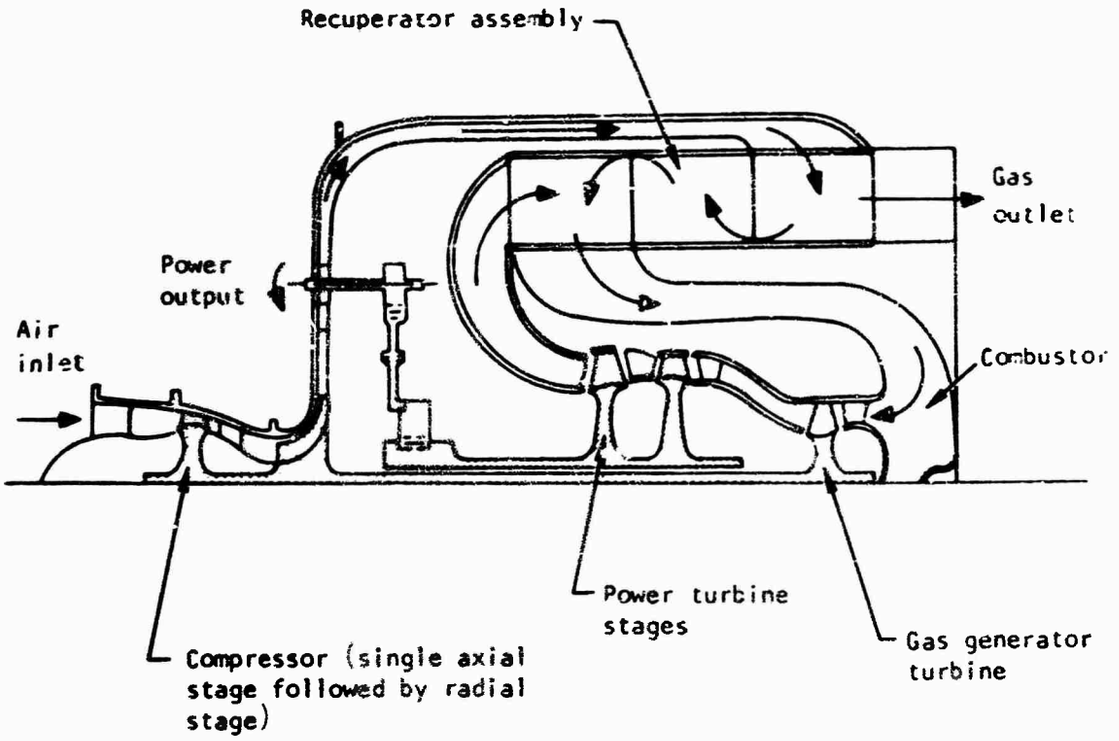

Figure 20. Engine Configuration A-15.

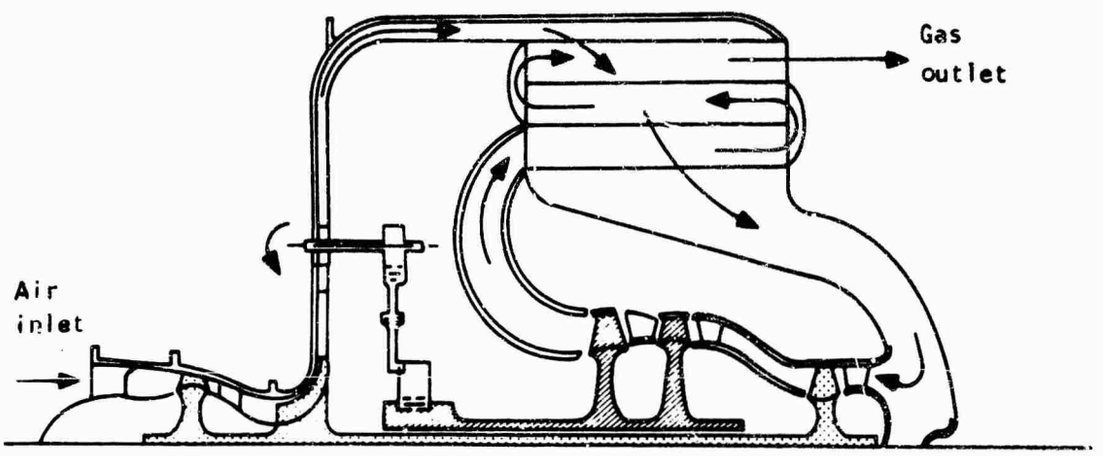

Figure 21. Engine Configuration A-16.

DESIGN CONCEPTS FOR INTERNAL ENGINE INSTALLATION (B)

The conceptual designs shown in Figures 22 through 31 illustrate the gas flow paths envisaged for an integral unit; the actual recuperator surface geometries for the selected configurations will be evaluated in the parametric study. With this type of installation, the engine assembly is physically hidden from external view by aircraft structure.

Configuration B-1 shown in Figure 22 is a two-pass cross-counterflow arrangement, and as drawn, shows the single-pass high pressure air inside the tubes and the two-pass low pressure gas outside the tubes. As for most of the designs shown, plate-fin or finned-tube surface geometries could also be utilized. The recuperator is considered to be prime engine package. The exhaust gas exits from the recuperator tube bundle in a radial direction. As for the previous designs in which the recuperator was wrapped around the rotating components, the turbomachinery layout is conventional, and the engine can be quickly split into the two basic power modules.

Configuration B-2 shown in Figure 23 is a two-pass cross-counterflow design with the high pressure compressor discharge air flowing two pass inside the tubes and the low pressure turbine exhaust gas flowing single pass outside the tube bundle. This flow pattern could also be realized with plate-fin or finned-tube surface geometries. The recuperator is again assumed to be prime engine structure giving an integral engine unit. The exhaust gas exits from the recuperator in a radial direction.

Configuration B-3 shown in Figure 24 is an arrangement in which both fluids are multipassed. The low pressure gas flows three pass outside the tubes, and the high pressure air flows two pass inside the tubes. Multipassing on both sides of the unit necessitates the use of low compactness surfaces to satisfy the low pressure loss requirements, and this results in a heat exchanger core weight and volume penalty. The exhaust gas exits from the recuperator in a radial direction.

Configuration B-4 shown in Figure 25 is a two-pass cross-counterflow design in which the low pressure gas flows single pass inside the tubes and the high pressure air flows two pass across the tube bundle. The exhaust gas exits from the front of the engine in an axial direction.

Configuration B-5 shown in Figure 26 is a pure counterflow tubular design in which the low pressure gas flows inside the tubes. The high pressure air flows in an axial direction outside the tubes. To fully utilize the annular envelope available for the heat exchanger, the tubes are radiused at the ends to form the headers. This type of design would probably have a large volume and weight because of the poor heat transfer coefficient associated with the axial airflow outside the tubes.

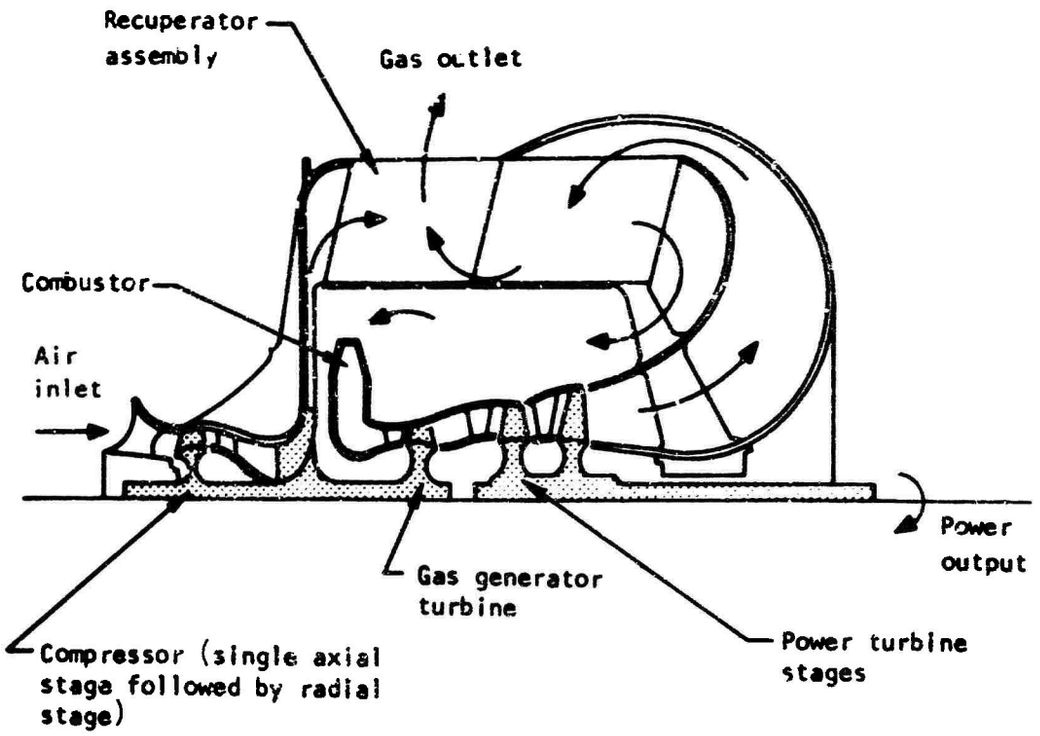

Figure 22. Engine Configuration B-1.

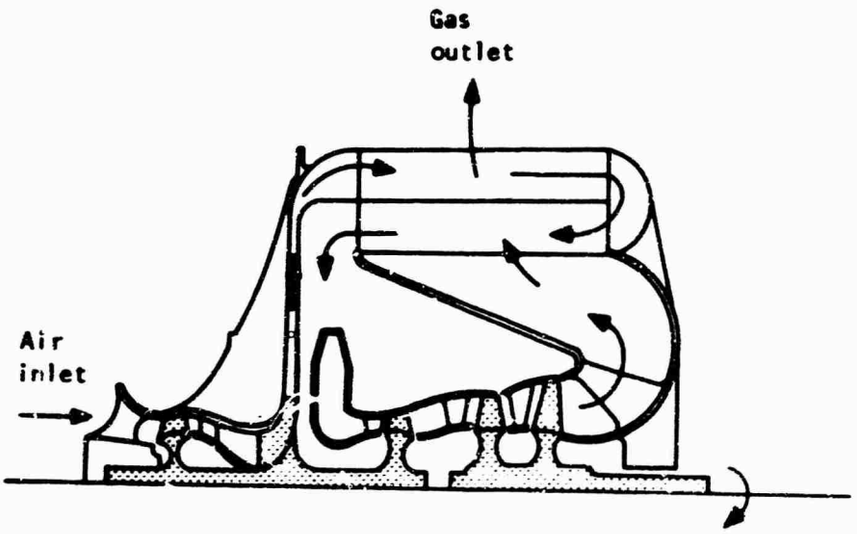

Figure 23. Engine Configuration B-2.

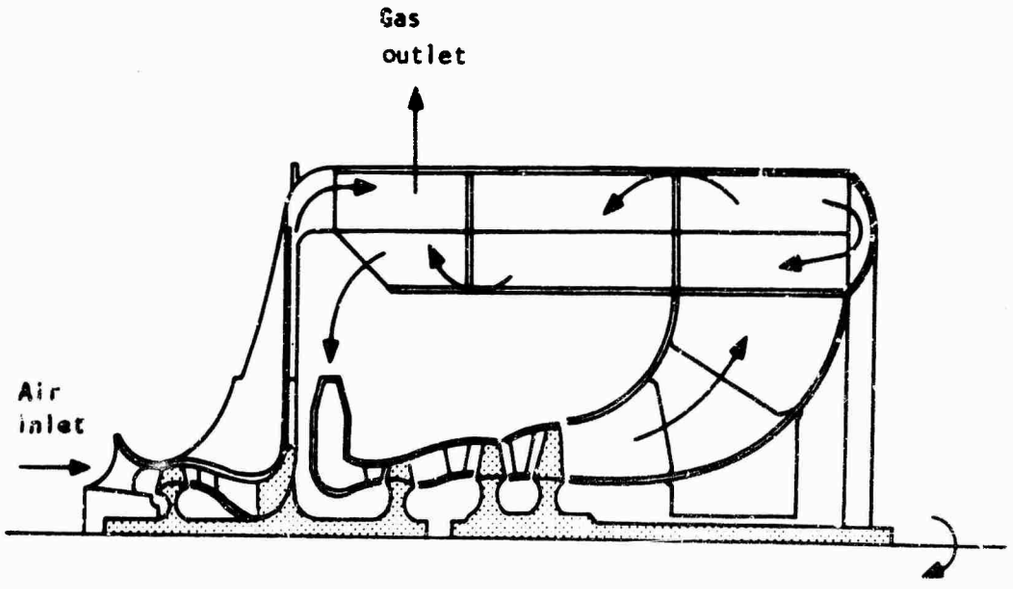

Figure 24. Engine Configuration B-3.

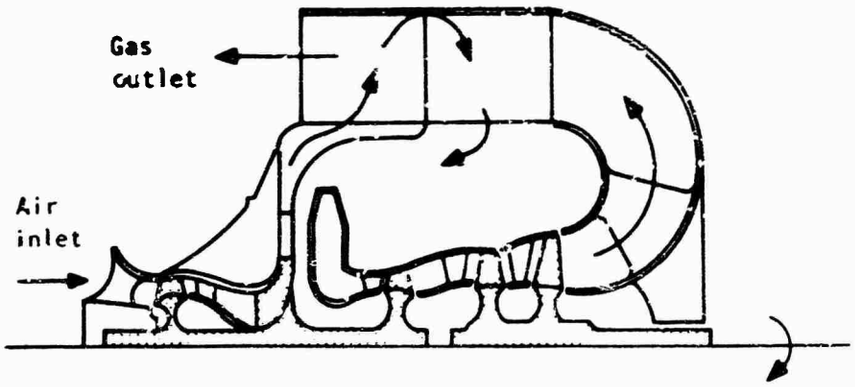

Figure 25. Engine Configuration B-4.

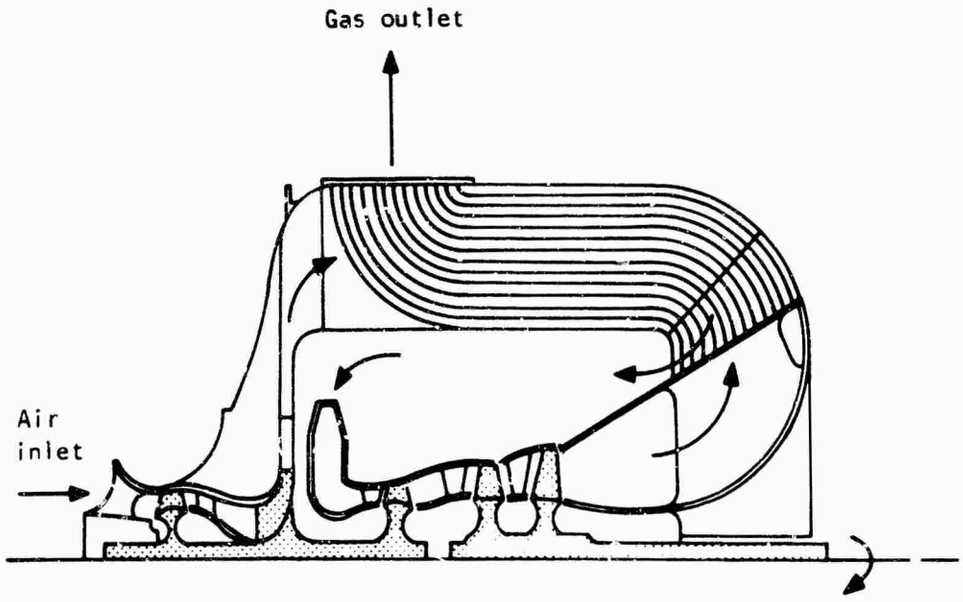

Figure 26. Engine Configuration B-5.

Configuration B-6 shown in Figure 27 is a tubular design in which the high pressure air flows two pass inside the tubes and the low pressure gas flows in an axial direction outside the tubes. The design is poor from the heat transfer standpoint because of the cross-counterflow-parallel-flow configuration, together with the low heat transfer coefficient for axial flow outside the tubes.

Configuration B-7 shown in Figure 28 is a three-pass cross-counterflow design with the high pressure air flowing single pass through the tubes and the low pressure gas flowing three pass across the bundle. For this type of turbomachinery arrangement, a concentric shaft system is utilized, and this necessitates an offset drive through the compressor diffuser. The exhaust gas exits from the recuperator in a radial direction as shown.

Configuration B-8 shown in Figure 29 is a three-pass cross-counterflow design with the high pressure air flowing three pass inside the tubes and the low pressure exhaust gas flowing radially outward across the tube bundle.

Configuration B-9 shown in Figure 30 is a three-pass cross-parallel-flow design with the high pressure air flowing single pass inside the tubes and the exhaust gas flowing three pass across the tube bundle. Thermodynamically, the cross-parallel-flow arrangement is poor, and with capacity rate ratios in the order of unity, only very low effectiveness levels are attainable.

Configuration B-10 shown in Figure 31 represents a radical change in turbomachinery gas flow path compared with all of the above designs. During the configuration study, no restrictions were placed on the designer as regards engine package shape and drive shaft arrangement, although the basic number of compressor and turbine stages and their respective position in the air flow path through the engine were adhered to. This gas turbine, perhaps not practical for airborne application, is included to illustrate that radical approaches were considered to try to establish engine configurations to satisfy the problem statement. In this design the gas-generator and power turbine spools are at 90 deg to each other, and a two-pass cross-counterflow recuperator is utilized. With this design, cross-over ducting between the turbines is necessary in addition to the ducting required to take the air and gas to and from the recuperator, so that this arrangement does not represent a truly integrated design. With the turbine shafting arrangement as shown, extreme care in the mechanical design would be necessary to avoid mechanical problems resulting from the thermal gradients likely to be experienced in such an engine with an unsymmetrical structure. The engine consists essentially of three basic modules: the gas-generator section, the power turbine section and the recuperator assembly.

Some of the above designs are not practical from the heat transfer and structural standpoints, but they have been included as a part of the overall configuration study aimed at selecting two configurations for each type of engine installation. Summaries of the above designs for the two types of installation are given in Tables V and VI.

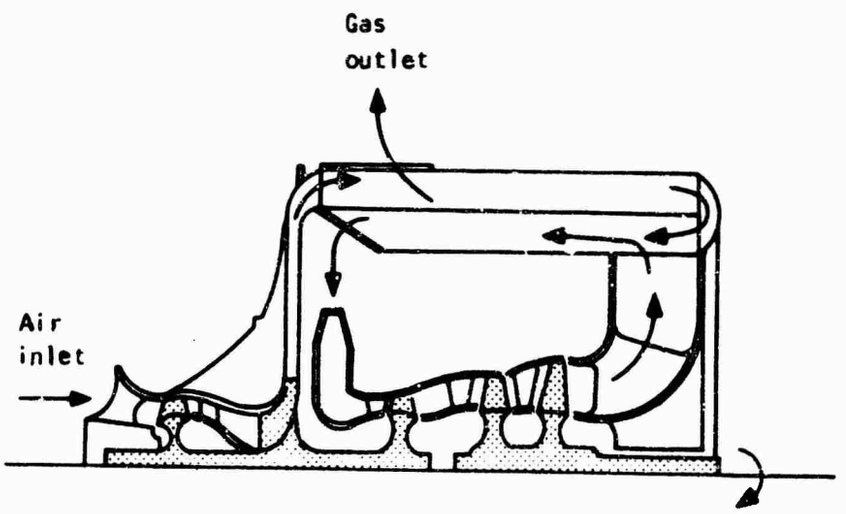

Figure 27. Engine Configuration B-6.

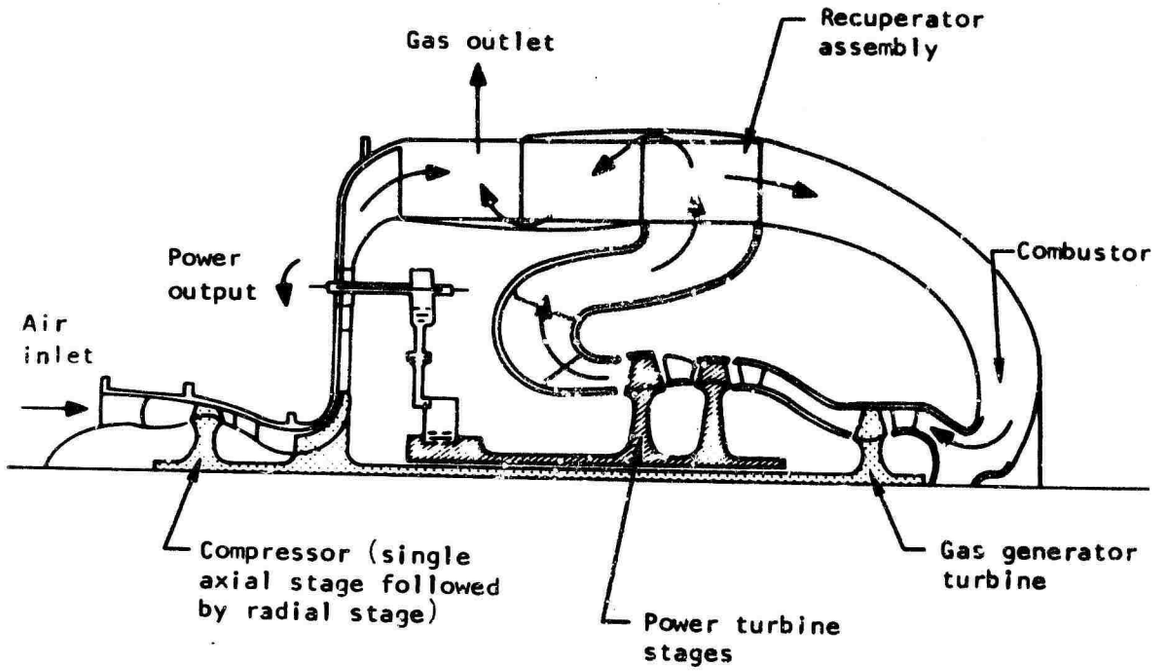

Figure 28. Engine Configuration B-7.

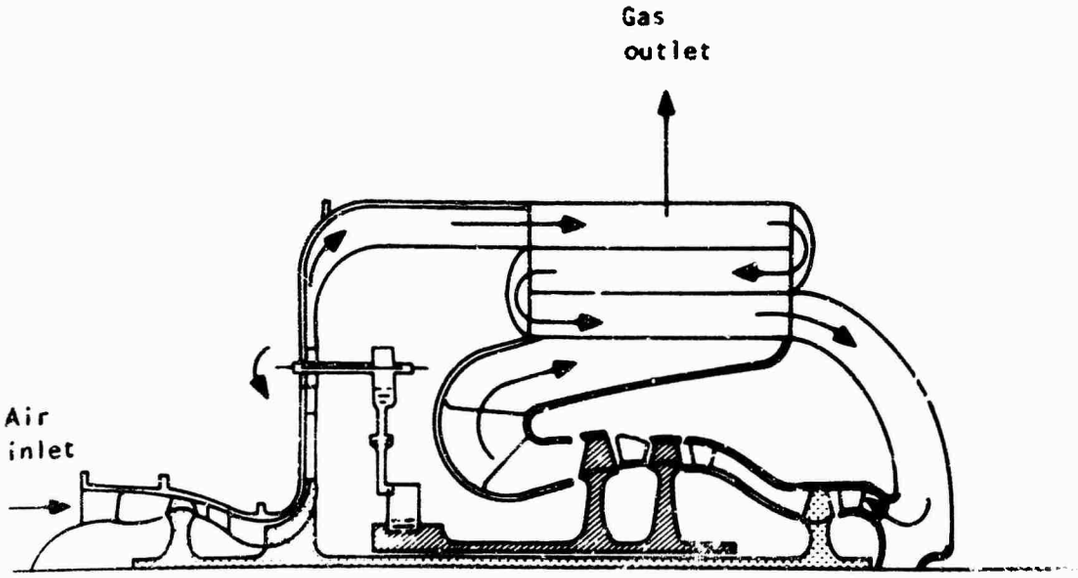

Figure 29. Engine Configuration B-8.

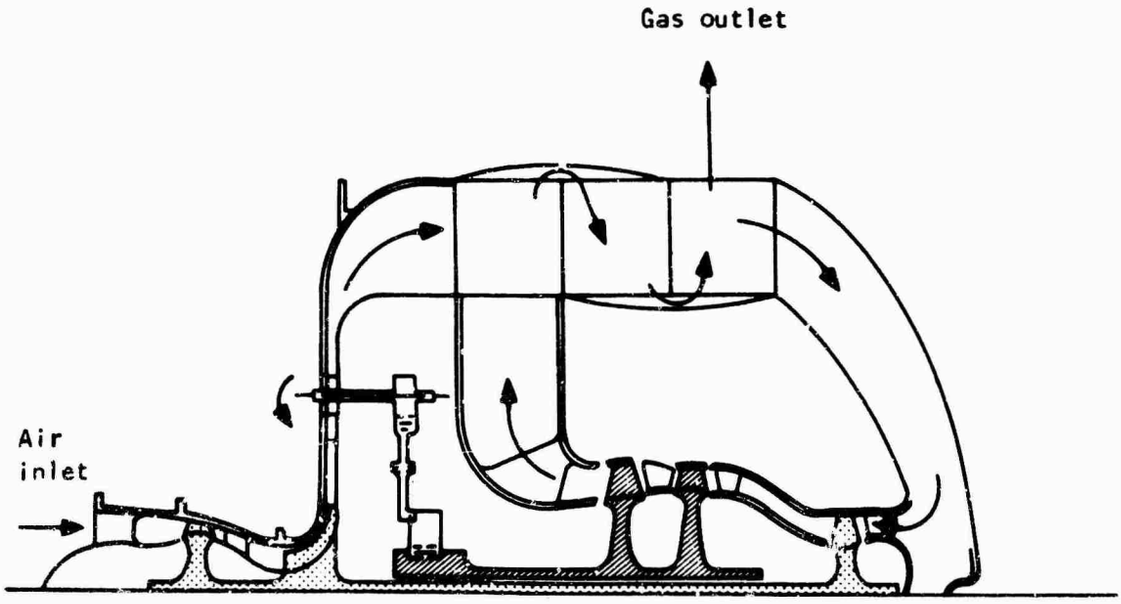

Figure 30. Engine Configuration B-9.

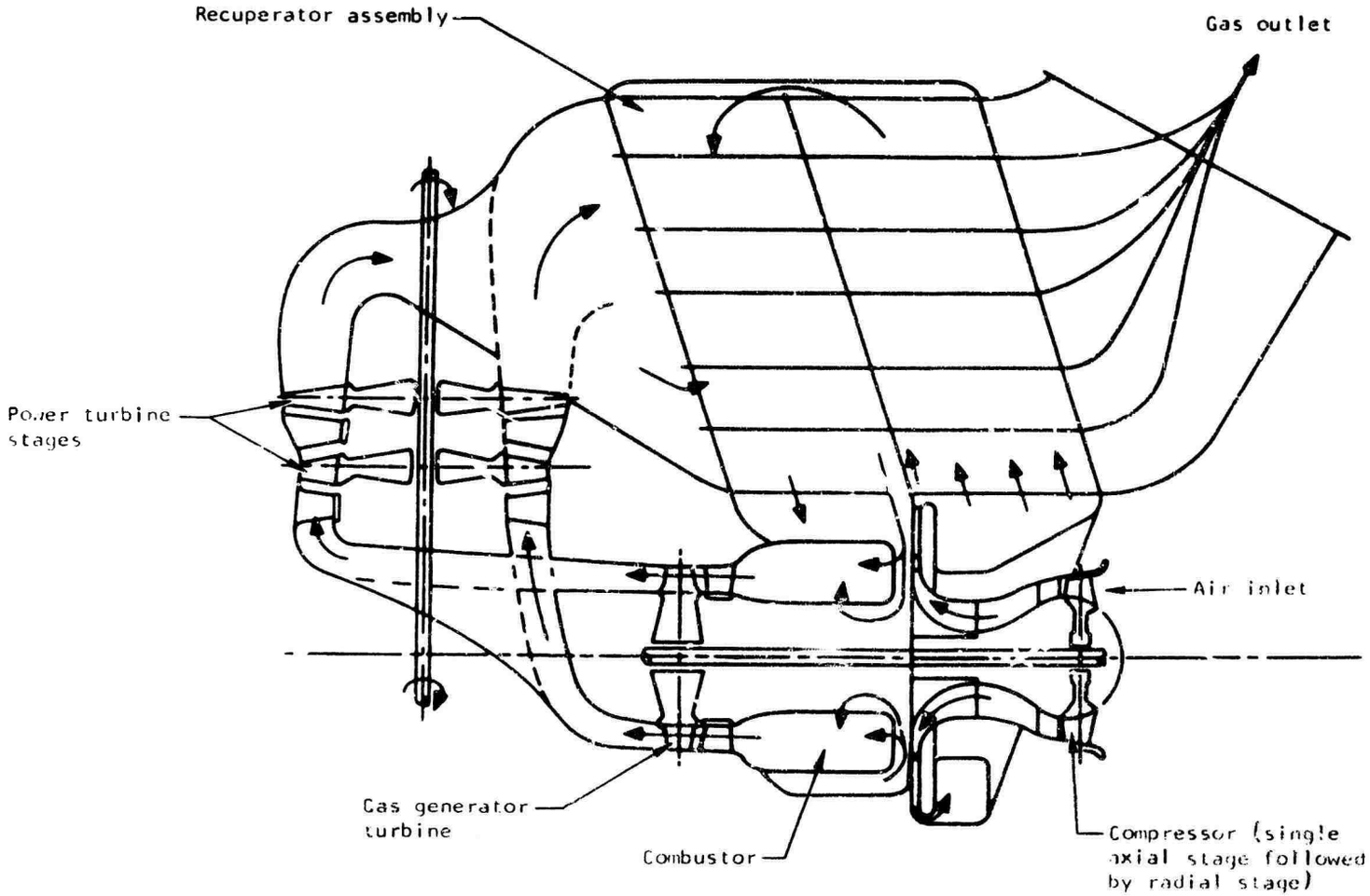

Figure 31. Engine Configuration B-10.

TABLE V. RELATIVE COMPARISON OF RECUPERATIVE ENGINE VARIANTS FOR EXTERNAL INSTALLATION

Engine Configuration	Recuperator Flow Configuration	Heat Transfer Aspects	Structural Aspects	Gas Flow Paths	Degree of Integration with Engine
A-1	Two-pass cross-counterflow	Good	Good	Good	Good
A-2	Three-pass cross-counterflow	Good	Good	Good	Good
A-3	Four-pass cross-counterflow	Fair	Good	Fair	Good
A-4	Two-pass cross-counterflow	Good	Fair	Poor	Poor
A-5	Counterflow	Good	Good	Good	Good
A-6	Counterflow	Good	Good	Good	Good
A-7	Two-pass cross-counterflow	Fair	Poor	Good	Good
A-8	Folded three-pass crossflow	Poor	Poor	Poor	Fair
A-9	Counterflow	Poor	Fair	Fair	Fair
A-10	Parallel flow	Poor	Fair	Poor	Fair
A-11	Two-pass cross counterflow	Fair	Poor	Poor	Poor
A-12	Counterflow	Good	Poor	Poor	Poor
A-13	Two-pass cross-counterflow	Fair	Poor	Poor	Poor
A-14	Folded three-pass Crossflow	Poor	Poor	Poor	Poor
A-15	Three-pass cross-counterflow	Poor	Poor	Poor	Fair
A-16	Three-pass cross-counterflow	Poor	Poor	Poor	Poor

TABLE VI. RELATIVE COMPARISON OF RECUPERATIVE ENGINE VARIANTS FOR INTERNAL INSTALLATION

Engine Configuration	Recuperator Flow Configuration	Heat Transfer Aspects	Structural Aspects	Gas Flow Path	Degree of Integration with Engine
B-1	Two-pass cross-counterflow	Good	Good	Good	Good
B-2	Two-pass cross-counterflow	Good	Good	Good	Good
B-3	Folded three-pass crossflow	Poor	Poor	Poor	Fair
B-4	Two-pass cross-counterflow	Fair	Poor	Good	Good
B-5	Counterflow	Poor	Poor	Poor	Fair
B-6	Two-pass cross-counterflow	Poor	Fair	Fair	Fair
B-7	Three-pass cross-counterflow	Good	Fair	Poor	Poor
B-8	Three-pass cross-counterflow	Good	Fair	Fair	Poor
B-9	Three-pass cross-parallel flow	Poor	Fair	Poor	Poor
B-10	Two-pass cross-counterflow	Fair	Fair	Poor	Poor

SELECTION OF TWO CONFIGURATIONS FOR EXTERNAL INSTALLATION

In studying the various configurations, the most attractive integrated concept appears to be an annuluar recuperator wrapped around the turbomachinery to give a compact package. This concept is structurally desirable in that the recuperator and turbine exit diffuser can be formed as one unit, and any axial or radial forces (either pressure or thermal) can be accommodated satisfactorily. Adding the recuperator to the back of the engine, or utilizing a side-mounted module, necessitates extra ducting and supporting structure and results in heavier weight arrangements that cannot be regarded as truly integrated designs.

In the configurations with the rear-mounted conical combustor, the power turbine is interposed between the compressor and the gas-generator turbine and the output shaft centerline must be offset from the centerline of the rotating assembly. The offset shaft could be replaced with a rear drive by placing the power turbine upstream of the gas-generator turbine. However, with this arrangement it is questionable whether the design values of turbine efficiency could be realized, and part-load performance would be jeopardized because of swirl in the interstage diffuser.

In the bulk of the configurations examined, the turbine output shaft was located at the rear of the engine to obtain a simplified shafting and bearing system. By minimizing the shaft dynamics problem, and by isolating the gas-generator and power-turbine rotating assemblies, it is expected that turbine tip clearance can be kept to a minimum and thus a high level of turbine efficiency can be ensured.

In reviewing the 16 conceptual designs summarized in Table V, configurations A-1, A-2, A-5 and A-6 satisfy the design goals of establishing a compact, integrated engine unit. In these configurations, the proposed engine design concept divides the components into two basic modules.

Configuration A-1

As outlined in the engine performance section of this report, a design was carried out for an engine with a recuperator effectiveness and pressure loss of 0.65 and 6 percent respectively. The flow paths chosen for this reference engine design correspond to configuration A-1, and details of the engine design were shown in Figure 4. The tubular recuperator shown is a two-pass cross-counterflow design with the high pressure air flowing single pass inside the tubes and the low pressure gas flowing two pass across the bundle. The recuperator could be designed with tubular, finned-tube, or plate-fin surface geometries. The high pressure air delivery to the recuperator is by means of an annulus at the engine outer diameter, and this provides a pressure vessel, which, in conjunction with the annular recuperator assembly and power turbine diffuser duct, forms a structure from which the power turbine bearing housing is supported. The exhaust gas exits from the engine in an axial direction through an annulus formed by the turbine diffuser and a flange on the recuperator assembly inner diameter. With the

power turbine shaft drive at the rear of the engine, the exhaust gas must be collected in an annular volute for final discharge to ambient conditions through a single circular or rectangular exhaust duct. No details of the final reduction gearbox have been shown on any of the engineering layouts presented in this report.

Configuration A-2

Details of engine configuration A-2 are shown in Figure 32. To compare engine size with that of configuration A-1, the recuperator has again been sized for the reference engine value of effectiveness and pressure loss (i.e., 0.65 and 6 percent respectively). The tubular recuperator shown is a three-pass cross-counterflow design with the high pressure air flowing single pass inside the tubes and the low pressure gas flowing three pass across the bundle. The recuperator could be designed and built from tubular, finned-tube, or plate-fin type surface geometry. As for the A-1 design, an outer annulus, which is an integral part of the engine structure, is used to deliver air from the compressor discharge to the recuperator inlet. This pressure vessel, in conjunction with the annular recuperator assembly and power turbine diffuser, forms a structure which supports the power turbine bearing housing. The exhaust gas exits from the recuperator through a series of radial ducts fabricated within the air delivery annulus. The geometry of these ducts would be optimized to give minimum flow area blockage within the air delivery annulus. After exiting from the recuperator, the exhaust gas is collected in an annular scroll for final discharge to ambient conditions through a single circular or rectangular exhaust duct.

Configurations A-5 and A-6

Details of engine configurations A-5 and A-6 are shown in Figures 10 and 11. The two designs are both pure counterflow variants and differ only as regards the flow pattern in the mitered end sections. Unlike configurations A-1 and A-2, which could be designed and built from tubular, finned-tube, or plate-fin type surface geometry, configurations A-5 and A-6 are limited to plate-fin construction only. With this limiting feature, it is concluded that configurations A-1 and A-2 are the most attractive for the external engine installation.

SELECTION OF TWO CONFIGURATIONS FOR INTERNAL INSTALLATION

As for the external installation, the most attractive concept to achieve the desired goal of a fully integrated, compact, lightweight package appears to be an annular recuperator wrapped around the turbomachinery. Since the same basic turbomachinery arrangement is utilized, the various comments given in the previous section on mechanical aspects and engine modulization for the external installations also apply to the selected internal installations. In reviewing the ten conceptual designs summarized in Table VI, configurations B-1 and B-2 satisfy the design goals of establishing a compact, integrated, lightweight engine unit.

A

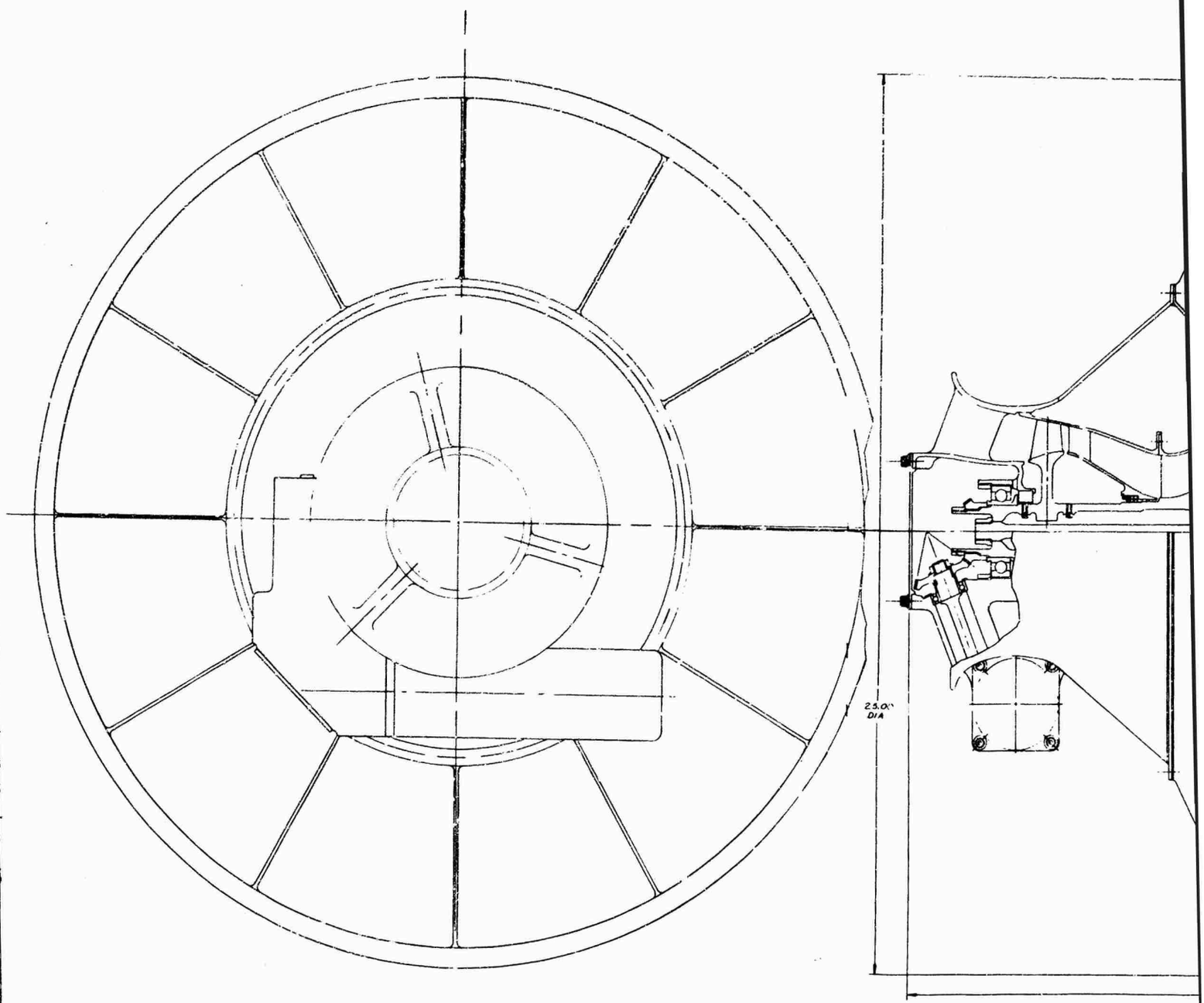

Figure 32. Engine Configuration A-2.

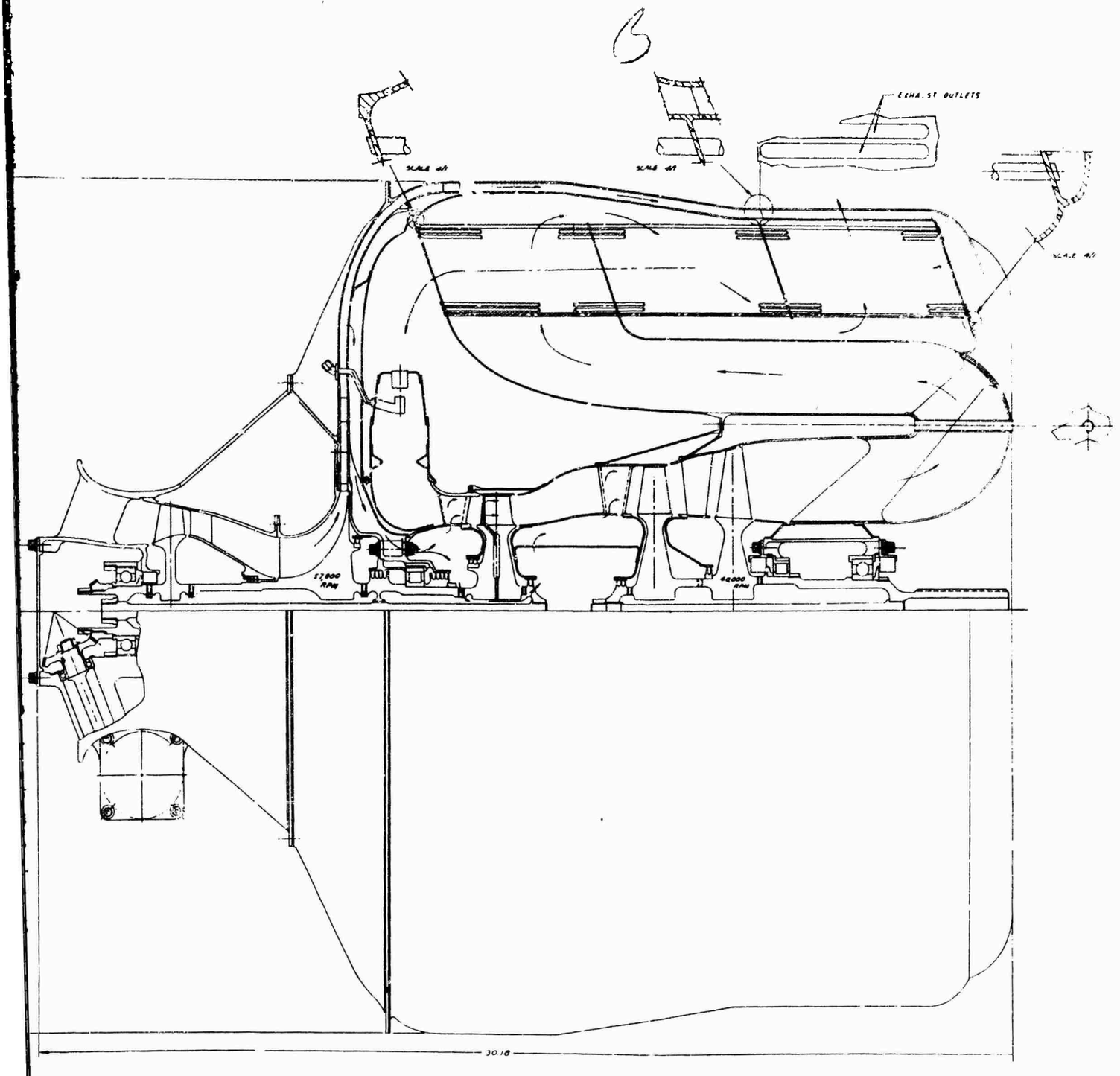
6
EXHA. ST OUTLETS
SCALE 4/1
SCALE 4/1
SCALE 4/1
57,000 RPM
42000 RPM
3018

Configuration B-1

Details of engine configuration B-1 are shown in Figure 33. To compare engine size with the sizes of the other configurations, the recuperator has been sized for the reference engine value of effectiveness and pressure loss (i.e., 0.65 and 6 percent respectively). The tubular recuperator shown is a two-pass cross-counterflow design with the high pressure air flowing single pass inside the tubes and the low pressure gas flowing three pass across the bundle. Thermodynamically, the basic flow path is the same as for the A-1 engine configuration. The recuperator could be designed and built from tubular, finned-tube, or plate-fin type surface geometry. After leaving the compressor diffuser, the air flows directly into the recuperator core and passes through the tubes in a single pass. After leaving the recuperator core, the air is turned through 180 deg in a duct formed by the turbine exit diffuser assembly. The power turbine stators are supported by two members which are bolted to a flange on the recuperator inner ducting. Elliptical ports are formed in these members to allow the heated air from the recuperator to flow back into the combustor. Additional seals are required after each of the power turbine stages to prevent the leakage of high pressure air directly into the turbine duct. The power turbine bearing housing is supported by a structure formed from the turbine exit diffuser, connected through a series of struts to the recuperator inner diameter. After exiting from the recuperator, the exhaust gas is collected in an annular scroll for final discharge to ambient conditions through a single circular or rectangular exhaust duct.

Configuration B-2

Details of engine configuration B-2 are shown in Figure 34. To compare engine size with that of configuration B-1, the recuperator has been sized for the reference engine value of effectiveness and pressure loss (i.e., 0.65 and 6 percent respectively). The tubular recuperator shown is a two-pass cross-counterflow design, with the high pressure air flowing two pass inside the tubes and the low pressure gas flowing single pass across the bundle. The high pressure, low temperature air flows toward the rear of the engine in the outer pass of the annular tube bundle. A simple turnaround pan is used to turn the air back through 180 deg into the second pass of the recuperator. The recuperator could be designed and built from tubular, finned-tube, or plate-fin type surface geometry. The power turbine stators are supported by two structural members which are bolted to a flange on the recuperator assembly. The power turbine bearing housing is supported by a structure formed from the turbine exit diffuser, connected through a series of struts to the recuperator assembly. After exiting from the recuperator, the exhaust gas is collected in an annular scroll for final discharge to ambient conditions through a single circular or rectangular exhaust duct.

SUMMARY OF CONFIGURATION STUDY

The same basic turbomachinery elements have been used in each of the four recuperative engine configurations chosen. A direct size comparison of the

four designs can be made since the recuperators were all sized for the same effectiveness and pressure loss and thus have the same power and specific fuel consumption.

In all four cases, the output shaft was located at the rear of the engine to obtain a simplified bearing system, consistent with the goal of establishing a series of truly integrated turbomachinery-recuperator engine designs. In each case, the accessories are driven from the front end of the gas generator shaft. Starter, fuel control, fuel pump, and oil pump are all sized to operate at 30,000 rpm. A considerable reduction in weight is realized both in the accessories and in the accessory drive components by allowing this relatively high rotative speed.

In each of the configurations selected, the simplicity of engine disassembly has been emphasized, particularly the fact that the gas-generator and power turbine sections can be separated by the removal of bolts from one flange only. The recuperator assembly can then be rapidly separated from the power turbine assembly. With the recuperator wrapped around the turbomachinery to give a compact, integral unit, additional secondary benefits can be realized. One bullet could severely damage a simple cycle engine, but the heat exchanged variant is less vulnerable because the recuperator protects the rotating components; even with local damage in the matrix, resulting in loss of performance, the helicopter could still fly back to base. With the configurations proposed, the heat exchanger will provide turbine self-containment and should reduce the noise level compared with existing designs.

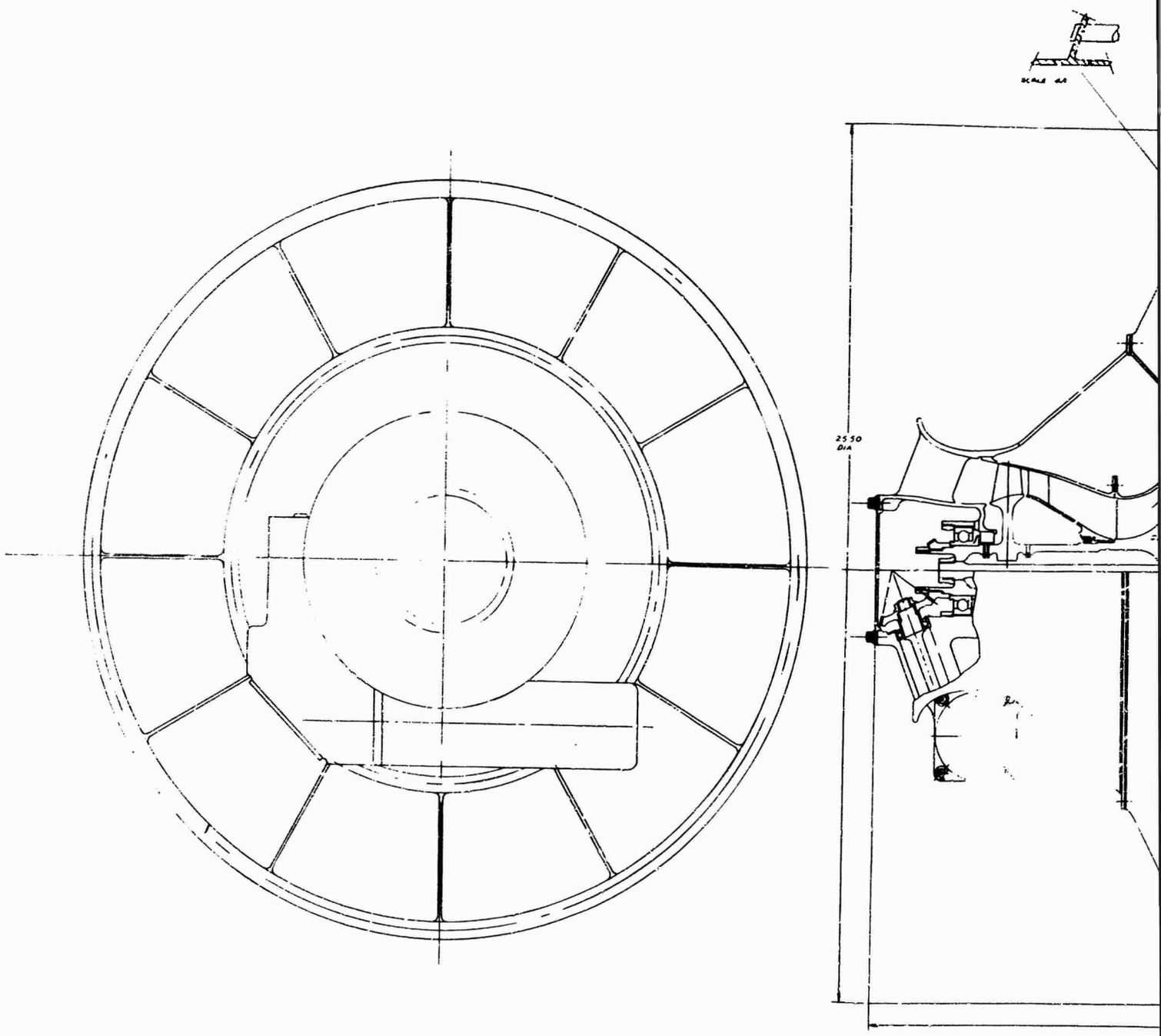

Figure 33. Engine Configuration B-1.

B

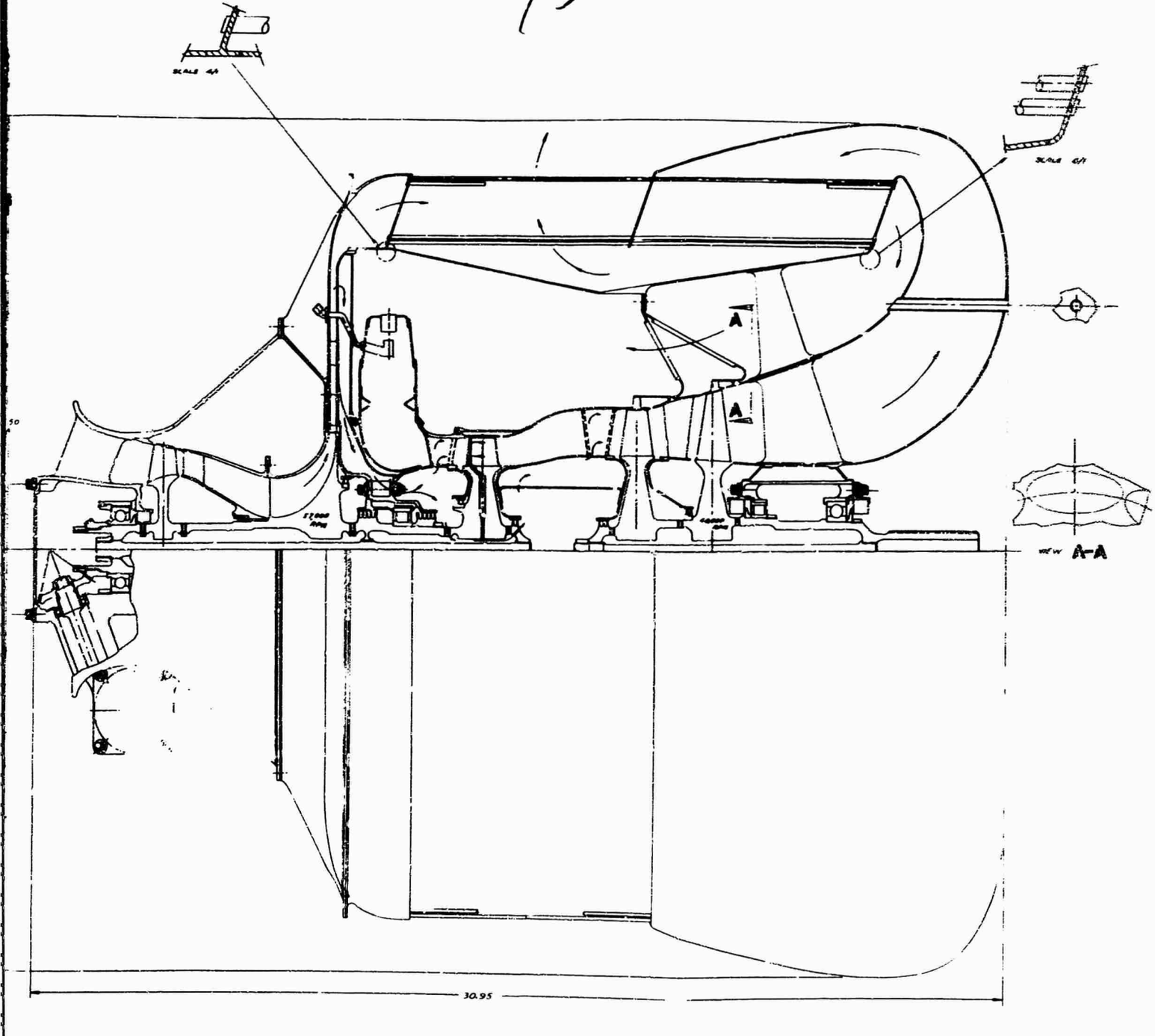

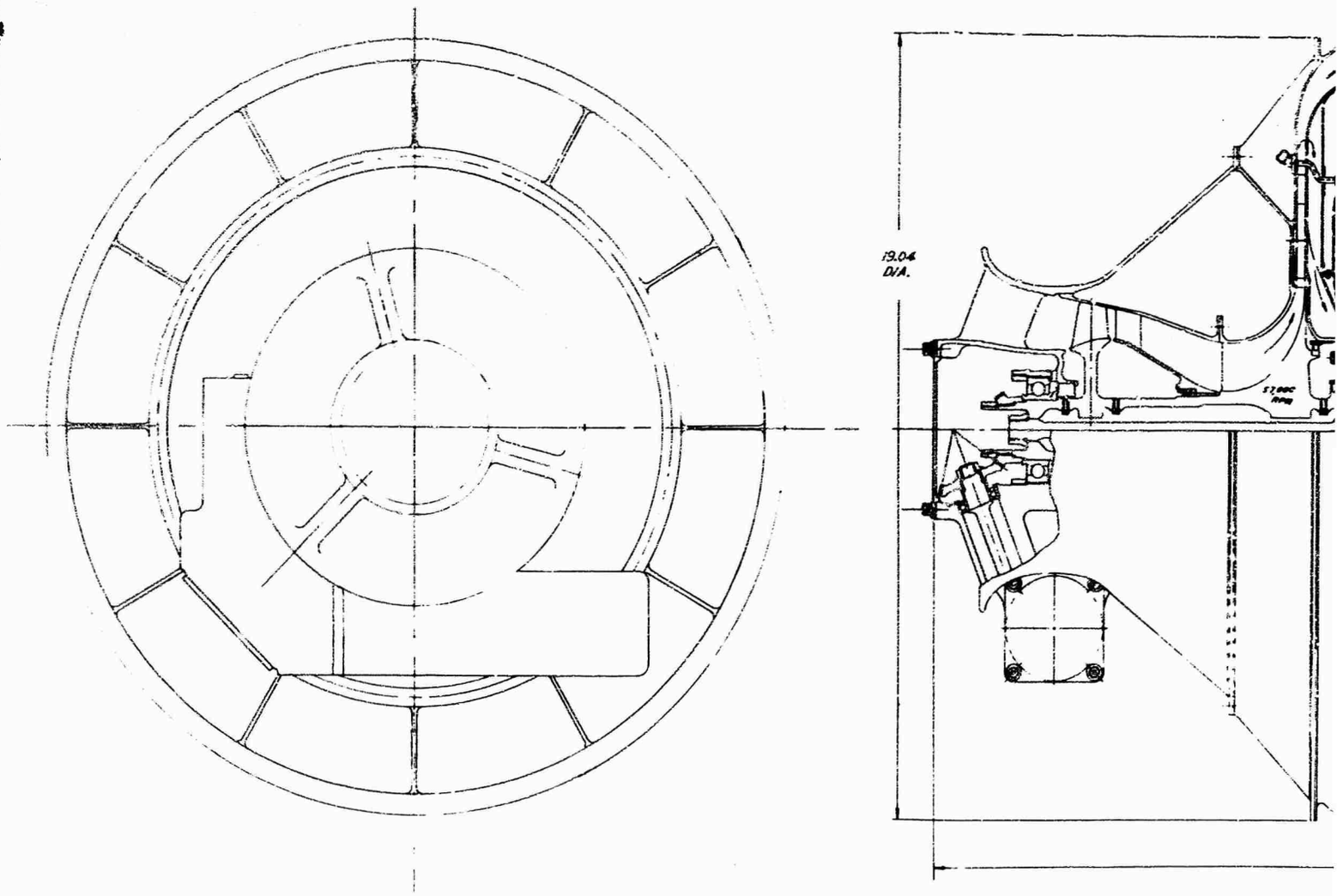

Figure 34. Engine Configuration B-2.

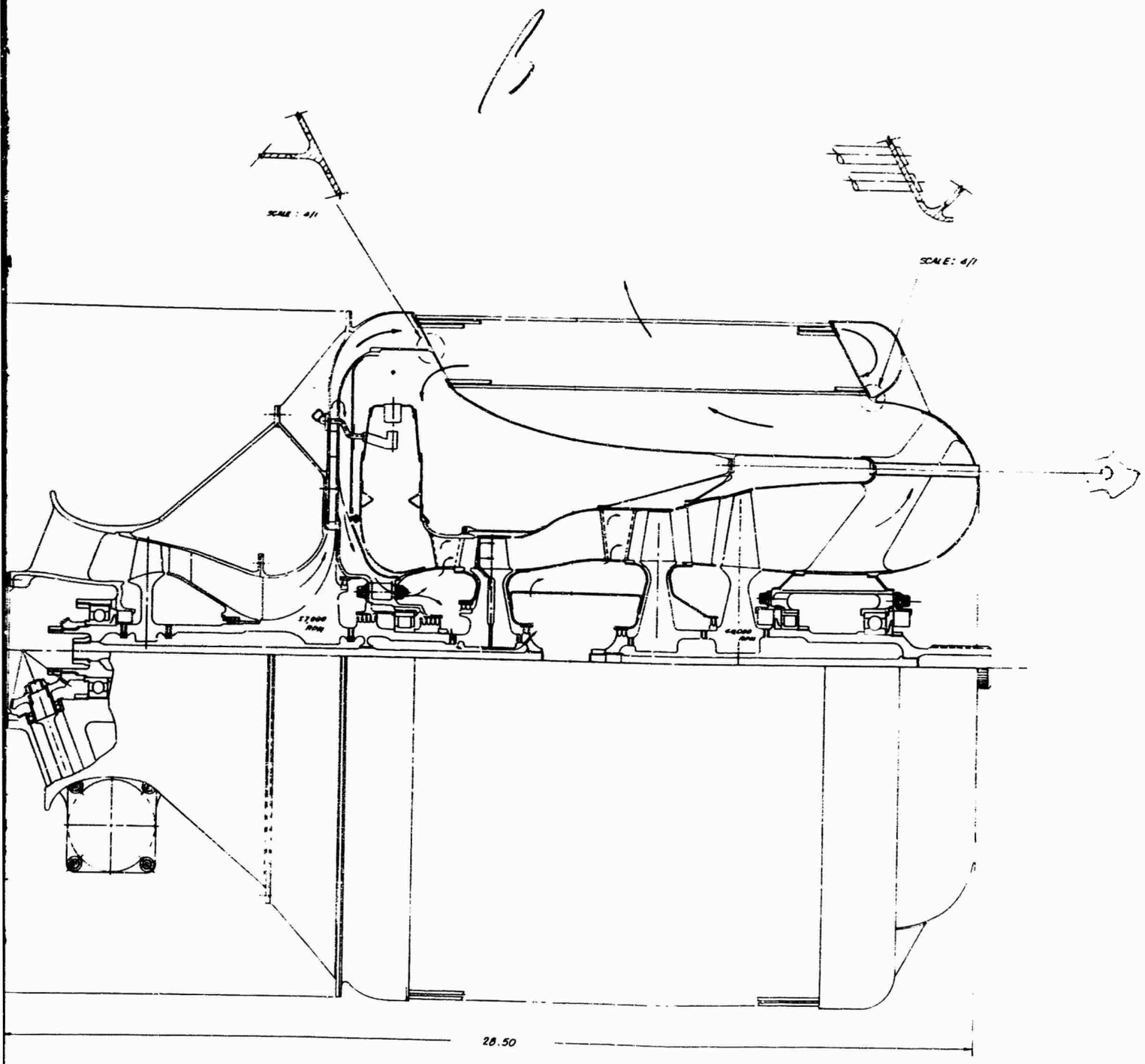
SCALE : 4/1
SCALE: 4/1
28.50

RECUPERATOR PARAMETRIC STUDY

ENGINE CYCLE DATA

Data generated during the engine performance calculations were used in the recuperator analysis. The mass flow rates used in the turbine and recuperator analysis are given below:

Compressor discharge flow	5.00 lb/sec
Turbine nozzle and blade cooling airflow	3.5%
Leakage at compressor exit	1.5%
Recuperator inlet (cold side)	5.0 $(1.5\% W_L + 3.5\% W_C)$ = 4.75 lb/sec
Gas generator turbine inlet	4.75 + $(2\% W_F)$ = 4.85 lb/sec
Power turbine inlet	4.85 = $(3\% W_C$ reentered) = 5.00 lb/sec
Recuperator inlet (hot side)	5.00 lb/sec

Temperature and pressure data used in the recuperator parametric study are given in Table VII. Based on the reference engine conditions, with an effectiveness and pressure loss of 0.65 and 6 percent respectively, an engine fuel/air ratio of 0.02 was computed. Throughout the study, the fluid properties on the recuperator gas side were taken to be those associated with the 0.02 fuel/air ratio value.

In the recuperator analysis, account was taken of the pressure loss in the ducting of the air and gas to and from the recuperator core faces. The recuperator pressure loss values quoted throughout the study refer to the total loss associated with the core and ducts. An air side pressure loss from the compressor diffuser exit to the recuperator air inlet face of 0.25 percent was assumed. A gas side pressure loss from the recuperator outlet face to the engine exhaust outlet of 0.50 percent was assumed. In the engine cycle analysis, a gas side pressure loss from the power turbine exit to the recuperator gas inlet face of 4.0 percent was assumed, but this is not included as a part of the recuperator pressure loss. With the integrated recuperator concept, no additional ducting is required from the recuperator air side exit to the combustor inlet; thus, no pressure loss is assumed to occur between these stations.

TABLE VII. DATA USED IN RECUPERATOR PARAMETRIC STUDY

Recuperator Pressure Loss ($\Delta P/P$), percent	2	4	6	8	10
Airflow, lb/sec	4.75	4.75	4.75	4.75	4.75
Gas Flow, lb/sec*	5.00	5.00	5.00	5.00	5.00
Recuperator Air Inlet Temperature, °R	1061.5	1061.5	1061.5	1061.5	1061.5
Recuperator Gas Inlet Temperature, °R	1776.6	1783.9	1791.7	1799.5	1807.4
Recuperator Air Inlet Pressure, psia**	131.95	131.95	131.95	131.95	131.95
Recuperator Air Outlet Pressure, psia	131.20	130.14	129.09	128.03	126.97
Recuperator Gas Inlet Pressure, psia***	14.87	15.05	15.24	15.43	15.63
Exhaust Gas Outlet Pressure, psia****	14.69	14.69	14.69	14.69	14.69

*Fluid properties on the recuperator gas side taken to be those associated with a fuel/air ratio of 0.02

**Air side pressure loss from compressor diffuser exit to recuperator air inlet face assumed to be 0.25 percent

***Gas side pressure loss from power turbine exit to recuperator gas inlet face assumed to be 4.0 percent

****Gas side pressure loss from recuperator outlet face to ambient assumed to be 0.5 percent

RANGE OF VARIABLES USED IN ANALYSIS

In the heat transfer analysis, the following range of recuperator parameters was evaluated:

Effectiveness, ε	0.40, 0.50, 0.60, 0.65, 0.70, 0.80, 0.90
Pressure Loss $(\Delta P/P)$, %	2.0, 4.0, 6.0, 8.0, 10.0

The recuperator effectiveness is defined as

$$\varepsilon = \frac{(W.C_P)_{AIR} (T_{OUT} - T_{IN})_{AIR}}{(W.C_P)_{MIN} (T_{IN\ GAS} - T_{IN\ AIR})}$$

where W = Mass flow rate

C_P = Specific heat

T = Total temperature

The recuperator pressure loss $(\Delta P/P)$ is defined as

$$\left(\frac{\Delta P}{P}\right) = \left(\frac{\Delta P_{AIR}}{P_{AIR\ IN}}\right) + \left(\frac{\Delta P_{GAS}}{P_{GAS\ OUT}}\right)$$

where the air side and gas side pressure losses include those incurred in the heat exchanger ducting as well as in the matrix.

Another variable considered in the heat exchanger analysis was the effect of the recuperator pressure loss split $(\Delta P/P)_{GAS}/(\Delta P/P)_{AIR}$. For each surface geometry examined, a series of solutions was run to find the pressure loss split that gave a minimum weight recuperator core. The following range of pressure loss splits was considered:

Pressure Loss Split $(\Delta P/P)_{GAS}/(\Delta P/P)_{AIR}$,	90/10, 80/20, 70/30, 60/40, 50/50, 40/60

For each combination of effectiveness and pressure loss, the corresponding fluid temperatures and pressures from Table VII were factored into the recuperator analysis.

FLOW CONFIGURATIONS EVALUATED

For the configuration study, it was concluded that the most attractive engine arrangements from the standpoint of minimum envelope volume could be realized by wrapping the recuperator around the turbomachinery in such a manner that the heat exchanger becomes a part of the engine prime structure. With this integrated concept, there is still a degree of freedom as regards recuperator internal flow configuration.

From the tubular core geometries, two-, three-, and four-pass cross-counterflow arrangements were examined and consideration was given to both the air and the gas as the multipass fluid. A similar analysis was carried out for the finned-tube core geometries.

For the plate-fin core geometries, a counterflow arrangement was examined in addition to the two-, three-, and four-pass cross-counterflow configurations. Multipassing the gas side only was considered for the plate-fin cross-counterflow cases.

TUBULAR SURFACE GEOMETRY EVALUATION

For the effectiveness and pressure loss range outlined above, a variety of tubular surface geometries of the type shown in Figure 35a was considered in the recuperator parametric study. The following variables have been used in the analysis.

Flow Configurations

Two-pass cross-counterflow (AIT* one pass, EOT** two pass)

Two-pass cross-counterflow (AIT two pass, EOT one pass)

Three-pass cross-counterflow (AIT one pass, EOT three pass)

Four pass cross-counterflow (AIT one pass, EOT four pass)

*Air inside tube

**Exhaust outside tube

All four engine configurations chosen have the high pressure air inside the tubes and the exhaust gas outside the tubes. This arrangement results in lightweight designs, since the inside Reynolds number is in a range where ring-dimpling of the tube wall provides an effective means of increasing the inside heat transfer coefficient. Since the exhaust gas is the lower pressure fluid, lighter weight recuperators generally result with the exhaust gas outside the tubes because, in additon to the above heat transfer considerations, the shell weight will be lower and the tubes will have thinner walls when loaded in tension with internal pressure than when loaded in compression with external pressure.

Tube Sizes

A fairly wide range of tube diameters has been considered as outlined below.

Tube outer diameter, 0.075, 0.10, 0.125, 0.15, 0.20, 0.25 in.

Tube wall thickness of 0.004 in. was used in heat transfer analysis

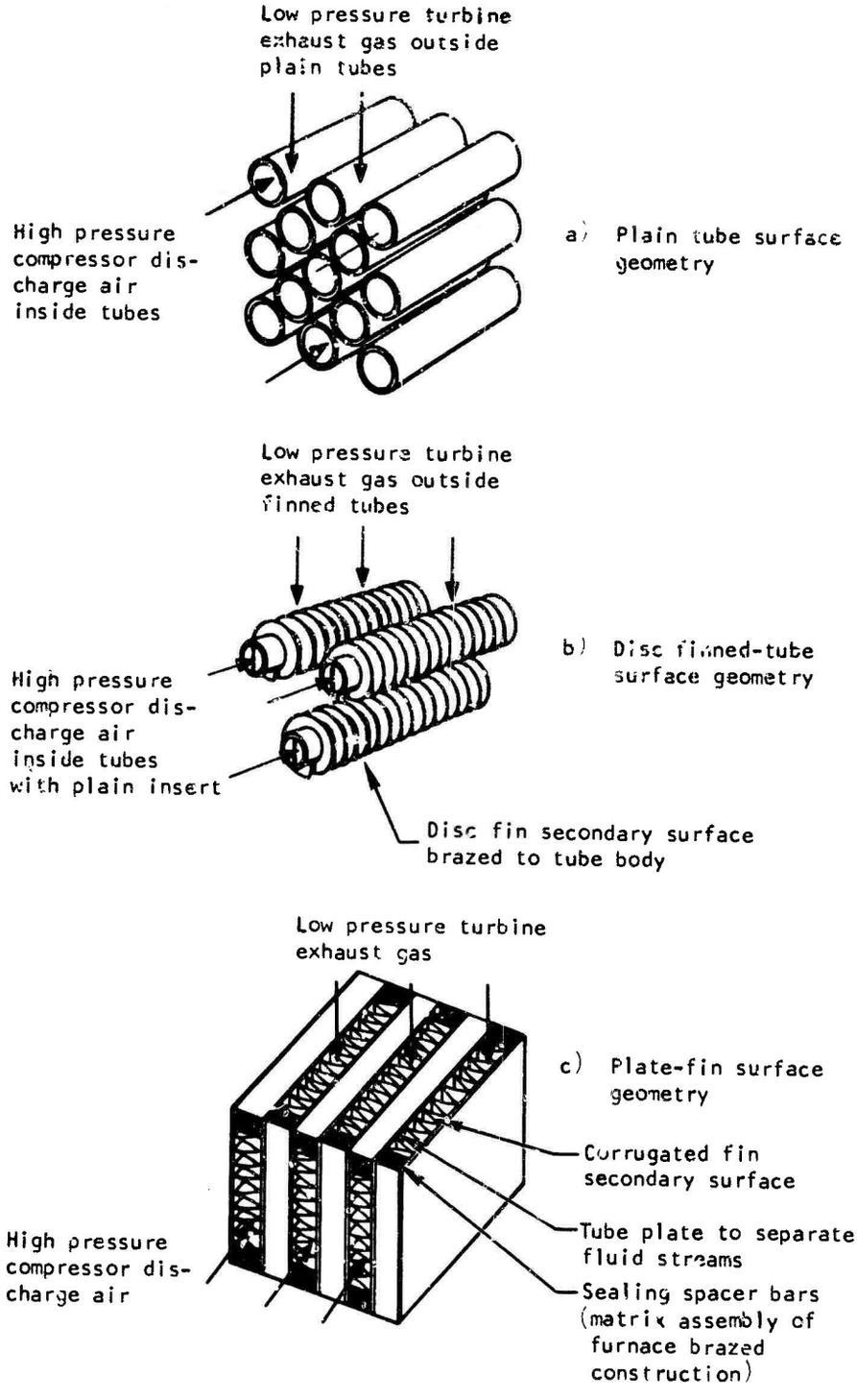

Figure 35. Typical Recuperator Surface Geometries

In the range of thicknesses being considered (0.0035 - 0.006 in.), the effect of tube wall thickness on matrix volume for a tubular design is insignificant, but the effect on weight and cost is important; this will be discussed in a later section when optimum solutions have been established.

Tube Inside Surface Geometry

To achieve a balance of heat transfer conductances between inside and outside tubular surfaces, some form of internal turbulator is usually employed, since the heat transfer coefficient for flow inside plain (nonturbulated) tubes is several times less than the coefficient for flow outside an optimized tube bundle. The best type of internal turbulator, (one that maximizes the ratio of heat transfer conductance to fluid pumping power) was found to be ring-dimpling of the tube wall. This was determined during a previous program in which extensive heat transfer and pressure loss tests were conducted for a number of tube surfaces of the type shown in Figure 36, including smooth, ring-dimpled, venturi-shaped ring-dimpled, roughened ring-dimpled, knurled, locally (spot) dimpled (spiral and ring) spiral-dimpled, external (outward) ring-dimpled, and others. The results of these tests were compared on the basis of thermal conductance versus friction power. The use of an internal strip turbulator is also a possibility but is advantageous only for Reynolds numbers below about 1500, where tube wall dimpling is ineffective in promoting turbulence.

AiResearch bases its dimpled tube design data on the heat transfer and pressure loss tests mentioned above. These tests were conducted over a Reynolds number range from 1,000 to 40,000 for a wide range of tube and dimple geometries. The results are correlated with a single geometry parameter, involving dimple depth, dimple spacing, and tube diameter, so that the friction factor and Colburn modulus for flow in dimpled tubes are obtained as a function of the Reynolds number and ψ only. Details of the ring dimple geometry used in the tubular recuperator analysis are shown in Figure 37a. Values of the dimple parameter ψ used in the analysis are given below.

Dimple Parameter ψ 0 (plain tube) 0.02, 0.04, 0.06, 0.08

Dimple Parameter defined as $= (\delta/d)\sqrt{s/d}$

where δ = dimple depth

d = tube inner diameter

s = dimple pitch

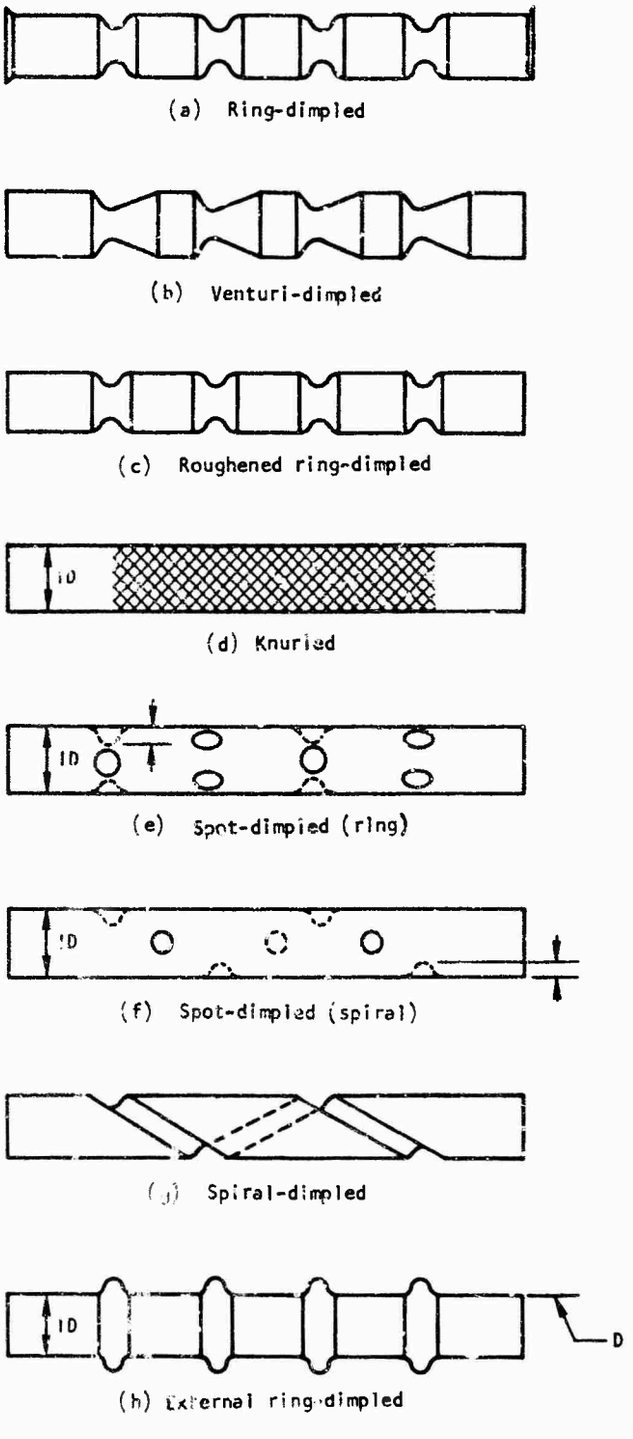

Figure 36. Tube Dimple Geometries.

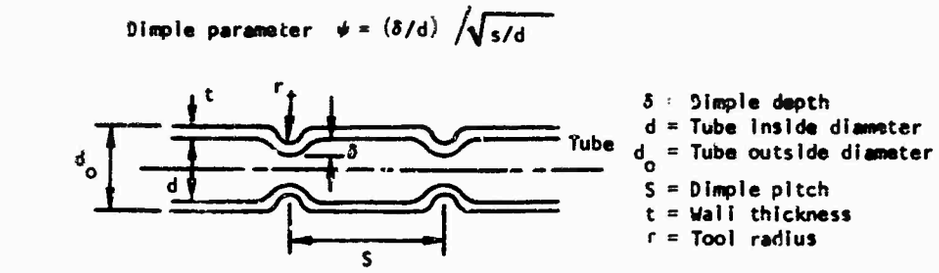

a) Ring dimple tube geometry

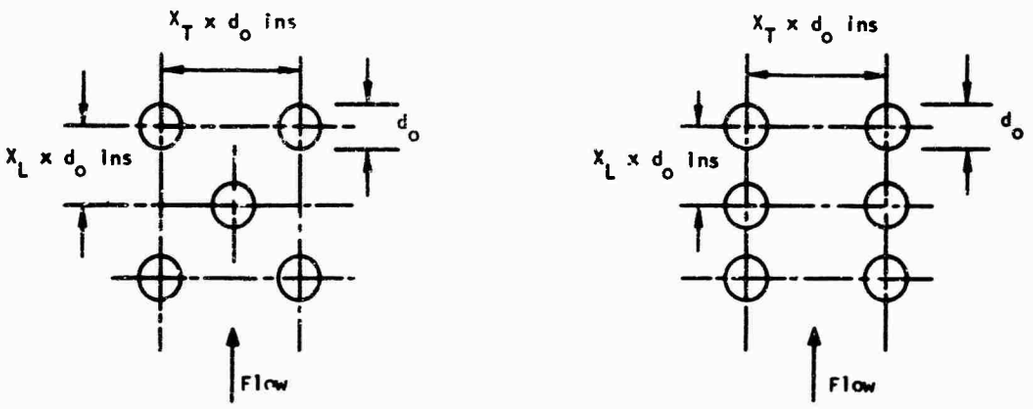

Staggered tube bundle (SB)

In-line tube bundle (IB)

d_o = Tube outside diameter

X_T = Transverse pitch as defined in sketch

X_L = Longitudinal pitch as defined in sketch

Terminology used in recuperator parametric study is illustrated by the four following examples:

SB 300100 - Staggered tube bundle $X_T = 3.00$, $X_L = 1.00$

IB 200125 - In-line bundle $X_T = 2.00$, $X_L = 1.25$

PLNTD - Plain tube diameter

DMP - Dimple

b) Tube outside surface geometries

Figure 37. Plain Tube Surface Geometries.

Outside Tube Geometries

Both staggered tube and in-line tube arrangements have been considered in the analysis, and details of the tube patterns are shown in Figure 37b. In the analysis the following values of longitudinal and transverse tube pitches were used:

Longitudinal tube pitch X_L = 1.00 (staggered tube rows)

Longitudinal tube pitch X_L = 1.24, 1.25, 2.00 (in line tubes)

Transverse tube pitch X_T = 1.50, 1.70, 2.00, 2.40, 2.70, 3.0 (staggered tube rows)

Transverse tube pitch X_T = 1.24, 1.50, 2.00 (in line tubes)

Heat transfer and pressure drop performance for flow outside of staggered and in-line tube matrices is based on AiResearch test data compiled on a series of close-packed cores in conjunction with data available from the literature, for several other matrix geometries. Considerations of geometric and dynamic similarity allow these data to be applied to a wide range of staggered and in-line tube geometries.

For each of the four engine configurations, extensive use was made of a computer program written for designing multipass tubular heat exchangers. In this program multipass cross-counterflow and multipass cross-parallel flow, tubular two-fluid heat exchangers are defined by an iteration procedure. Any fluid combination of liquids and gases can be utilized. The friction factor and Colburn modulus data for both inside and outside tubes are available in the form of Lagrangian tables. The outside of the tubes can either be plain or have circular disc fins or continuous-strip fins. The inside of the tubes can be plain, dimpled, or have internal fins or turbulators. Input parameters required include effectiveness, pressure drop, inlet temperatures and pressures, and the weight flow rate of the two fluids. Fluid properties, with the exception of the specific heats in the heat balance calculation, are evaluated at average film temperature. Core fluid velocity is evaluated at the bulk average temperature. Allowances for shock and turning losses are made as specified multiples of the core velocity head. Momentum pressure losses associated with change of flow area from the ducts to the heat exchanger face are also calculated. Gas density is calculated on the basis of the perfect gas law and compressibility factors are used. Multipassing can be accomplished either inside or outside of the tubes. Surface input information required includes the tube diameter, the internal surface (dimple detail, etc), the transverse and longitudinal tube pitch, all material thicknesses, the number of passes, tube material density and thermal conductivity, and the tube bundle configuration.

The important outputs from the program include tube bundle inner and outer diameters, tube number, tube length, and tube weight. Naturally all of the combinations of surface geometries did not give practical heat exchanger sizes and weights. From the thousands of computer solutions generated for

each engine configuration, a series of designs was selected and the data plotted. The initial analysis was aimed at establishing the optimum recuperator pressure loss split to give minimum weight solutions. Engine configurations A-1 and B-1 have identical recuperator flow paths (i.e., AIT one pass and EOT two pass), and a survey of the effect of pressure loss split on tube weight over a range of effectiveness and pressure loss for these configurations is shown in Figure 38. At the high levels of effectiveness, with a low pressure loss allowance, the tube weight is quite sensitive to the recuperator pressure loss split. At the low levels of effectiveness, the pressure loss split has a very small effect on tube weight. From this curve array, it has been concluded that practical designs close to minimum weight could be achieved with a recuperator pressure loss split $(\Delta P/P)_{GAS}/(\Delta P/P)_{AIR}$ of 60/40 [i.e., $(\Delta P/P_{GAS} = 1.5\ (\Delta P/P)_{AIR}$]. This value has been used throughout the tubular recuperator study

During the initial analysis, it was observed that the core sizes and weights at the 90 percent effectiveness level were excessively large. Even with the smallest hydraulic diameter surfaces and most compact tube spacings considered in this study, the minimum core weights were still in the order of hundreds of pounds, and the tube bundle dimensions were large and incompatible with the turbomachinery. For realistic designs, an upper limit on effectiveness of 80 percent has been used on the graphical plots, although computer solutions up to the 90 percent effectiveness level were obtained as a part of the parametric study.

For the A-1 and B-1 configurations, which thermodynamically have the same flow pattern, staggered tube patterns were used and both two-pass and four-pass cross-counterflow arrangements were evaluated with the compressor discharge air as the single-pass fluid and the turbine exhaust gas as the multipass fluid. With the four-pass cross-counterflow arrangements, it was found that less compact surfaces had to be utilized because of the small pressure loss allowance; this resulted in a weight and volume penalty compared with the two-pass arrangements. At the 90 percent effectiveness level, the four-pass designs showed smaller core sizes and weights, but the units were extremely large and incompatible with the turbomachinery. In the graphical presentation of the recuperator parametric data, only the two-pass cross-counterflow solutions are shown. The salient core dimensions for a series of selected staggered tube surface geometries are shown in Figure 39. The selected designs for the B-1 and A-1 engine configurations at the reference engine conditions (effectiveness = 0.65 and pressure loss = 6 percent) are shown respectively on pages 71 and 73.

The design of the A-2 configuration is based on a three-pass cross-counterflow arrangement; to achieve minimum weight solutions that were compatible with the turbomachinery, it was necessary to utilize in-line tube patterns. The heat transfer characteristics of this tube pattern are inferior to those associated with the staggered tube bundle, but the inherently lower friction factor means that the surface compactness of the

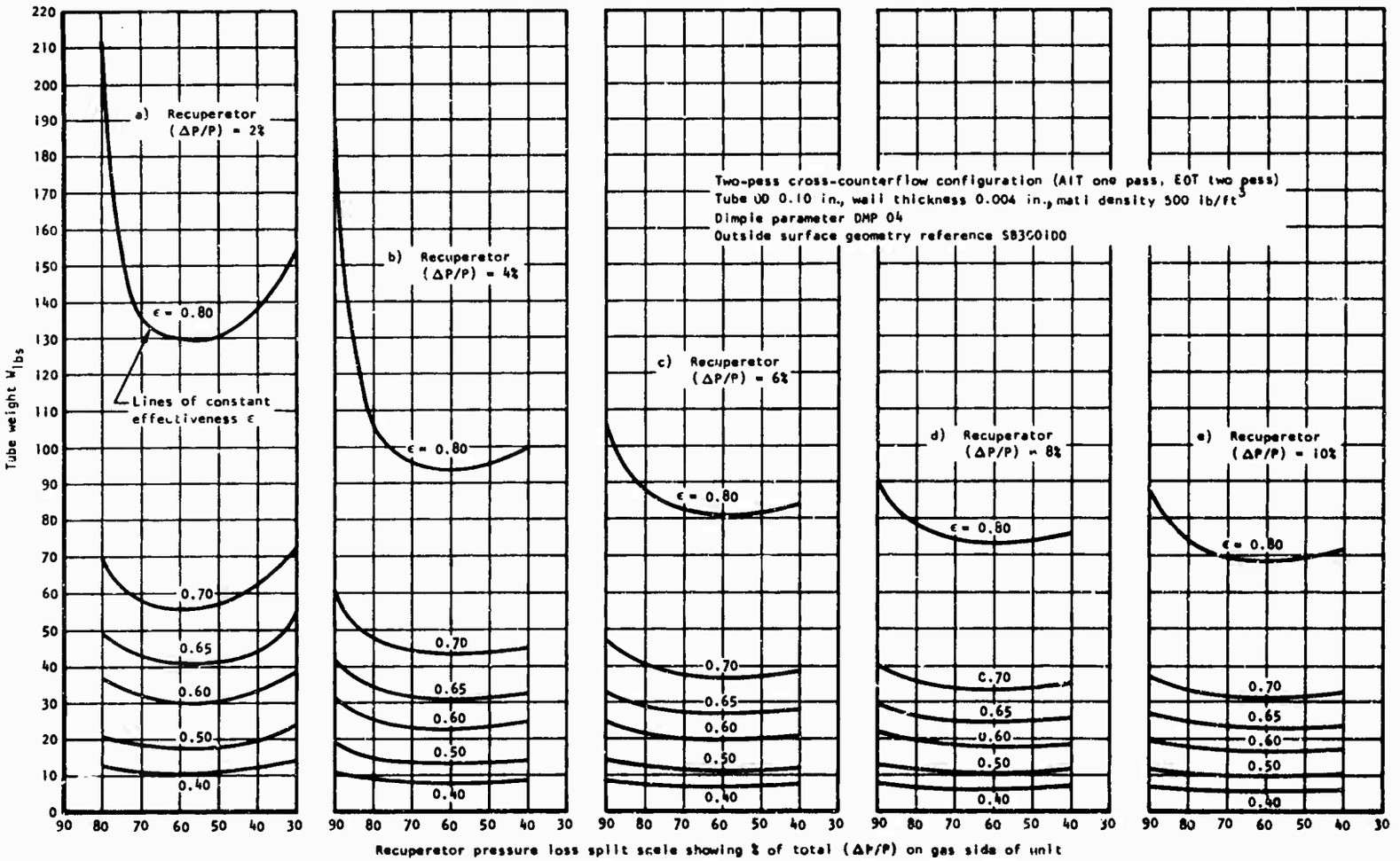

Figure 38. Effect of Pressure Loss Split on Weight for a Tubular Recuperator Over a Range of Effectiveness and Pressure Loss.

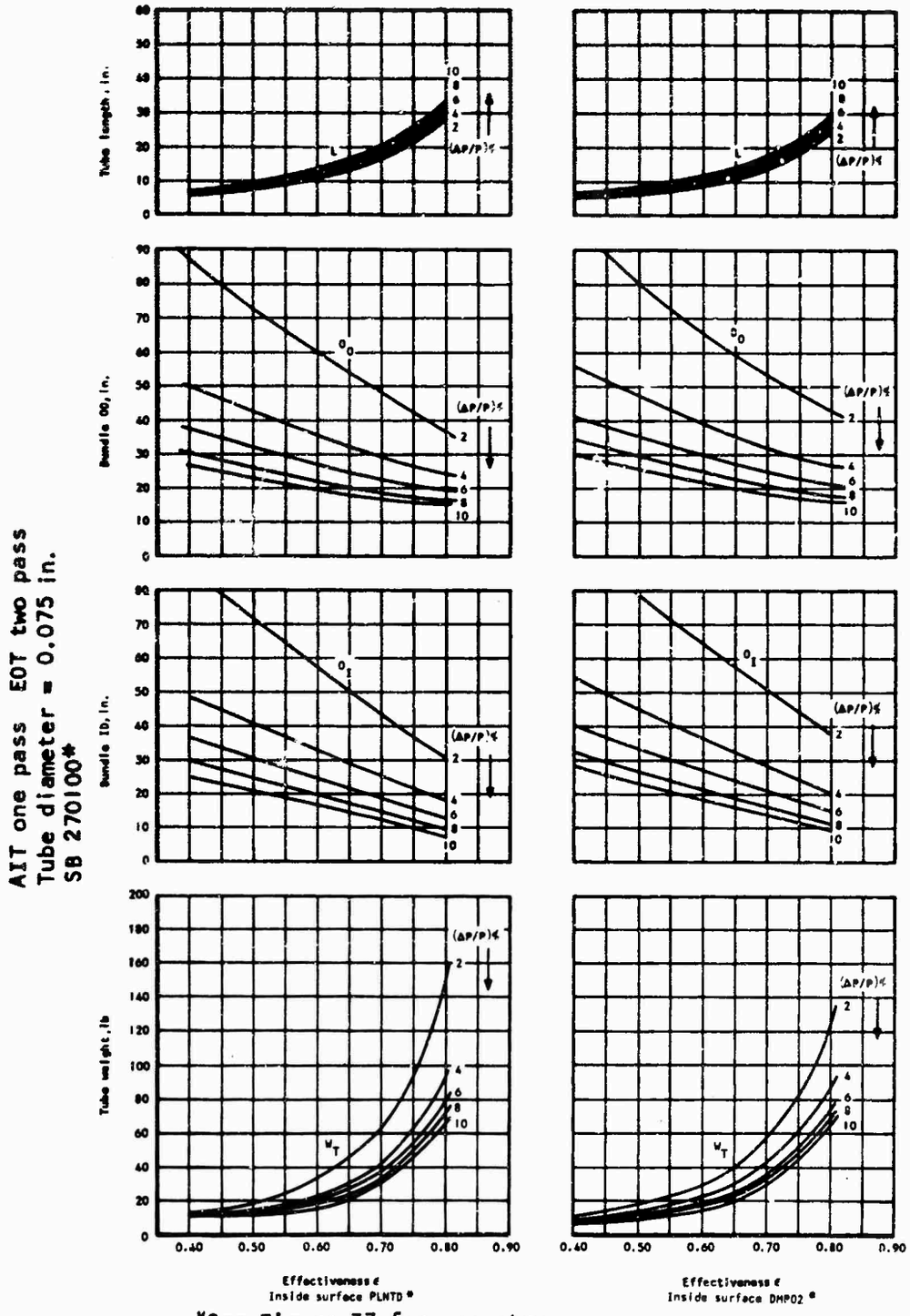

*See Figure 37 for geometry

Figure 39. Recuperator Parametric Data for Engine Configurations A-1, B-1.

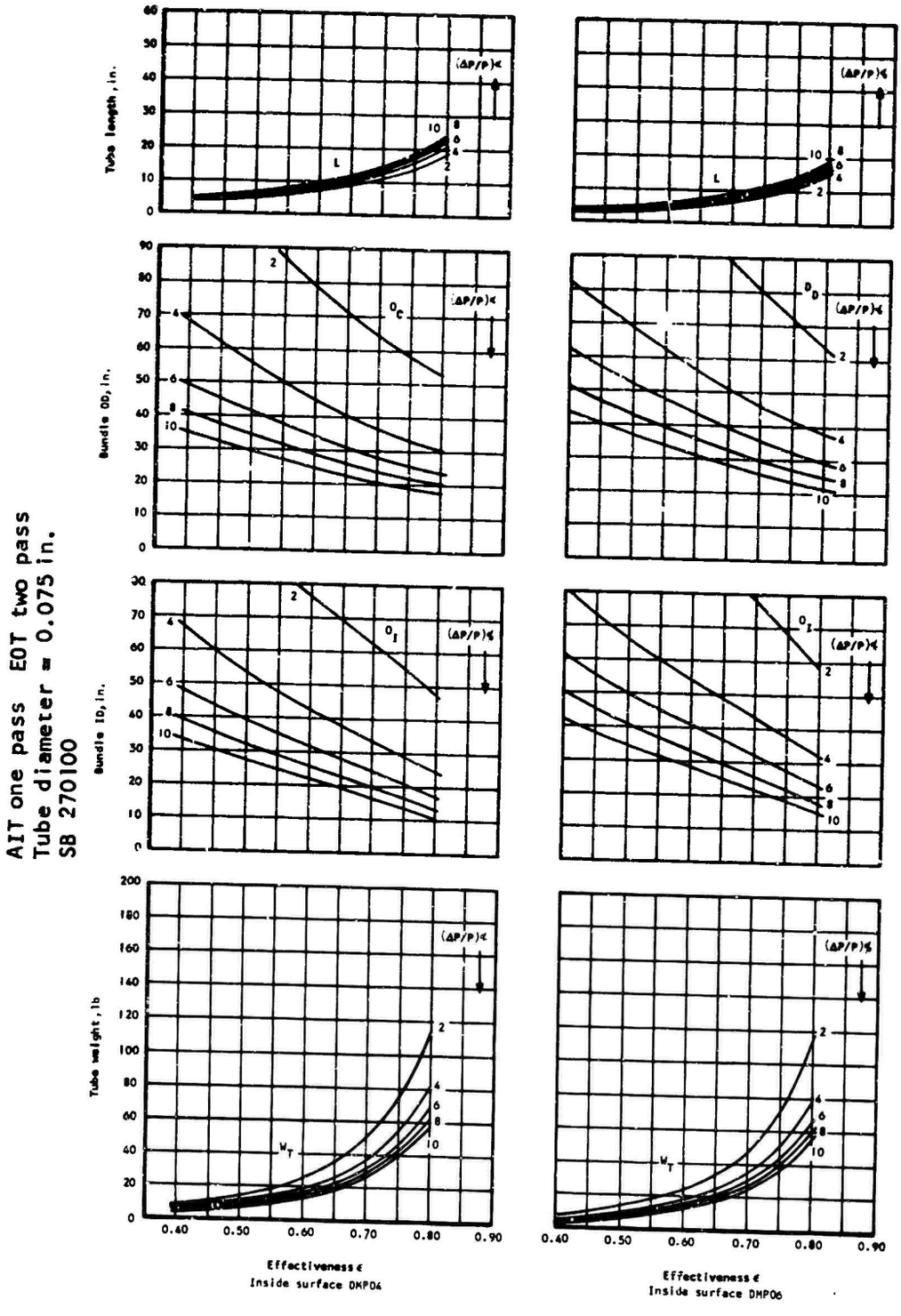

Figure 39. Continued.

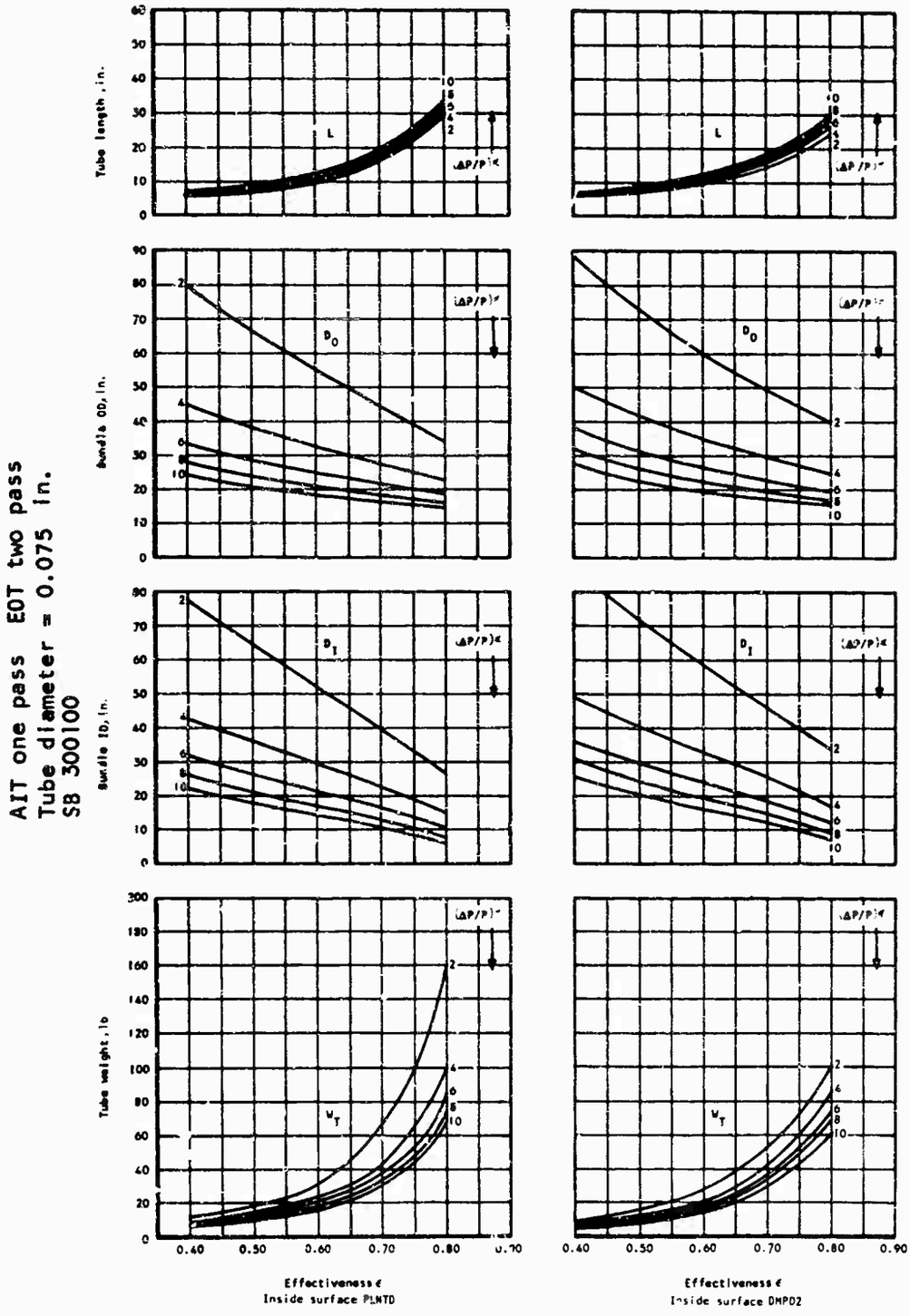

Figure 39. Continued.

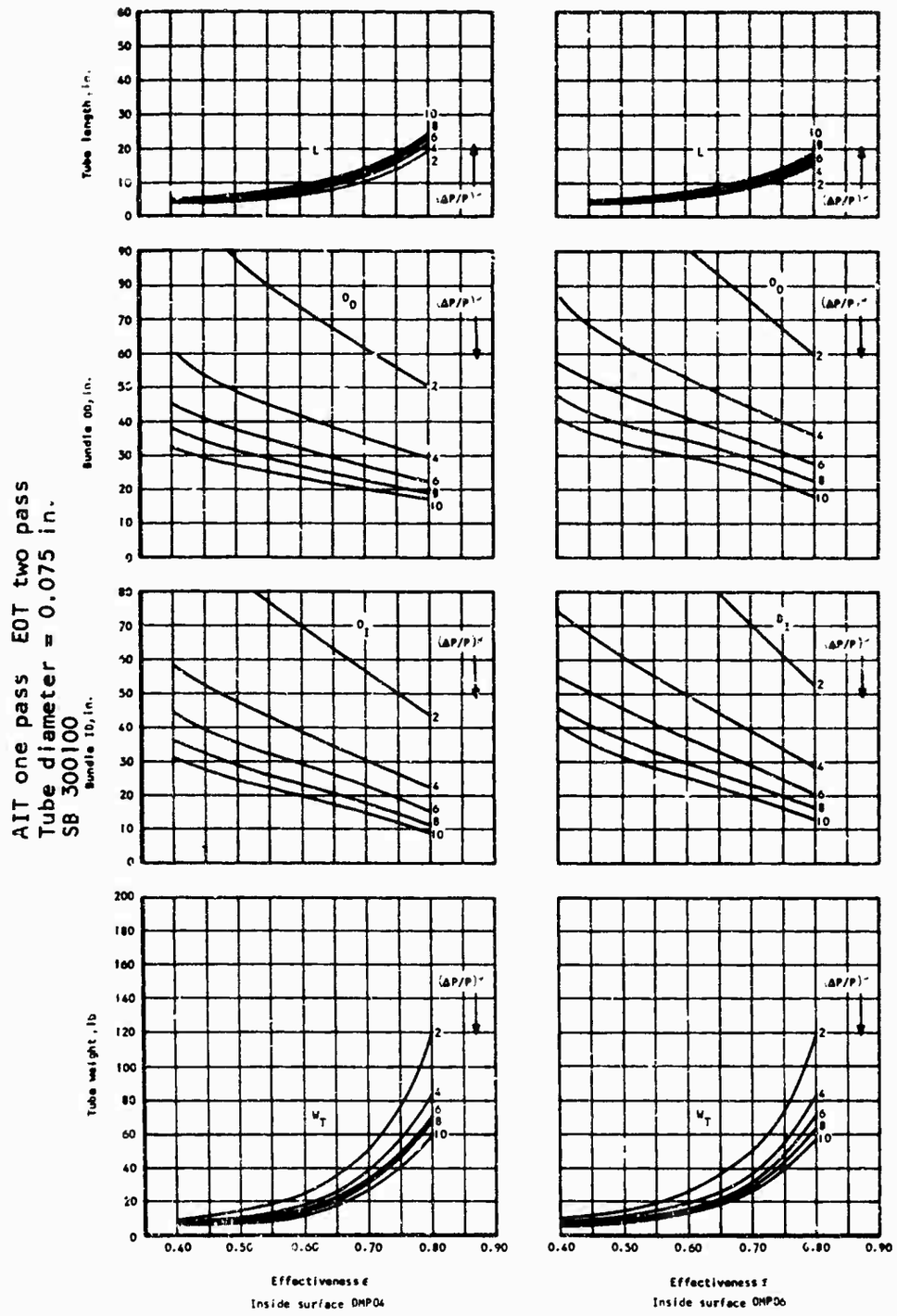

Figure 39. Continued.

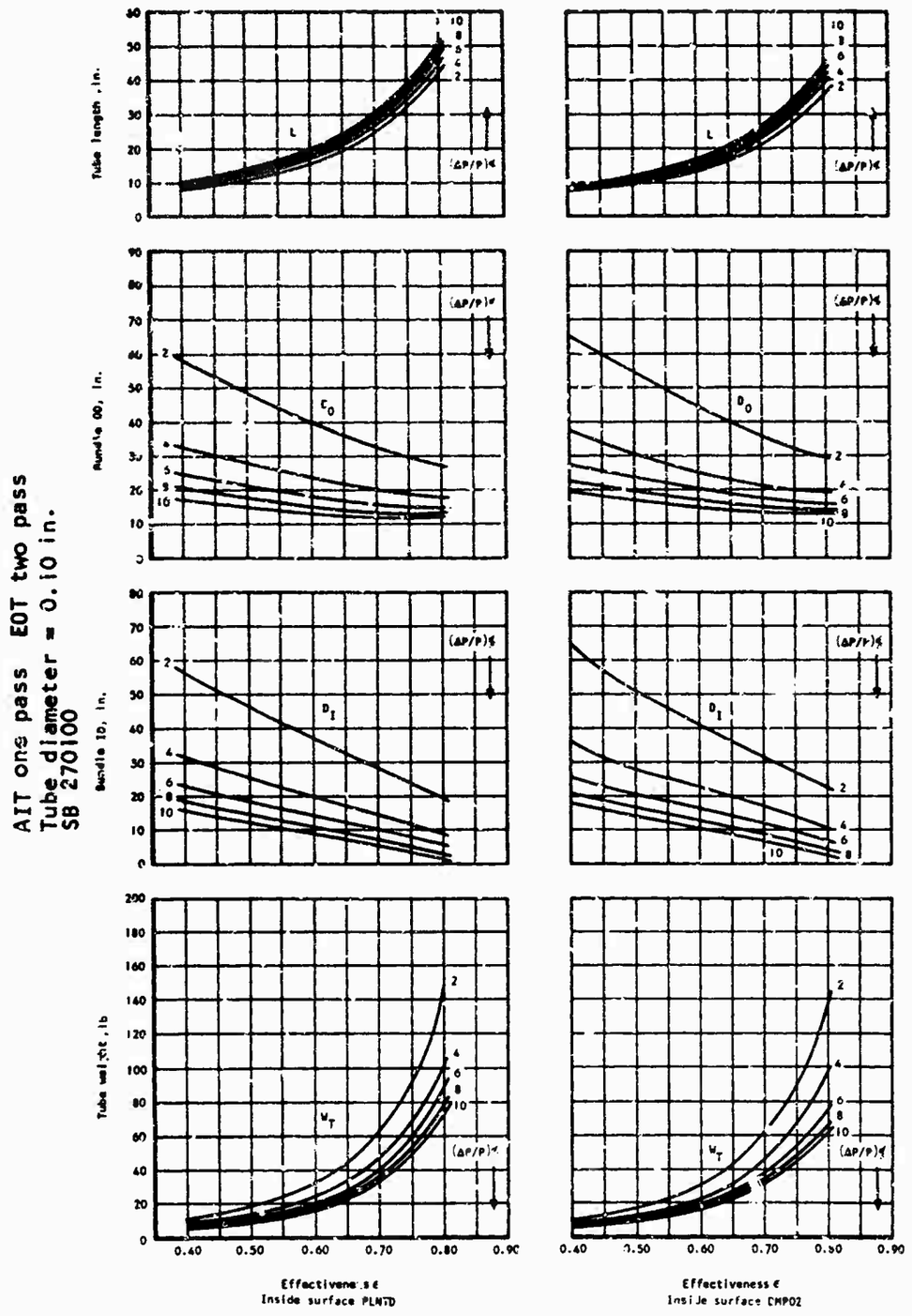

Figure 39. Continued.

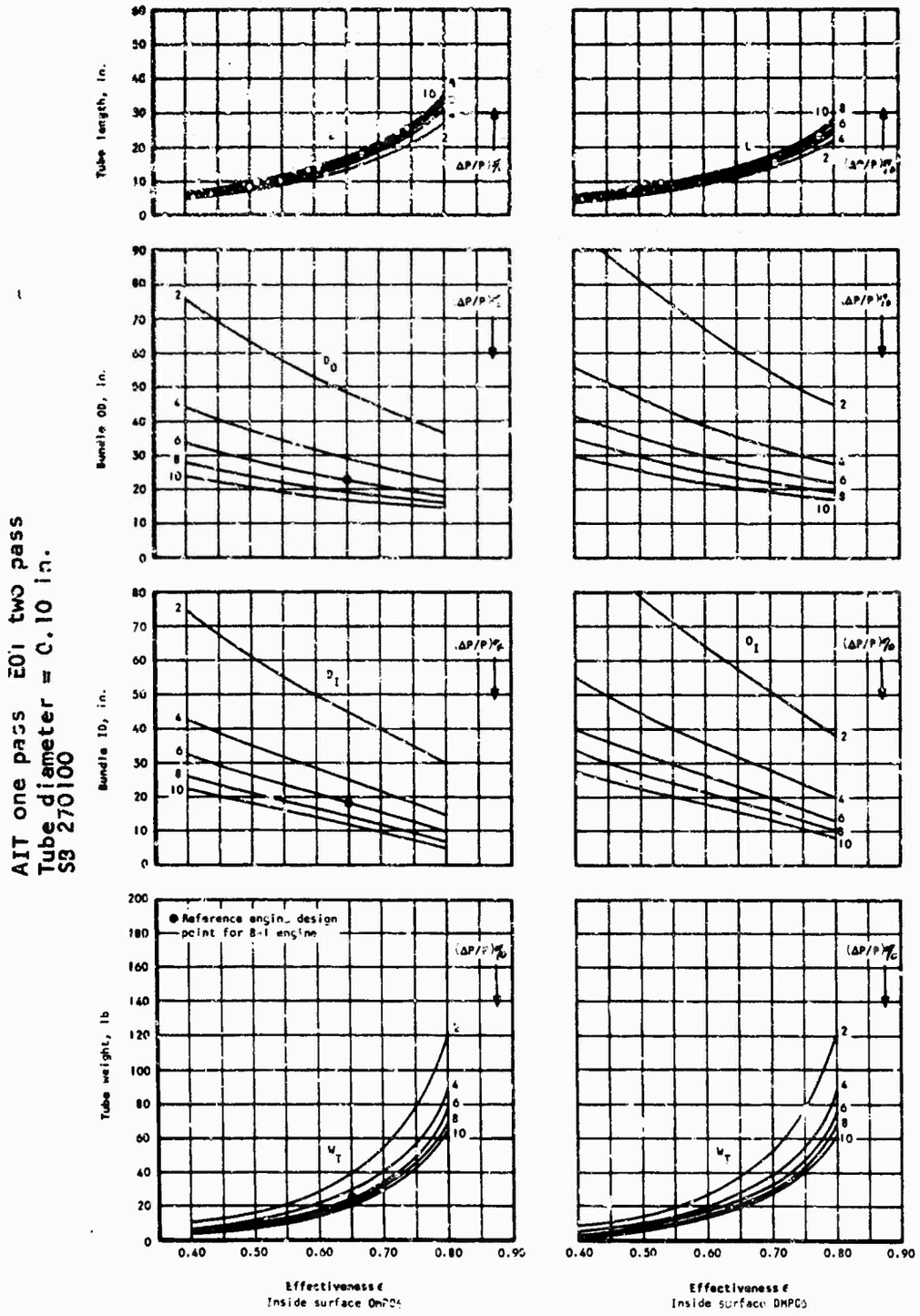

Figure 39. Continued.

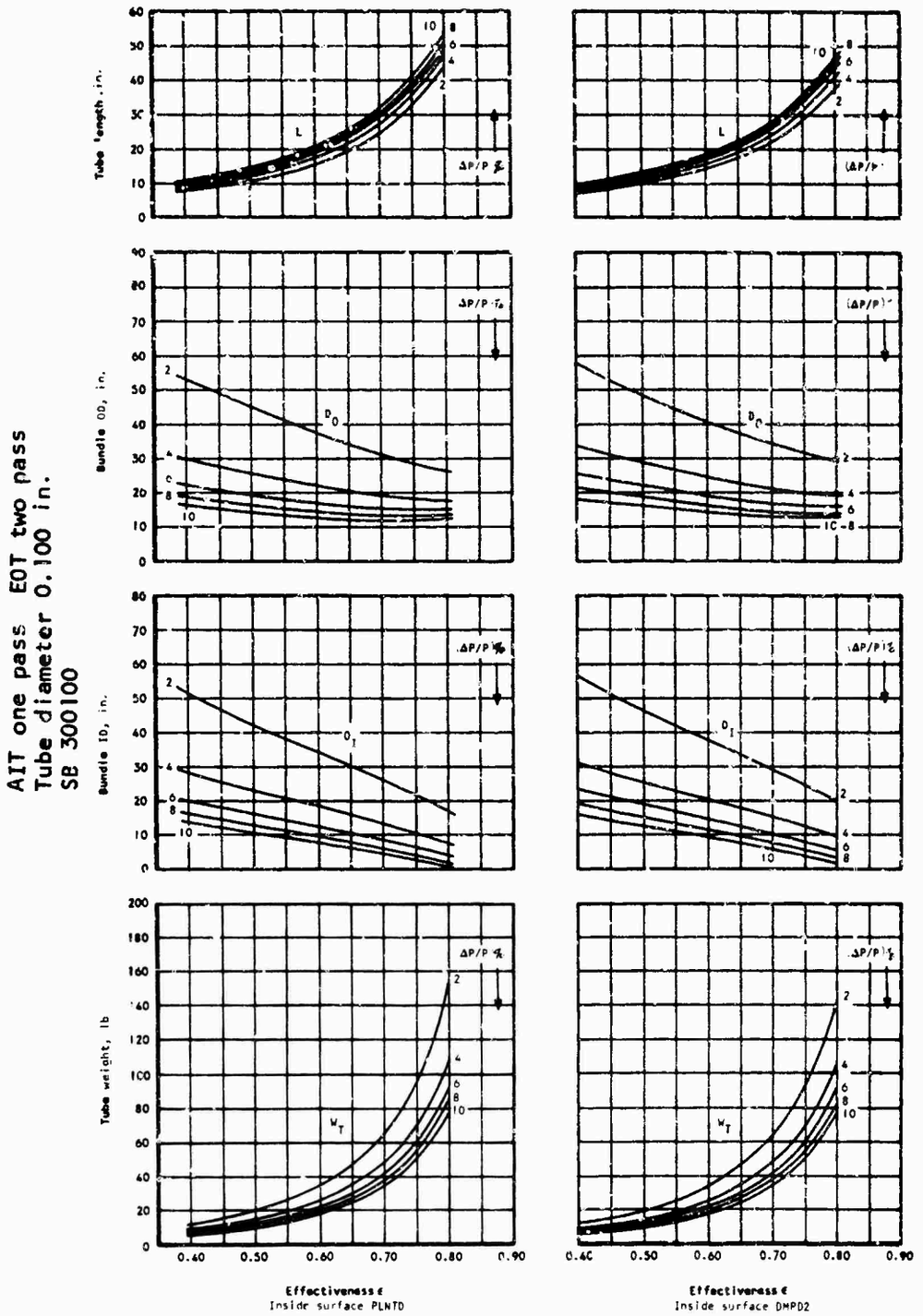

Figure 39. Continued.

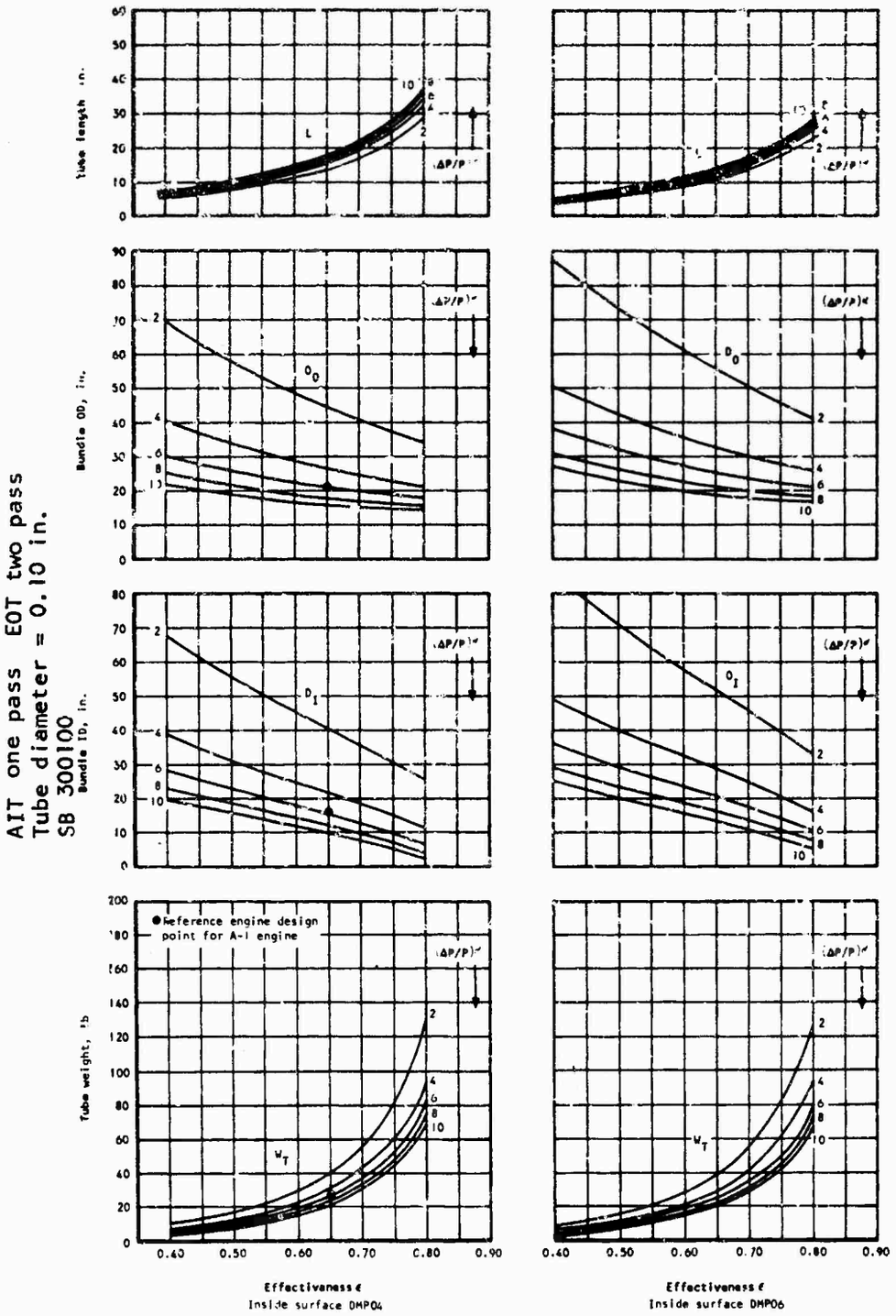

Figure 39. Continued.

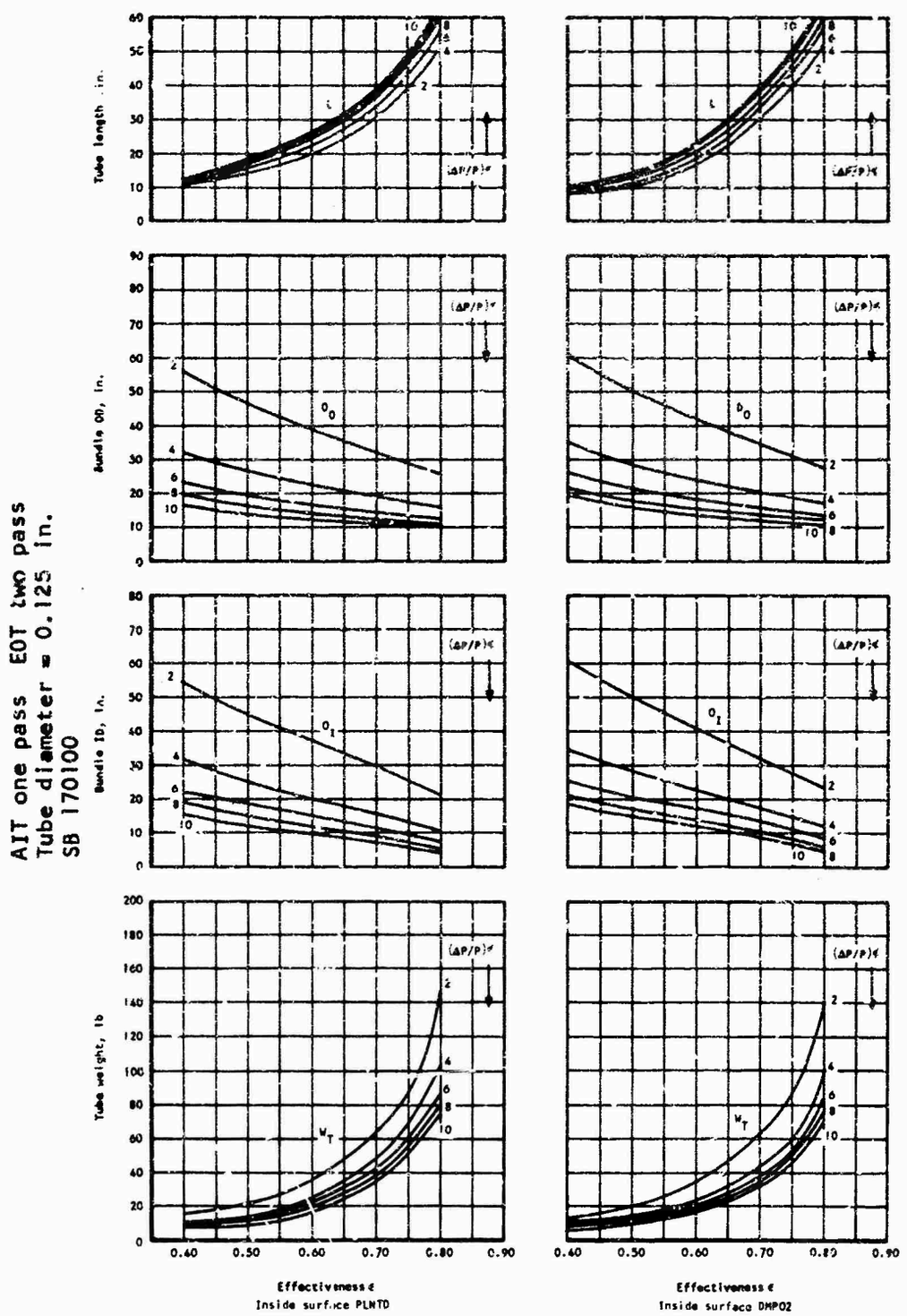

Figure 39. Continued.

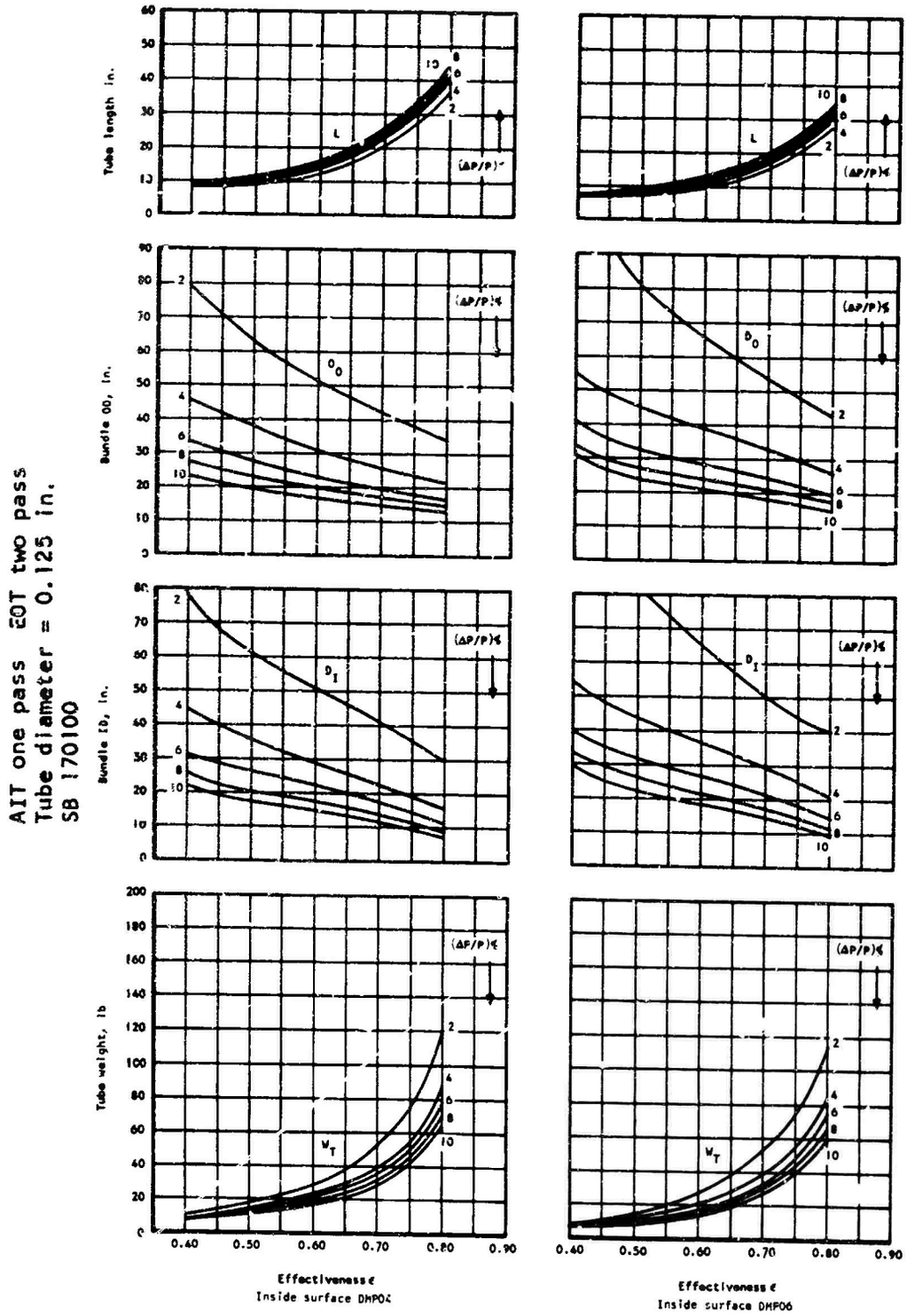

Figure 39. Continued.

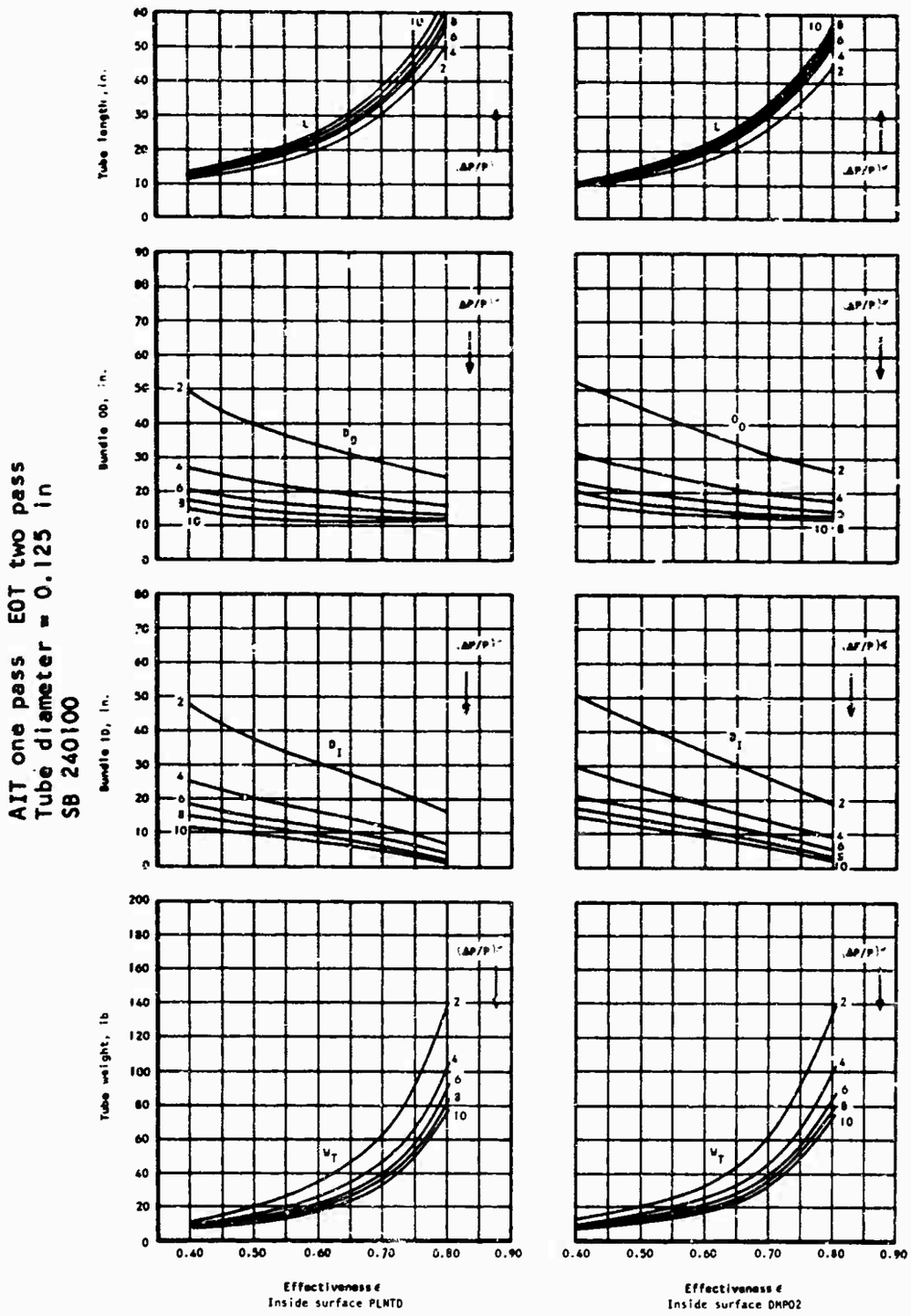

Figure 39. Continued.

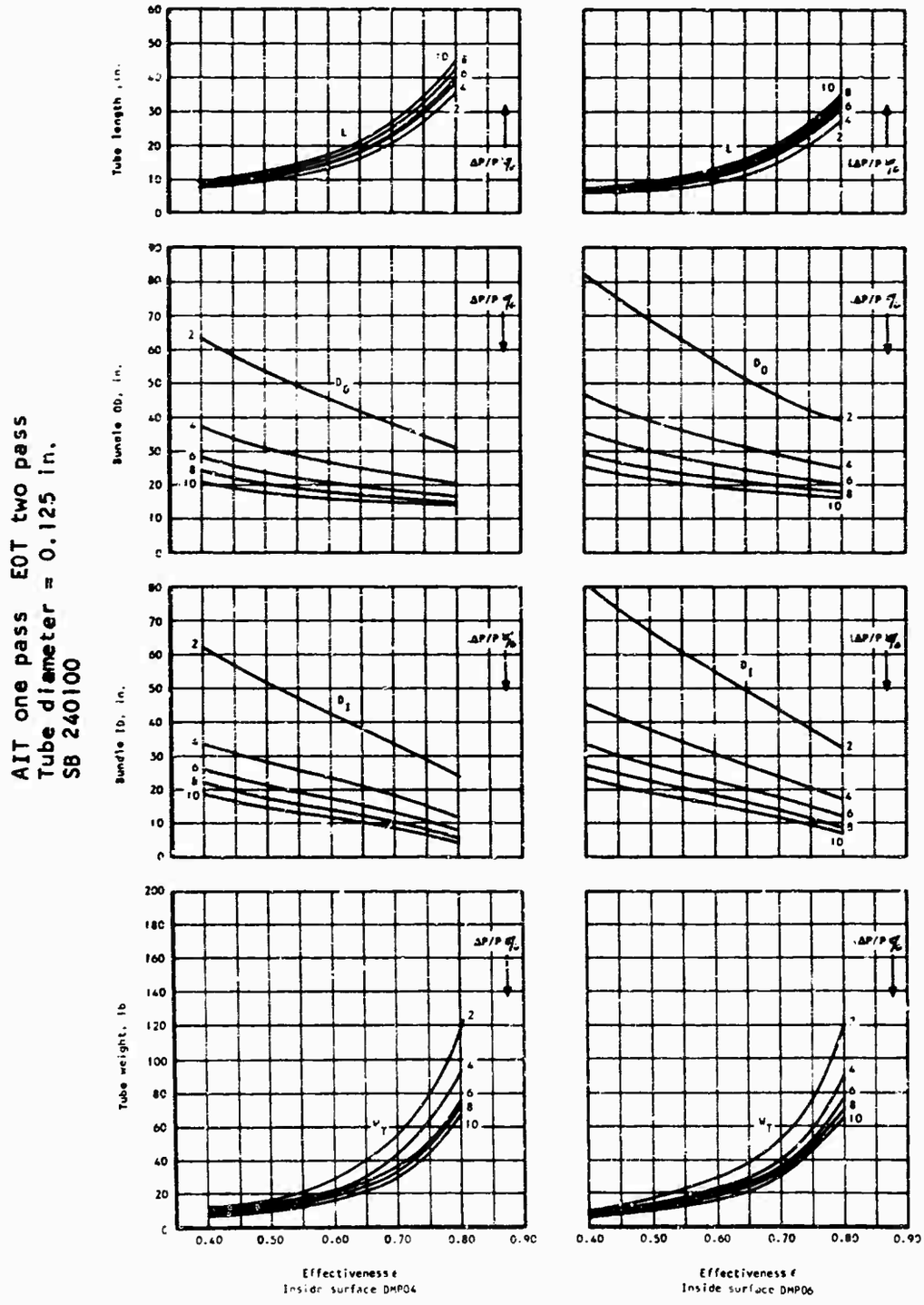

Figure 39. Continued.

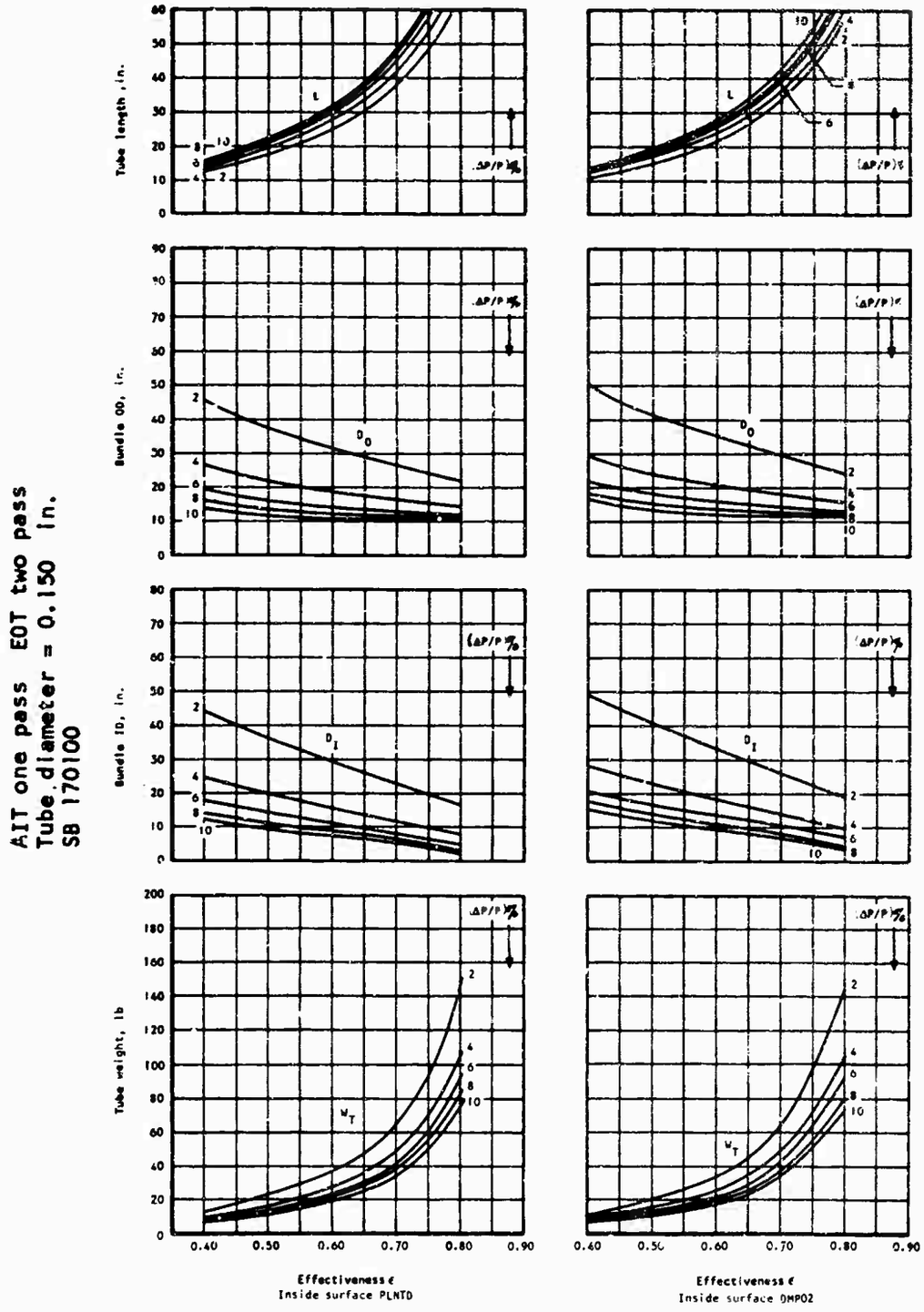

Figure 39. Continued.

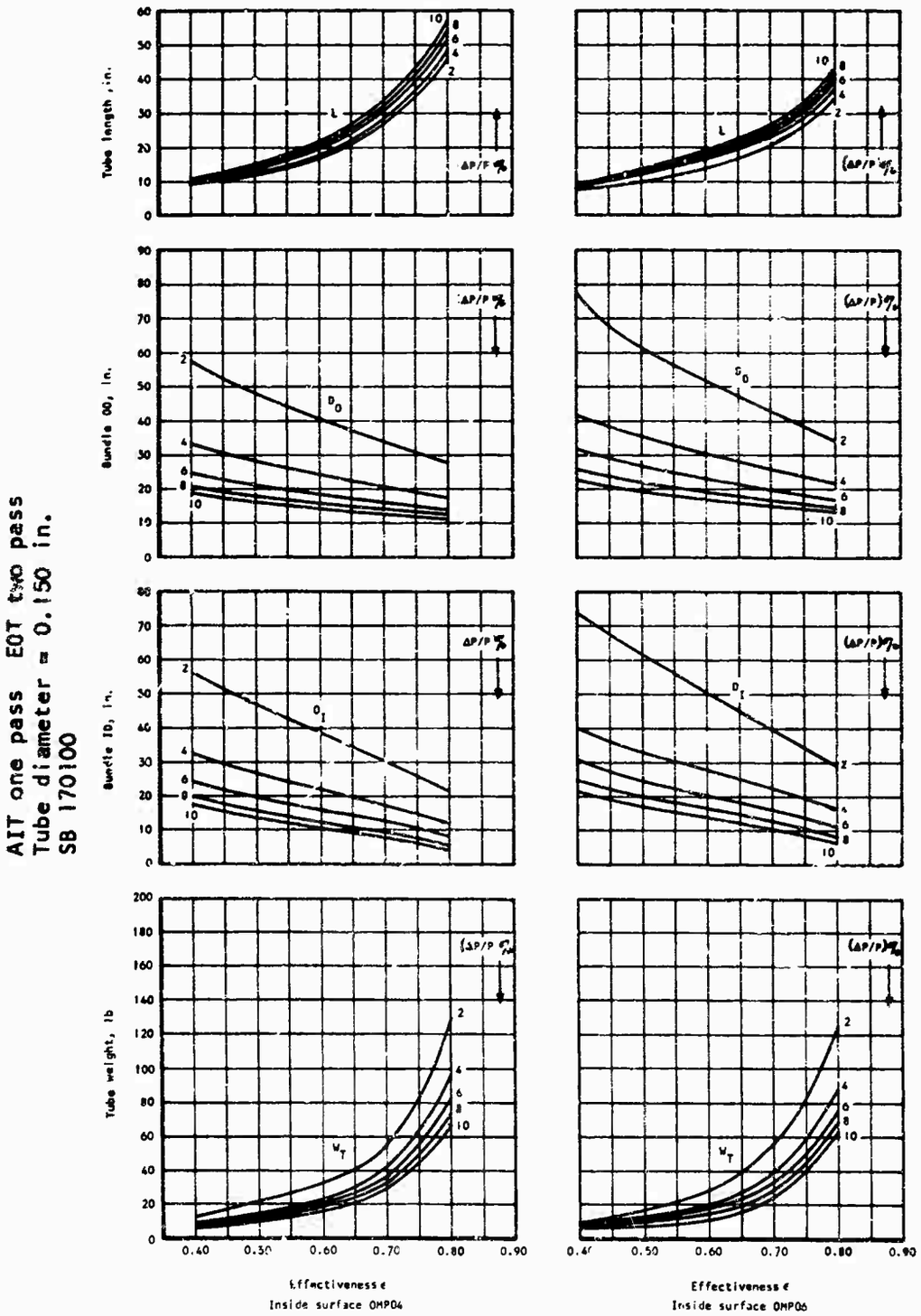

Figure 39. Continued.

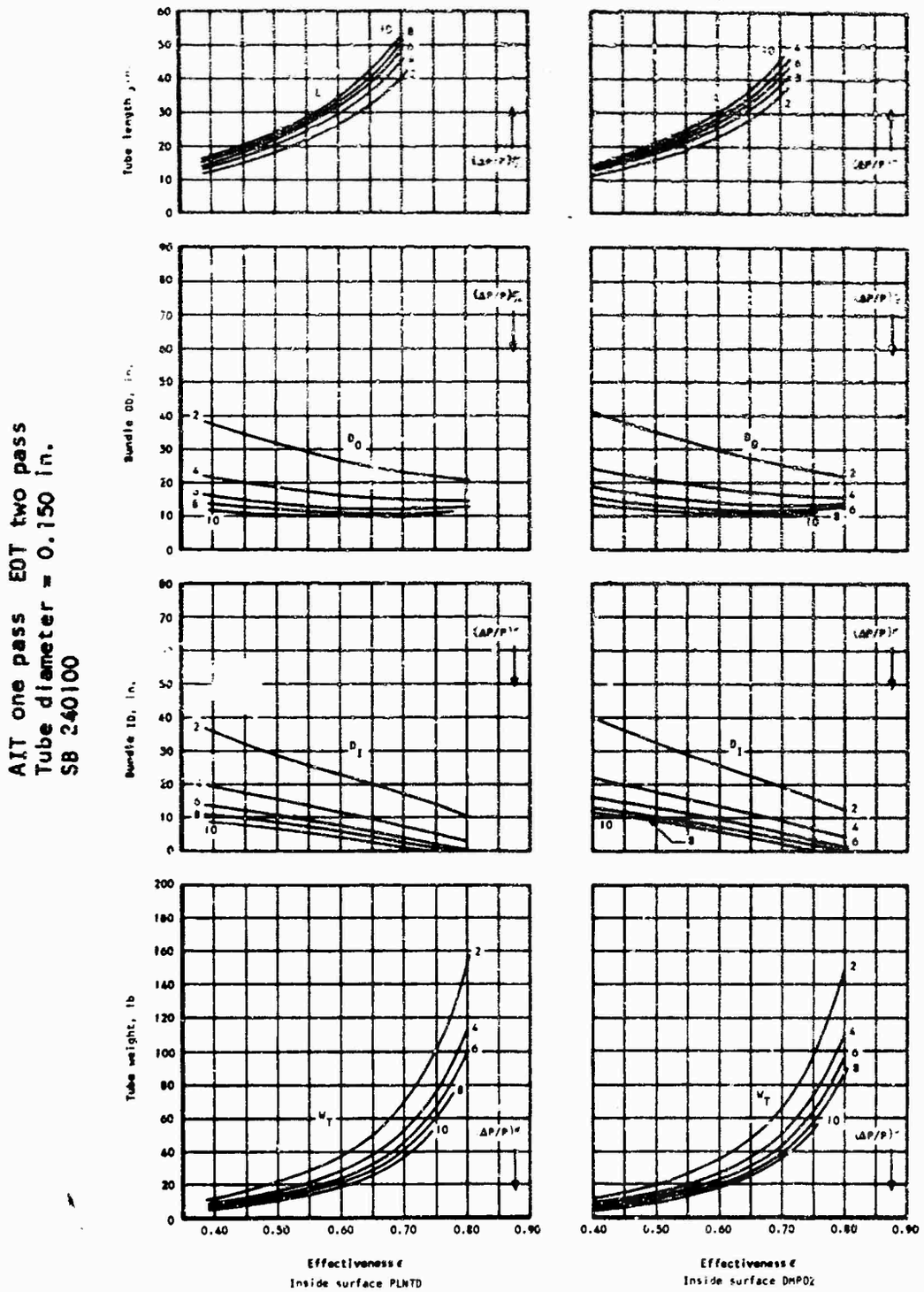

Figure 39. Continued.

AIT one pass EOT two pass
Tube diameter = 0.150 in.
SB 240100

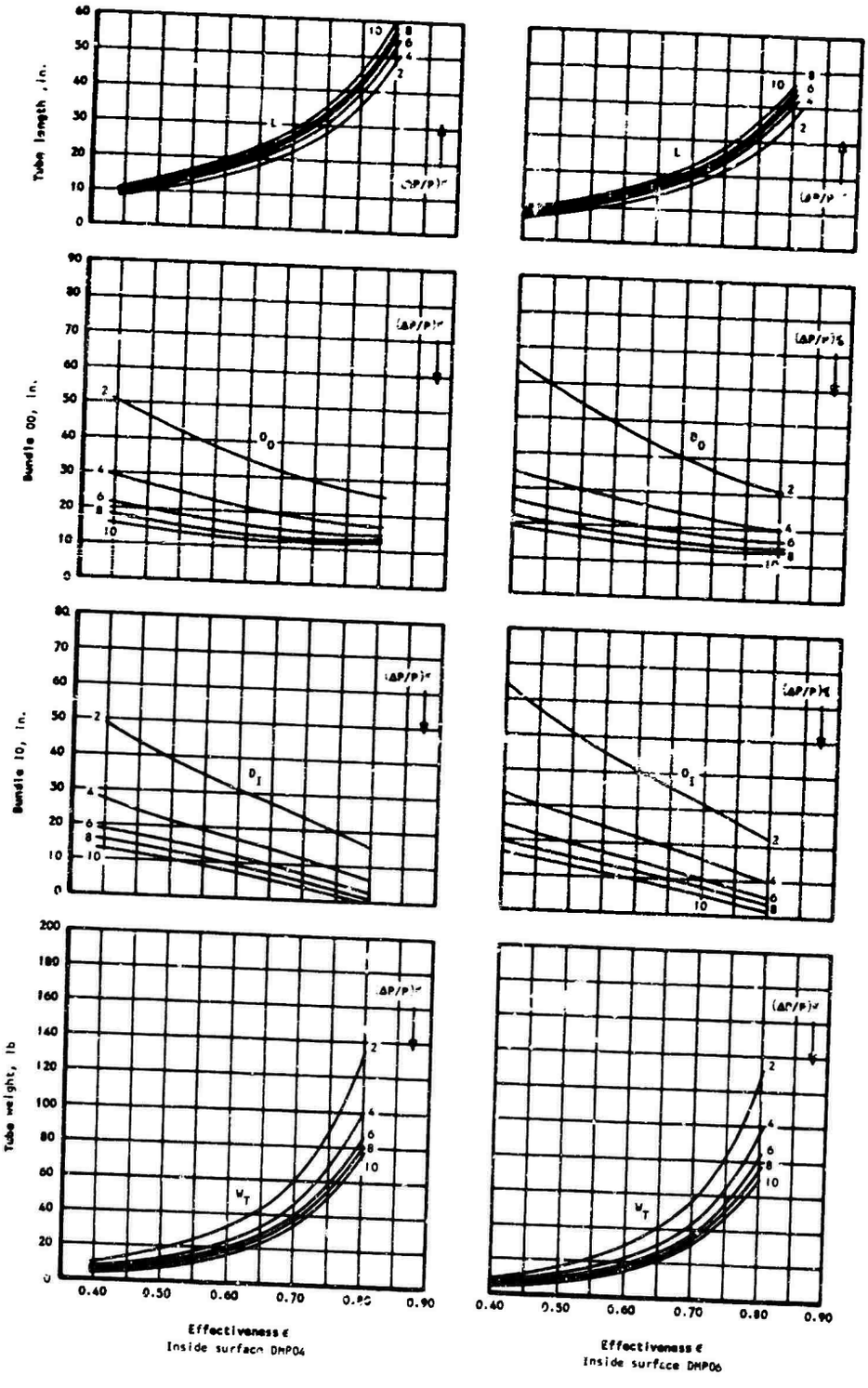

Figure 39. Continued.

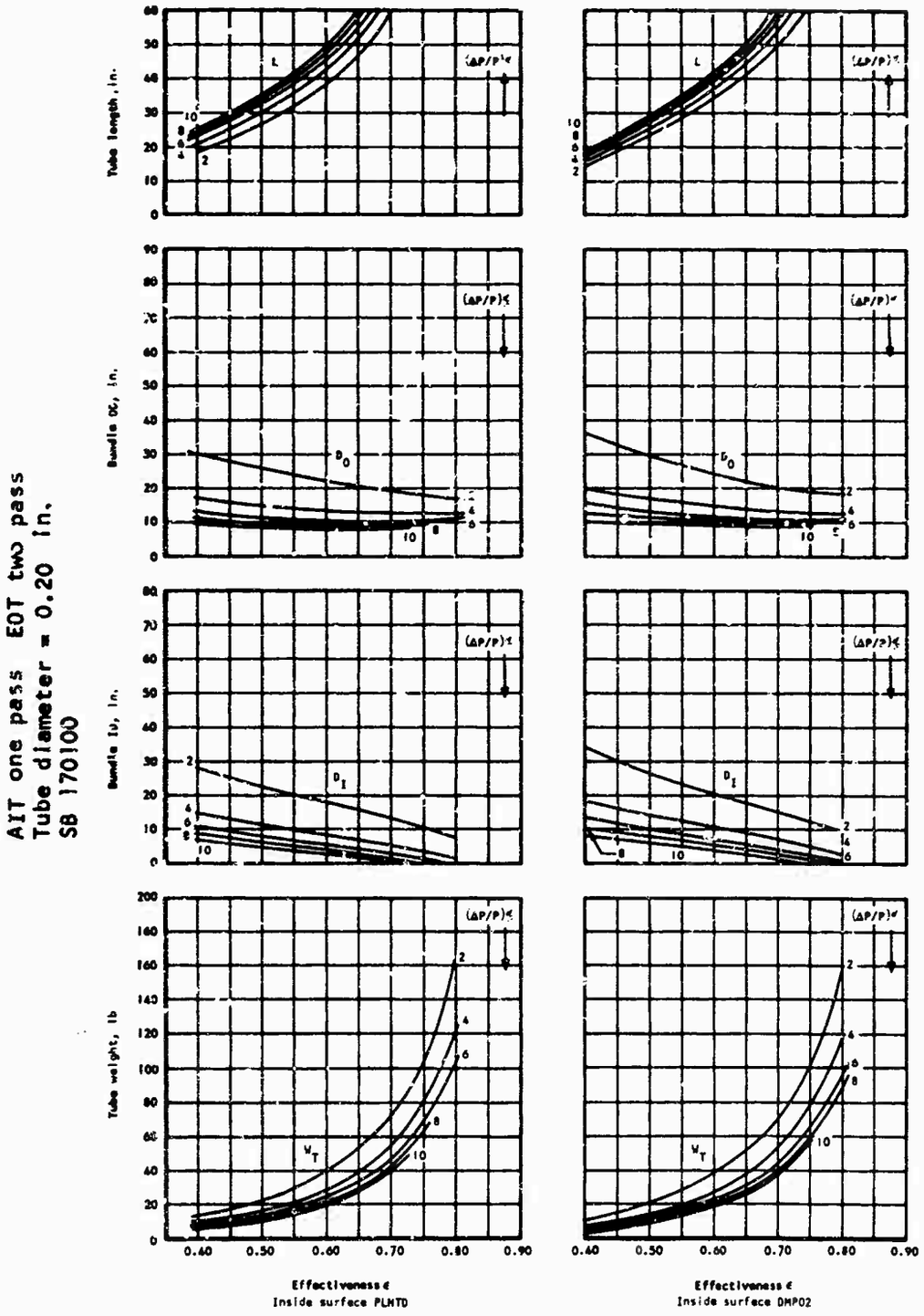

Figure 39. Continued.

AIT one pass EOT two pass
Tube diameter = 0.20 in.
SB 170100

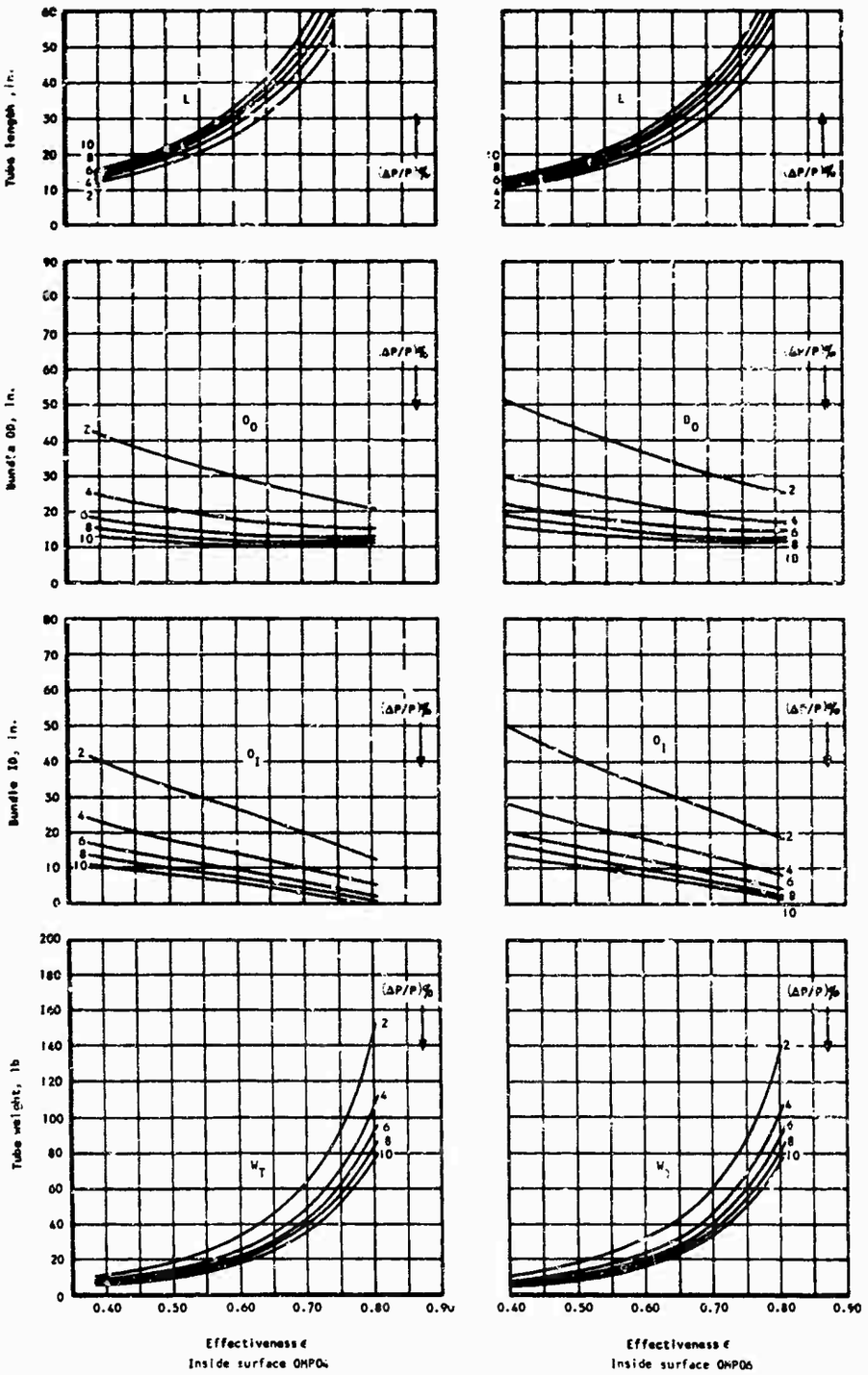

Figure 39. Continued.

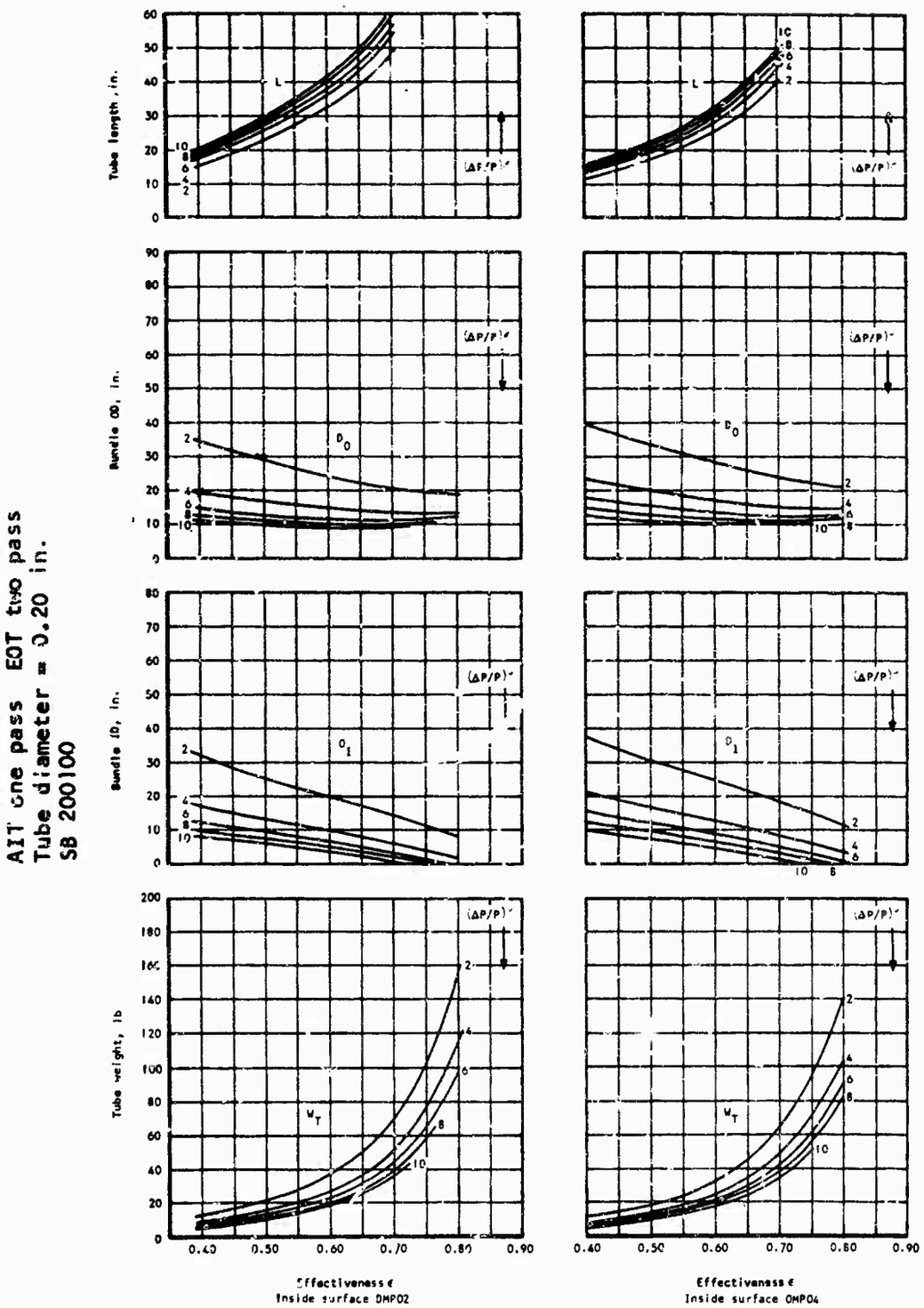

Figure 39. Continued.

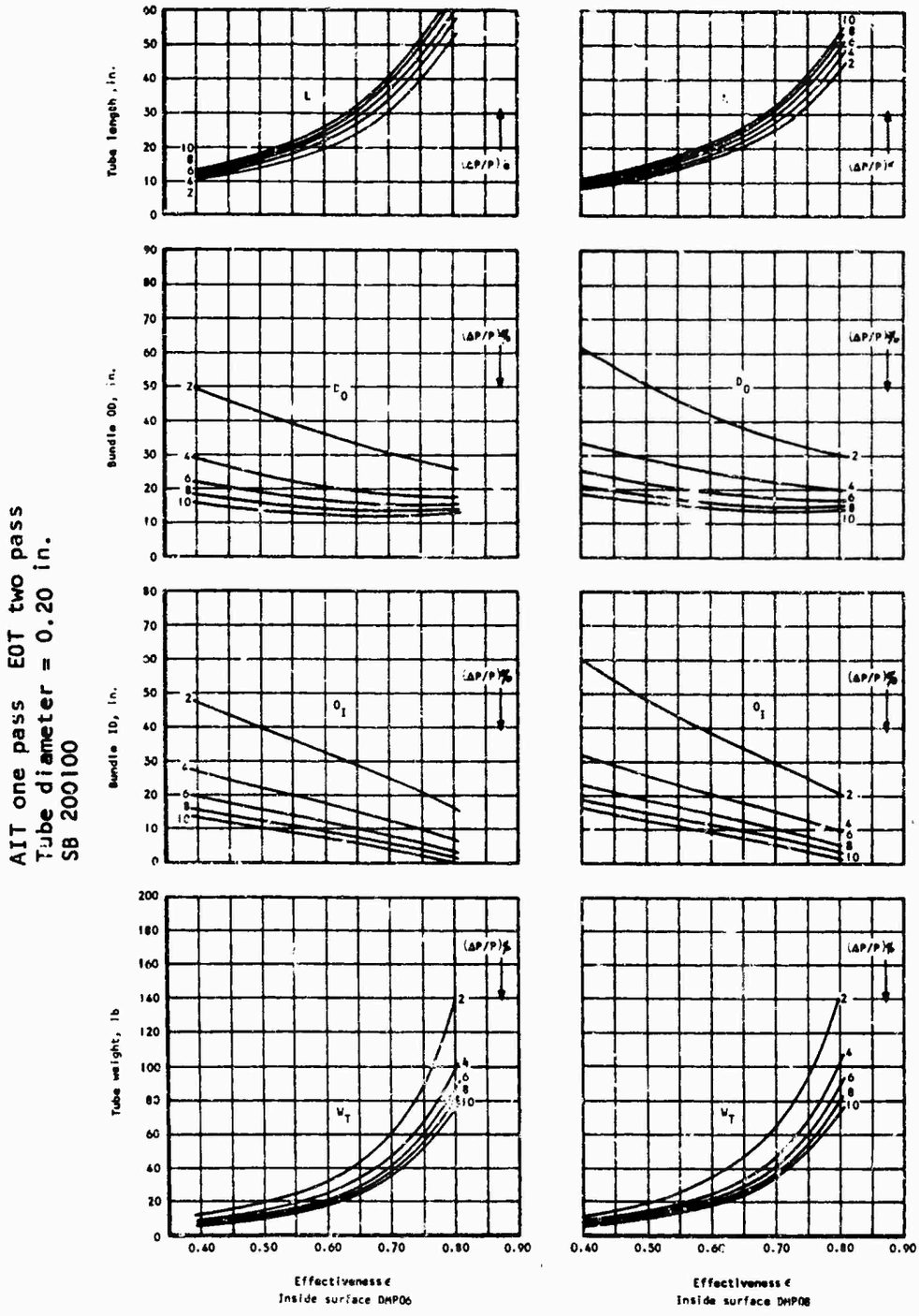

Figure 39. Concluded.

in-line tube pattern can be increased to give practical, lightweight recuperator designs that are compatible with the turbomachinery. The salient core dimensions for a series of selected in-line tube surface geometries are shown in Figure 40. The selected design for the A-2 engine configuration at the reference engine conditions is shown on page 90.

For the B-2 configuration, there is a choice of two-pass or four-pass cross-counterflow arrangement. As for the A-1 and B-1 designs, it was found that the relaxation in core surface compactness necessary for the four-pass arrangements resulted in a weight and volume penalty compared with the two-pass designs. In the graphical presentation of the recuperator parametric data, only the two-pass cross-counterflow solutions are shown. The salient core dimensions for a series of selected staggered tube surface geometries are shown in Figure 41. The selected design for the B-2 engine arrangement at the reference engine condition is shown on page 106.

A summary of the selected designs for the four engine configurations, at the reference engine conditions, for the tubular recuperator surface geometries is shown in Table VIII.

FINNED-TUBE SURFACE GEOMETRY EVALUATION

For the effectiveness and pressure loss range outlined in a previous section, a variety of finned-tube surface geometries of the type shown in Figure 35b was considered in the recuperator parametric study. The analytical procedures were similar to those described for the plain tubular surface geometries. The following variables have been used in the analysis.

Flow Configurations

The flow configurations examined were identical to those described in the tubular surface geometry section.

Tube Sizes

A fairly wide range of tube diameters was considered. Tube outer diameters of 0.075, 0.10, 0.125, 0.15, 0.20 and 0.25 inch were evaluated, and a tube wall thickness of 0.004 inch was used.

Tube Inside Geometry

In the tubular recuperator section, lightweight solutions were presented where the inside heat transfer coefficient was substantially increased by ring-dimpling of the tube wall. With a gas-to-gas heat exchanger made from small diameter tubes, the addition of finned secondary surfaces on the outside of the tubes poses a severe, if not prohibitive, problem in fabricating

AIT one pass EOT two pass
Tube diameter = 0.075 in.
IB 200125 *

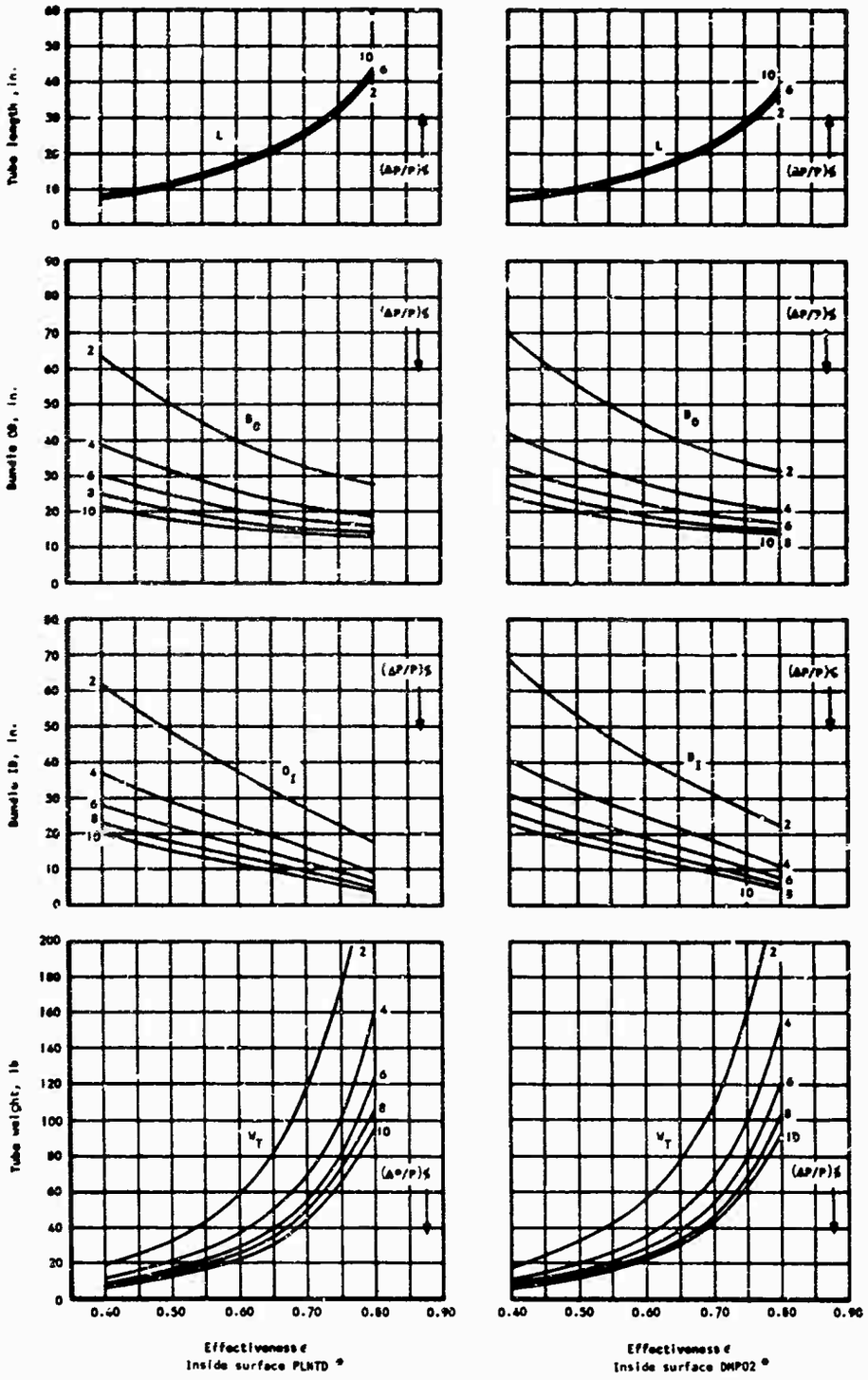

*See Figure 37 for geometry

Figure 40. Recuperator Parametric Data for Engine Configuration A-2.

AIT one pass EOT three pass
Tube diameter = 0.075 in.
IB 200125

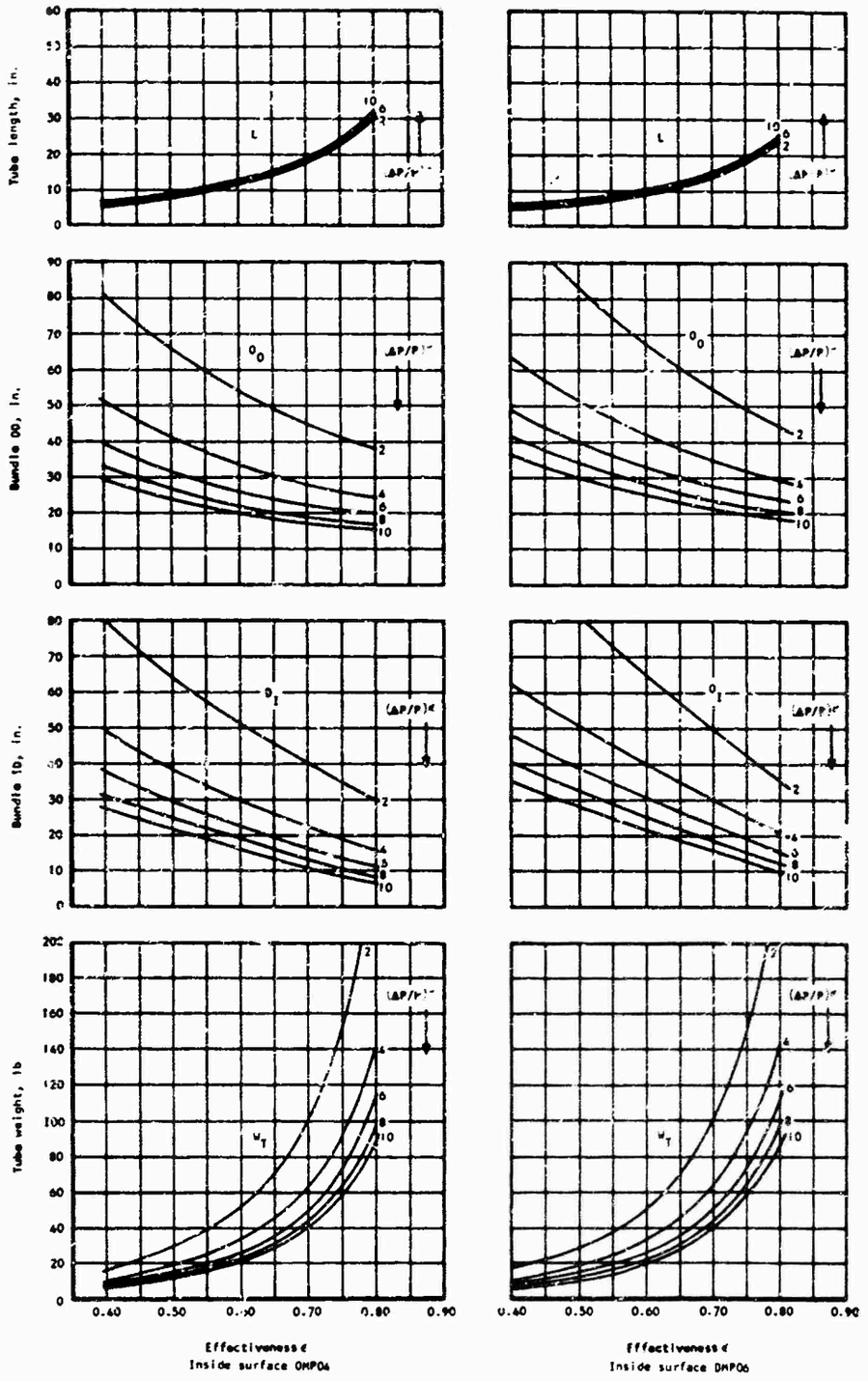

Figure 40. Continued.

AIT one pass EOT three pass
Tube diameter = 0.10 in.
IB 200125

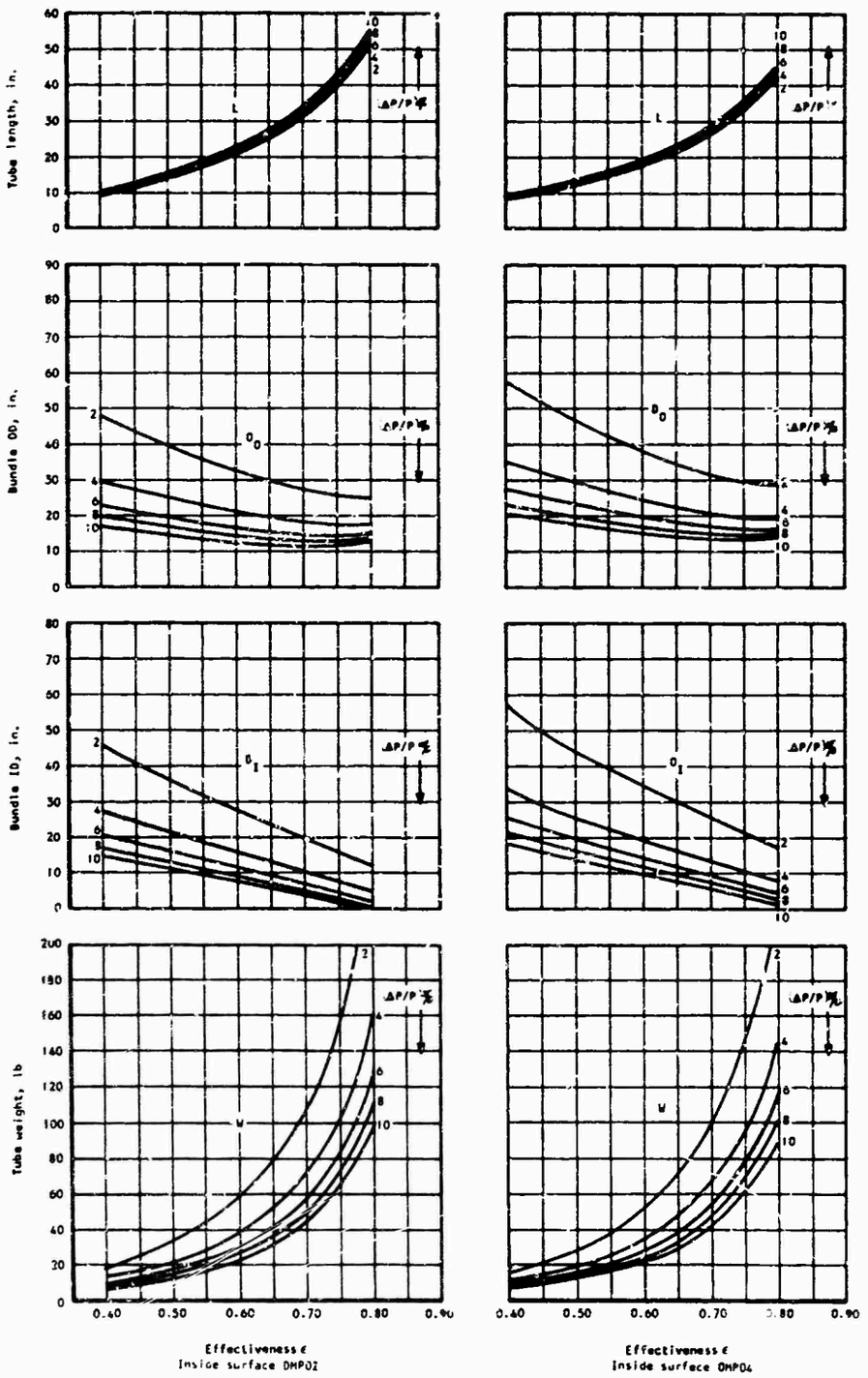

Figure 40. Continued.

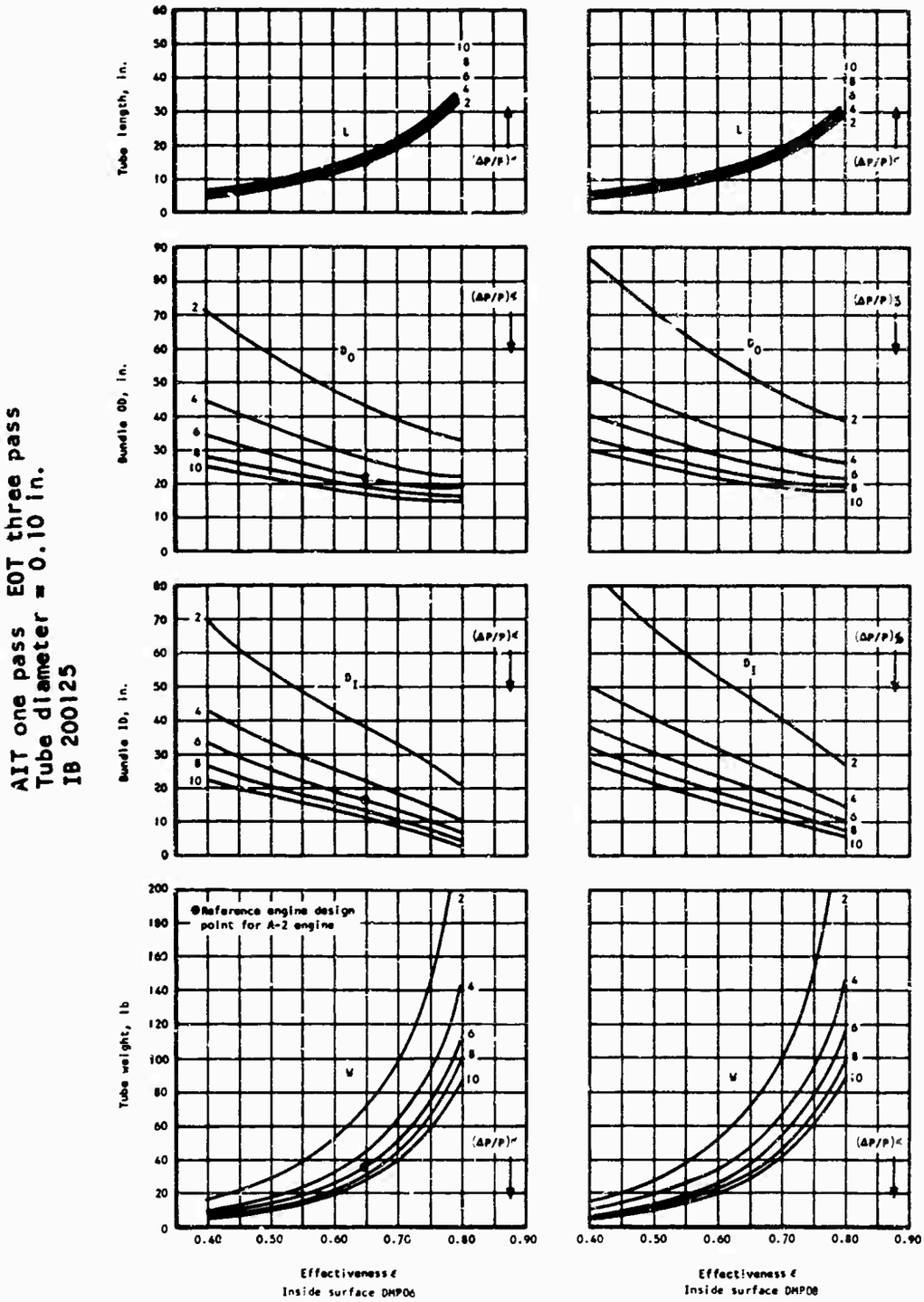

Figure 40. Continued.

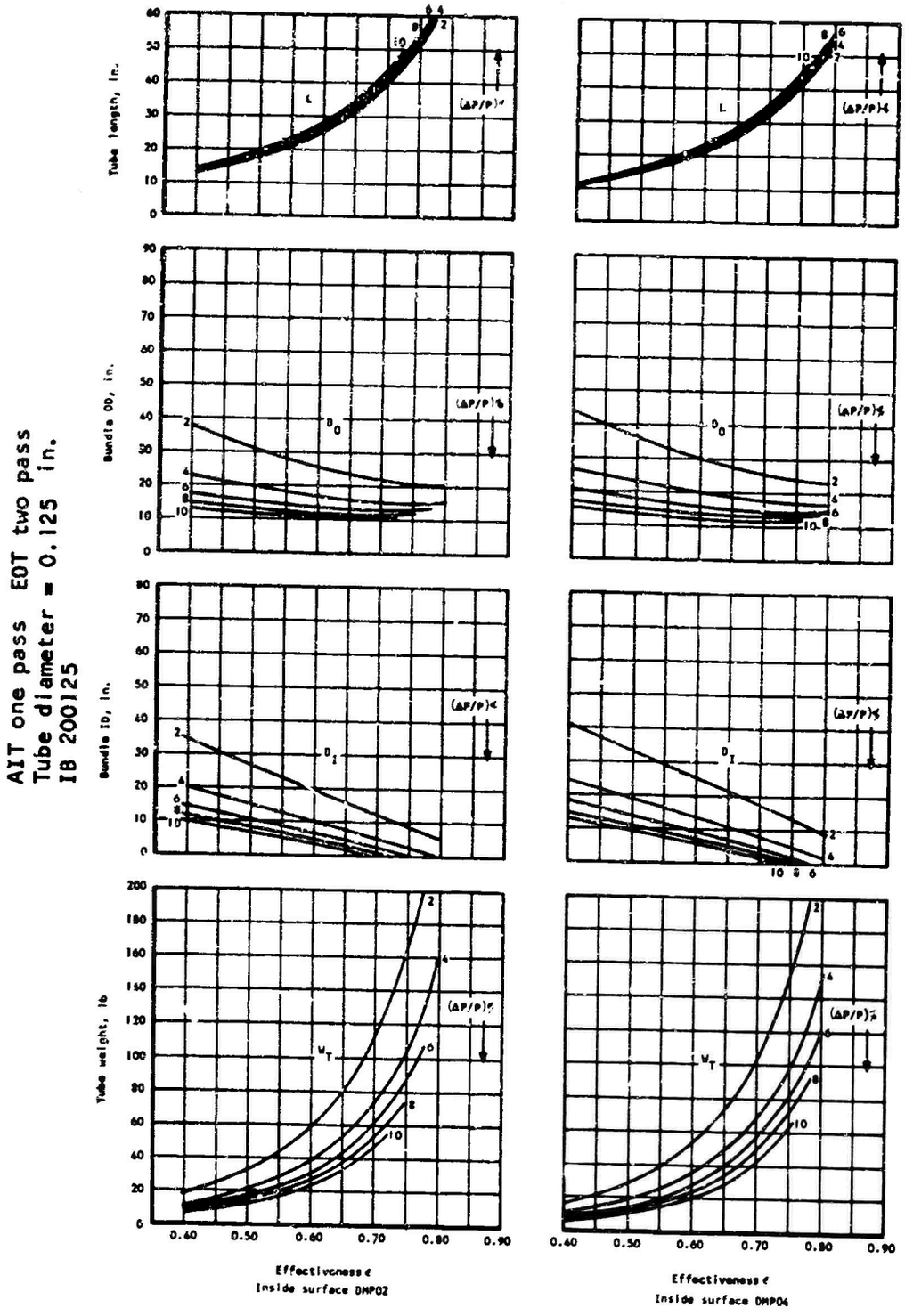

Figure 40. Continued.

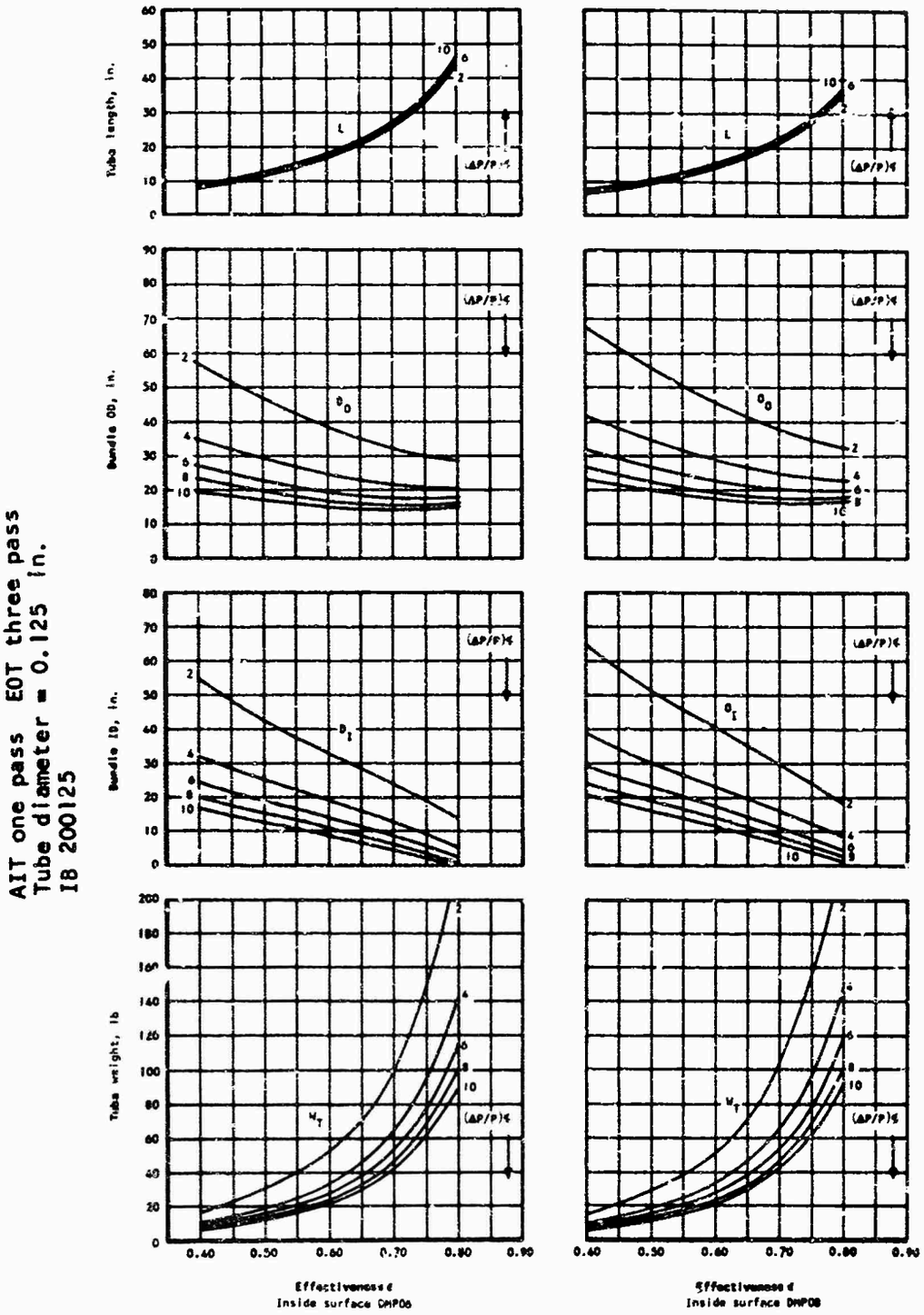

Figure 40. Continued.

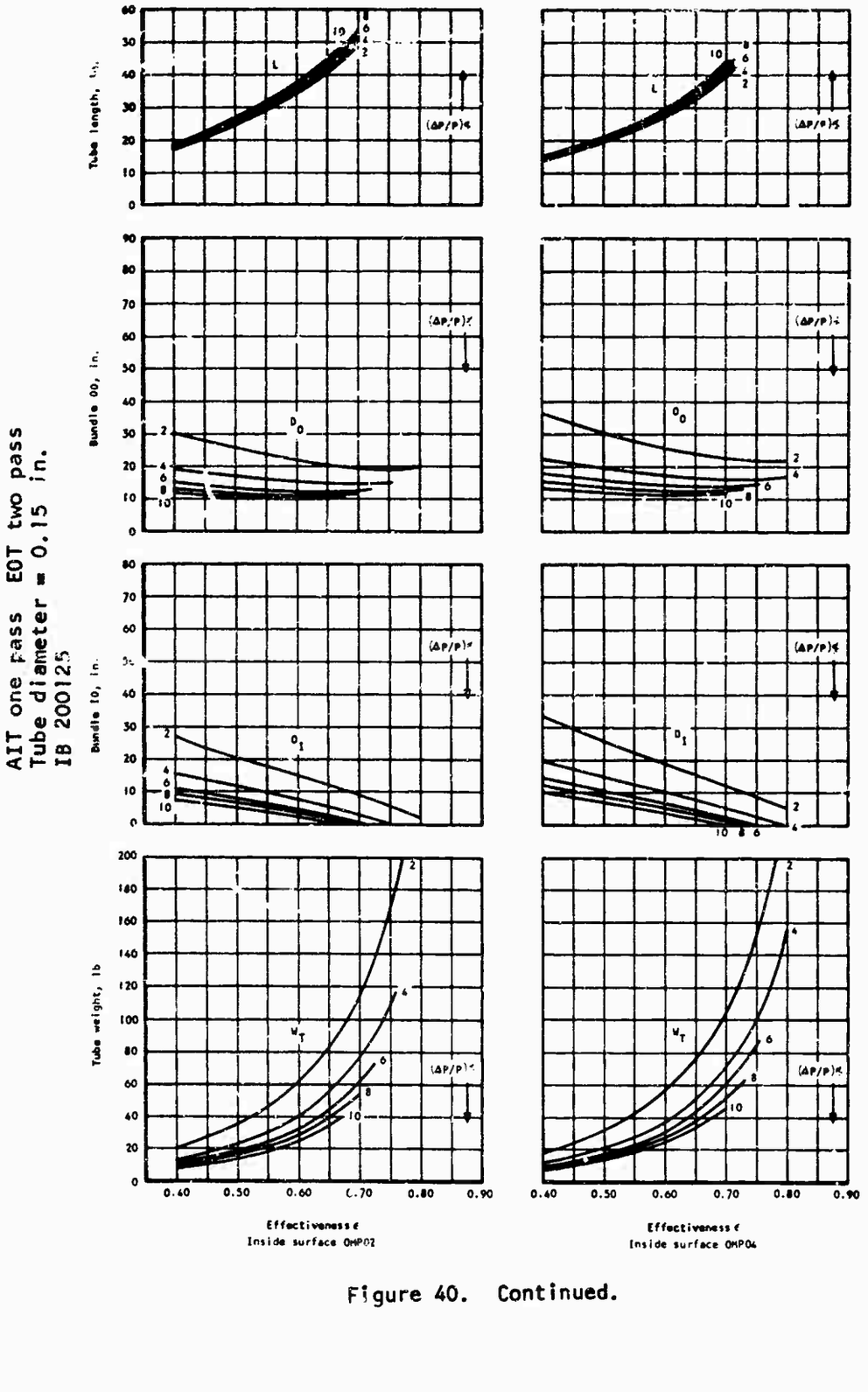

Figure 40. Continued.

AIT one pass EOT three pass
Tube diameter = 0.15 in.
IB 200125

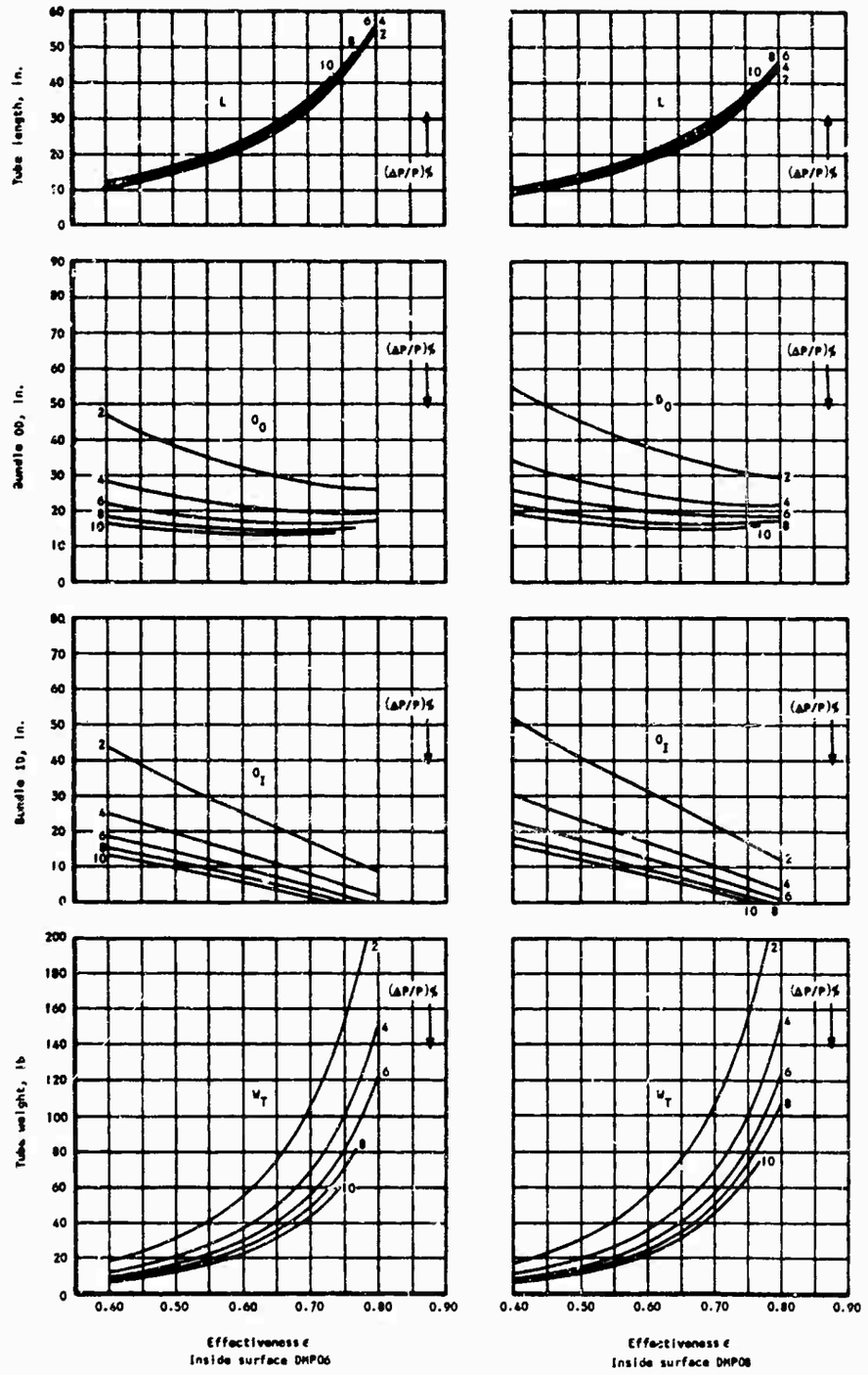

Figure 40. Concluded.

AIT two pass EOT two pass
Tube diameter = 0.075 in.
SB 240100

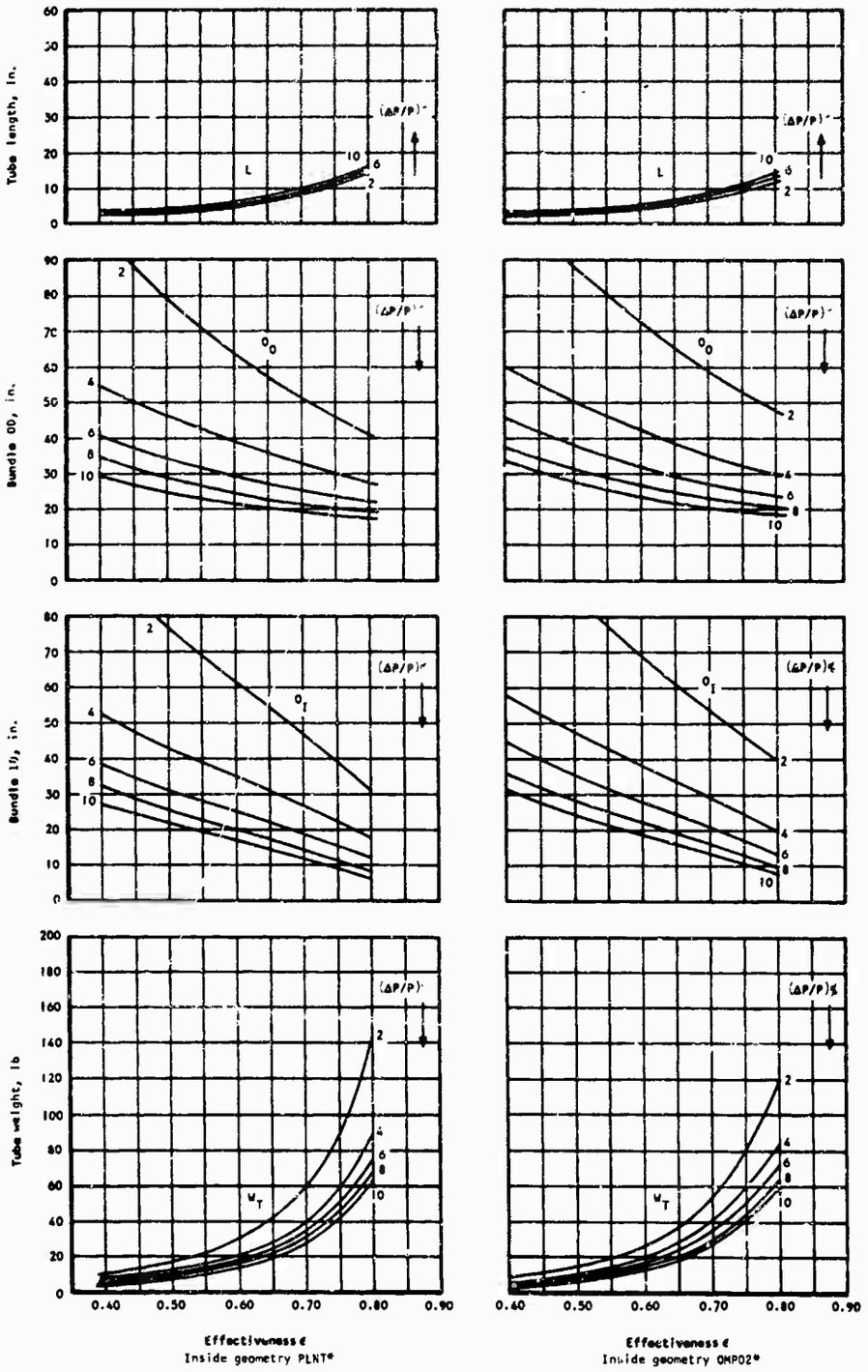

*See Figure 37 for geometry

Figure 41. Recuperator Parametric Data for Engine Configuration B-2.

AIT two pass EOT two pass
Tube diameter = 0.075 in.
SB 270100

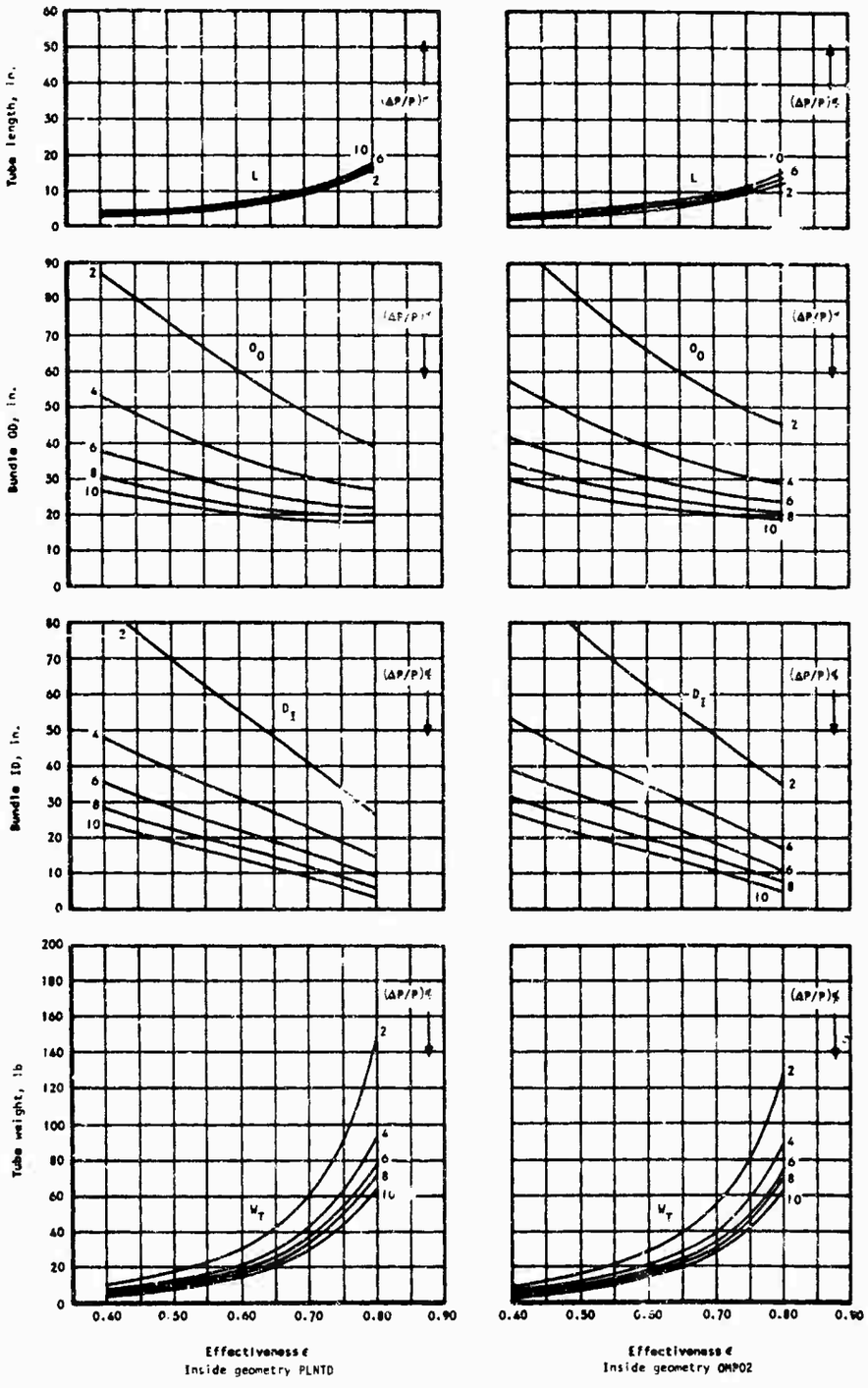

Figure 41. Continued.

AIT two pass EOT one pass
Tube diameter = 0.075 in.
SB 300100

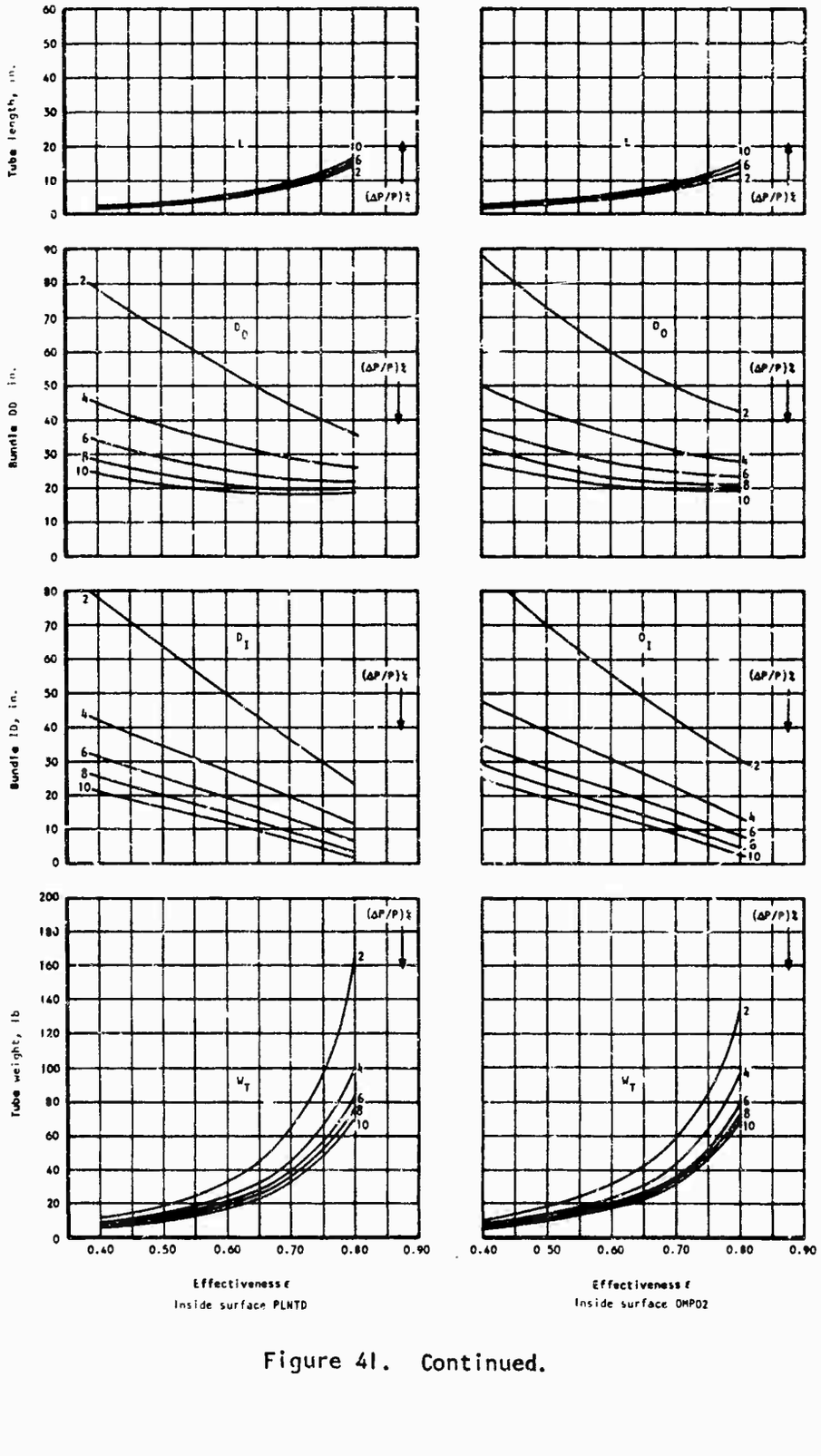

Figure 41. Continued.

AIT two pass EDT one pass
Tube diameter = 0.10 in.
SB 150100

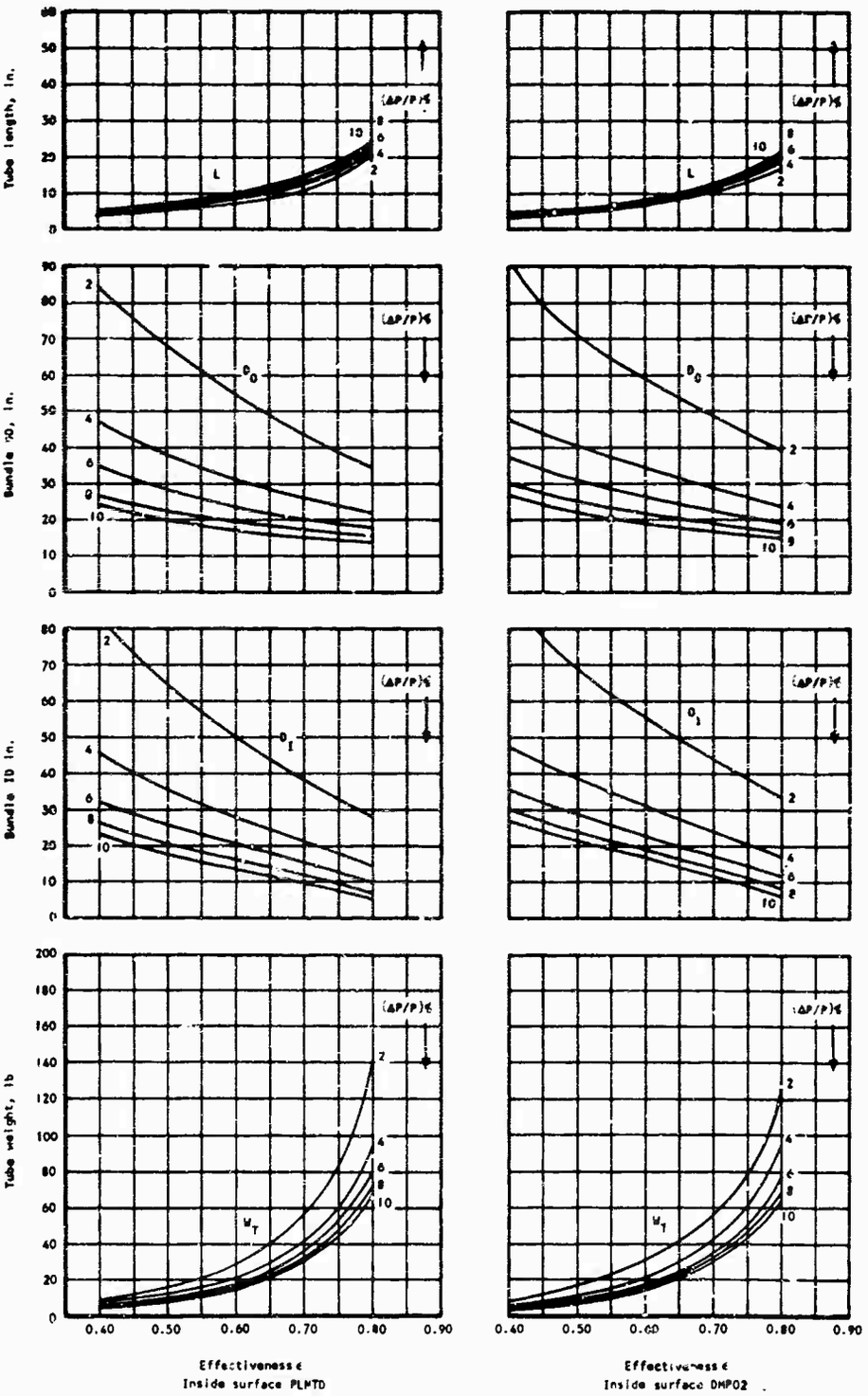

Figure 41. Continued.

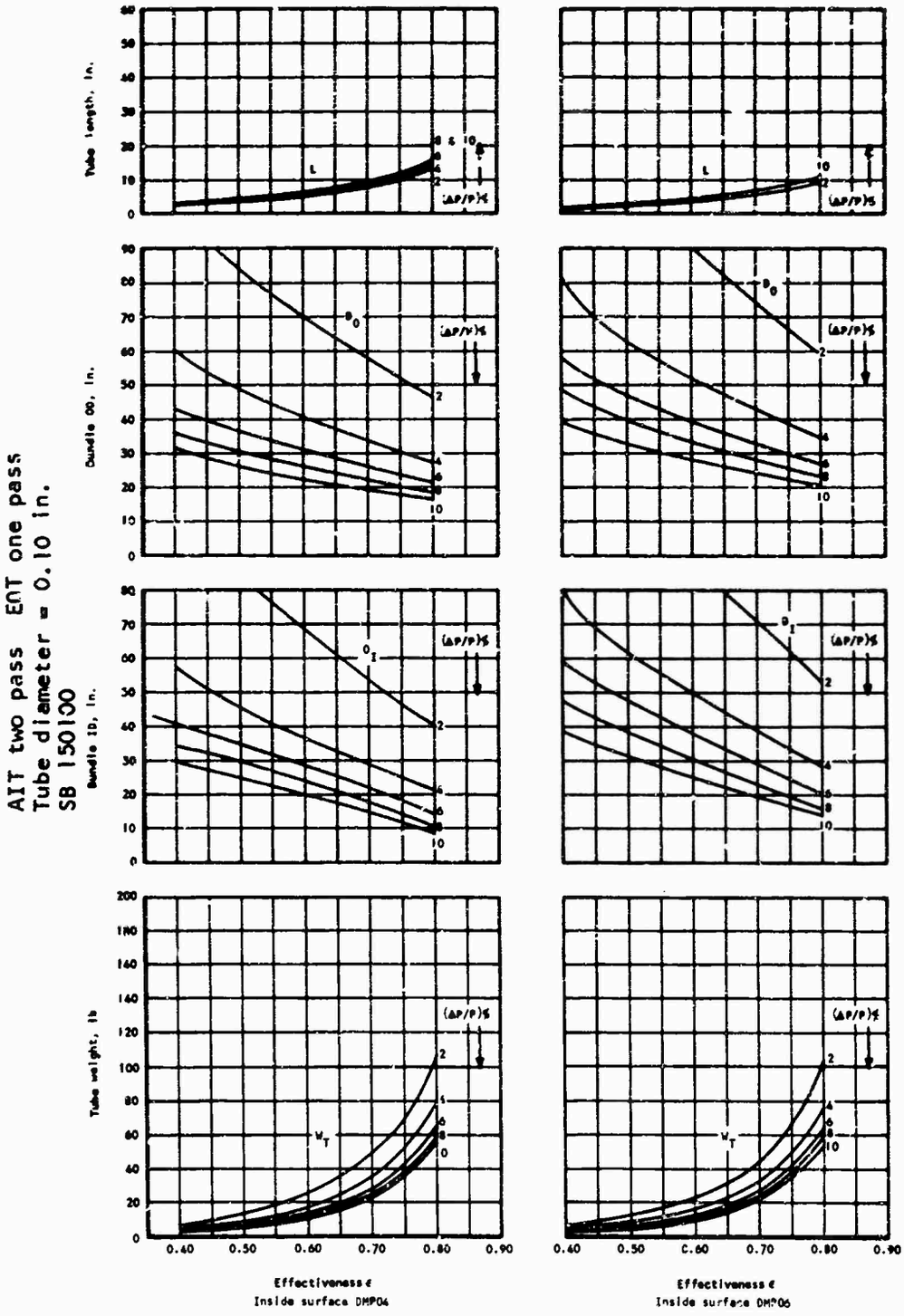

Figure 41. Continued.

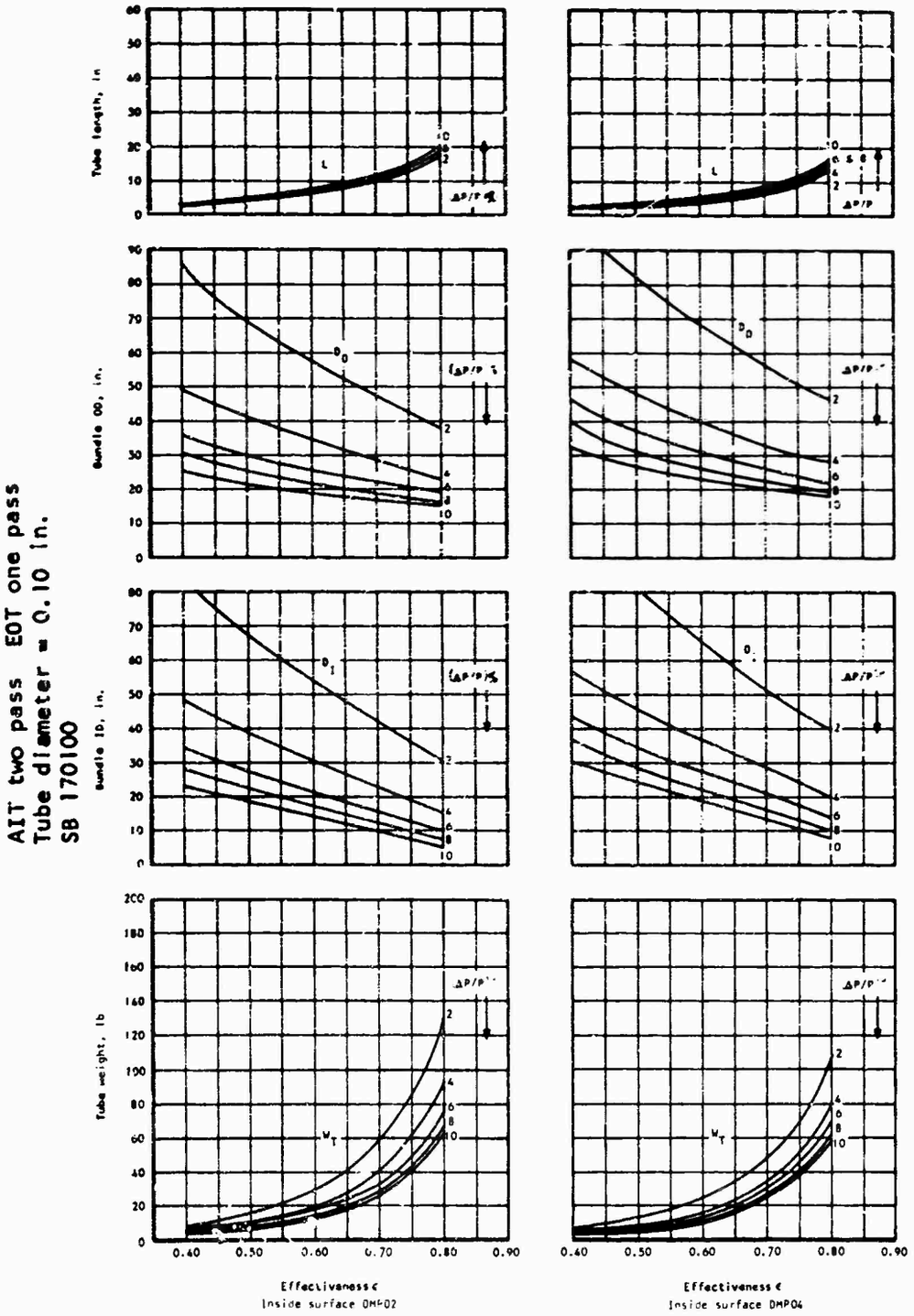

Figure 41. Continued.

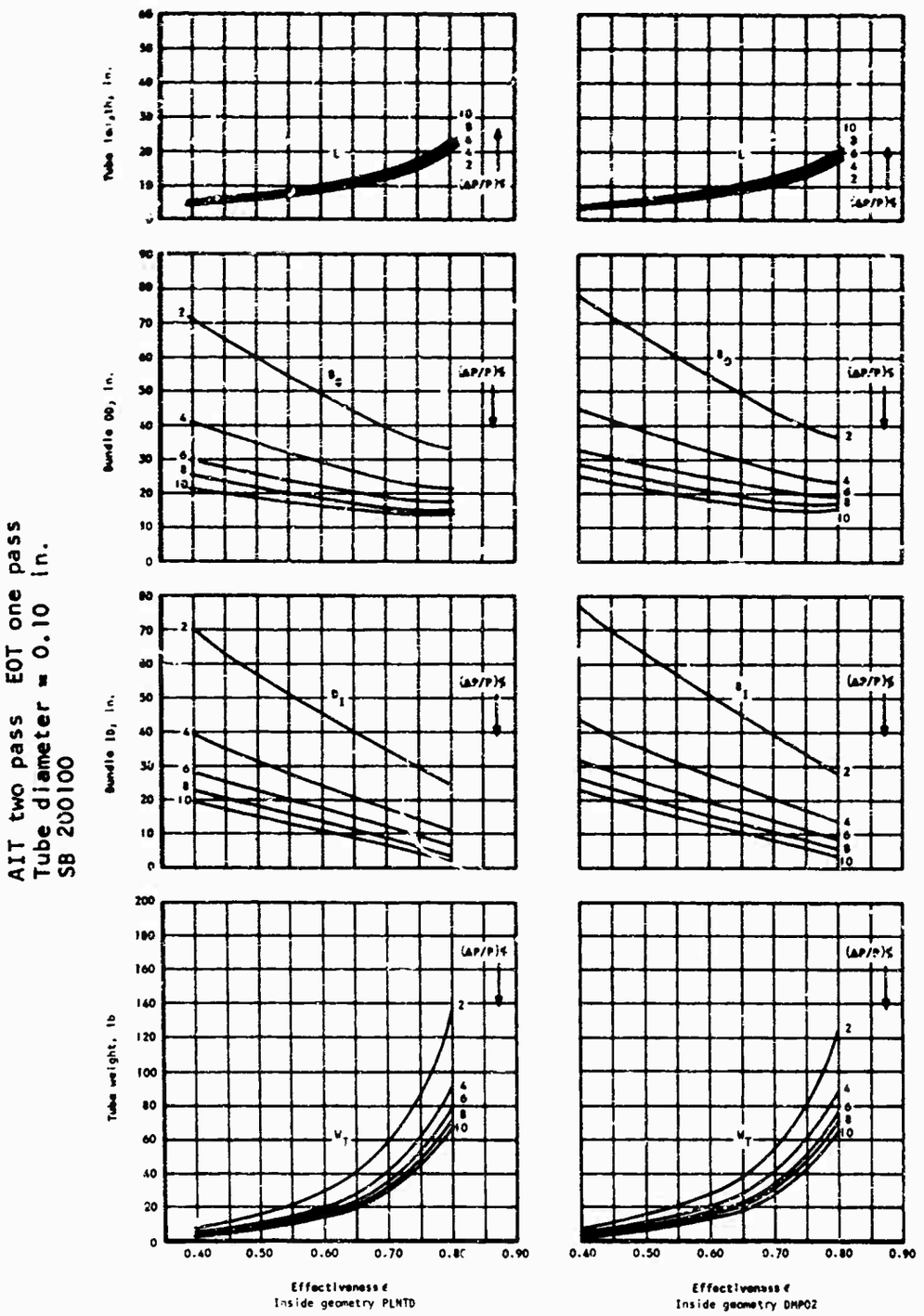

Figure 41. Continued.

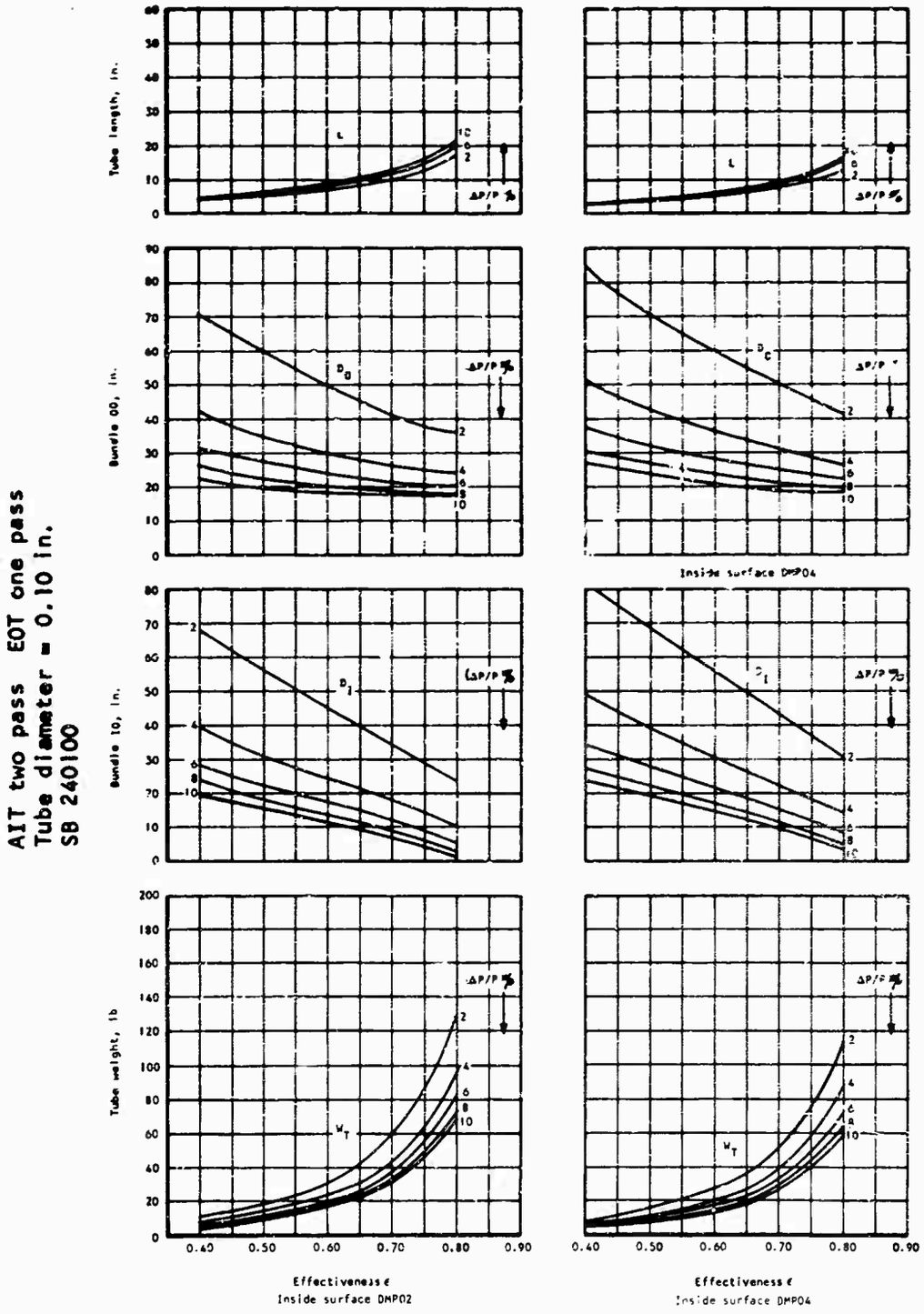

Figure 41. Continued.

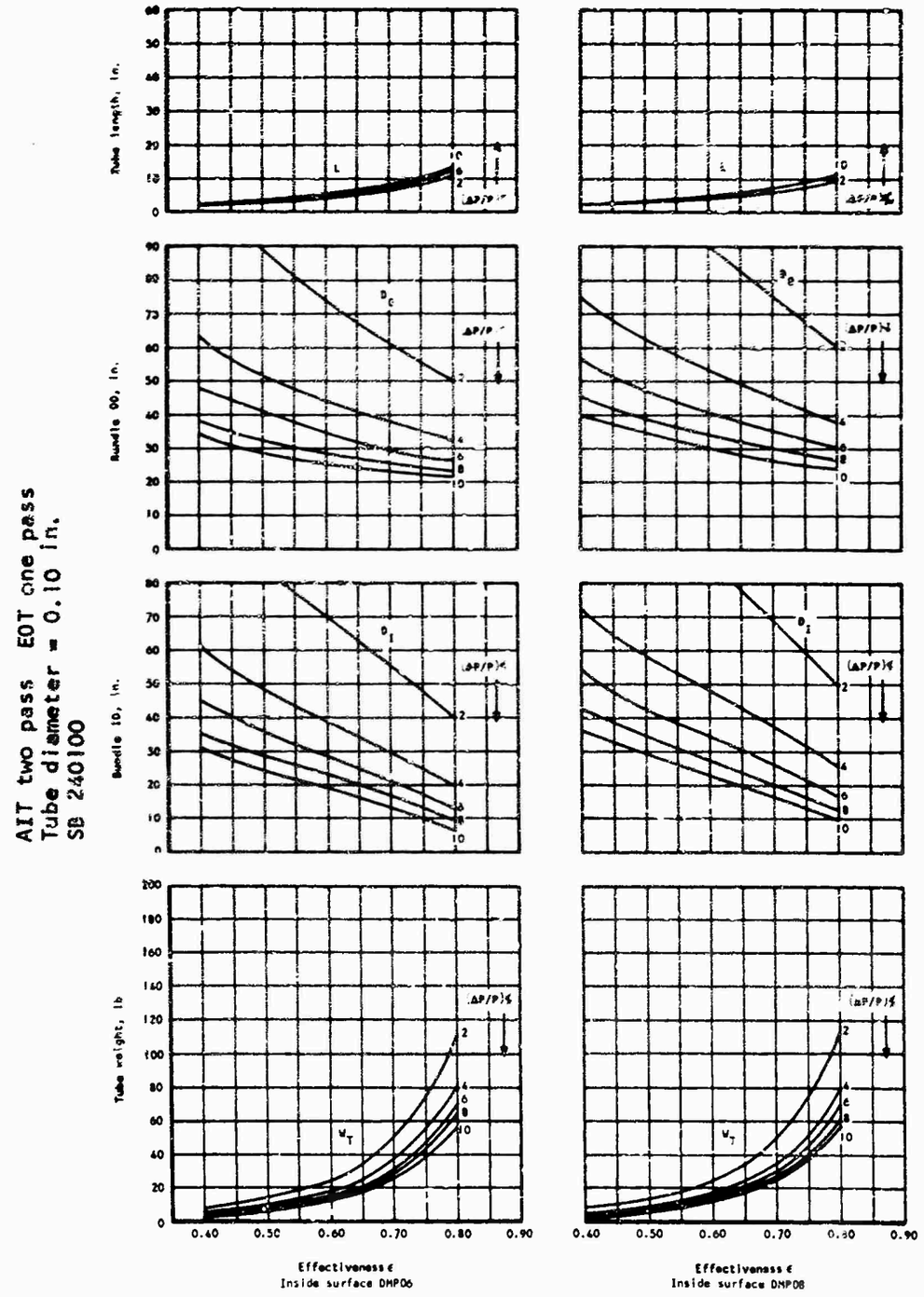

Figure 41. Continued.

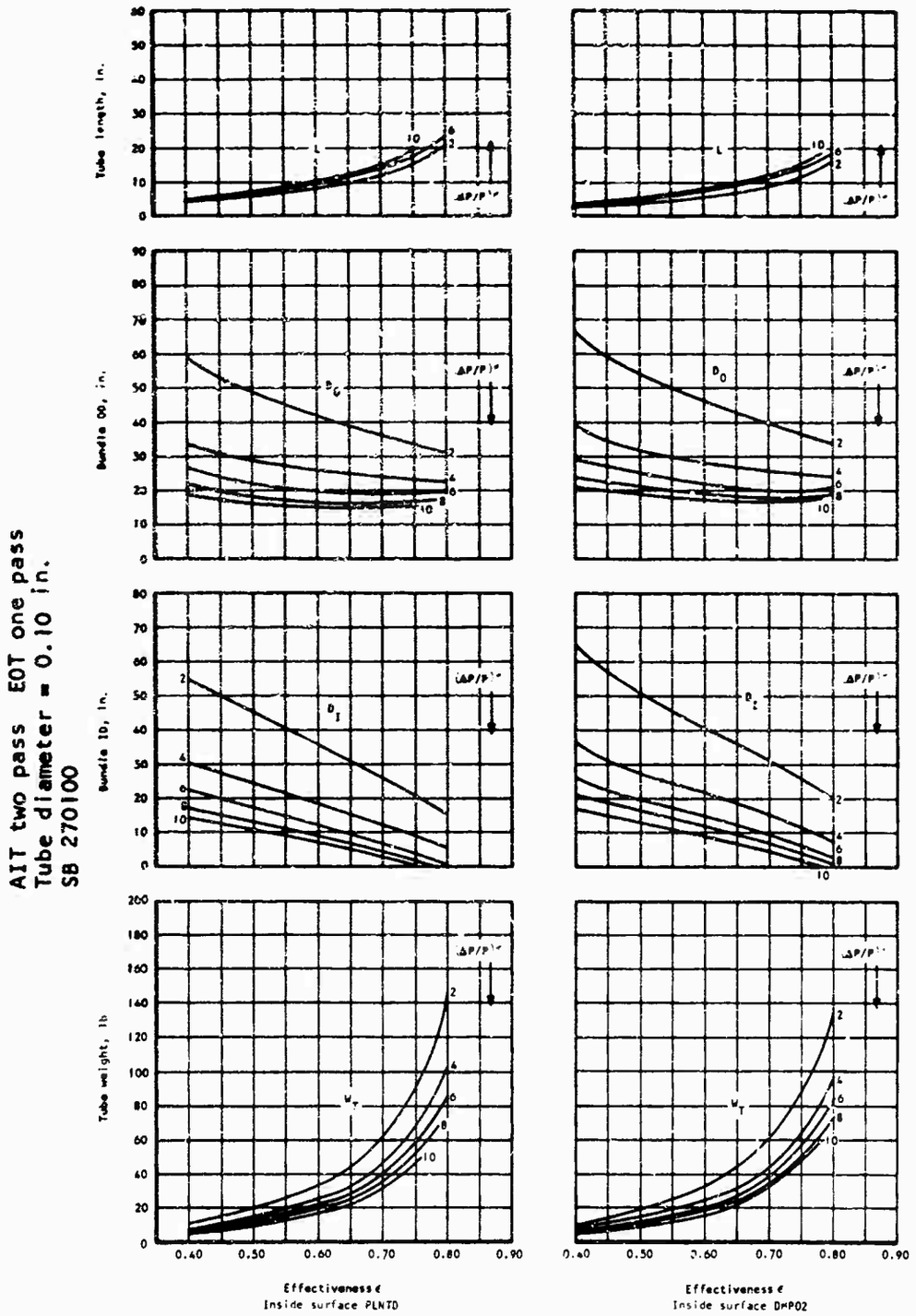

Figure 41. Continued.

AIT two pass EOT one pass
Tube diameter = 0.10 in.
SB 270100

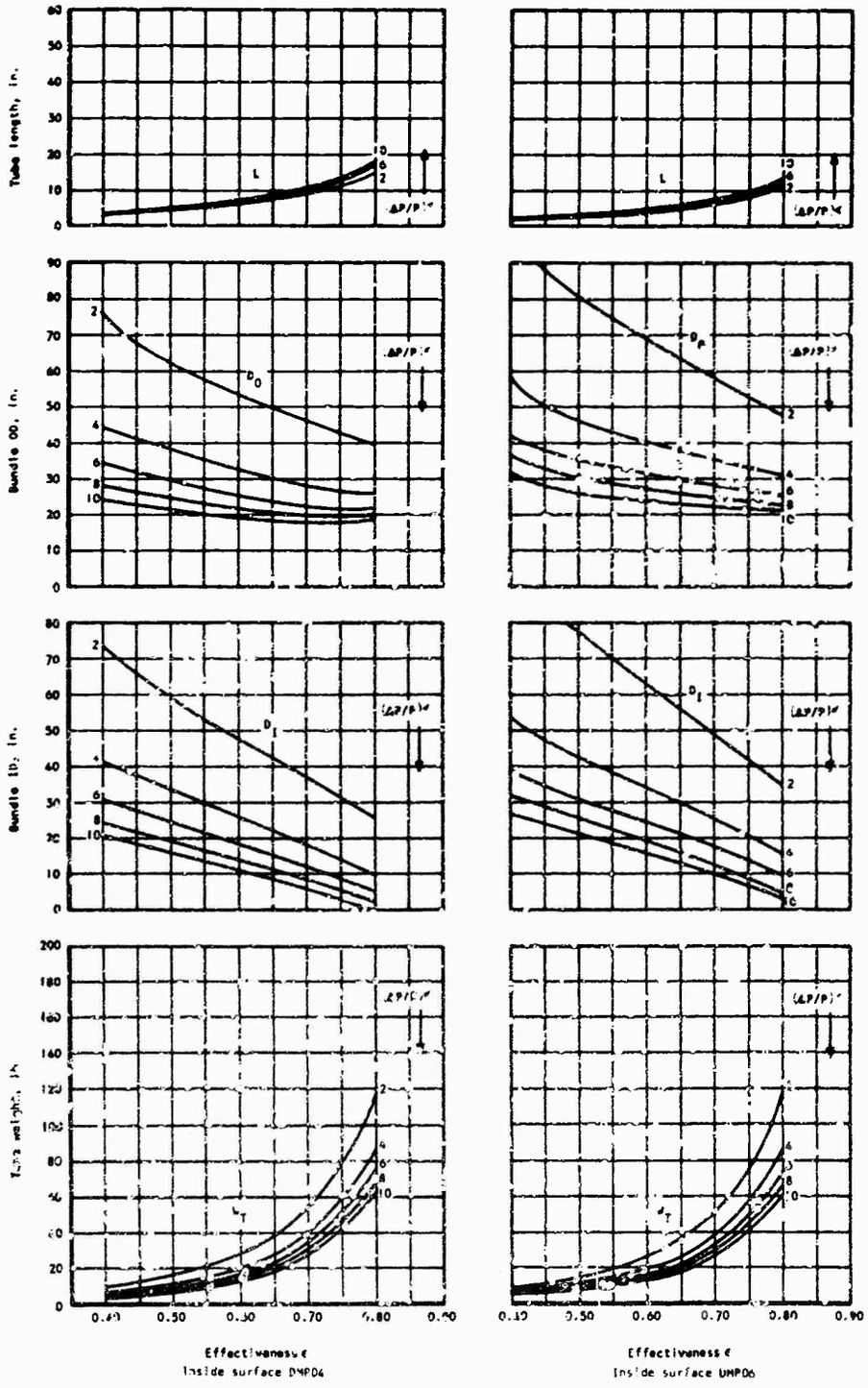

Figure 41. Continued.

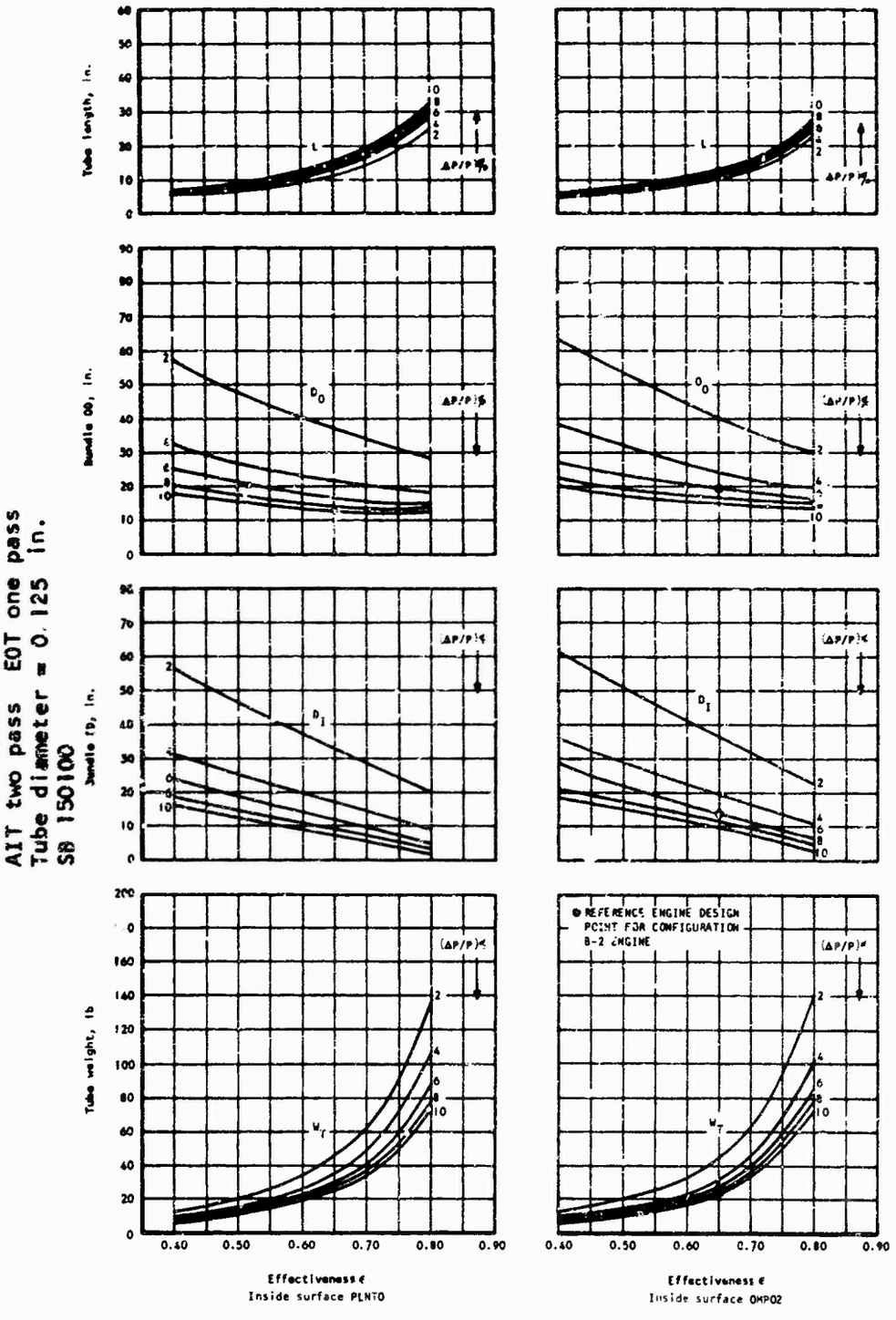

Figure 41. Continued.

AIT two pass EOT one pass
Tube diameter = 0.125 in.
SB 150100

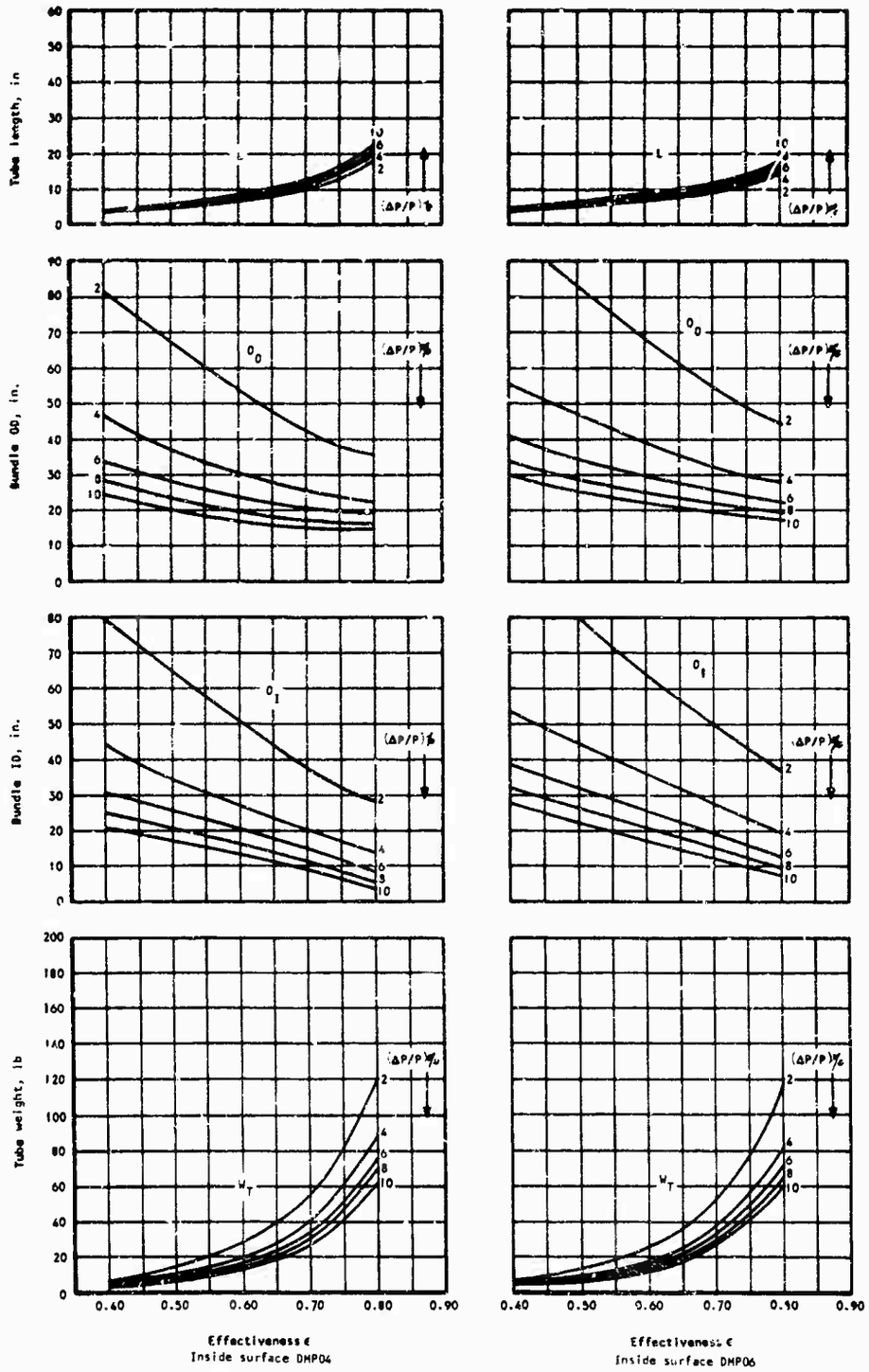

Figure 41. Continued.

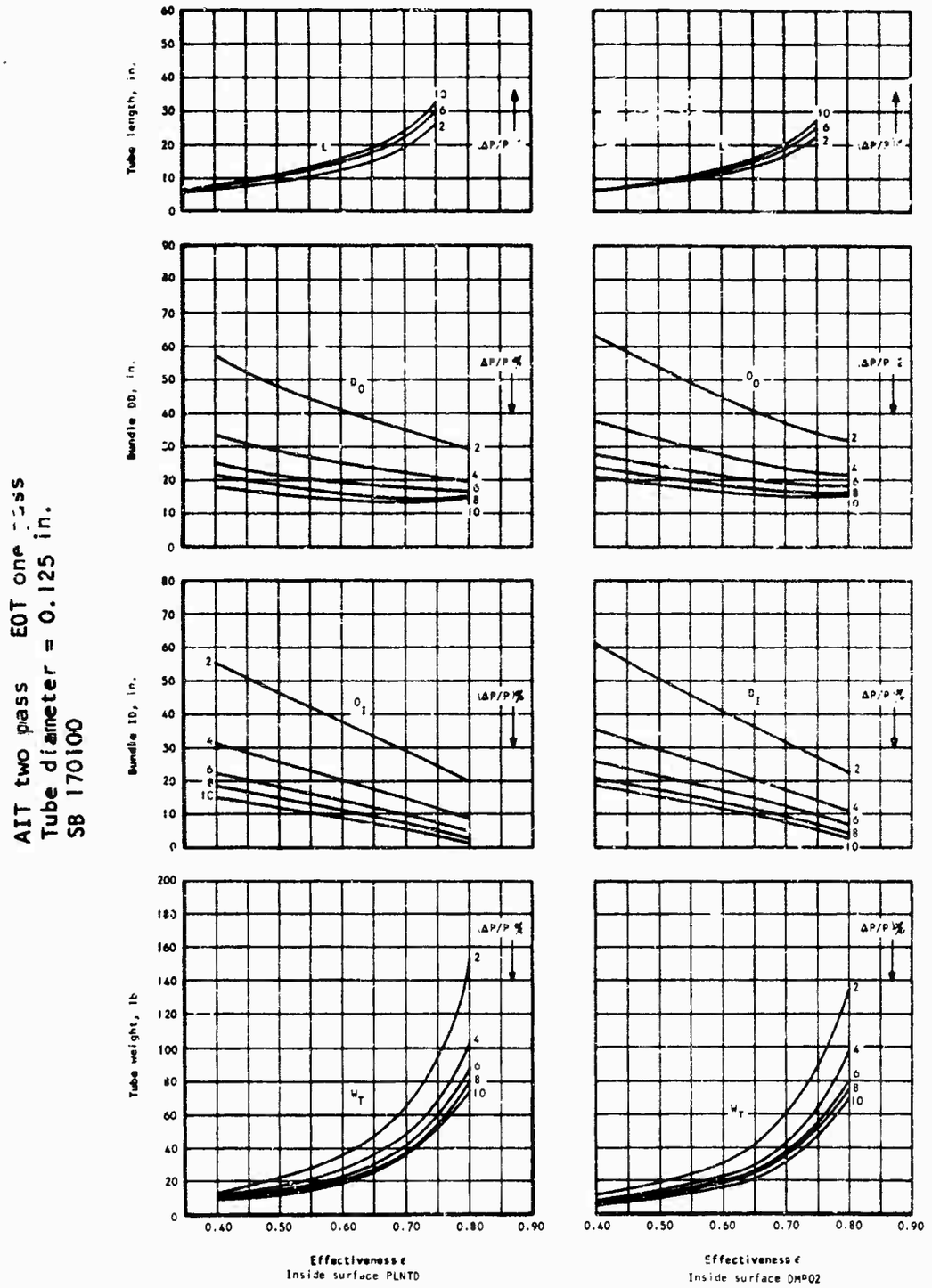

Figure 41. Continued.

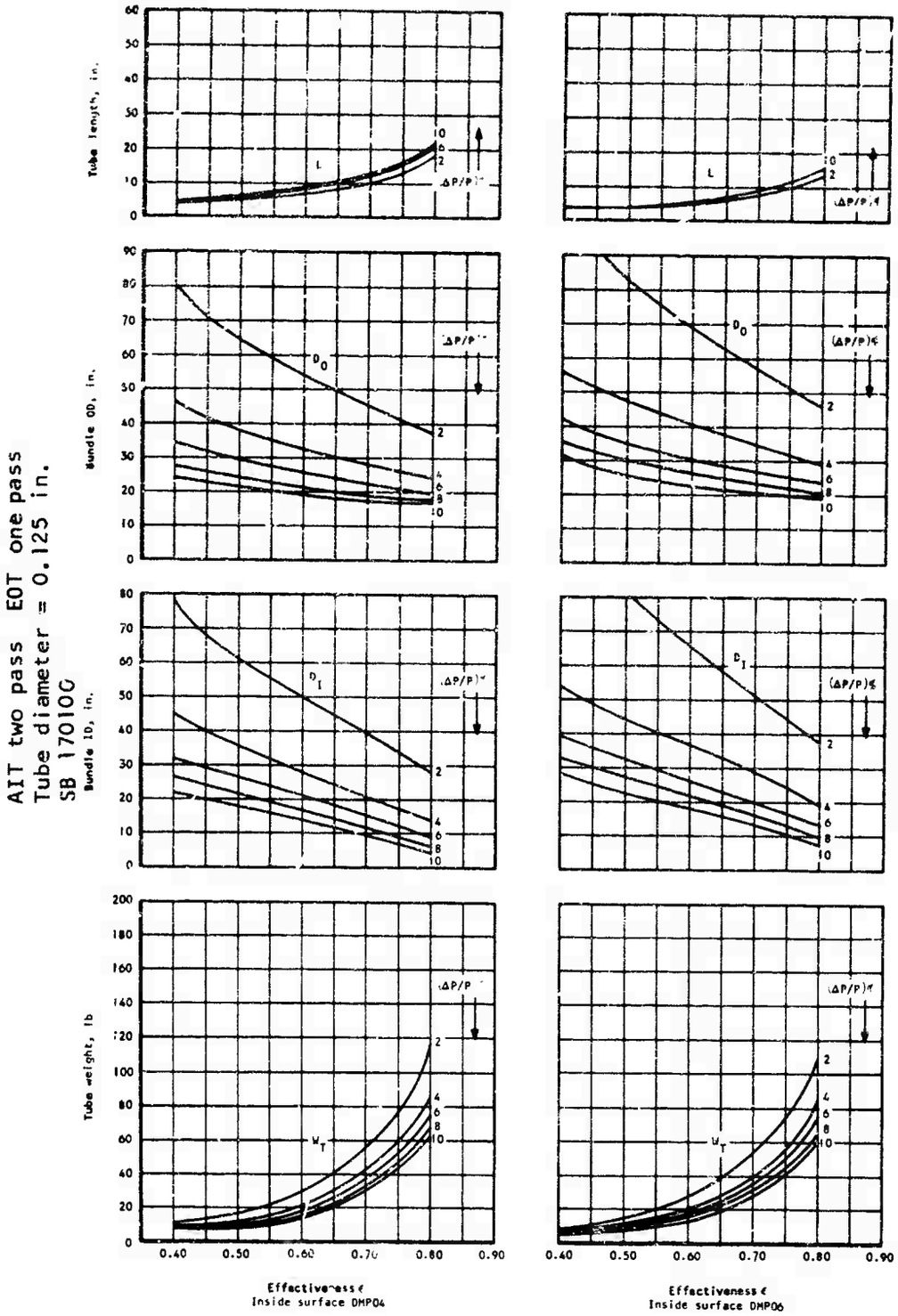

Figure 41. Continued.

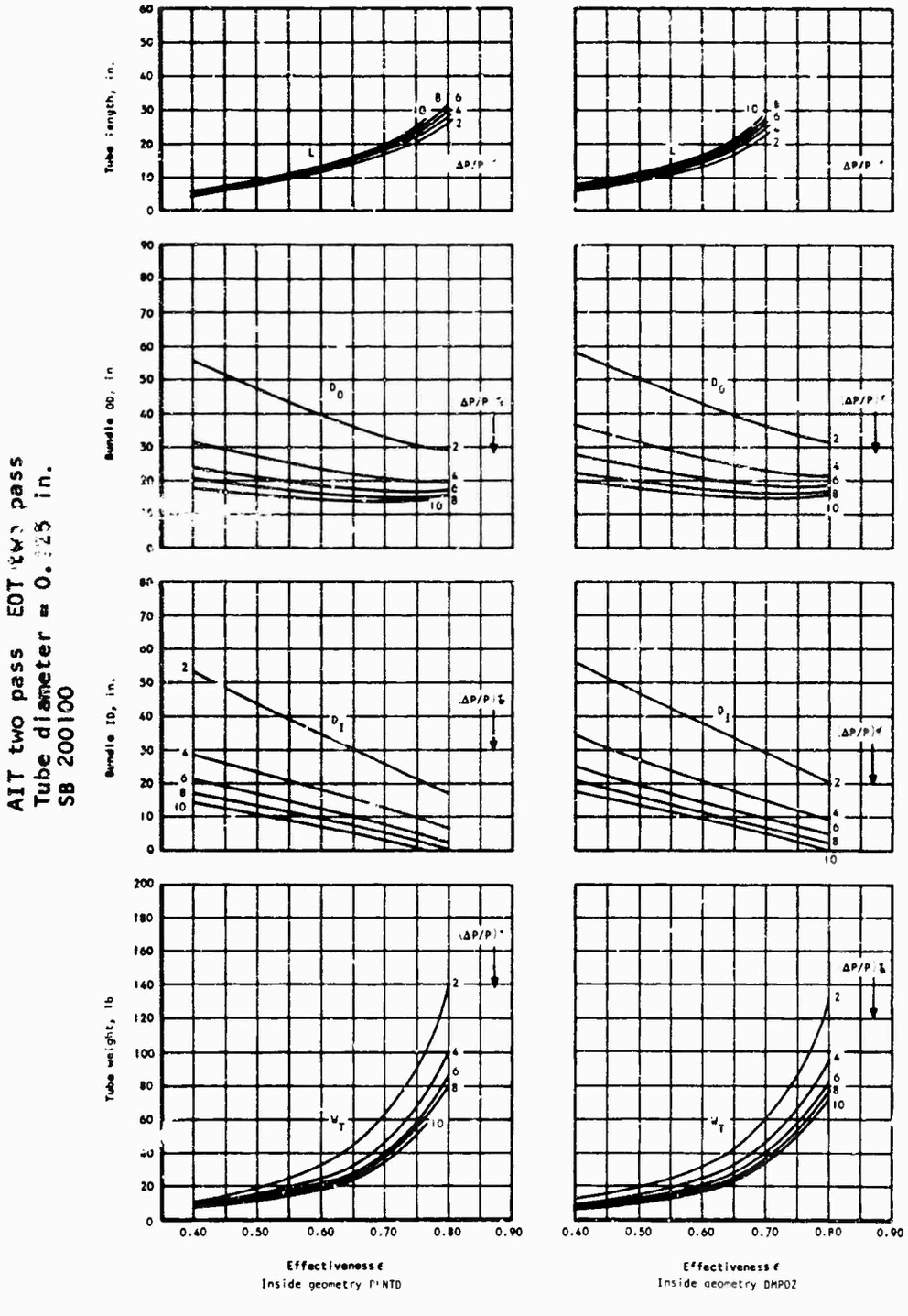

Figure 41. Continued.

AIT two pass EOT one pass
Tube diameter = 0.125 in.
SB 200100

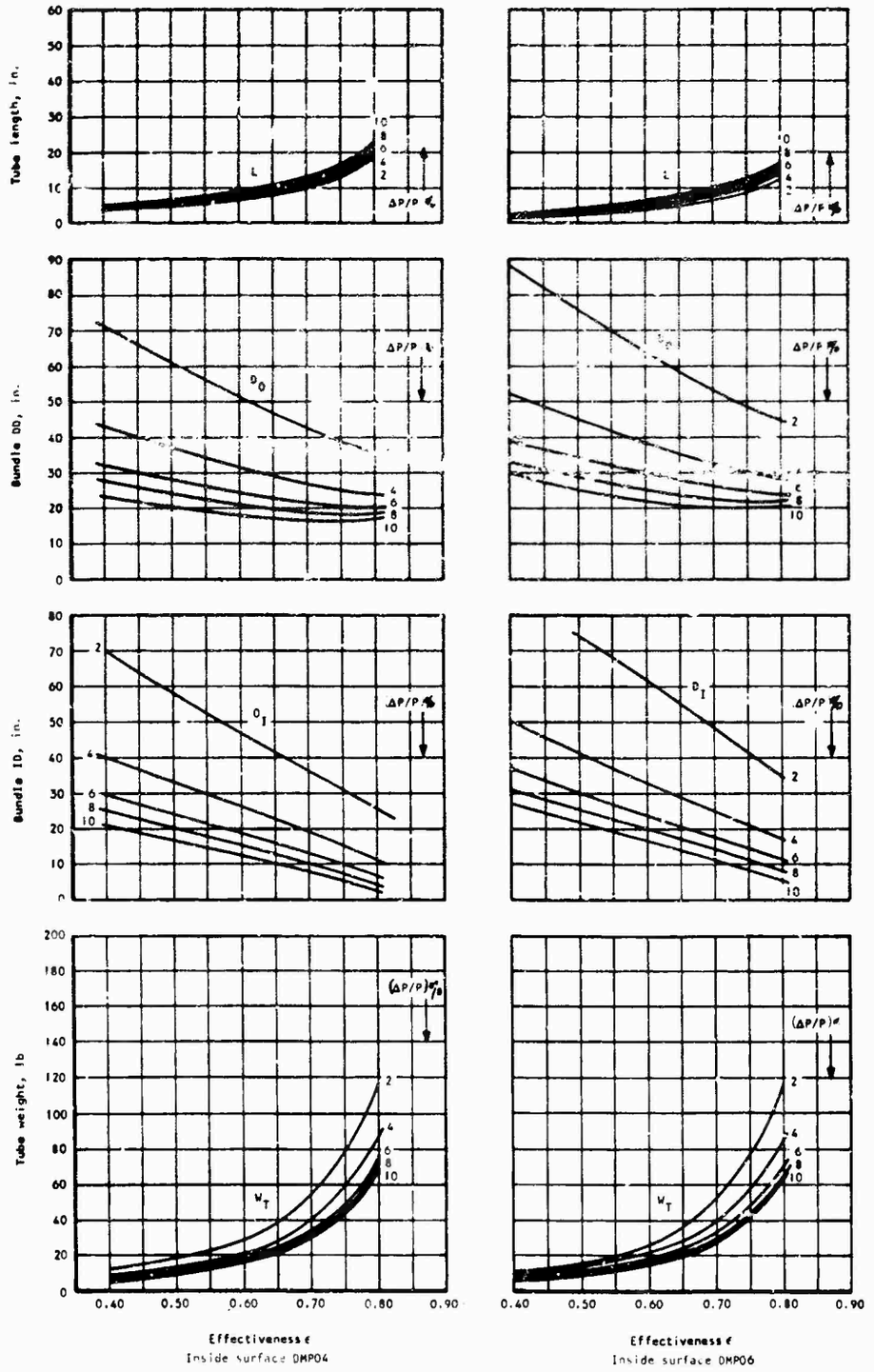

Figure 41. Continued.

AIT two pass EOT one pass
Tube diameter = 0.15 in.
SB 170100

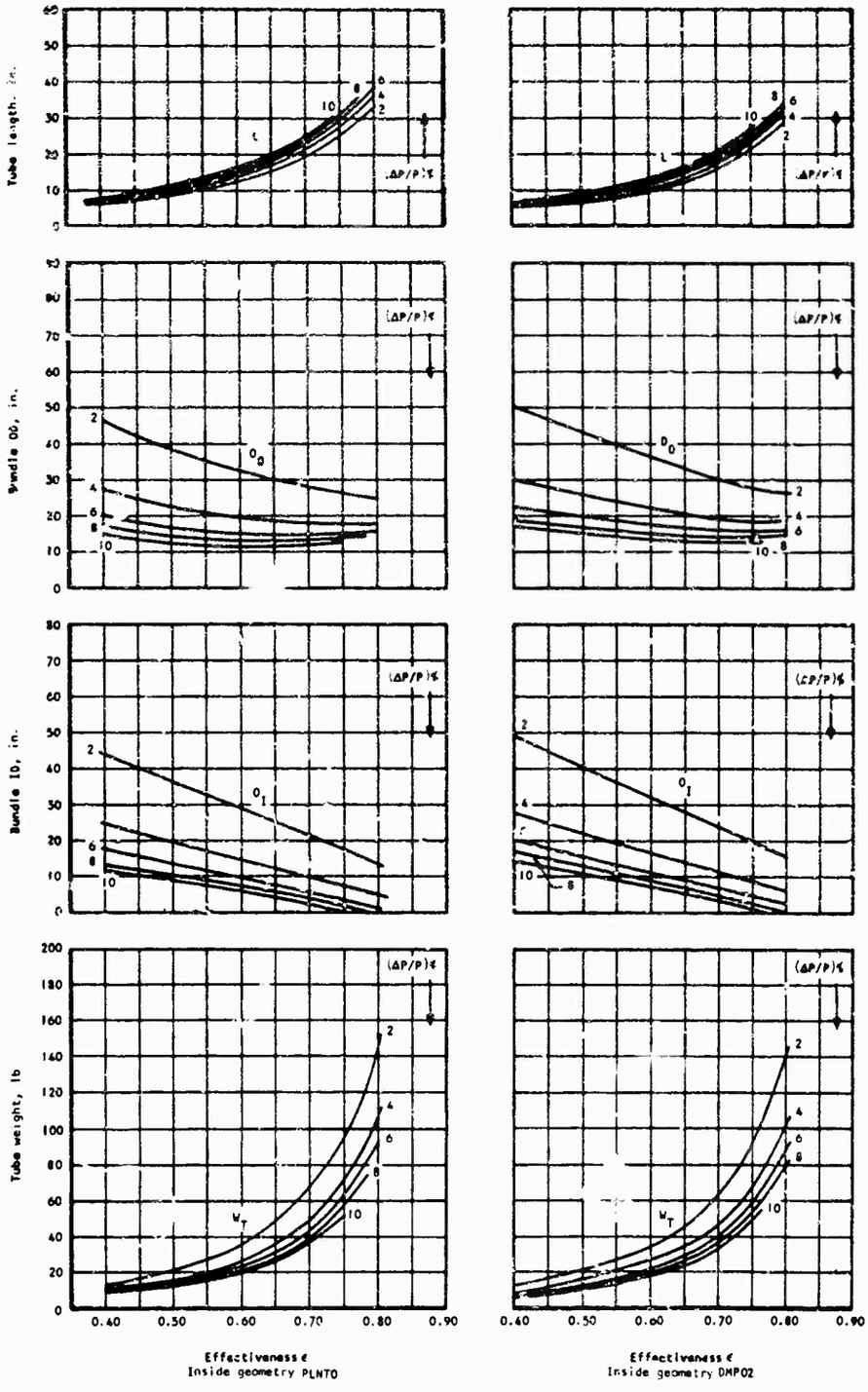

Figure 41. Continued.

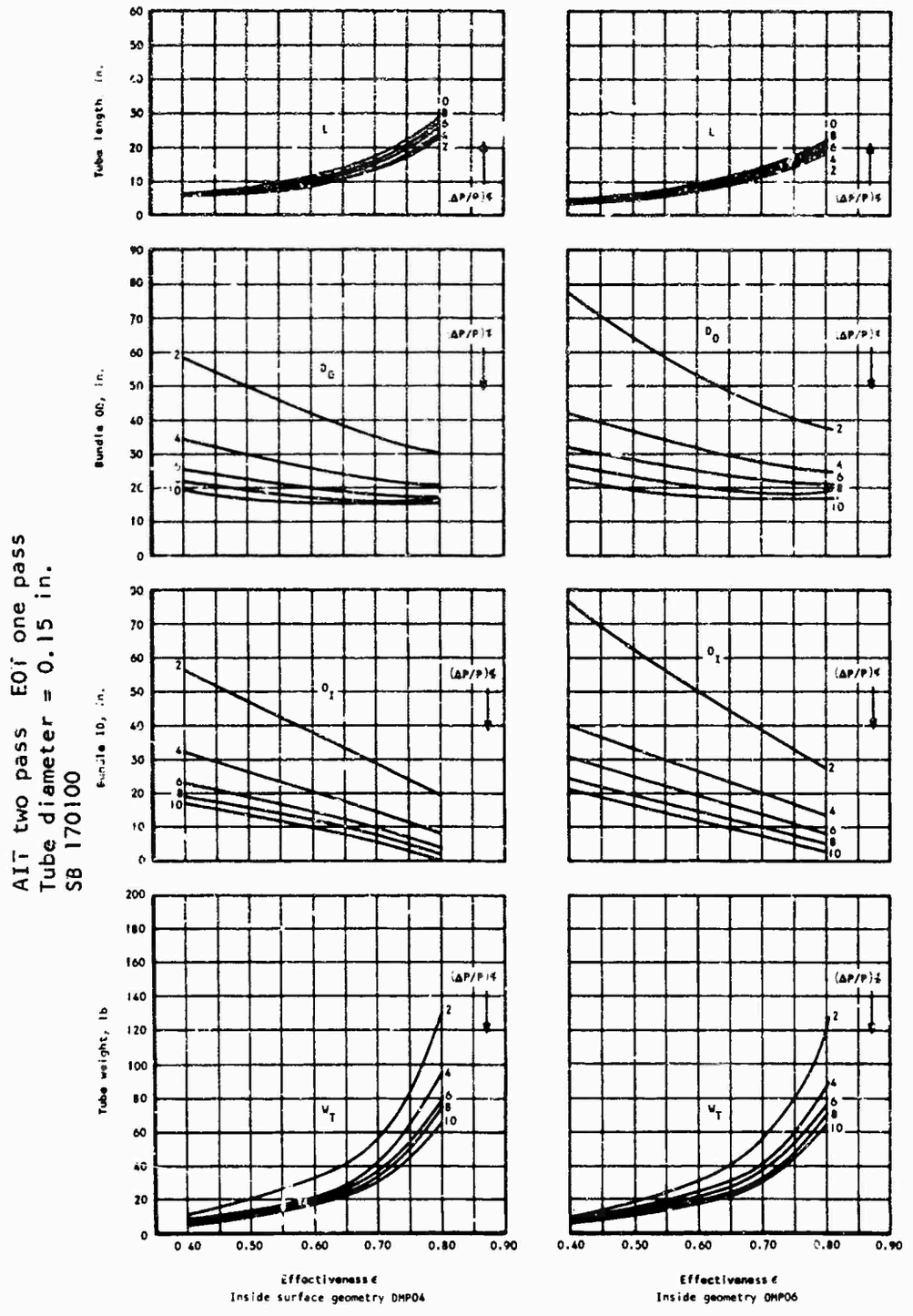

Figure 41. Continued.

AIT two pass EOT one pass
Tube diameter = 0.15 in.
SB 200100

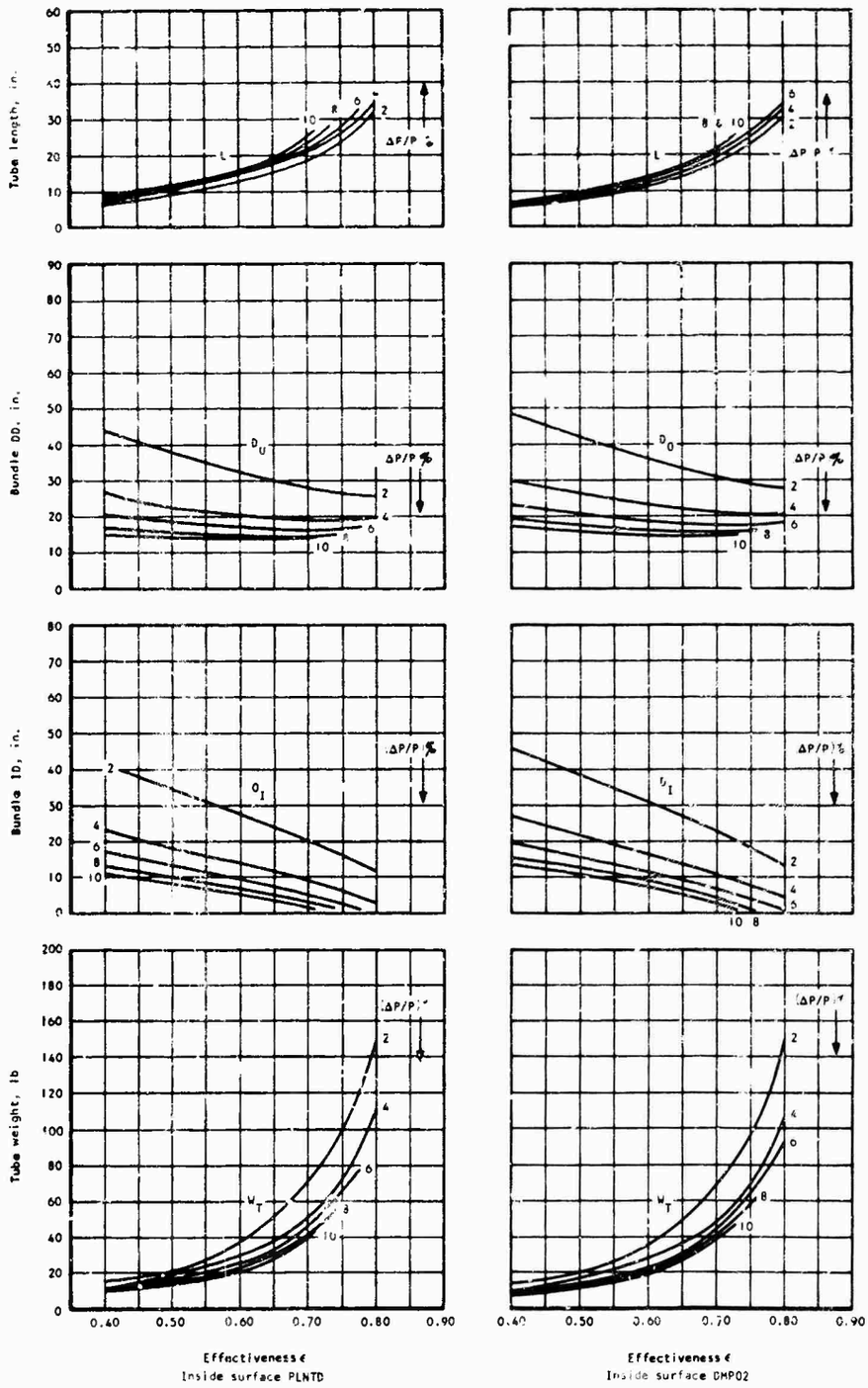

Figure 41. Continued.

AIT two pass EOT one pass
Tube diameter 0.15 in.
SB 200100

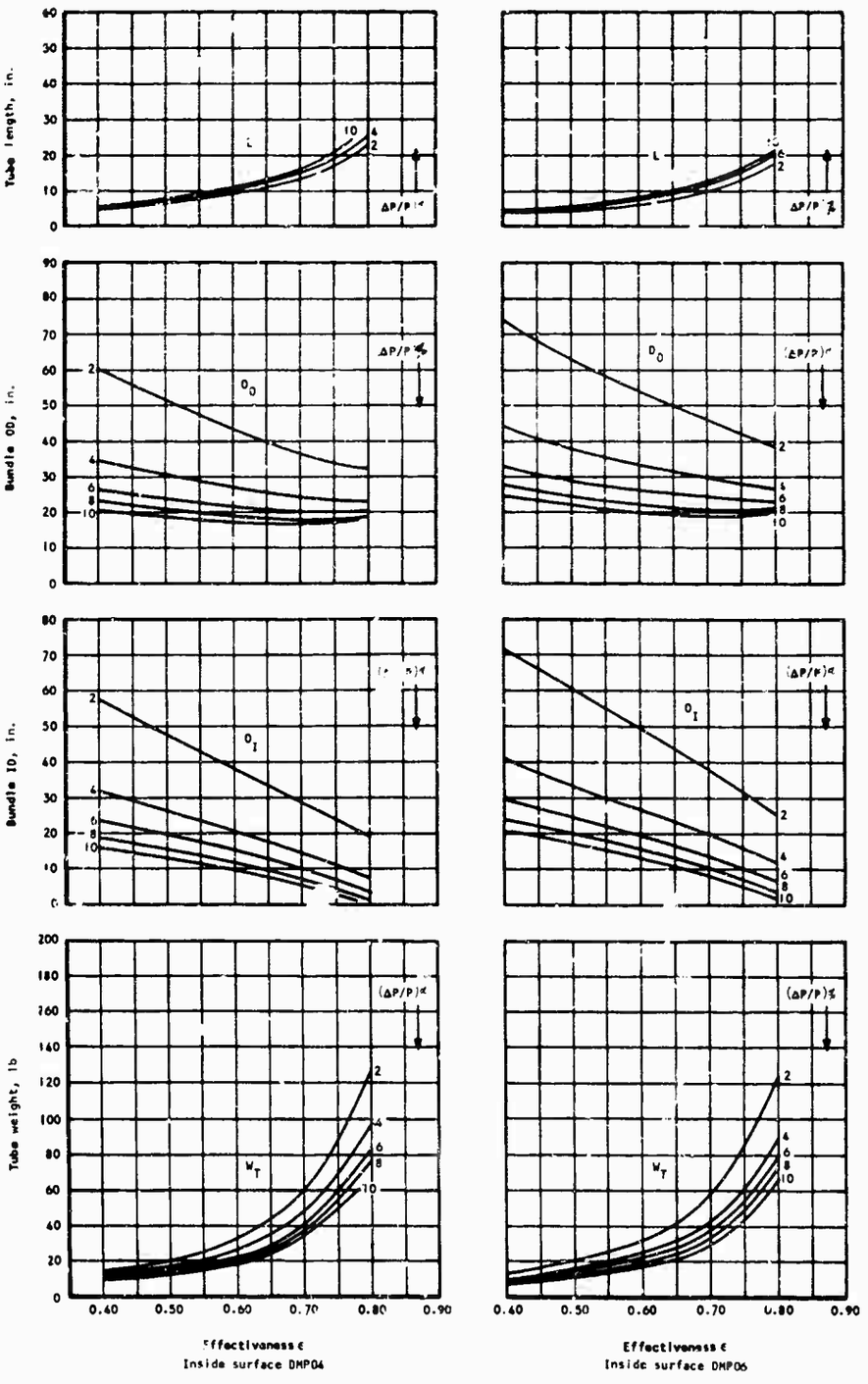

Figure 41. Continued.

AIT two pass EOT one pass
Tube diameter = 0.15 in.
SB 240100

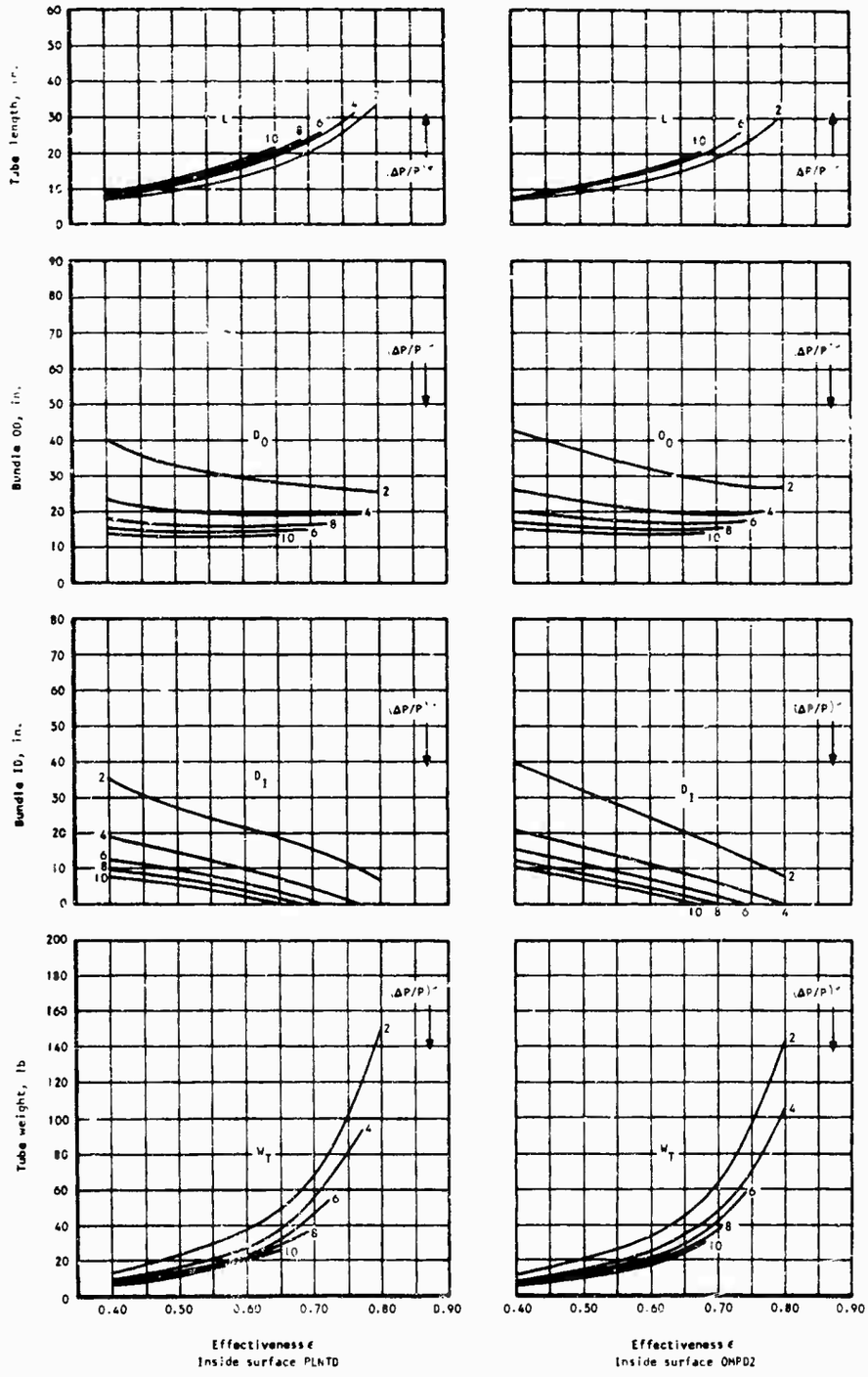

Figure 41. Continued.

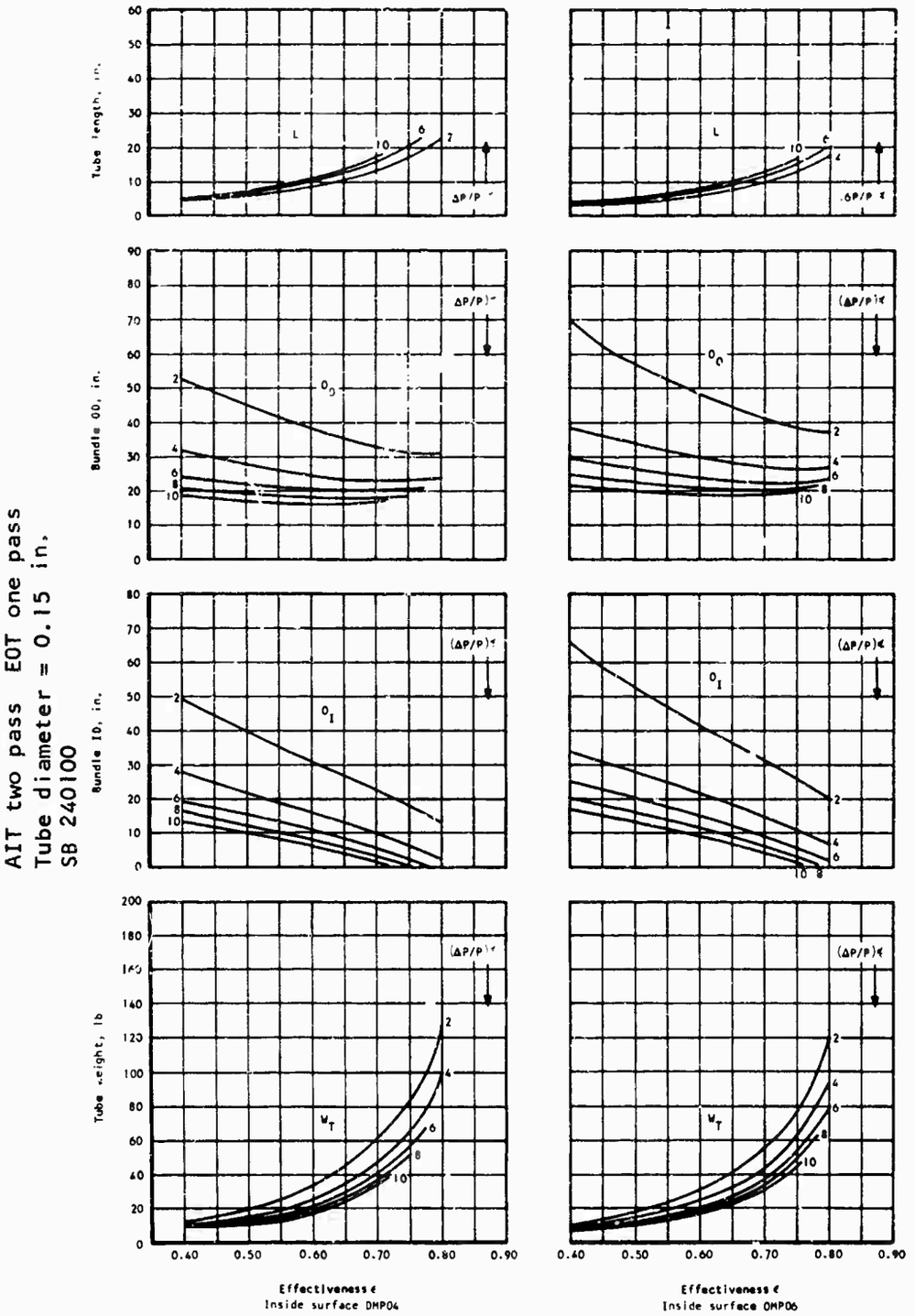

Figure 41. Continued.

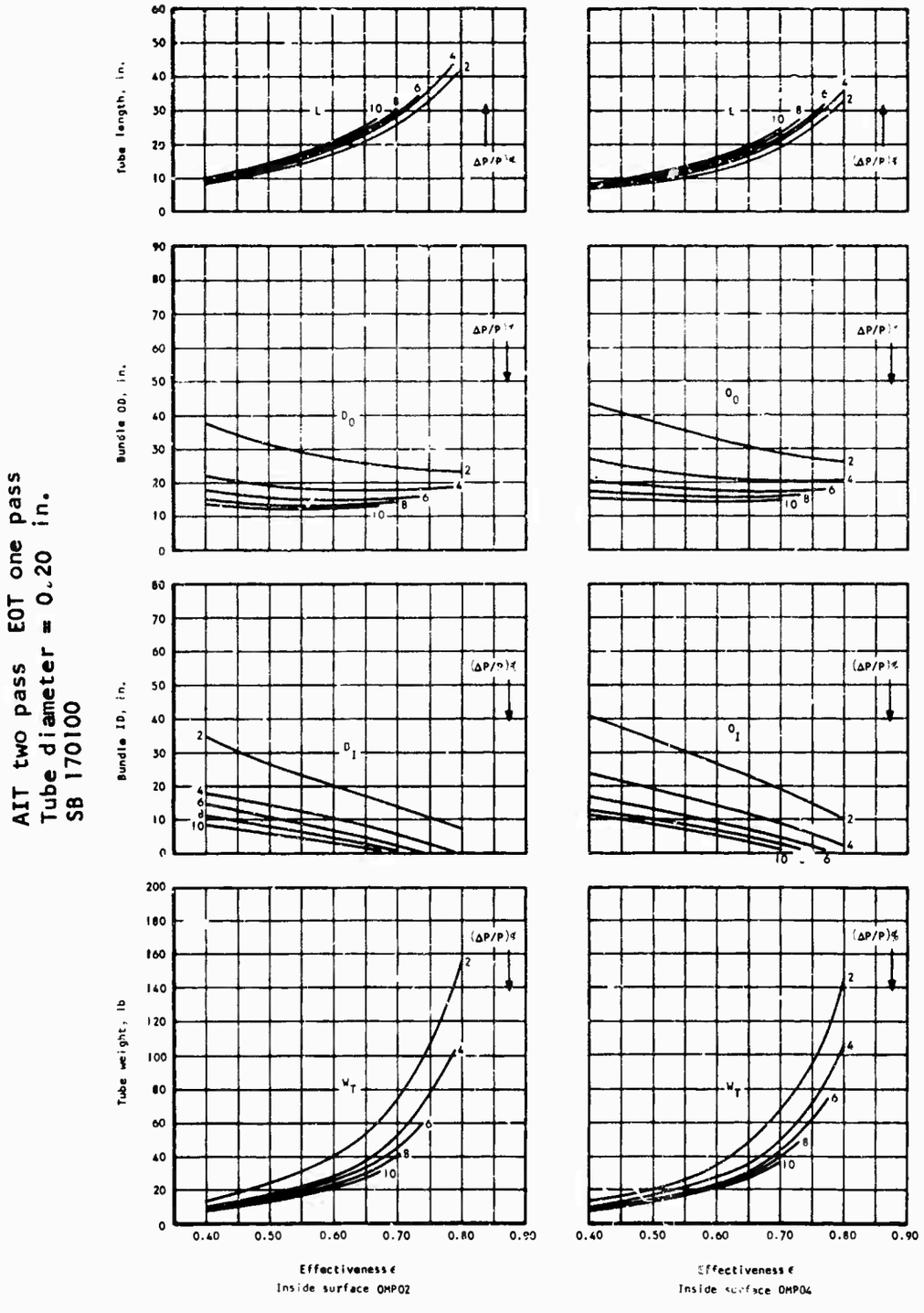

Figure 41. Continued.

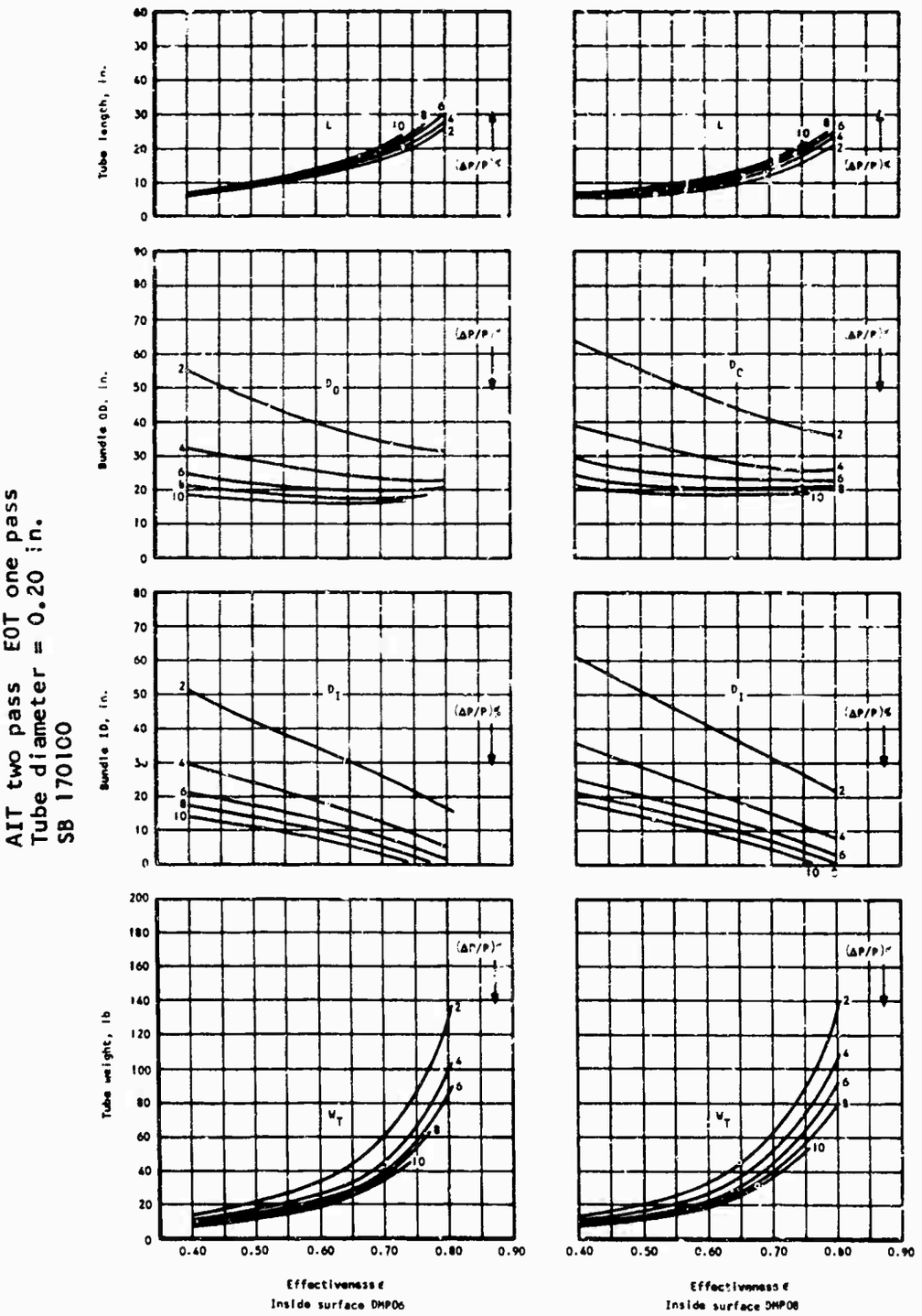

Figure 41. Concluded.

TABLE VIII. SUMMARY OF TUBULAR RECUPERATOR SOLUTIONS FOR REFERENCE ENGINE CONDITIONS (EFFECTIVENESS = 0.65, PRESSURE LOSS = 6 PERCENT)

Engine Configuration	A-1	A-2	B-1	B-2
Flow Configuration	Two-Pass Cross Counterflow	Three-Pass Cross Counterflow	Two-Pass Cross Counterflow	Two-Pass Cross Counterflow
Number of Air Passes	1 AIT	1 AIT	1 AIT	2 AIT
Number of Gas Passes	2 EOT	3 EOT	2 EOT	1 EOT
Tube Outer Diameter, in.	0.100	0.100	0.100	0.125
Tube Pattern	Staggered	In Line	Staggered	Staggered
Transverse Pitch X_T	3.00	2.00	2.70	1.50
Longitudinal Pitch X_L	1.0	1.25	1.00	1.00
Outside Surface Reference	SB300100	IB200125	SB270100	SB150100
Dimple Parameter ψ	0.04	0.06	0.04	0.02
Tube Bundle ID, in.	15.83	17.18	18.15	14.36
Tube Bundle OD, in.	20.83	22.50	22.15	18.86
Tube Length, in.	16.20	16.18	15.45	12.22
Tube Weight, lb	27.14	37.59	25.29	26.90
Number of Tubes	4800	6656	4690	5004
Core Volume, ft^3	1.35	1.55	1.13	0.83
Surface Compactness, ft^2/ft^3	241.0	289.0	268.0	389.0

the tube dimples. For designs with external secondary surfaces, the inside heat transfer coefficient can be increased by utilizing a plain strip, a spiral strip or a flap turbulator inside the tube. Details of these turbulence promoting devices are shown in Figure 42. With the plain strip brazed inside the tube, the hydraulic diameter is effectively reduced; this, together with the increase in heat transfer surface area, results in an improved internal conductance. Although the spiral strip and the flap turbulator are more effective heat transfer promoters, the associated large increase in friction factor results in core sizes of very large flow frontal area and small flow length for units such as a gas turbine recuperator where a very limited pressure loss is allowed. In the recuperator analysis, plain tubes, plain tubes with an internal strip, and plain tubes with an internal flap turbulator were evaluated.

Outside Surface Geometries

Disc-finned arrangements of the type shown in Figure 43a were evaluated for both staggered and in-line tube patterns. From a 33-disc-finned-tube inventory, 5 surfaces were selected as being representative for air-to-gas heat exchanger application. Using the finned-tube terminology given in Figure 43a and b, details of the selected surfaces are outlined in Table IX.

Heat transfer and pressure drop data used in the analysis for flow outside the selected in-line and staggered tube arrangements are based on AiResearch test data obtained from a series of small test cores. For each of the four engine configurations, extensive use was made of the same computer program as used in the tubular recuperator analysis and described in the previous section.

The initial analysis was aimed at establishing the optimum recuperator pressure loss split to give minimum weight solutions. As in previous recuperator studies, a survey of the computer output showed that the finned-tube geometry was not very attractive, primarily because finning of the tubes adds area to the side of the heat exchanger that already has the higher conductance (i.e., flow across the tube bundle). The addition of heat transfer area to the high-conductance side represents an inefficient use of heat transfer area, and thus results in a high-weight design. The recuperators with the flap turbulators inside the tubes yielded the lightest weight solutions, but the core flow frontal areas were so large that the units were incompatible with the turbomachinery. The designs with the plain strip inserted in the tube gave slightly lighter weight solutions than the plain tube. From the thousands of computer solutions, the most attractive designs from the standpoints of minimum weight and compatibility with the turbomachinery were associated with the IFT 12 surface. At the 65 percent effectiveness and 6 percent pressure loss levels, the effect of pressure loss split on tube and fin weight for a range of tube diameters is shown in Figure 44 for the IFT 12 outside surface geometry, for plain tubes with plain strip inserts as the inside surface. As can be seen, a 60/40 hot-to-cold side pressure loss split results in units close to minimum core weight. This value is in agreement with the findings of the plain

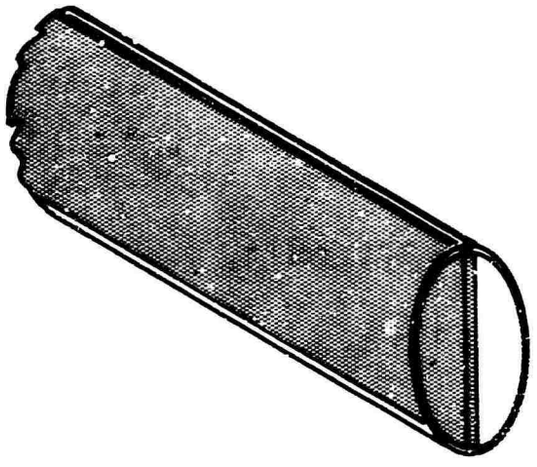

(a) Internal plain strip

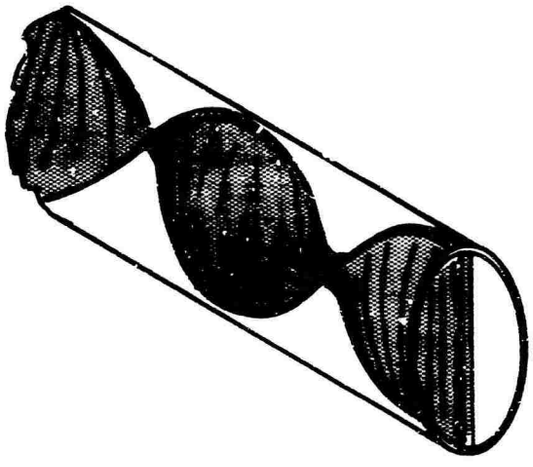

(b) Internal spiral strip

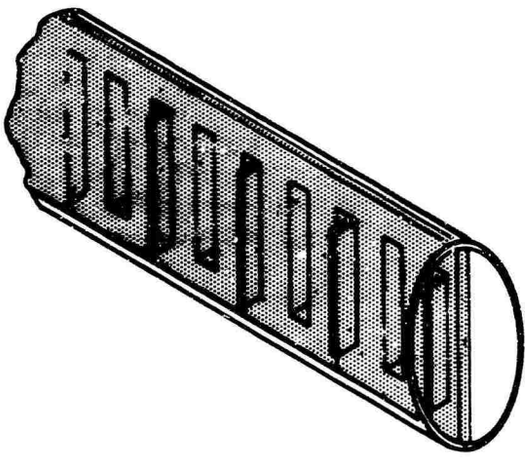

(c) Internal flap turbulator

Figure 42. Internal Turburlence-Promoting Devices.

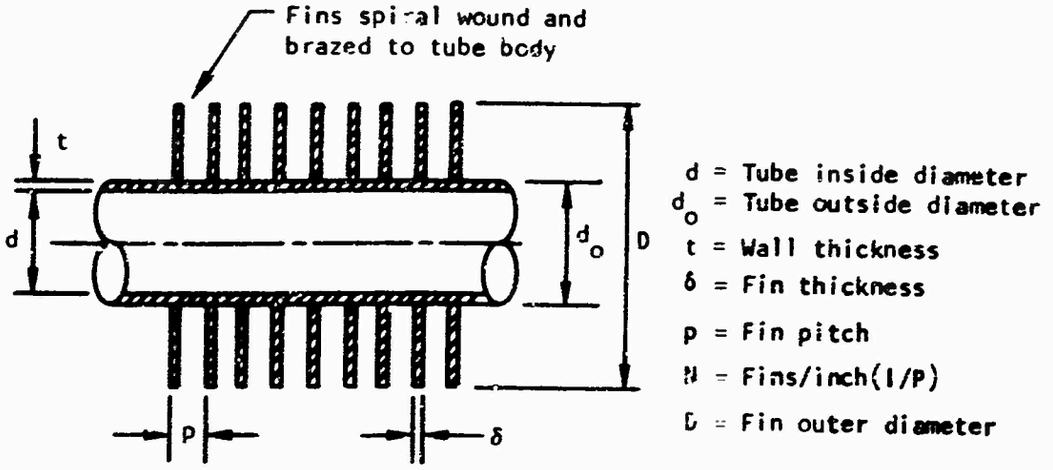

a) Disc-finned tube geometry

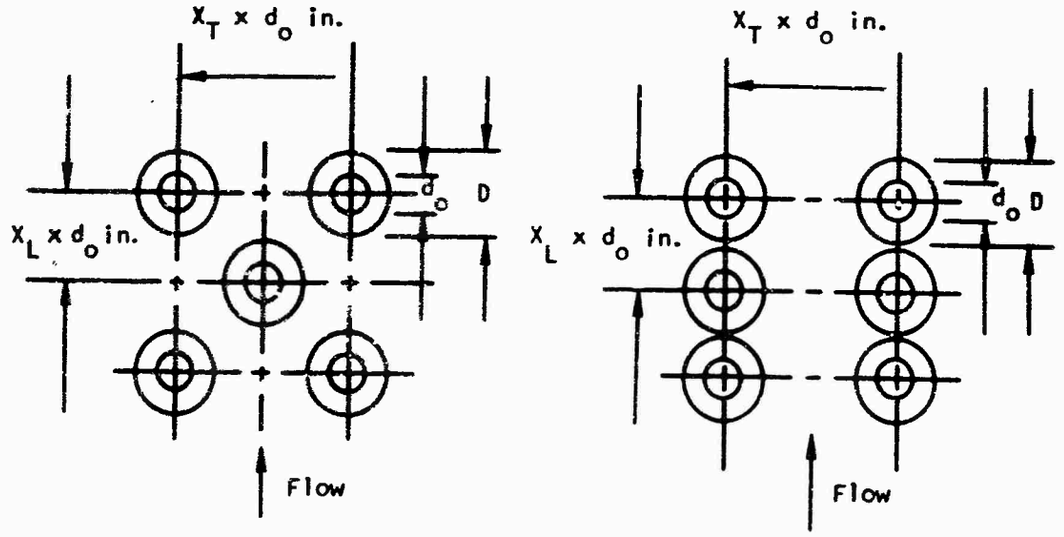

Staggered tube arrangement (SFT)

In-line tube arrangement (IFT)

d_o = Tube outside diameter

X_T = Transverse pitch as defined in sketch

X_L = Longitudinal pitch as defined in sketch

b) Outside surface geometries

Figure 43. Finned-Tube Surface Geometries.

TABLE IX. FINNED-TUBE SURFACE GEOMETRY DETAILS

Surface Designation	Tube Pattern	$\frac{\text{Fin Dia } D}{\text{Tube Dia } d_o}$	Transverse Pitch, X_T	Longitudinal Pitch, X_L	No. Fins per Inch, N	Tube Wall Thickness t, in.	Fin Thickness δ
IFT 3	In-Line	2.0	2.83	2.50	30.0	0.004	0.004
IFT 9	In-Line	2.5	2.83	2.50	30.0	0.004	0.004
IFT 12	In-Line	2.18	2.20	2.20	25.8	0.004	0.004
SFT 16	Staggered	2.50	2.60	2.26	30.0	0.004	0.004
SFT 18	Staggered	1.25	2.00	1.00	30.0	0.004	0.004

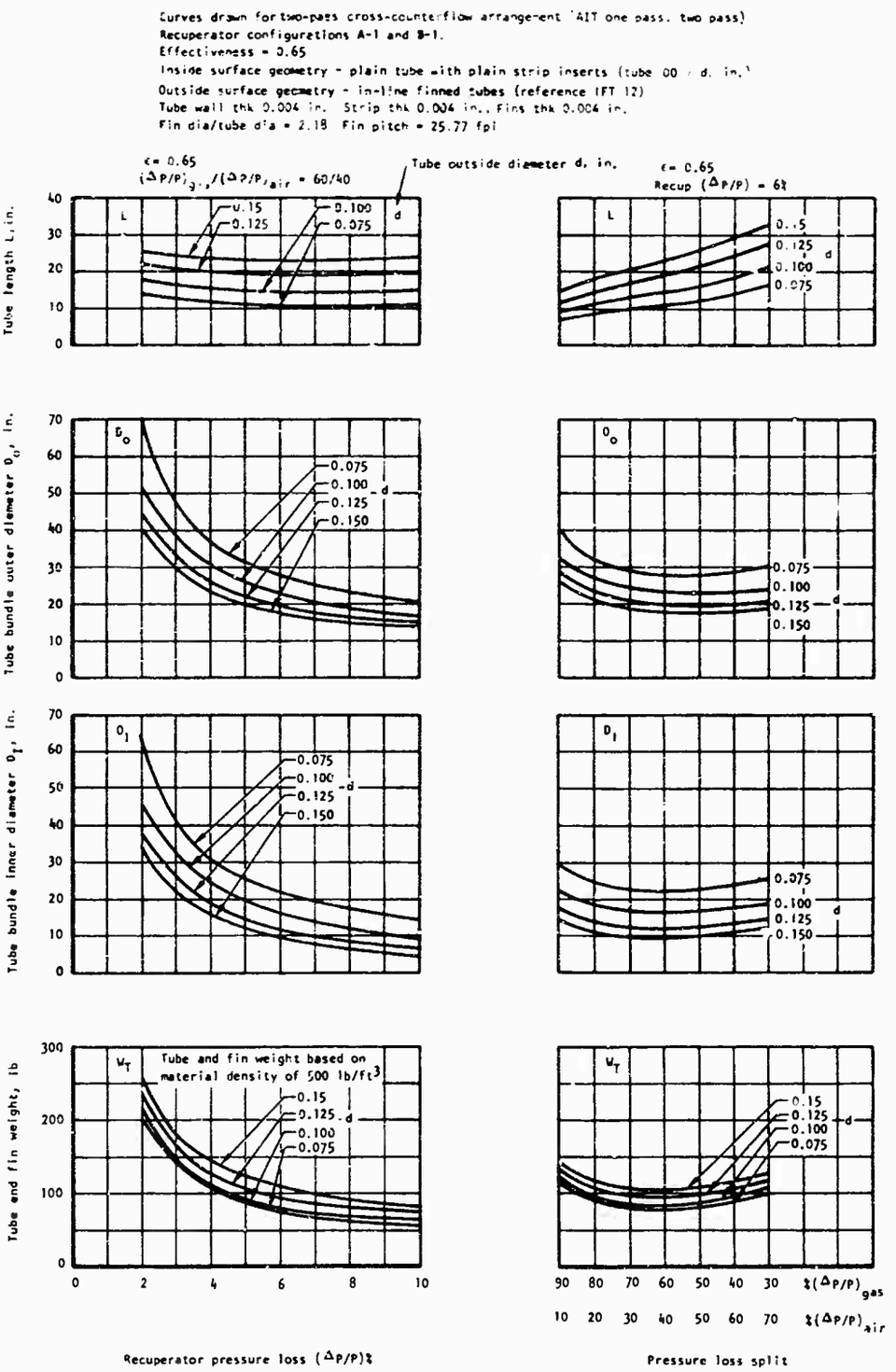

Figure 44. Effect of Pressure Loss Split on Finned-Tube Recuperator Size.

tube analysis discussed in the previous section. With this pressure loss split, the effect of pressure loss level on core size and weight for the two-pass cross-counterflow A-1 and B-1 engine configurations at the 65 percent effectiveness level is also shown on Figure 44. The relationship between effectiveness and core size and weight for a series of tube diameters, with and without a plain internal insert, for engine configurations A-1 and B-1 are shown in Figure 45. In Figures 46 and 47, similar relationships are shown for engine configurations A-2 and B-2 respectively. Because the finned-tube core weights are so much higher than the dimpled plain tube variants, the curves shown on Figures 45, 46, and 47 have been drawn only for a recuperator pressure loss of 6 percent. Typically, the effect of pressure loss on core size and weight was shown in Figure 44 for a given effectiveness and surface geometry. Based on the analysis, it is concluded that finned-tube surface geometries are not attractive for small gas turbine recuperators where the overall allowable pressure loss is small and the main design goal is to produce a unit of minimum weight.

The main application for finned-tube surface geometries is in liquid-to-air heat exchangers. A typical example is an air-cooled oil cooler where a high inside oil pressure drop can be tolerated, and thus the inside heat transfer coefficient can be increased substantially by the use of internal turbulators.

PLATE-FIN SURFACE GEOMETRY EVALUATION

For the effectiveness and pressure loss range outlined in a previous section, a variety of plate-fin surface geometries of the type shown in Figure 35c was considered in the recuperator parametric study. The following variables have been used in the analysis.

Flow Configurations

Counterflow

Two-pass cross-counterflow

Three-pass cross-counterflow

Four-pass cross-counterflow

In all four engine configurations, it has been assumed that the high pressure compressor discharge air is the single-pass fluid and the turbine discharge gas is the multipass fluid, flowing through the heat exchanger in a pattern to give a cross-counterflow arrangement.

Surface Geometry

A wide range of secondary surfaces was evaluated. Both plain triangular and rectangular offset fins of the type shown in Figure 48 were examined.

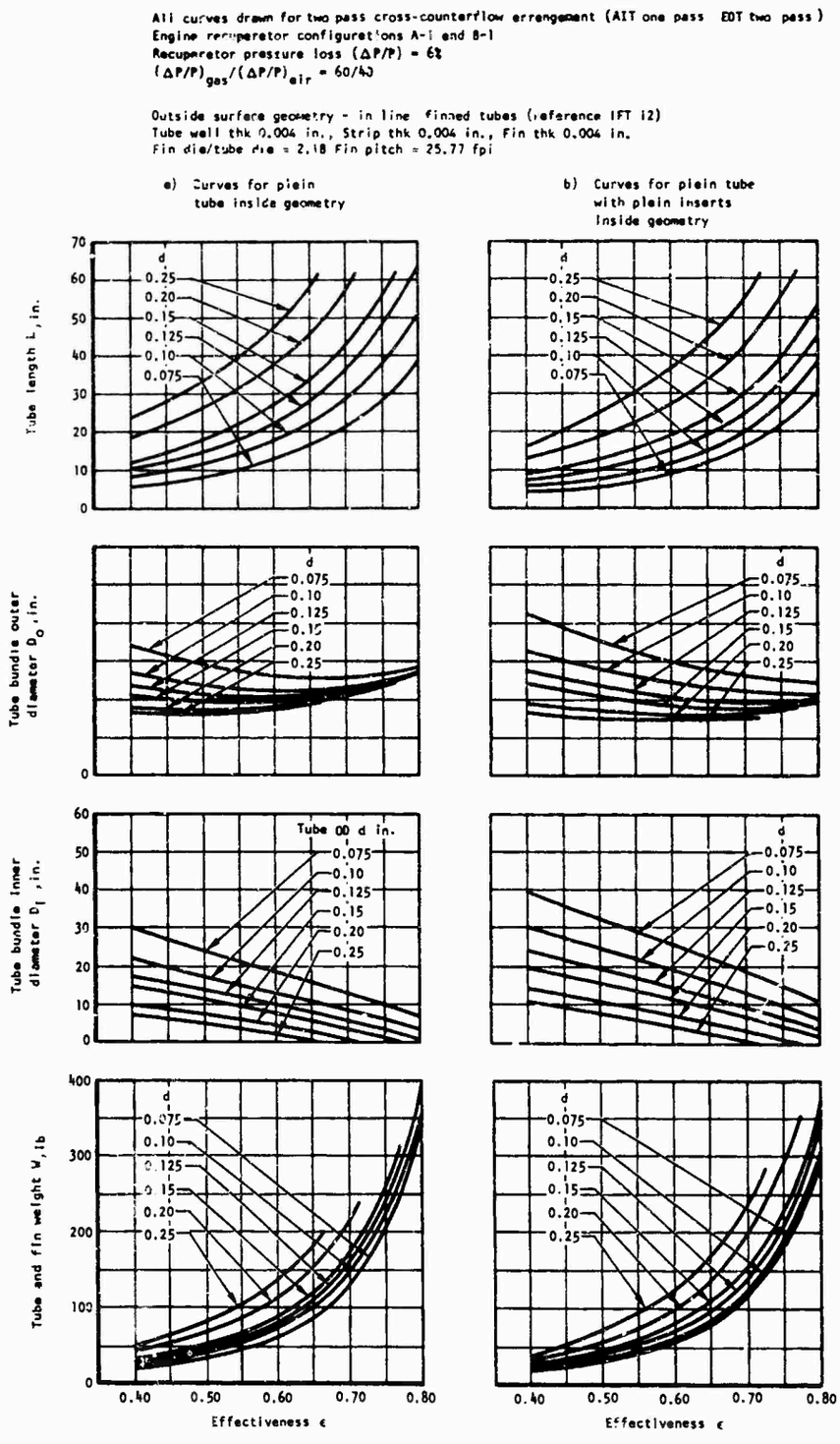

Figure 45. Relationship Between Effectiveness and Finned-Tube Recuperator Size for Engine Configurations A-1, B-1.

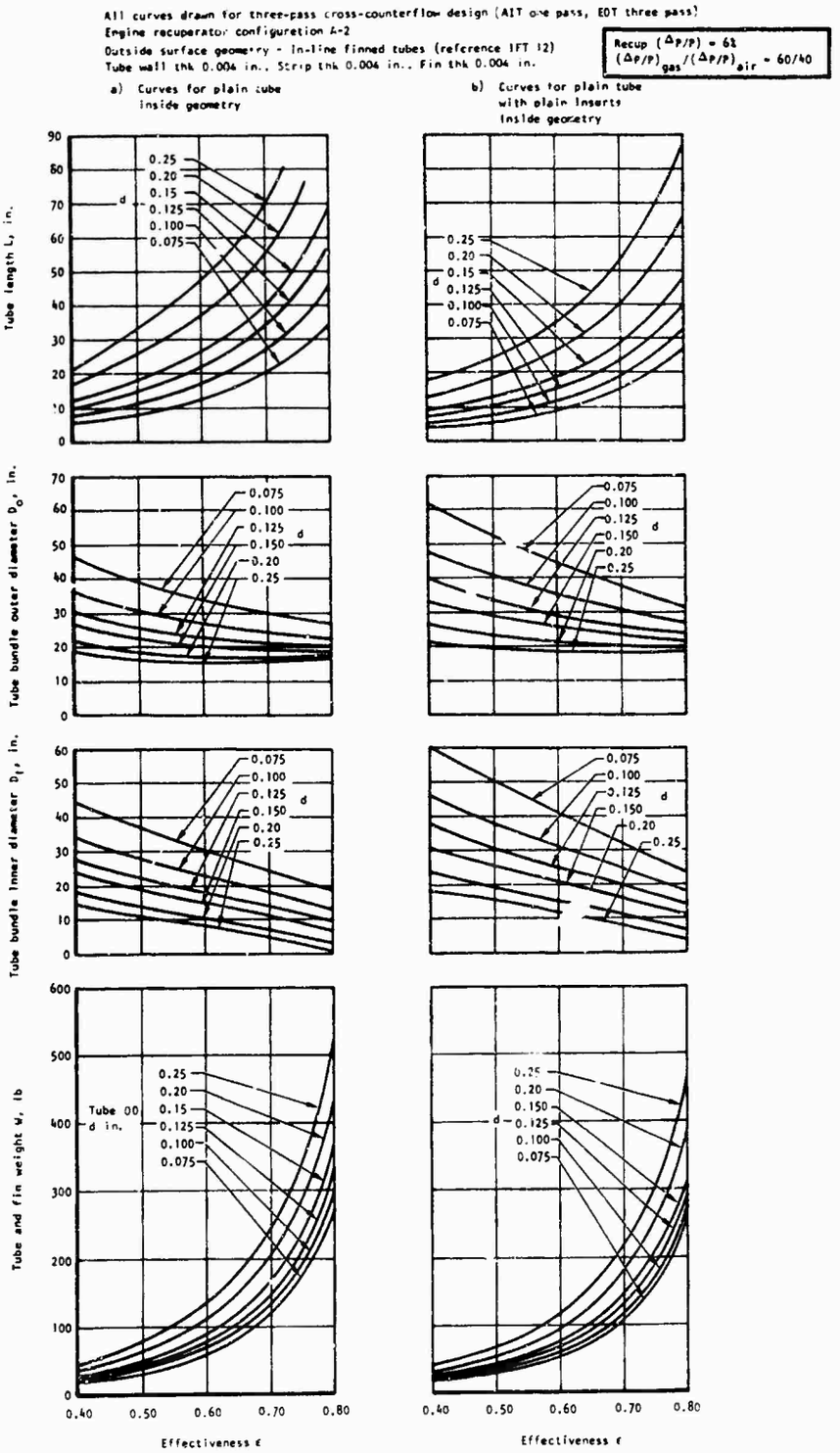

Figure 46. Relationship Between Effectiveness and Finned-Tube Recuperator Size for Engine Configuration A-2.

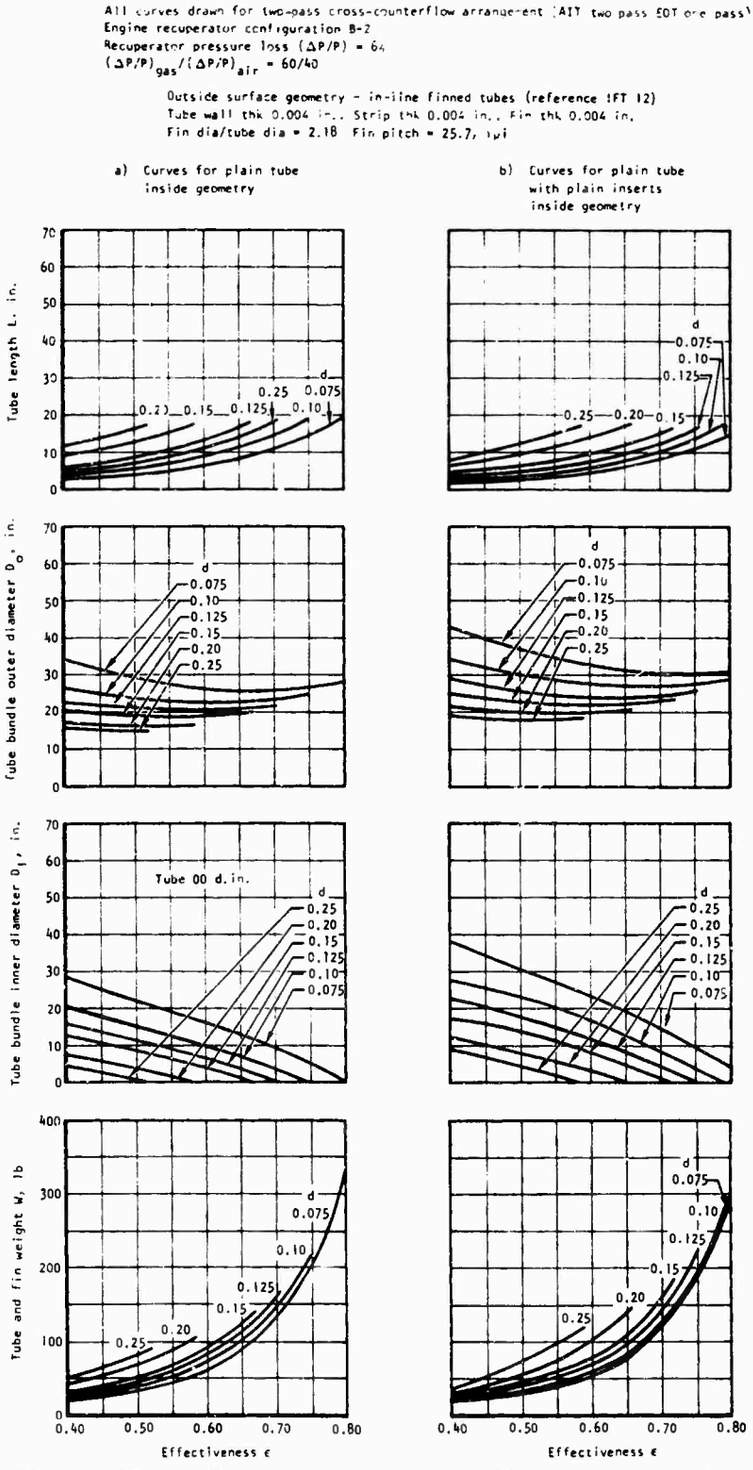

Figure 47. Relationship Between Effectiveness and Finned-Tube Recuperator Size for Engine Configuration B-2.

In the majority of recuperator industrial and automotive applications, offset finned surfaces are utilized for minimum volume and weight. With this type of surface, the fins are systematically pierced in the direction of flow, and offset normal to the direction of flow, as shown in Figure 48. This provides periodic dissipation of the boundary layers and thereby increases the heat transfer coefficients. Boundary layer dissolution incurs a smaller pressure drop penalty than artificial turbulence promotion such as that obtained with the wavy or herringbone configurations. In the development of many thousands of plate-fin heat exchangers for aircraft and industrial applications, a large number of AiResearch fin geometries have been generated for which heat transfer and friction data are available. In comparing the characteristics of the various types of surfaces, including offset, plain, louvered, perforated, herringbone, and pin-fin, it has been observed that the compact offset rectangular fins result in matrices of minimum volume and weight, and thus represent a very effective type of secondary surface.

The range of surface geometries evaluated varied from a very compact configuration (38 fins/inch, 0.025 inch passage height) to a relatively loose corrugation (10 fins/inch, 0.55 inch passage height). Details of the 20 surfaces considered are given in Table X. All combinations of these surfaces on both the high and low pressure sides of the unit were considered.

For the plate-fin geometries, extensive use was made of two computer programs written for designing counterflow and multipass cross-counterflow heat exchangers. Both programs design gas-to-gas plate-fin heat exchangers by an iteration procedure for a range of finned surfaces. The friction factor (f) and Colburn modulus (j) for each of the fin surface are available in a tubular form as a function of heat exchanger Reynolds number. Heat transfer and pressure drop data used in the plate-fin analysis are based on AiResearch test data obtained from a series of small test cores. When given the required performance, fluid properties, fin information, and heat exchanger details, the programs calculate the size and weight of the required heat exchanger core. The programs were also directed to search for fin combinations giving the lightest weight solution. Perfect gas behavior and normal operating temperature and pressure levels are assumed. Density for the core friction pressure drop is the reciprocal of the average specific volume. Each side of the heat exchanger is designed separately and the sides are combined. There is no mixing inside each pass, but mixing between passes is assumed. Checks are made for thermodynamically impossible problems and for core and duct Mach numbers. The specific heat ratios in the compressibility equations are calculated from the specific heat by means of perfect gas relations. Duct and core end losses are calculated as fixed multiples of the velocity pressure. Fin effectivenesses are determined by iteration.

Required input performance parameters include weight flows, inlet total temperatures and total pressures, total-to-total overall pressure drops, and effectiveness. Required input fin and heat exchanger information includes material thickness, thermal conductivities, and densities. In

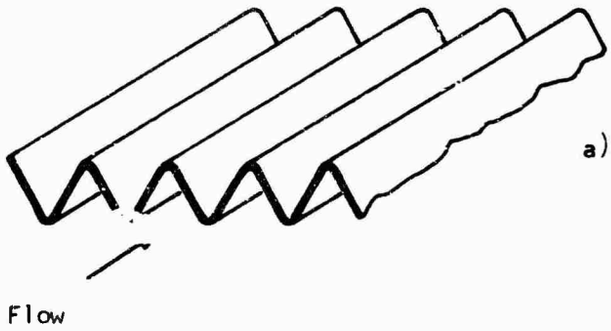

a) Enlarged view of typical plain triangular fin heat transfer surface

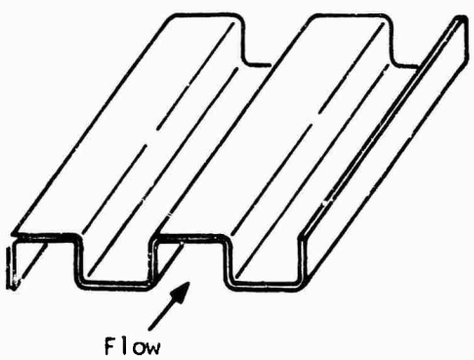

b) Enlarged view of typical plain rectangular fin heat transfer surface

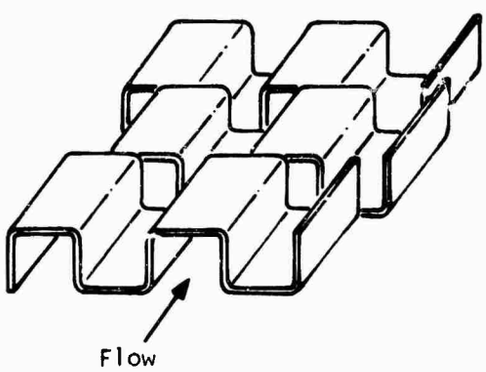

c) Enlarged view of a typical rectangular offset-fin heat transfer surface

Figure 48. Typical Plate-Fin Surface Geometries.

TABLE X. PLATE-FIN SURFACE GEOMETRIES EVALUATED IN RECUPERATOR PARAMETRIC STUDY

Number	Fin Type	Fins/Inch	Passage Height, in.
1	Rectangular offset	38	0.025
2	"	20	0.050
3		24	0.075
4		20	0.075
5		20	0.100
6		16	0.100
7		16	0.125
8		16	0.153
9		24	0.200
10		24	0.300
11		16	0.250
12		28	0.250
13		16	0.100
14		12	0.175
15	Rectangular offset	12	0.117
16	Plain triangular	17	0.125
17	"	19	0.250
18		17	0.125
19		12	0.250
20	Plain triangular	10	0.544

the counterflow analysis, the effect of the inlet and outlet crossflow sections, which are necessary to distribute the gas flows into and out of the pure counterflow section, on the size and performance of the unit was not calculated. In the analysis, 400 fin surface combinations were evaluated and a search was directed for the fin surface combination that resulted in the lightest weight heat exchanger solution. The results of the search for the minimum weight counterflow recuperator matrix are plotted on Figure 49. The values given are for pure counterflow only and do not include the end headering sections. Based on current manufacturing technology, a minimum fin thickness of 0.004 in. has been assumed, together with a tube plate thickness of 0.006 in. These curves, drawn for pure counterflow, can be applied to each of the four engine configurations and are valid whether a modular or full annular core arrangement is assumed. Radially tapered passages have not been considered; thus, for the full annular type of core, the elements would have to be spirally wrapped or formed into an involute to maintain a constant passage height.

For the reference engine design point effectiveness and pressure loss of 0.65 and 6 percent respectively, it can be seen from Figure 49 that the minimum matrix weight is 66 lb and the minimum volume is 0.714 ft^3. Above an effectiveness of about 0.70, the volume and weight increase very rapidly. In general, utilization of extremely compact plate-fin surfaces results in cores in which the weight is greater and the volume is smaller than an equivalent unit with tubular surface geometry. To achieve the smaller volume, it is necessary to use extremely compact surfaces, with the result that the frontal areas tend to be large and the flow lengths small, for a counterflow configuration with small allowable pressure losses. The weights and volumes given in Figure 49 are the minimum that can be obtained from the fin surface inventory selected for the plate-fin recuperator parametric study. It is realized that the choice of surface geometry for the minimum weight solution may not give a core shape that is compatible with the turbomachinery, and Figure 49 is drawn merely to show the theoretically obtainable minimum volumes and weights. Relaxation of the surface compactness to reduce flow frontal area would result in an increase in core weight and volume. Addition of the end sections to direct the air and gas into and out of the pure counterflow section also results in an increase in core weight and volume over the values shown in Figure 49.

Figure 50 shows the effect of material thickness on the weight and volume of a counterflow core. The datum for this study is the minimum weight core for the reference engine conditions from Figure 49 (effectiveness 0.65, pressure loss 6 percent). As one would expect, the biggest weight savings results from a reduction in the corrugation fin thickness. However, as the fin thickness is reduced, the fin efficiency falls off, resulting in an increased volume requirement for the same thermal duty; the volume increases rapidly if the fin thickness is reduced much below 0.003 in. For a particular application, the minimum material thickness would be determined from a detailed stress analysis of the core for a given life requirement. The minimum fin and plate thicknesses for current stainless steel recuperators are 0.004 in. and 0.006 in. respectively. For lightweight aerospace application, slightly thinner foils could probably be used, but this would result

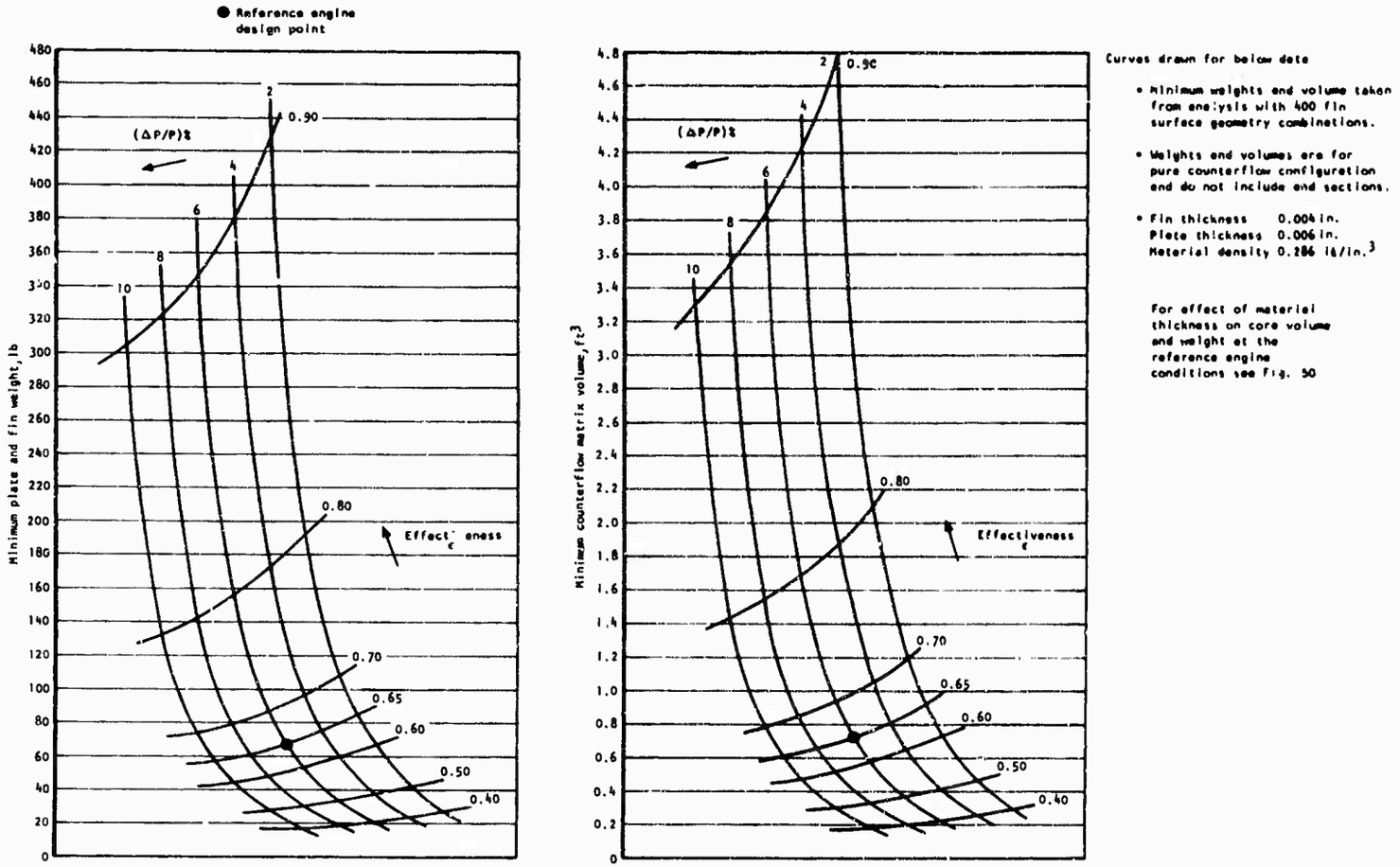

Figure 49. Counterflow Plate-Fin Minimum Matrix Volume and Weight Relations.

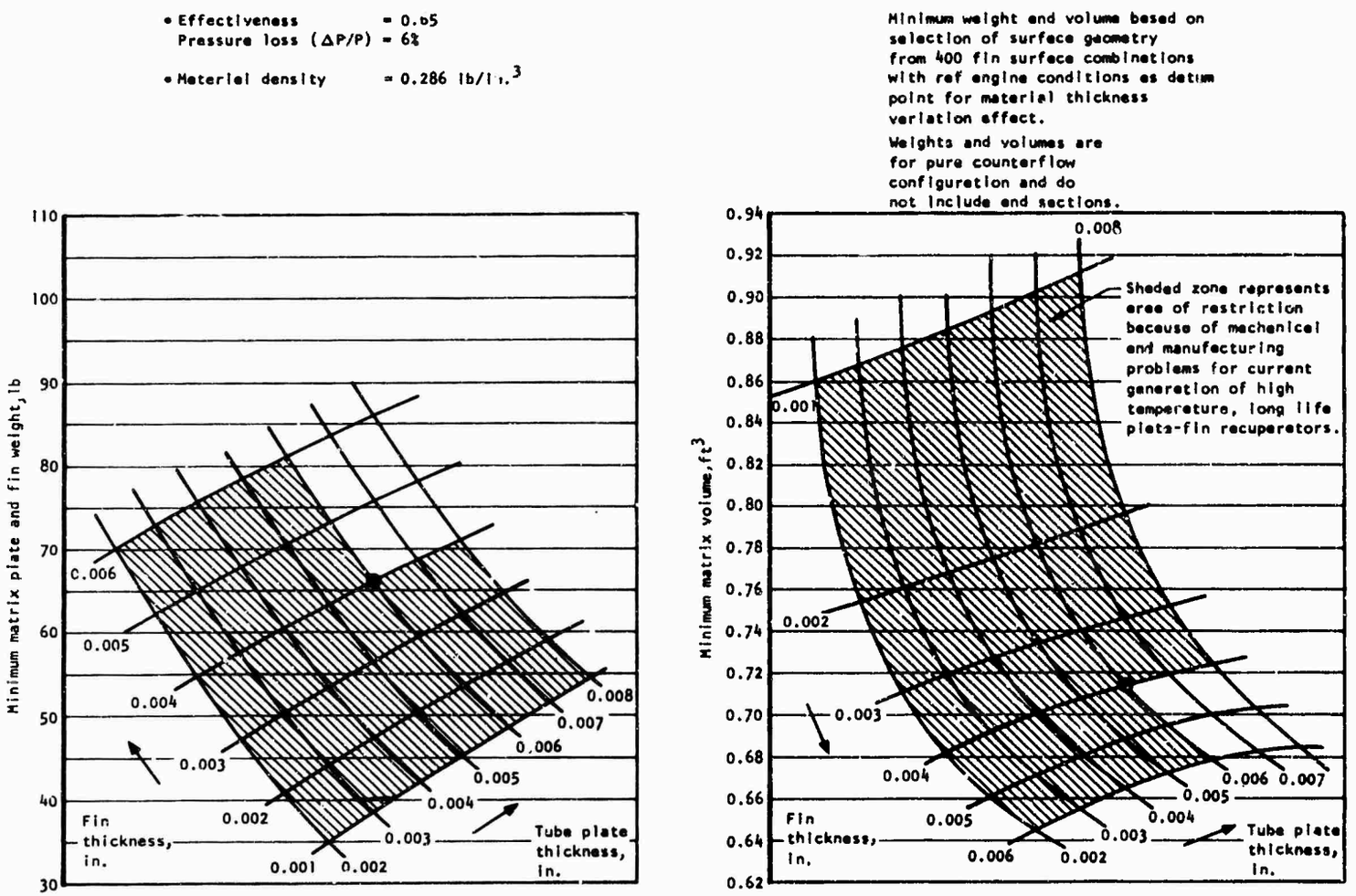

Figure 50. Effect of Material Thickness on Matrix Volume and Weight for Counterflow Plate-Fin Recuperator.

in much tighter control of the manufacturing tolerances, particularly in the brazing operation where extremely close temperature control would be necessary to minimize local braze alloy erosion, etc.

In addition to the pure counterflow variant, plate-fin arrangements of two-, three-, and four-pass cross-counterflow have been analyzed. As carried out for the tubular units, the effect of pressure loss split on core weight was examined (Figure 51). For the two-pass cross-counterflow design, the matrix weight is a minimum when 60 percent of the available pressure loss is used up on the gas side of the unit. For the three- and four-pass arrangements, the minimum weight is achieved at a slightly higher percentage on the gas side. To show the effect of pressure loss split on core weight and volume, these curves were drawn at the reference engine effectiveness and pressure loss. With the limited pressure loss available and the small recuperator inside diameter, the surface compactness has to be reduced for the three-, and four-pass arrangements with the result that the minimum matrix weight and volume increase compared with the two-pass configuration.

In Figure 52, the relationships between effectiveness and pressure loss and between minimum core weight and volume are shown for a two-pass cross-counterflow arrangement. As for the counterflow arrangement, the data presented are valid for a modular or full annular core, and the comments given previously regarding material thickness are equally applicable. The curves shown in Figures 52, 53, and 54 again represent minimum weight solutions taken from a search involving 400 fin surface combinations and are drawn for the case where 60 percent of the available pressure loss is used up on the gas side of the unit. For the two-pass cross-counterflow arrangement, the data given on Figure 52 are applicable for engine configurations A-1, B-1, and B-2. The three-pass cross-counterflow data on Figure 53 are for engine configuration A-2, and the four-pass data on Figure 54 can be applied to configurations A-1, B-1, and B-2.

Based on the plate-fin analysis, a series of minimum weight solutions has been established, and these are compared with solutions from the tubular and finned-tube studies at the reference engine conditions as outlined in Table XI.

From the surface geometry comparison, it can be seen that the minimum weight counterflow plate-fin matrix weight, while lighter than the finned-tube variant, is much heavier than the dimpled plain tube design. Therefore, the main emphasis in establishing an optimum design will be concentrated on the dimpled plain tube geometries.

Curves drawn for below data

- Minimum weights and volumes taken from parametric analysis with 400 fin surface geometry combinations
- Fin thickness 0.004 in.
  Tube plates 0.006 in.
  Material density 0.286 lb/in.^{3}

Curves drawn for
$\epsilon = 0.65$
$(\Delta P/P)_{ov} = 0.06$

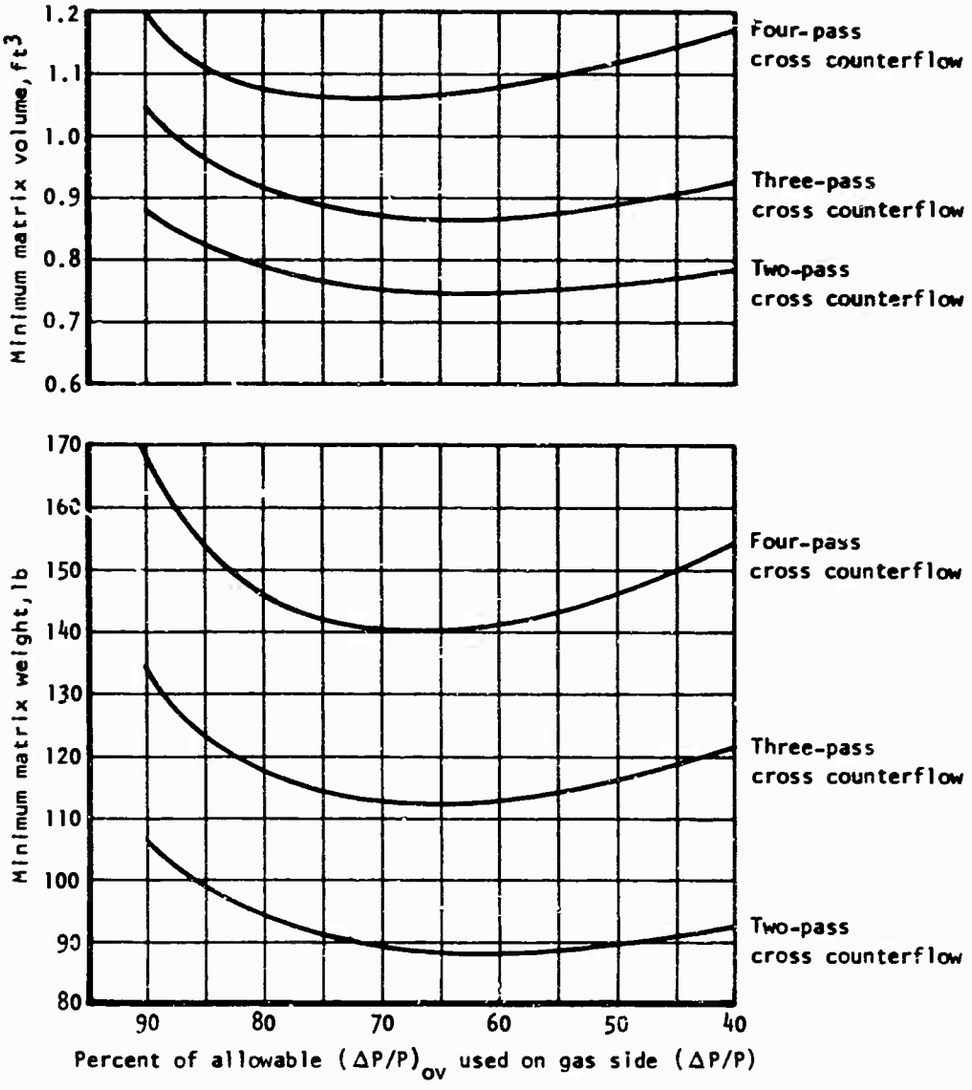

Figure 51. Effect of Pressure Loss Split on Minimum Recuperator Matrix Plate-Fin Weight and Volume for Cross-Counterflow Arrangement.

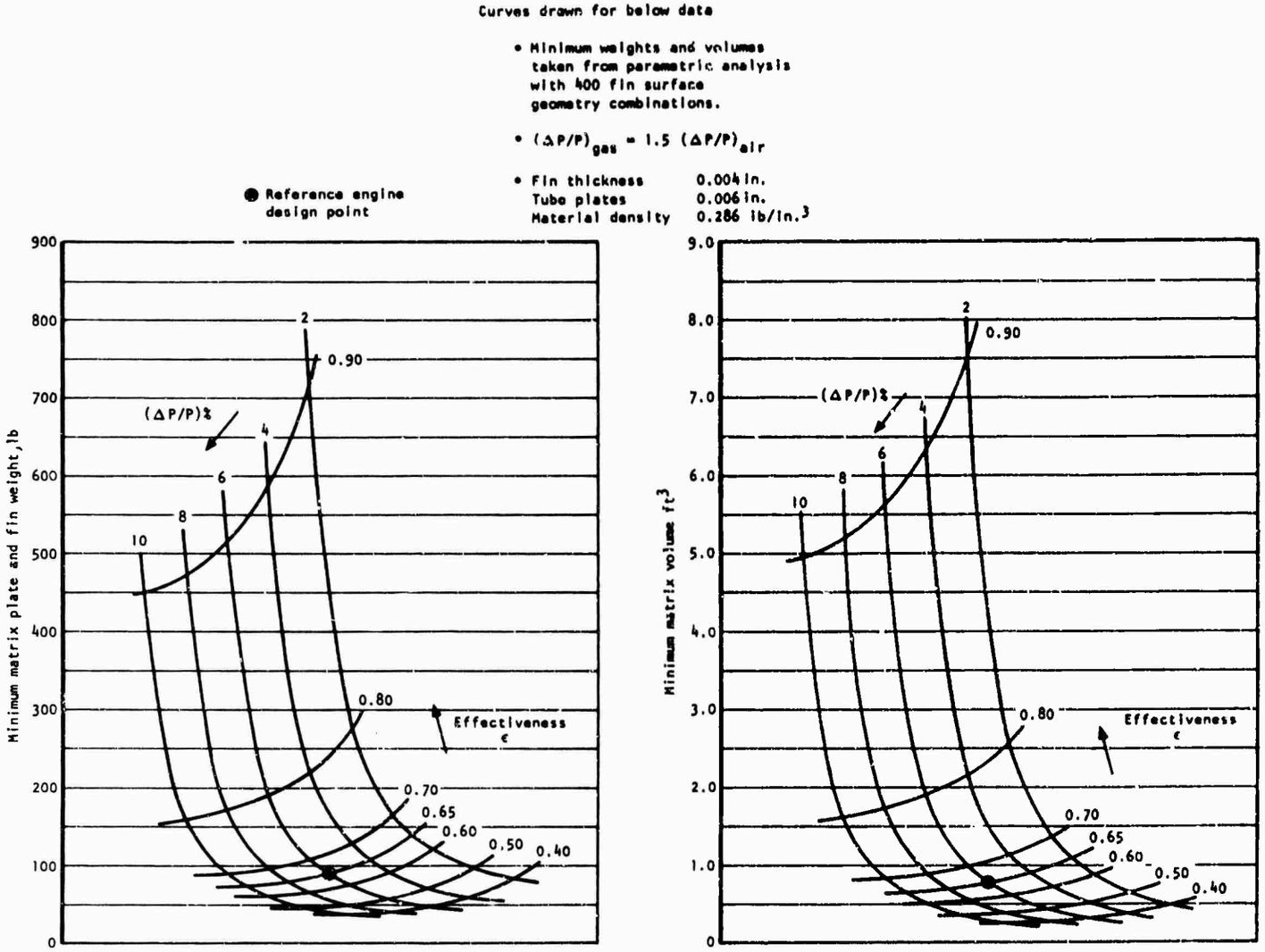

Figure 52. Minimum Plate-Fin Matrix Volume and Weight for a Two-Pass Cross-Counterflow Recuperator.

Curves drawn for below dete

- Minimum weights end volumes teken from perometric anelysis with 400 fin surfece geometry combinetions.
- $(\Delta P/P)_{ges} = 1.5\ (\Delta P/P)_{air}$
- Fin thickness 0.004 in.
  Tube pleting 0.006 in.
  Meteriel density 0.286 lb/in.^{3}

● Reference engine design point

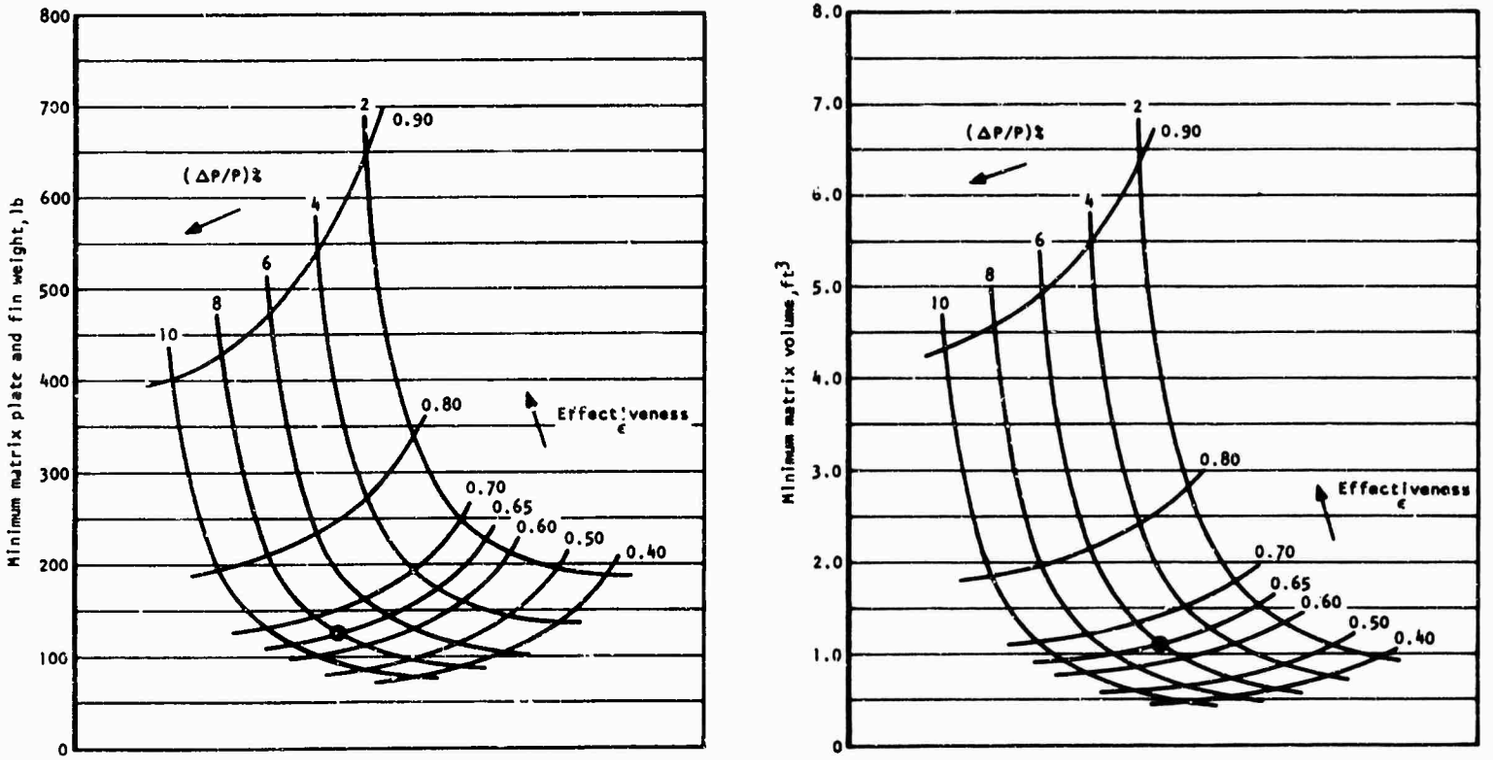

Figure 53. Minimum Plate-Fin Matrix Volume and Weight for a Three-Pass Cross-Counterflow Recuperator.

Curves drawn for below date

- Minimum weights and volumes taken from parametric analysis with 400 fin surface geometry combinations
- $(\Delta P/P)_{gas} = 1.5\ (\Delta P/P)_{air}$
- Fin thickness 0.004 in.
  Tube plates 0.006 in.
  Material density 0.286 lb/in.^{3}

● Reference engine design point

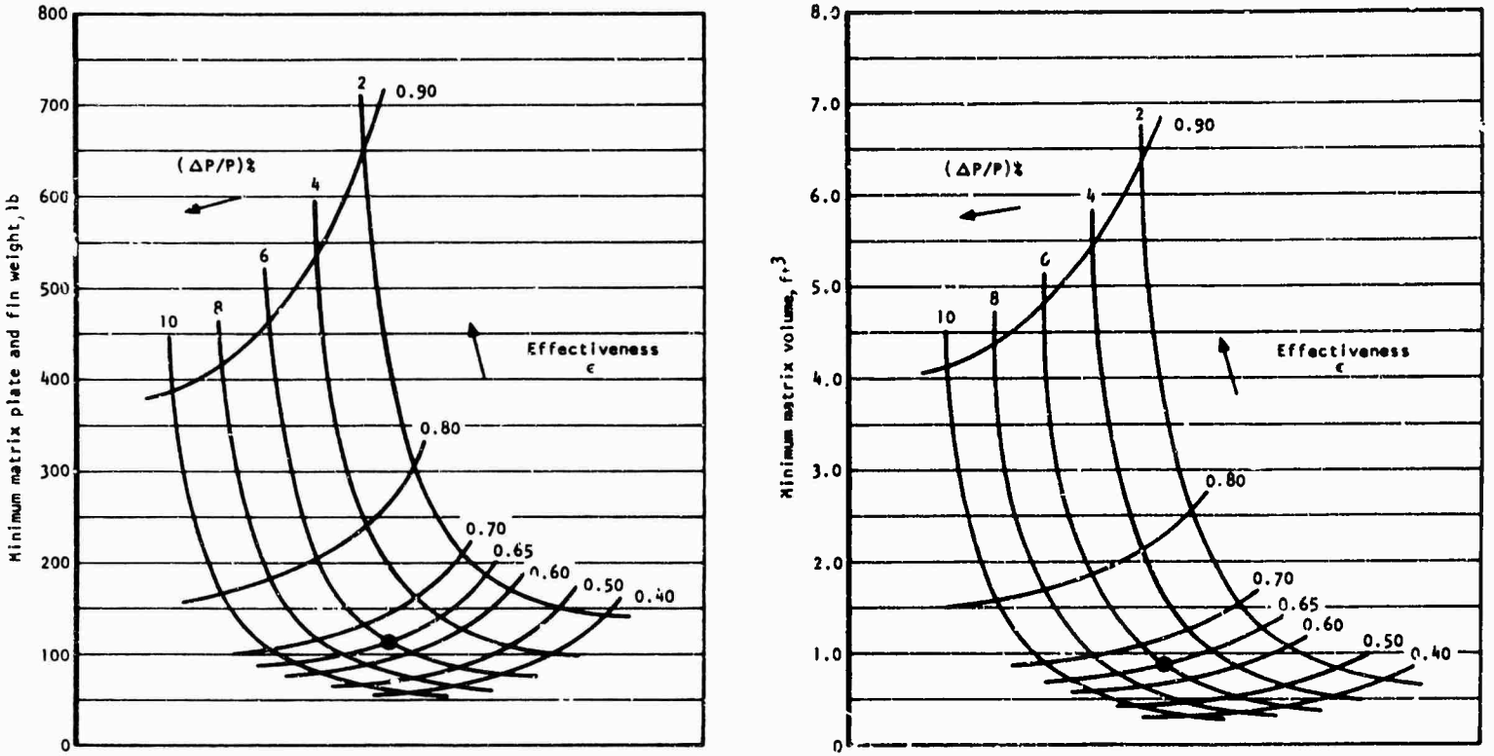

Figure 54. Minimum Plate-Fin Matrix Volume and Weight for a Four-Pass Cross-Counterflow Recuperator.

TABLE XI. COMPARISON OF MINIMUM WEIGHT SOLUTIONS FOR TUBULAR, FINNED-TUBE, AND PLATE-FIN GEOMETRIES

Surface Geometry	Dimpled Plain Tube	Finned Tube With Plain Insert	Plate Fin			
Flow Configuration	Two-Pass Cross Counterflow		Counterflow		Two-Pass Cross Counterflow	
Engine Configuration	A-1 B-1	A-1 B-1	A-1 B-1	A-2 B-2	A-1 B-1	B-2
Effectiveness	0.65	0.65	0.65		0.65	
Pressure Loss, %	6.0	6.0	6.0		6.0	
Minimum Weight, lb	27.14	82.53	66.0		88.0	

RECUPERATOR MATERIALS

The factors of primary importance in the selection of recuperator materials are mechanical properties, hot-corrosion resistance, fabricability, compatibility with brazing filler metals, metallurgical stability, and cost.

Mechanical Properties

A recuperator material must have adequate mechanical properties during its design lifetime to withstand the stresses due to thermal transients and fluctuating and steady-state pressure differentials.

It is insufficient merely to measure the properties of new, unexposed material, because mechanical properties are almost always degraded by environmental attack and by metallurgical changes such as aging reactions and carbide precipitation. Metallurgical stability and corrosion resistance cannot be considered apart and are important in evaluating mechanical properties.

Erosion resistance is also an important mechanical property. Erosion is caused by solid or liquid particles (dust, sand, carbon, or molten salt droplets) in the gas turbine environment battering against the surface of a material. Although dynamic yield strength and endurance limit can give indications, there is no accurate way to calculate erosion resistance. Among the stainless steels and superalloys considered as recuperator meterials, those with higher yield strength should have the higher resistance to erosion.

Hot Corrosion

Hot corrosion is the attack on metal alloy components caused directly or indirectly by contact with products of combustion of gas turbine engines. Included in this term are all synergistic effects that contribute to hot corrosion such as sulfidation, oxidation, erosion, stress corrosion, and both static and cyclic stresses.

In an Army Aviation Materiel Laboratories sponsored research program at AiResearch (Reference 4), it has been shown that hot-corrosion attack of stainless steels and superalloys definitely occurs at current levels of recuperator operating temperatures.

Fabricability

Materials selected for formed parts, such as fins and pans, must have adequate formability at room temperature and must be amenable to brazing, welding, and all other contemplated manufacturing operations.

Compatibility with Brazing Filler Metals

Since brazing is the most economical means of producing recuperator structures, the compatibility of structural materials with candidate brazing filler metals is of primary importance. The selected base metal/filler metal combinations must satisfy the following requirements:

1. Compatible brazing temperature. Metallurgical changes must not occur in the parent metal as a result of the brazing temperature cycle.

2. Minimum erosion and penetration into the base metal.

3. Adequate wetting and flow.

4. Adequate brazed joint strength and hot-corrosion resistance.

5. Little or no embrittlement of the base metal by diffusion of brazing filler metal constituents into the base metal.

6. If galvanic attack appears to be a problem under service conditions, galvanic potential between base metal and filler metal should be low. The base metal should preferably be the anode, since it has much greater surface area.

Metallurgical Stability

The mechanical properties and corrosion resistance of a recuperator material must not be detrimentally affected by internal metallurgical changes, such as carbide precipitation, sigma formation, internal oxidation, or diffusion reactions between dissimilar materials, e.g., between base metals and filler metals or coatings.

AiResearch has acquired an extensive background relating to the effects of wall thickness, temperature, gas atmosphere composition, and brazing filler metals on the creep strength, rupture strength, ductility and high temperature corrosion of a variety of stainless steel and superalloys.

A reduction in strength of thin-walled materials has also been demonstrated in a program on hot corrosion of recuperator alloys (Reference 4). The purpose of the program was to evaluate the hot-corrosion resistance of the materials and brazing alloys in gas turbine combustion products at 1100°, 1300°, and 1500°F. Preliminary hot-corrosion tests at 1500°F were conducted for 100 hr to screen candidate braze alloys. Following this, tubes containing disks brazed with selected braze alloys were pressurized at maximum temperatures of 1100°, 1300°, and 1500°F to cause failure-at-time intervals up to 1000 hr. Specimens were thermally cycled under stress after 2-hour hold times at temperatures and alternately exposed to oxidizing and reducing gases containing 5 ppm sea salt to simulate startup, operating, and cooldown conditions of a gas turbine engine. Tubing and brazed joints were metallographically examined to evaluate hot corrosion of various brazing alloy tubing material combinations. Hot-corrosion stress rupture data for a material are shown in Figure 55. Figure 56 shows the range of gas and core metal temperatures being considered in the recuperator parametric study. The estimated maximum tube wall metal temperatures are based on a heat exchanger with balanced thermal conductances (i.e., $hA_{GAS} = hA_{AIR}$). This assumption is fairly valid since the goal of the parametric study was to identify surface geometries to give minimum volume and weight solutions.

MATERIAL COSTS

Foil and tube costs were obtained for candidate recuperator materials over a representative range of material thicknesses and tube diameters. With the main emphasis being placed on dimpled plain tube surface geometries to give minimum weight units, detailed cost analysis of the tubular heat exchangers was carried out. Tube price data used in the cost analysis for a selected reference material is shown in Figure 57.

STRUCTURAL CONSIDERATIONS

Structural considerations related to recuperator design were investigated for the severe pressure, temperature and vibratory load environment associated with turbine operations. Design conditions are discussed and a typical set of material stress criteria is provided for the various loadings. Applicable material properties for a candidate superalloy material are included to indicate approximate acceptable stress levels. Critical structural design areas such as the tubes and tube supports, headers, and shells are discussed to outline the general approach necessary for a successful design.

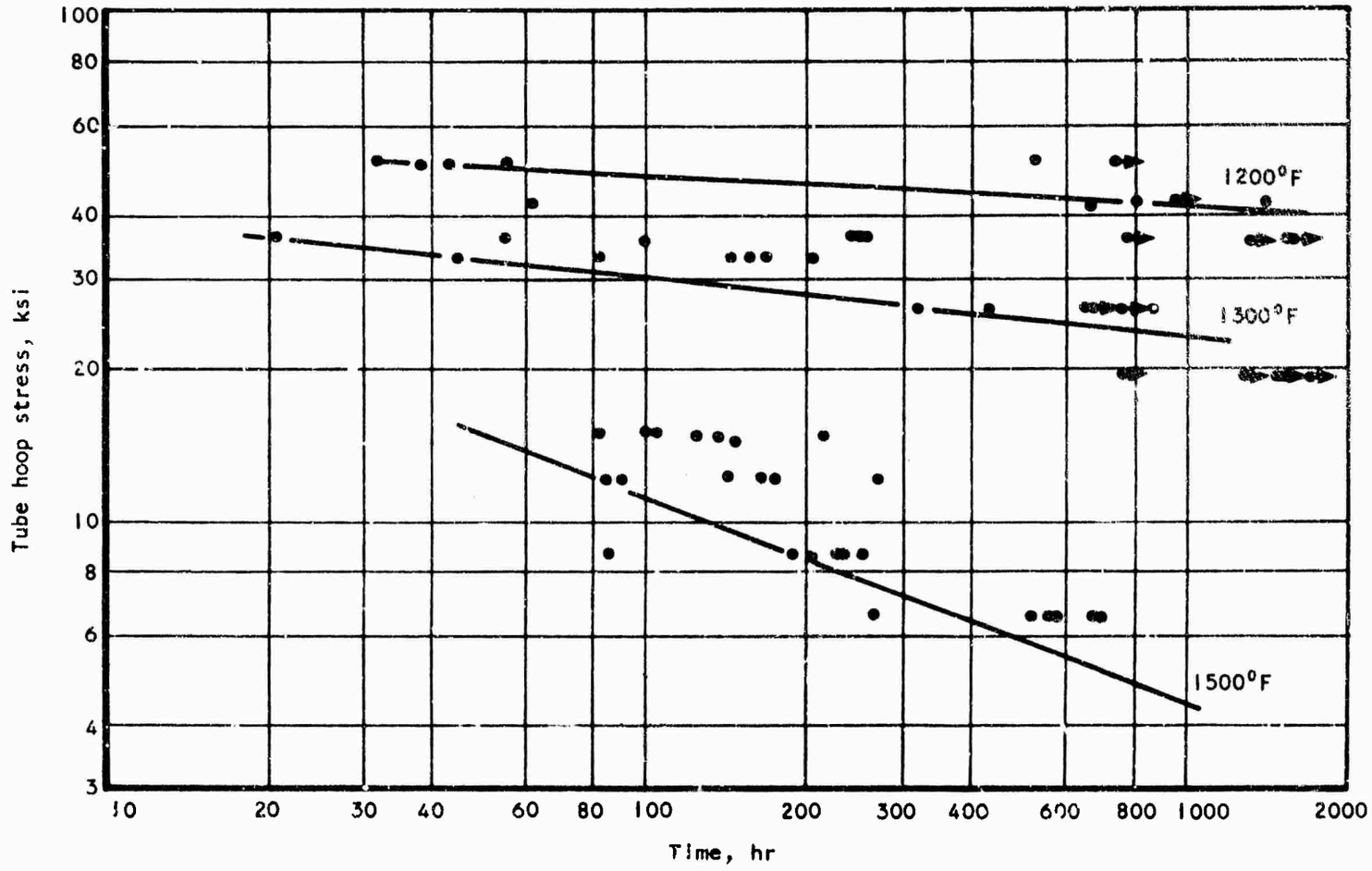

Figure 55. Cyclic Hot-Corrosion Stress-Rupture Data (Reference 4).

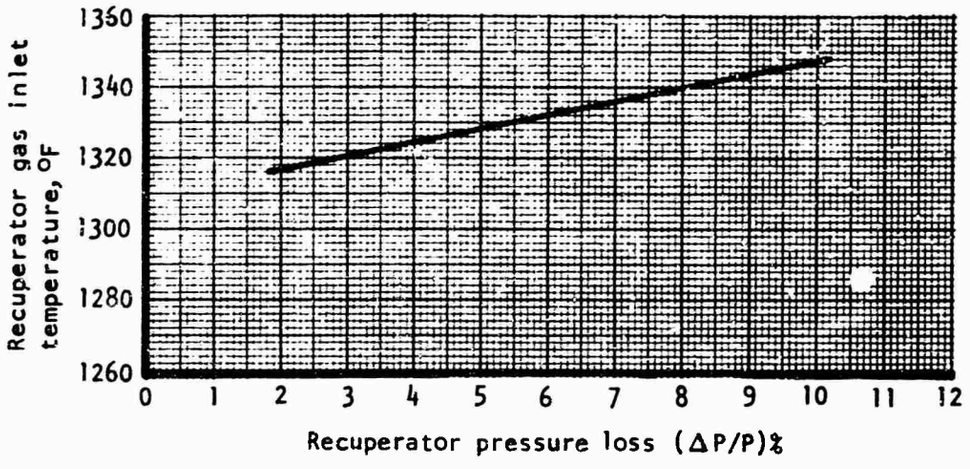

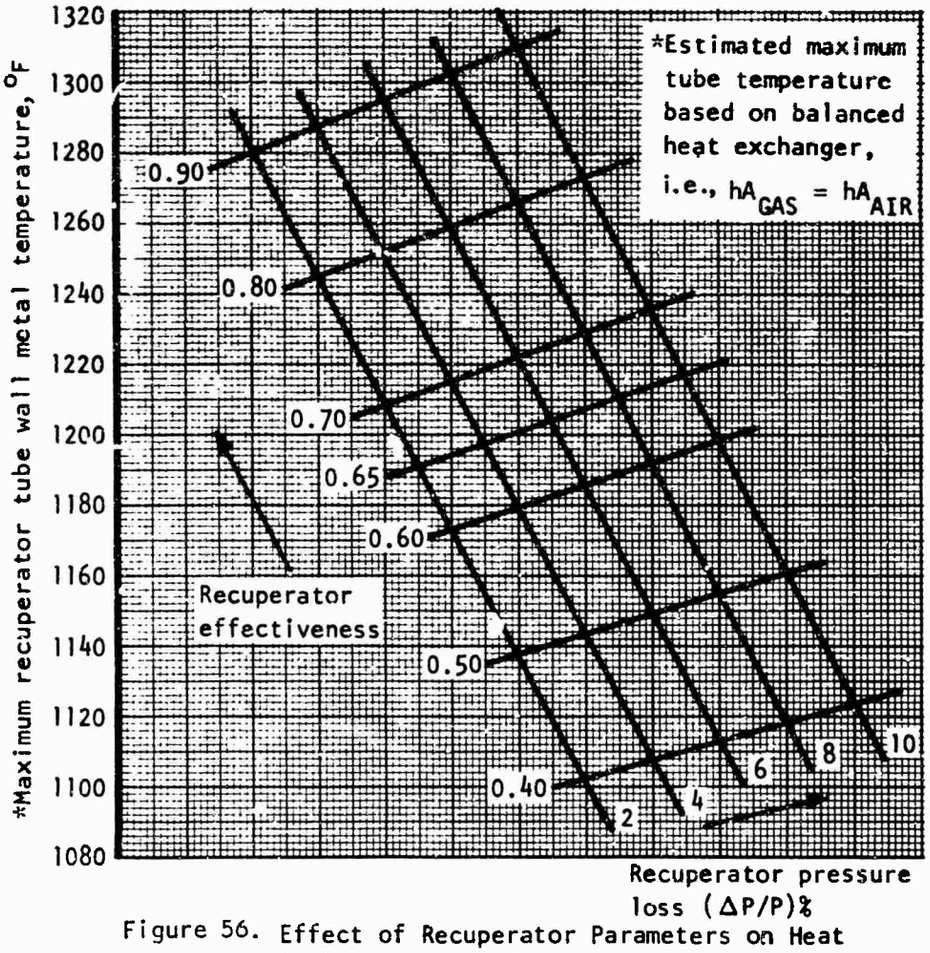

Figure 56. Effect of Recuperator Parameters on Heat Exchanger Gas Inlet Temperature and Maximum Tube Wall Metal Temperature.

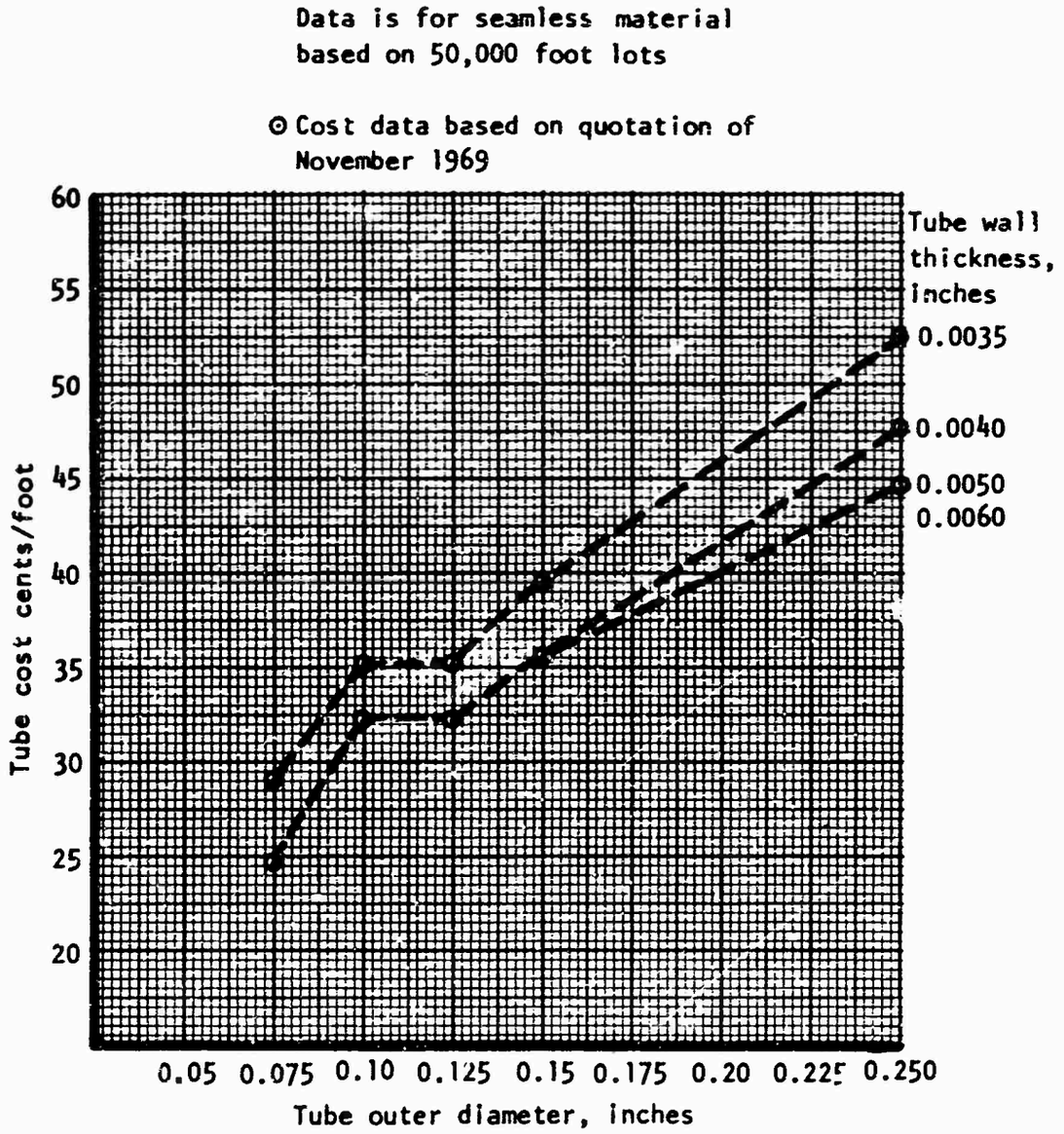

Figure 57. Tube Cost Data for a Reference Material.

Design Criteria

The recuperator is expected to operate for a minimum of 1000 hr in a high temperature environment which will have metal temperatures of about 1300°F and gas pressures up to about 130 psi. The combined effects of high temperature and extended life require that the recuperative material provide adequate creep strength properties. Transient temperature conditions, particularly during startup, must be accommodated for in the heat exchanger design, so that the selected material will have adequate fatigue strength. In this low-cycle fatigue range, stresses exceeding the material yield strength are acceptable, and fatigue life is related to the plastic strain per cycle and to the material ductility. Therefore, to provide adequate thermal fatigue life, the material must have acceptable reduction in area properties. An extensive shock and vibration spectrum is expected due to aircraft and engine operating characteristics with the engine mount and rotational frequencies being the most critical to the recuperator. If a recuperator resonance coincides with an engine operating frequency, large vibratory amplifications can occur which will cause recuperator fatigue. Many cycles can be accumulated during the operating life, so, in contrast to low-cycle thermal fatigue, the design stresses must be below the fatigue limit of the material which is about the yield strength for typical recuperator materials.

A variety of load conditions, stress conditions, and types of failure mode possibilities would be experienced by the unit during its life. The detailed set of design criteria discussed below would be used to design the various components.

Allowable Stresses for Internal Pressure Design

The standard design practice employed by AiResearch is to design the pressure carrying structure for proof pressures of 1.5 times the working pressures and for burst pressures of 2.5 times the working pressures. The structure must not yield at proof pressure or rupture at burst pressure. This implies that the proof pressure is the governing design condition if the ratio of yield stress to ultimate stress is less than 0.6 and that the burst pressure will govern if the ratio is greater than 0.6. The allowable stress at working pressure is, therefore, the lesser of the following:

$$\sigma_{all} = (\sigma_{ult})/2.5 \quad \text{- (1a)}$$

$$\sigma_{all} = (\sigma_{y})/1.5 \quad \text{- (1b)}$$

At elevated temperature for extended operating times, the above conditions must be satisfied, and in addition, the component must be satisfactory for creep effects. A set of criteria for creep must be comparable to those for the short-time loading. Accordingly, limitations based upon stress

to rupture and stress to 1-percent creep must be established. For the rated design life of the unit, it will be designed for sustained pressure operation at maximum operating temperature throughout the entire design life. Allowable stresses at working pressure must be the lesser of the following:

$$\sigma_{all} = [(\text{1-percent creep stress})_{1000\ hr}]/1.2 \quad - - - - \text{(2a)}$$

$$\sigma_{all} = [(\text{creep-rupture stress})_{1000\ hr}]/1.5 \quad - - - - - \text{(2b)}$$

Allowable Stresses for Inertia Loads

Inertia loads, both static and vibratory, may be experienced during any phase of the operating cycle of the unit. The component must, therefore, be designed to carry the inertia loads at elevated temperature. Since the maximum loads generally occur for a relatively short time duration, the short-time material properties will be used. The design allowable stress used for the inertia loads will, therefore, be governed by Equation (1).

Allowable Thermal Fatigue Stresses

The magnitude of thermal stress due to temperature differences developed during the rapid heat-up cycle of the system results in plastic deformations in various components, particularly in the hot operating regions. For a minimum operating life requirement of 1000 thermal cycles, a minimum design life of 4000 cycles would be used to ensure that the life is achieved. The required analysis was based on the accumulated plastic strain approach for estimating fatigue life. The number of cycles to failure N is determined from the formula

$$N = \frac{2C^2}{(\epsilon_p)^2_{1-2} + (\epsilon_p)^2_{4-5}} \quad - - - - - - - - - - - - - - - \text{(3)}$$

where N = cycles to failure

ϵ_p = plastic strain

C = material ductility constant

The ductility constant is based upon the material reduction of area property, RA, and the formula below is based on work outlined in Reference 5.

$$C = 0.79\ \text{Ln}\ \frac{100}{100 - RA}$$

The reduction area at fracture is determined from standard tensile tests and the plastic strain is estimated from a typical load cycle for the material. Cumulative effects for different load cycles during the material life are handled by a fatigue damage rule similar to Miner's rule. In addition, since both creep and fatigue are occurring simultaneously, the effects of the two material damage phenomena are important.

Material Properties

The allowable pressure stresses vs temperature for a reference recuperator material are shown in Figure 58. The allowable stresses were determined from the yield stress and the stress for 1-percent creep in 1000 hr using the design criteria in Equations (1) and (2). The yield and the 1-percent creep stress conditions provide lower allowable stresses than the ultimate stress and 1000-hr creep rupture stress. Additional properties required for design are included in Table XII.

Tube Design

Tube dimensions were based on the heat transfer analysis and then checked for structural capability. Typical tube lengths were from 10 to 15 in., diameters were 0.1 and 0.125 in., and wall thickness was 0.004 in. Maximum tube operating temperature was estimated to be 1200°F for 0.65 effectiveness case based on a gas inlet temperature of 1330°F and an air outlet temperature of 1070°F. Loads on the tubes included pressure and thermal and vibratory inertia, as discussed in the following paragraphs.

Pressure containment capability can be determined from the cylindrical membrane stress by the standard relation

$$\sigma = PR/t$$

The stress for a 0.125-in.-diameter tube with a wall thickness of 0.004 in. at the compressor outlet pressure of 132 psi is therefore 4100 psi. The allowable stress from Figure 58 at 1200°F is 31,000 psi, so tube strength is more than adequate for pressure containment.

Axial thermal loads in the tubes due to differential growth between the tubes and adjacent structures must be avoided whereas differential tube growth and thermal bending stresses can be tolerated. The thermal analysis for this study was restricted to considering the axial temperature differential which will require moving, or floating, headers between the tubes, shells and tube supports except for a single fixed point which is assumed to be the header at the one end. The header at the hot end would generally

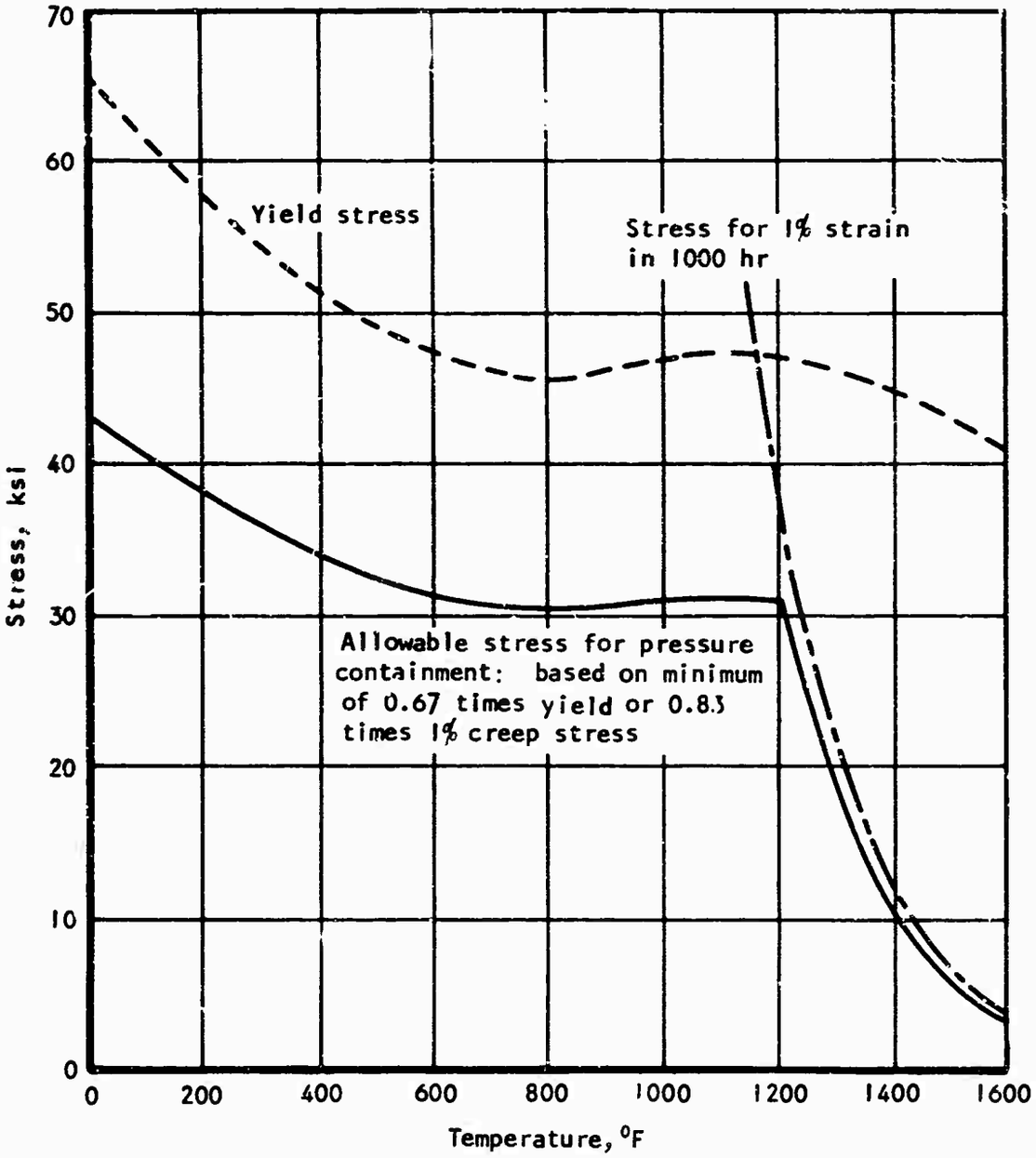

Figure 58. Allowable Pressure Stresses Versus Temperature for a Reference Recuperator Material.

TABLE XII. TUBE MATERIAL PROPERTIES VS TEMPERATURE

Temperature, ^{0}F	Thermal Expansion Coefficient, in./in./$^{0}F \times 10^{6}$	Elastic Modulus, psi x 10^{-6}	Reduction in area, percent(1)
70	-	29.8	43
200	7.1	29.2	-
400	7.3	28.4	-
600	7.4	27.5	-
800	7.6	26.6	-
1000	7.8	25.6	-
1200	8.2	24.4	-
1400	8.5	23.1	48
1600	8.8	-	73

(1)Typical values for sheet material based on tests conducted at AiResearch.

be selected as the fixed point so that the required flexible joints or seals could be designed for the lower temperature operating regions. An example of the temperature differentials that can be expected is provided by the differential between the outer shells for the ducting, the compressor air to the tubes, and the tubes themselves in design configuration A-1. At steady-state conditions, the shell temperature will be about 600°F, whereas the average tube temperature is estimated to be about 1000°F. The tubes adjacent to the shell will therefore be in compression. A 400°F temperature differential occurs during steady conditions, whereas the allowable difference to avoid tube buckling in compression would be about 200°F. During start conditions, the tubes respond more rapidly than the shells and a transient difference of 700° to 900°F would be expected. Transient conditions would therefore be about twice as severe as steady-state conditions, and strengthening the tube to avoid buckling is not practical. The floating header design approach was therefore assumed in the analysis that follows.

The design for inertia loads was based on a 25g tube capability and tube resonance frequencies greater than 150 Hz. Assuming that the tubes are readily excited by the turbine, and that an isolation system is not desirable, this approach assumes that tube resonances giving very large amplifications will be avoided. If resonances above 150 Hz occur, it is assumed that 25g capability for the tubes will be sufficient for extended operations. The allowable tube length for a 25g uniform load can be estimated for simple support conditions where the beam bending stress is

$$\sigma = \frac{M}{Z}$$

where, for a thin wall tube

$$Z = \pi R^2 t$$

and $$M = 25\ \gamma\ (2\ \pi R t)\ L^2/8$$

Combining, and using a typical metal density, γ, of 0.3 lb/in.^{3},

$$\sigma = 1.8\ L^2/R$$

For an allowable bending stress at 1200°F of 31,000 psi the allowable unsupported length of a 0.1-in.-diameter tube is 41 in. However, the allowable span for the same tube is only 6.7 in. based on the natural frequency relation

$$f = 1.57\sqrt{EI/\mu\ L^4} \qquad (4)$$

where E = material elastic modulus, psi

μ = tube mass per unit length, lb-sec^2/in.^{2}

I = ZR, in.^{4}

The allowable span based on frequency was used for the tube support design that follows.

Tube Supports

Tube supports include flow guides, intermediate baffles, and supports for the flow guides and baffles. The design load for the flow guides and baffles (required when allowable span is exceeded between flow guides or headers, depending on the configuration) is the tube weight over the span loading the baffle, multiplied by 25 to account for amplifications (see tube design). The baffle thicknesses required for this loading are small, and the size will generally be set by minimum fabricable size limitations. The selected minimum for this design was a thickness of 0.03 in.

A system of support beams parallel to the tubes will be required to support these flow guides and baffles for inertia loads perpendicular to the tube axis. The approach to designing these beams is similar to tube inertia load design and therefore includes capability for 25g load and stiffness to place resonances above 150 Hz. In addition, since the support beam is parallel to the tubes, one end will be fixed and the other free to slide so that thermal restraint of the tubes does not occur.

Header Design

The header plate on the one end will support the tubes, headers and baffles for inertia loads and also will be a pressure-carrying member. Due to the short span between the inner and outer radii of the header annulus, plate size for inertia loads will be less than the selected minimum thickness of 0.04 in. Pressure loads cause edge moments on the inner and outer radii, and local reinforcements may be required. The header at the other end is a pressure-carrying member, and the design will be similar for both headers.

Shell Design

The manifolding for the recuperator consists of several different types of pressure containing members including the outer cylinder shells in the A-1 and A-2 designs, conical inner shells and a radial inlet manifold for the compressor air. The outer cylindrical shells and radial manifold can be of sandwich construction to provide efficient pressure containment and strength for inertia loads. A typical outer sandwich shell for the A-1 and A-2 configurations would consist of 0.02 in. sheets and plain triangular fins between the inner and outer shells.

An important design consideration for the shells would be the incorporation of flexible sections to accommodate differential growth between tubes and shells. A typical flexible element would be a cylindrical formed metal bellows which would contain pressure and supply the needed axial flexibility.

SYSTEMS COMPARISON AND EVALUATION

An evaluation of the parametric data is presented to establish an engine configuration-recuperator design that is optimum for each of the two engine installation types. Evaluations of surface geometry, flow-path configurations, total engine-recuperator weight, and cost are given below.

RECUPERATOR SURFACE GEOMETRY EVALUATION

For the tubular recuperator designs, all four engine configurations chosen have the high pressure compressor discharge air inside the tubes and the low pressure turbine exhaust gas outside the tubes. As found in previous studies, this arrangement results in lightweight designs, since the inside Reynolds number is in a range where ring-dimpling of the tube wall provides an effective means of increasing the inside heat transfer coefficient.

For the finned-tube designs, the addition of finned secondary surfaces on the outside of the tubes virtually precludes ring-dimpling of the tube wall. The inside heat transfer coefficient can be increased by utilizing a plain strip, a wire spiral, or a flap turbulator inside the tube. With the plain strip brazed inside the tube, the combination of reduced hydraulic diameter and increased surface area results in an improved internal conductance. The data from the recuperator parametric study showed that the finned-tube geometry was not very attractive, primarily because finning of tubes adds area to the side of the heat exchanger that already has the higher conductance. The addition of heat transfer surface area to the high conductance side represents an inefficient use of heat transfer area, and thus results in a high-weight design.

Based on practical material thicknesses, a series of minimum weight solutions for plate-fin surface geometries was generated for a wide range of surface compactness. Using efficient offset secondary surfaces resulted in the cores in which the weight was greater, and the volume smaller, than an equivalent unit with a tubular surface geometry. To achieve the smaller volume, extremely compact surface geometries were necessary, and this resulted in impractical core sizes with large flow frontal areas and small flow lengths. In the parametric study, it was found that the minimum weight counterflow plate-fin matrix, while lighter than the finned-tube variant, was much heavier than the dimpled plain tube design.

With one of the major goals of the study being to identify the type of recuperator surface geometry to give minimum weight units that are compatible with the turbomachinery, it is concluded that optimum designs will be realized with plain tube surface geometries.

RECUPERATOR FLOW-PATH CONFIGURATION

From the parametric study, it is apparent that at the extremes of the effectiveness and pressure loss ranges considered, unrealistic recuperator sizes as regards compatibility with the turbomachinery result for the practical range of internal and external surface geometries used in the heat transfer analysis. Even with the smallest hydraulic diameter surfaces evaluated, the minimum core weights at the 90 percent effectiveness level were in the order of hundreds of pounds, and for realistic designs an upper limit on effectiveness of 80 percent has been used in the comparison of configurations. At pressure losses of less than 4 percent, the recuperator inner and outer diameters become large and are not practical from the standpoint of engine integration. In the comparison of the various configurations, a low value of recuperator pressure loss of 4 percent has been used.

From the parametric study data, a comparison in core weights can be made between the two external configurations A-1 and A-2 over the range of effectiveness and pressure loss considered. In the design of the three-pass counterflow recuperators for the A-2 configuration, it was necessary to use in-line tube patterns to achieve minimum weight designs that were compatible with the turbomachinery. The heat transfer characteristics of this tube pattern are inferior to those associated with the staggered tube design used in the A-1 configuration. Although increased surface density surfaces were utilized for the A-2 design, by virtue of the inherently lower friction characteristics of the in-line tube arrangement, the increase in compactness was not sufficient to offset the poorer heat transfer characteristics of the in-line tubes. The net result of this was that, over the range of effectiveness and pressure loss considered, the core weights of the A-2 configuration were higher than those of the A-1 configuration when comparing two units on the basis of compatibility with the turbomachinery.

From the parametric study data, a comparison in core weights can be made between the two internal configurations B-1 and B-2 over the range of effectiveness and pressure loss considered. Both designs are of two-pass cross-counterflow arrangement with the high pressure air inside the tubes and the low pressure gas outside the tube bundle. In the B-1 design, the low pressure gas flows two-pass across the bundle, and for designs to be compatible with the turbomachinery there is a limit in surface compactness that can be used for the low available gas side pressure loss. In the B-1 design, the small flow length associated with the single pass across the bundle means that the gas side mass flow velocity can be increased considerably by utilizing a much more compact surface geometry. At the same time, full advantage of the ring-dimpling effect on internal heat transfer can be taken by the increased mass flow velocity on the air side by virtue of the two-pass flow arrangement. In comparing the two configurations, it is apparent that the B-2 flow arrangement results in designs with a much improved balance of internal to external thermal conductance. On the basis of compatibility with the turbomachinery, there is little difference in core weight between the B-1 and B-2 designs, but because of the much

more compact surfaces used in the B-2 arrangement, the core volume is much less and hence results in a much smaller engine package.

While configurations A-1 and B-2 can be identified as the most attractive from the standpoint of minimum heat exchanger core weight for the external and internal installations respectively, a further study was carried out to confirm this selection on the basis of overall engine-recuperator weight.

RECUPERATOR WEIGHT ESTIMATES

Detailed weight calculations were carried out for the four engine configurations at the reference engine design conditions (recuperator effectiveness of 0.65 and pressure loss of 6 percent). The weight of the recuperator may be readily broken down into a number of components, including tubes, headers, baffles, ducts, flanges and seals. To enable a series of simple equations to be generated which allows the total weight of a complete recuperator of a given type to be calculated from the data presented in the parametric study, the following were considered.

In addition to tube weight, the headers and baffles must be considered in the calculation of core weight. The weight of the blank header and baffle may be readily computed knowing the inside and outside core diameters and respective thicknesses. The number of tubes in the core can be established from the tube weight, diameter, length and wall thickness. It is then a simple step to compute the weight of the drilled headers and baffles. Simplifying equations were derived for weights of the shell, ducts, flanges and seals. Stress calculations were carried out to compute the necessary sheet metal thicknesses for pressure containment in the shells and ducts. Weights were calculated by computing the developed lengths of the ducts and their mean diameters in terms of the tube length, bundle inner and outer diameters, or some basic dimension fixed by the turbomachinery. A similar approach was used in the calculation of the flange and seal weights. The following equations were generated to give overall recuperator weight for the four engine configurations.

Engine Configuration A-1

$$\text{Recuperator weight} = W_T + 0.0392\,(D_o^2 - D_I^2) - \frac{0.0707\,W_T}{dL}$$

$$+ 0.00327\,D_o^2 L + 0.0393\,D_I L + 0.376L$$

$$+ 0.248\,D_o - 0.076\,D_I + \text{constant}$$

Engine Configuration A-2

$$\text{Recuperator weight} = W_T + 0.0467\,(D_o^2 - D_I^2) - \frac{0.0875\,W_T}{dL} + 0.00327\,D_o^2L + 0.0317\,D_IL + 0.376L + 0.248\,D_o - 0.053\,D_I$$

Engine Configuration B-1

$$\text{Recuperator weight} = W_T + 0.0583\,D_o^2 - 0.028\,D_I^2 - \frac{0.0707\,W_T}{dL} + 0.031\,D_oL + 0.0445\,D_IL + 0.267\,D_I + 0.033\,D_o - \text{constant}$$

Engine Configuration B-2

$$\text{Recuperator weight} = W_T + 0.0323\,(D_o^2 - D_I^2) - \frac{0.052\,W_T}{dL} + 0.015\,D_IL + 0.44L + 0.147\,D_o + 0.122\,D_I + \text{constant}$$

where W_T = total tube weight, lb

D_o = core outside diameter, in.

D_I = core inside diameter, in.

L = core length, in.

d = tube outer diameter, in.

t = tube wall thickness, in.

All four arrangements have the same basic turbomachinery arrangement, the weight of which was computed as 126.2 lb. Then, using this basic turbomachinery weight in conjunction with the above equations, the total engine weight can be calculated for any heat exchanger selected from the recuperator parametric study curves.

RECUPERATOR COST DATA

The first objective in the cost analysis was to develop detailed cost information on the four basic configurations at the reference engine effectiveness and pressure loss of 0.65 and 6 percent respectively. The second objective was to develop cost scalars for configurations A-1 and B-2 which would permit the generation of cost information over a range of

effectiveness from 0.40 to 0.80 and a range of pressure loss from 4 percent to 10 percent.

In the first task, cost considerations were given to the constituent parts and the labor involved in their assembly. The recuperator may be split into two major assemblies: the core and the shell with its associated ducting and structure.

Recuperator Core Cost Breakdown (Applicable to All Four Configurations)

The core can be further split into tubes, headers and baffles. Tube cost data was obtained from a number of manufacturers for a range of diameters and wall thicknesses for several materials. The tube cost data used in the analysis is shown in Figure 57. To the basic cost of the tubing must be added the cost of ring-dimpling where applicable. The cost is assessed on a linear-foot basis irrespective of tube diameter, wall thickness or material. Headers and baffles are considered together because of their similar configuration. Basic sheet metal costs were used to derive the cost of the blank headers, to which a charge was added for blanking and forming to the desired configuration. The major cost, however, is in the formation of the holes, which are most economically produced by the Electric Discharge Machining (EDM) process. This cost is assessed on the number of holes required irrespective of size or spacing. The assembly costs of the core can be broken down into stacking, brazing, and inspection. Stacking cost is assessed on the number of tubes and baffles through which the tubes must be passed, and is irrespective of tube diameter. Brazing costs are assessed on the basis of core volume, as this determines the number of units which may be brazed in any given furnace load. Inspection costs are based on the number of parts, which in this case is dominated by the number of tubes.

Recuperator Shell and Ducting Cost Breakdown

The recuperator shell and ducting costs are assessed on the basis of diameter, length, relative complexity, and basic sheet metal costs.

In configurations A-1 and A-2, the compressor discharge air is ducted to the recuperator in an outer annulus. The cost of these integral ducts is assessed on the basis of core length and core outside diameter, with an additional factor to cover their relative complexity. The turbine exhaust duct is assessed only on the basis of core internal diameter (its length for the most part is defined by the engine geometry) and relative complexity. Various flanges and seals associated with the recuperator are included in the duct cost. Their cost is assessed on their diameter, which may be taken as constant or may be approximated by the core inside or outside diameter, and their relative complexity.

In the second part of the cost study, a series of cost scalars was established for configurations A-1 and B-2 using the basic guidelines given above.

a. Core Costs for Configurations A-1 and B-2

$$\text{Tube cost} = (a\,C_T + b)\,\frac{W_T}{dt}$$

$$\text{Header cost} = \frac{C\,W_T}{L\,dt}$$

$$\text{Stacking cost} = \frac{d'\,W_T}{L\,dt}$$

$$\text{Inspection cost} = \frac{e\,W_T}{L\,dt}$$

$$\text{Brazing cost} = f\,LD_C$$

Combining the above equations gives

$$\text{Total core cost} = (a\,C_T + b)\,\frac{W_T}{dt} + \frac{g\,W_T}{L\,dt} + f\,LD_O$$

where a, b, c, d', e, f, and g are constants

C_T = tubing cost per foot for specific material

d = tube diameter

t = tube wall thickness

L = core length

D_O = core outside diameter

W_T = tube weight

b. Duct, Flange, Seal and Assembly Costs for Configurations A-1 and B-2

Ducts, flanges, seals and assembly costs associated with the core outside diameter are given by:

$$\text{A-1 configuration cost} = h\,D_O\,L$$

$$\text{B-2 configuration cost} = i\,D_O$$

Ducts, flanges, seals and assembly costs associated with the core inside diameters are given by:

$$\text{A-1 configuration cost} = j\,D_I$$

$$\text{B-2 configuration cost} = k\,D_I$$

where h, i, j and k are constants

D_I = core inside diameter

Combining the above equations gives the cost scalars used in determining the total recuperator costs over a range of effectiveness and pressure loss.

$$\text{A-1 Configuration Recuperator Cost} = (aC_T + b)\frac{W_T}{dt} + \frac{g\,W_T}{L\,dt} + (f + h)\,LD_o + j\,D_I$$

$$\text{B-2 Configuration Recuperator Cost} = (aC_T + b)\frac{W_T}{dt} + \frac{g\,W_T}{L\,dt} + fLD_o + i\,D_o + k\,D_I$$

SELECTION OF RECUPERATOR CONFIGURATIONS FOR INTERNAL AND EXTERNAL INSTALLATIONS

A survey of the recuperator parametric data was carried out to identify the surface geometries which gave minimum weight designs that were compatible with the turbomachinery. For the most attractive surface geometries, data was taken from the parametric study and replotted as shown for configuration A-1 in Figure 59. The units selected are identified on the curves in this figure. A summary of the designs selected for configurations A-1 and A-2 is given in Tables XIII and XIV respectively for the range of effectiveness and pressure loss being considered. The total recuperator weights computed and the engine weights are included in the tables.

Similarly, for the internal installation, data was taken from the parametric study and replotted as shown for configuration B-2 in Figure 60. The units selected are identified on the curves in this figure. A summary of the designs selected for configurations B-1 and B-2 is shown in Tables XV and XVI respectively for the range of effectiveness and pressure loss being considered.

To have established designs that had a common recuperator inside diameter would have meant running an infinite number of surface geometry combinations in the annular core recuperator design computer program. In the tables of selected minimum weight solutions, it can be seen that the inner diameters do vary; however, in the choice of these designs, consideration was given to compatibility with the turbomachinery. All of the solutions given in the four tables can be readily integrated with the basic turbomachinery to give compact engine packages.

Detailed cost analyses of the four basic configurations were carried out at the reference engine conditions The lowest recuperator cost estimate was for the B-2 configuration, and using this as a datum of say 100 percent, the relative costs of the other three configurations are as follows. The relative costs for configurations A-1, A-2, and B-1 were 136 percent, 186 percent, and 115 percent, respectively. For the two installation types, arrangements A-1 and B-2 are the most attractive from the standpoint of minimum cost. The cost scalars established from the detailed cost analyses at the reference engine conditions were used to generate the curves for

TABLE XIII. SELECTED HEAT EXCHANGER AND ENGINE SIZES AND WEIGHTS (FOR ENGINE CONFIGURATION A-1) FOR RANGE OF VARIABLES CONSIDERED IN PARAMETRIC STUDY

Pressure Loss	Effectiveness	0.80	0.75	0.70	0.65	0.60	0.50	0.40
($\Delta P/P$) = 4%	Bundle ID, in.	16.5 (1)	15.2 (5)	14.8 (9)	16.0 (13)	18.0 (17)	18.0 (21)	15.3 (25)
	Bundle OD, in.	24.0	22.7	21.1	21.9	21.9	20.6	17.9
	Tube length, in.	27.0	25.0	24.0	21.5	19.5	19.0	20.5
	Tube diameter, in.	.075	.10	.10	.10	.125	.20	.20
	Tube weight, lb	85.0	63.0	43.0	34.0	25.0	15.0	10.0
	Recuperator weight, lb	177.5	143.5	117.0	101.6	86.4	69.7	58.3
	Engine weight, lb	303.7	269.7	243.2	227.8	212.6	195.9	184.5
	Engine OD, in.	26.3	25.1	23.7	24.4	24.4	23.2	20.9
	Engine OV length, in.	40.5	39.0	32.5	35.0	33.0	32.5	34.0
($\Delta P/P$) = 6%	Bundle ID, in.	15.5 (2)	14.5 (6)	16.0 (10)	15.83 * (14)	14.6 (18)	16.4 (22)	16.7 (26)
	Bundle OD, in.	22.1	22.6	20.7	20.83	18.8	19.7	18.0
	Tube length, in.	22.0	20.4	17.5	16.20	17.0	13.0	14.5
	Tube diameter, in.	.075	.10	.075	.10	.10	.10	.20
	Tube weigh, lb.	71.0	51.0	36.0	27.14	22.0	13.0	8.5
	Recuperator weight, lb.	138.9	113.2	90.0	76.63	66.2	52.3	44.0
	Engine weight, lb.	265.1	239.4	216.2	202.8	192.4	178.5	170.2
	Engine OD, in.	24.6	25.0	23.3	23.45	21.7	22.5	21.0
	Engine OV length, in.	35.5	34.0	31.0	29.90	30.6	28.7	28.7
($\Delta P/P$) = 8%	Bundle ID, in.	14.2 (3)	14.5 (7)	17.5 (11)	16.4 (15)	14.5 (19)	15.0 (23)	17.0 (27)
	Bundle OD, in.	20.6	20.6	22.2	20.3	18.9	18.45	19.2
	Tube length, in.	21.5	16.2	13.7	14.5	14.5	12.0	11.5
	Tube diameter, in.	.075	.075	.075	.075	.10	.10	.125
	Tube weight, lb.	61.0	45.0	31.0	24.0	19.0	11.5	7.0
	Recuperator weight, lb.	121.4	92.9	77.5	66.6	58.5	46.1	39.5
	Engine weight, lb.	247.6	219.1	203.7	192.8	184.7	172.3	165.7
	Engine OD, in.	23.2	23.2	24.7	23.0	21.8	21.4	22.0
	Engine OV length, in.	35.0	29.9	28.7	28.7	28.7	28.7	28.7
($\Delta P/P$) = 10%	Bundle ID, in.	15.3 (4)	14.0 (8)	14.7 (12)	17.2 (16)	16.0 (20)	16.8 (24)	14.4 (28)
	Bundle OD, in.	21.6	19.0	20.1	21.4	20.4	18.6	16.4
	Tube length, in.	18.7	18.0	14.0	11.8	8.5	13.2	12.0
	Tube diameter, in.	0.075	0.075	0.075	0.075	0.10	0.15	0.125
	Tube weight, lb.	54.5	39.0	25.5	20.0	15.5	9.0	5.5
	Recuperator weight, lb.	109.2	85.3	70.2	59.3	53.0	42.0	34.9
	Engine weight, lb.	235.4	211.5	196.4	185.5	179.2	168.2	161.1
	Engine OD, in.	24.1	21.9	22.8	24.0	23.0	21.5	19.6
	Engine OV length, in.	32.3	31.6	28.7	28.7	28.7	28.7	28.7

*Reference engine conditions.

(1) Unit numbers referred to in Figure 59.

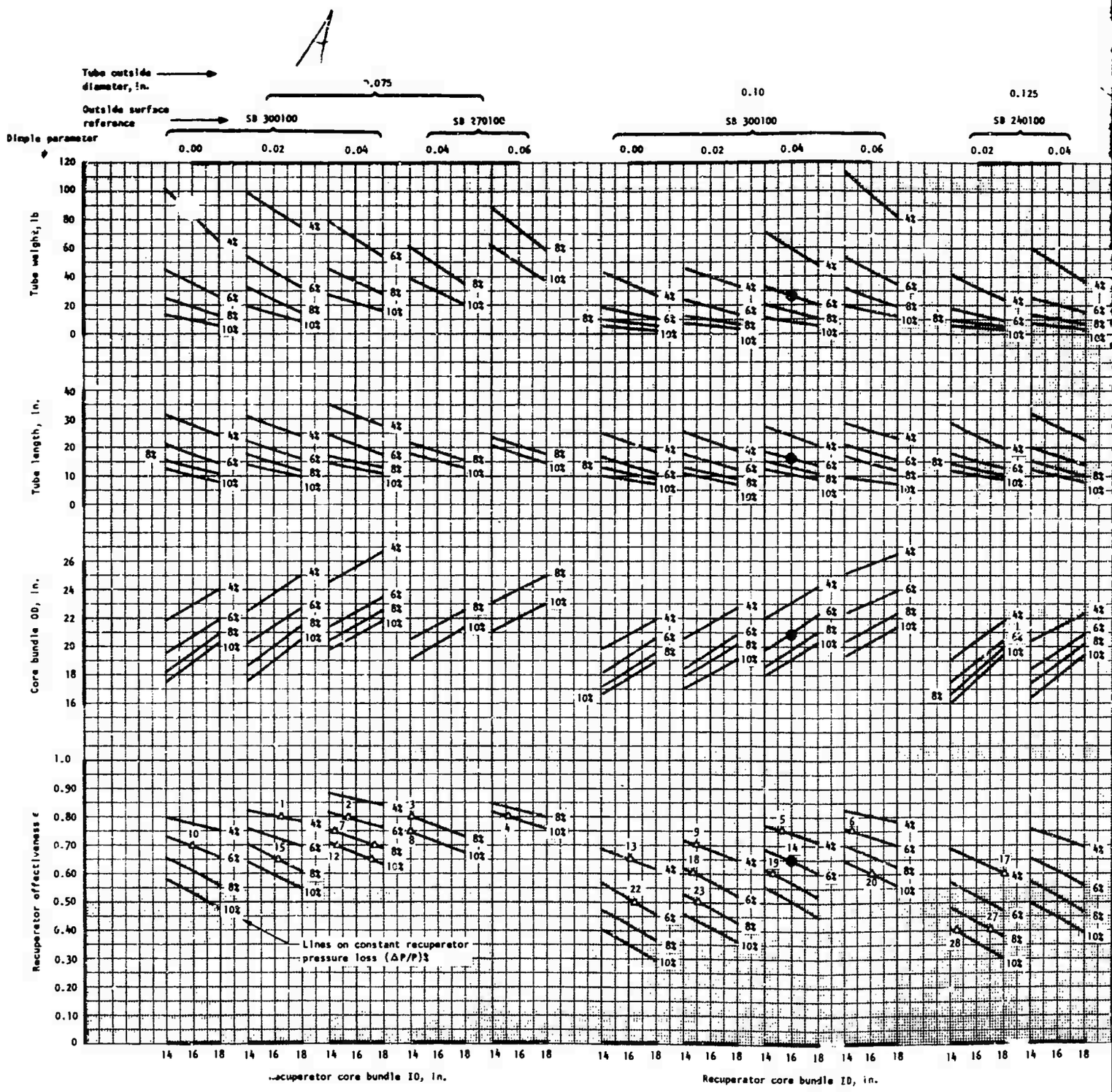

Figure 59. Summary of Recuperator Surface Geometries for Configuration A-1.

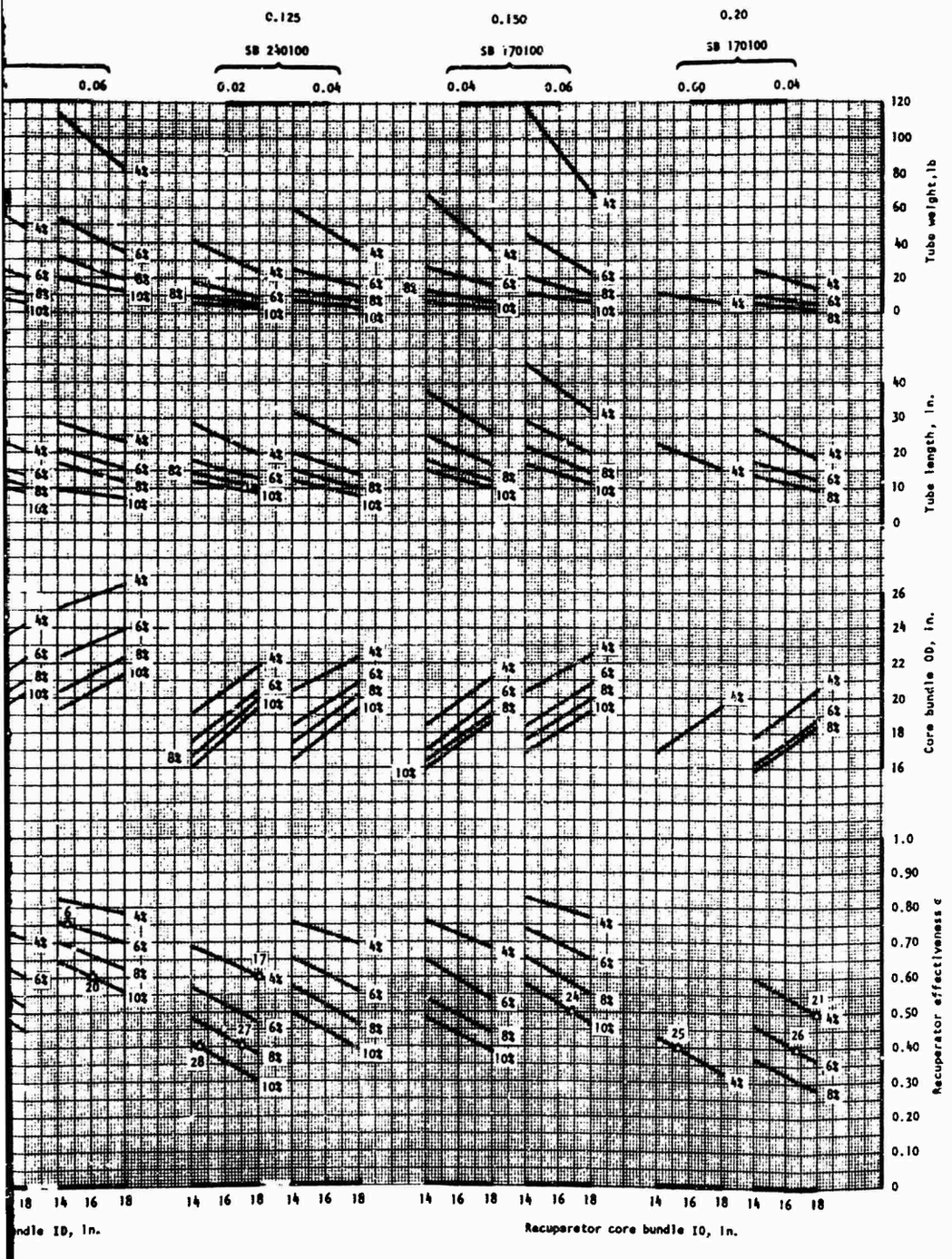

● Referenced engine design point date.

△ 19 Numbered units represent those selected from survey over the complete range of effectiveness and pressure loss being studied. These selected designs are summarized in table Tube weight based on wall thickness of 0.004"

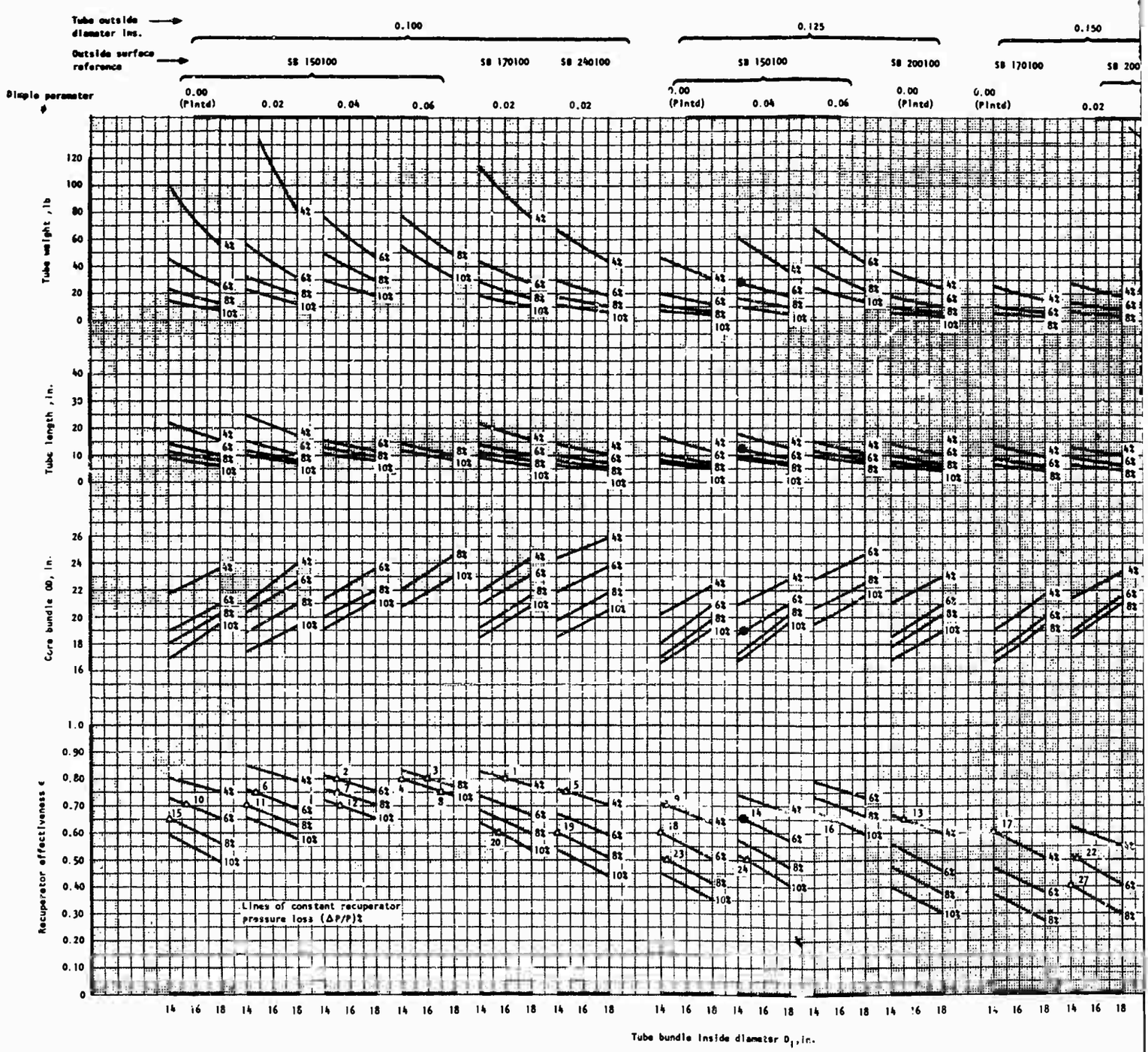

Figure 60. Summary of Recuperator Surface Geometries for Configuration B-2.

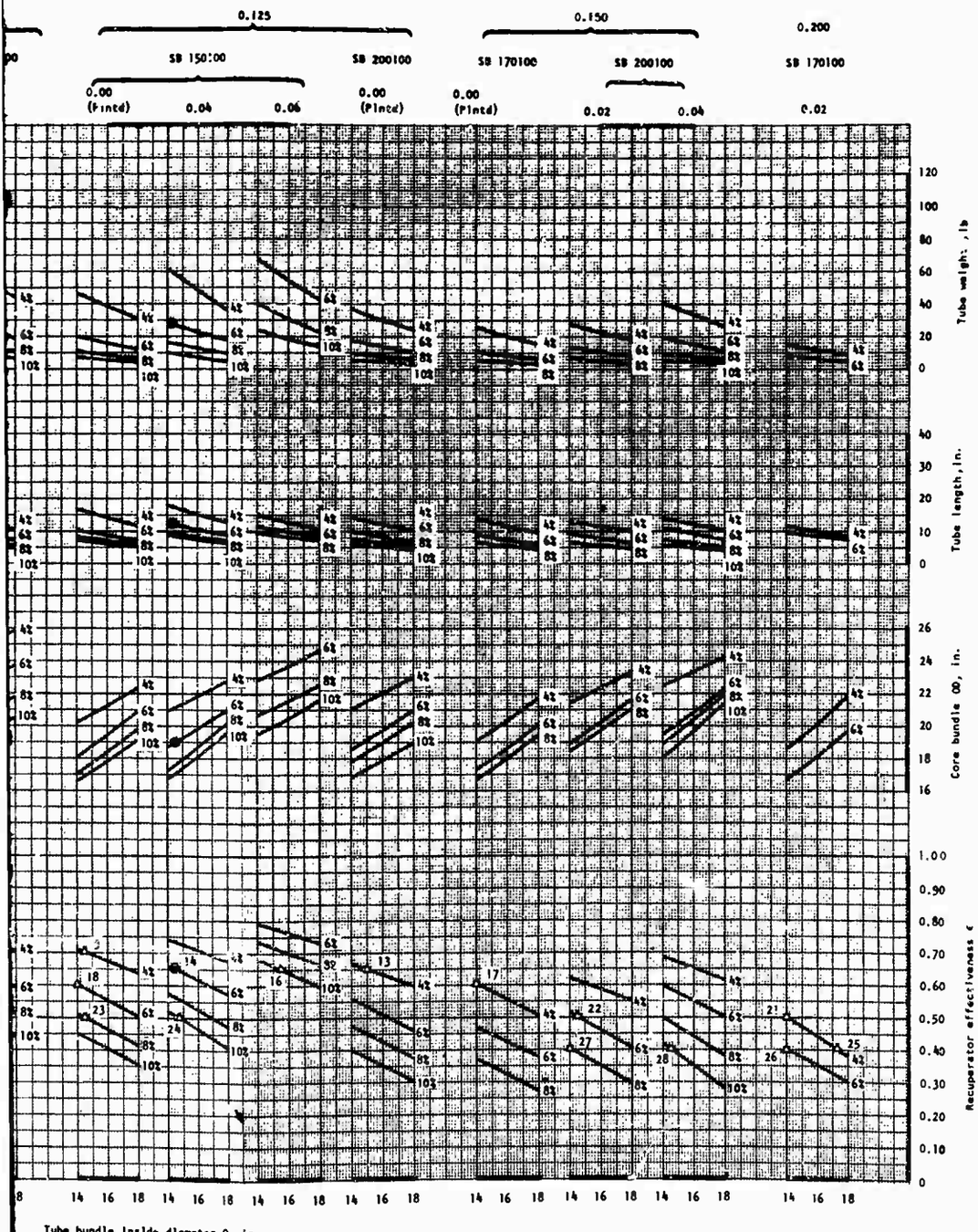

● Referenced engine design point data

△19 Numbered units represent those selected from survey over the complete range of effectiveness and pressure loss being studied.

These selected designs are summarized in table

Tube weights based on wall thickness of 0.004"

etries

TABLE XIV. SELECTED HEAT EXCHANGER AND ENGINE SIZES AND WEIGHTS (FOR ENGINE CONFIGURATION A-2) FOR RANGE OF VARIABLES CONSIDERED IN PARAMETRIC STUDY

Pressure Loss	Effectiveness	0.80	0.75	0.70	0.65	0.60	0.50	0.40
($\Delta P/P$)	Bundle ID, in.	16.0	15.5	16.5	16.0	15.0	15.0	16.0
= 4%	Bundle OD, in.	24.0	24.0	25.0	23.0	21.0	18.0	19.0
	Tube length, in.	30.0	28.0	22.0	20.5	21.5	15.0	16.0
	Tube diameter, in.	0.075	0.10	0.125	0.125	0.15	0.125	0.15
	Tube weight, lb	142.0	94.0	67.0	47.0	37.0	22.0	14.0
	Recuperator weight, lb	239.5	183.2	151.5	116.6	99.9	57.9	55.3
	Engine weight, lb	365.7	309.4	277.7	242.8	226.1	184.1	181.5
	Engine OD, in.	26.35	26.4	27.3	25.5	23.7	21.1	21.9
	Engine OV length, in.	44.0	40.0	36.0	34.5	35.5	29.0	30.0
($\Delta P/P$)	Bundle ID, in.	15.5	19.0	17.0	17.18*	15.0	16.0	15.0
=6%	Bundle OD, in.	24.0	25.5	22.0	22.50	19.5	19.5	18.0
	Tube length, in.	23.5	18.5	18.0	16.18	17.0	14.0	14.0
	Tube diameter, in.	.075	.075	.075	.10	.125	.10	.15
	Tube weight, lb	110.0	74.0	50.0	37.59	30.0	18.0	11.0
	Recuperator weight, lb	190.0	145.6	115.4	91.76	75.8	56.5	47.6
	Engine weight, lb	316.2	271.8	241.6	217.96	201.0	182.7	173.8
	Engine OD, in.	26.4	27.8	24.6	25.00	22.4	22.4	21.1
	Engine OV length, in.	37.5	32.5	32.0	30.18	31.0	28.5	28.5
($\Delta P/P$)	Bundle ID, in.	15.3	18.5	18.5	17.5	16.5	15.3	15.5
= 8%	Bundle OD, in.	24.0	22.0	23.5	22.5	21.0	19.5	18.0
	Tube length, in.	19.7	18.5	14.5	15.0	14.0	12.0	11.5
	Tube diameter, in.	.075	.075	.075	.10	.10	.125	.15
	Tube weight, lb	97.1	64.0	44.0	34.0	24.0	15.0	9.0
	Recuperator weight, lb	166.5	121.3	95.3	85.1	67.4	50.3	38.2
	Engine weight, lb	292.7	247.5	221.5	211.3	193.6	176.5	164.4
	Engine OD, in.	26.4	24.6	25.9	25.0	23.7	22.4	21.1
	Engine OV length, in.	33.7	32.5	28.5	29.0	28.5	28.5	28.5
($\Delta P/P$) = 10%	Bundle ID, in.			15.5	19.0	16.5	18.0	15.5
	Bundle OD, in.			21.0	23.0	20.0	20.0	17.5
	Tube length, in.	No	No	15.0	12.5	13.0	11.0	10.5
	Tube diameter, in.	Solu-tion	Solu-tion	.075	.075	.075	.075	.10
	Tube weight, lb			40.0	28.0	22.0	13.0	8.0
	Recuperator weight, lb			85.3	71.8	58.7	44.2	33.6
	Engine weight, lb			211.5	198.0	184.9	170.4	159.8
	Engine OD, in.			23.7	25.5	22.8	22.8	20.6
	Engine OV length, in.			29.0	28.5	28.5	28.5	28.5

*Reference engine conditions.

TABLE XV. SELECTED HEAT EXCHANGER AND ENGINE SIZES AND WEIGHTS (FOR ENGINE CONFIGURATION B-1) FOR RANGE OF VARIABLES CONSIDERED IN PARAMETRIC STUDY

Pressure Loss	Effectiveness	0.80	0.75	0.70	0.65	0.60	0.50	0.40
$(\Delta P/P)$ = 4%	Bundle ID, in.	16.5	15.5	17.0	18.0	18.0	18.0	19.5
	Bundle OD, in.	24.0	23.0	22.0	22.0	22.0	21.0	21.5
	Tube length, in.	27.0	14.5	22.5	20.5	19.5	17.5	14.0
	Tube diameter, in.	.075	.10	.10	.10	.125	.15	.15
	Tube weight, lb	85.0	62.0	45.0	34.0	24.0	16.0	10.0
	Recuperator weight, lb	150.7	105.9	98.8	85.4	74.4	60.6	51.6
	Engine weight, lb	276.9	232.1	225.0	211.6	200.6	186.8	177.8
	Engine OD, in.	27.10	26.2	25.4	25.4	25.4	24.5	24.9
	Engine OV length, in.	42.5	30.0	38.0	36.0	35.0	33.0	29.5
$(\Delta P/P)$ = 6%	Bundle, ID, in.	17.5	16.7	16.0	18.15*	16.5	16.5	17.0
	Bundle OD, in.	23.5	23.5	21.5	22.15	20.0	19.0	19.0
	Tube length, in.	21.5	19.5	19.0	15.45	16.0	16.0	14.5
	Tube diameter, in.	.075	.10	.125	.10	.10	.20	.15
	Tube weight, lb	69.0	48.0	35.0	25.29	21.0	12.0	9.0
	Recuperator weight, lb	125.0	102.2	82.5	69.7	60.1	49.0	44.5
	Engine weight, lb	251.2	228.4	208.7	195.9	186.3	175.2	170.7
	Engine OD, in.	26.6	26.7	24.9	25.5	23.6	22.8	22.8
	Engine OV length, in.	37.0	35.0	34.5	30.95	31.0	31.0	30.0
$(\Delta P/P)$ = 8%	Bundle ID, in.	16.0	16.0	17.5	17.0	16.5	16.5	16.0
	Bundle OD, in.	20.5	22.5	22.0	19.5	20.0	19.5	18.5
	Tube length, in.	18.0	17.5	13.5	15.5	13.5	12.0	10.5
	Tube diameter, in.	.075	.075	.075	.075	.10	.15	.15
	Tube weight, lb	64.0	43.0	31.0	24.0	17.0	11.0	7.0
	Recuperator weight, lb	104.6	90.2	71.1	60.5	52.8	43.8	35.4
	Engine weight, lb	230.8	216.4	197.3	186.7	179.0	170.0	161.6
	Engine OD, in.	24.10	25.8	25.4	23.3	23.6	23.3	22.4
	Engine OV length, in.	33.5	33.0	29.5	31.0	29.5	29.5	29.5
$(\Delta P/P)$ = 10%	Bundle ID, in.	15.5	14.0	16.5	16.0	18.0	17.0	17.5
	Bundle OD, in.	21.5	19.0	20.5	19.0	22.0	19.0	19.0
	Tube length, in.	18.5	18.5	14.5	16.5	11.0	13.0	11.0
	Tube diameter, in.	.075	.075	.075	.075	.10	.15	.15
	Tube weight, lb	56.0	40.0	27.0	20.0	14.0	9.0	6.0
	Recuperator weight, lb	100.9	77.9	64.7	56.6	51.5	41.9	36.2
	Engine weight, lb	227.1	204.1	190.9	182.8	177.7	168.1	162.4
	Engine OD, in.	24.9	22.8	24.1	22.8	25.4	22.8	22.8
	Engine OV length, in.	34.0	34.0	30.0	32.0	29.5	29.5	29.5

*Reference engine conditions.

TABLE XVI. SELECTED HEAT EXCHANGER AND ENGINE SIZES AND WEIGHTS (FOR ENGINE CONFIGURATION B-2) FOR RANGE OF VARIABLES CONSIDERED IN PARAMETRIC STUDY

Pressure Loss	Effectiveness	0.80	0.75	0.70	0.65	0.60	0.50	0.40
($\Delta P/P$) = 4%	Bundle ID, in.	16.0[1]	14.7[5]	14.5[9]	15.0[13]	14.0[17]	14.0[21]	17.3[25]
	Bundle OD, in.	23.0	24.6	20.6	21.5	19.0	18.5	21.2
	Tube length, in.	18.5	13.8	16.0	13.2	14.0	11.7	8.8
	Tube diameter, in.	.10	.10	.125	.125	.15	.20	.20
	Tube weight, lb	94.0	63.0	45.0	33.0	26.0	15.0	9.0
	Recuperator weight, lb	122.1	91.7	69.8	57.4	48.3	35.4	25.8
	Engine weight, lb	248.3	217.9	196.0	183.6	174.5	161.6	152.0
	Engine OD, in.	23.2	24.6	20.6	21.7	19.2	18.7	21.4
	Engine OV length, in.	33.0	28.5	30.5	28.5	28.5	28.5	28.5
($\Delta P/P$) = 6%	Bundle ID, in.	15.0[2]	14.1[6]	15.5[10]	14.36[14]*	14.0[18]	14.5[22]	14.0[26]
	Bundle OD, in.	21.9	20.7	19.7	18.86	18.0	19.1	16.7
	Tube length, in.	14.5	14.7	12.5	12.22	10.2	9.0	9.5
	Tube diameter, in.	.10	.10	.10	0.125	.125	.15	.20
	Tube weight, lb	69.0	52.0	37.0	26.9	20.0	12.5	8.0
	Recuperator weight, lb	93.4	75.6	58.0	47.4	39.0	29.5	24.0
	Engine weight, lb	219.6	201.8	184.2	173.6	165.2	155.7	150.2
	Engine OD, in.	22.1	20.9	19.9	19.04	18.2	19.3	16.9
	Engine OV length, in.	29.0	29.2	28.5	29.50	28.5	28.5	28.5
($\Delta P/P$) = 8%	Bundle ID, in.	16.0[3]	15.0[7]	14.0[11]	14.0[15]	14.0[19]	14.5[23]	14.0[27]
	Bundle OD, in.	23.2	20.5	18.8	18.0	19.7	17.3	18.4
	Tube length, in.	12.5	12.0	12.0	11.5	8.0	8.2	7.0
	Tube diameter, in.	.10	.10	.10	.10	.10	.125	.15
	Tube weight, lb	62.0	45.0	33.0	24.0	18.0	11.0	7.0
	Recuperator weight, lb	86.4	67.2	52.9	42.9	36.8	27.0	23.1
	Engine weight, lb	212.6	193.4	179.1	169.1	163.0	153.2	149.3
	Engine OD, in	23.4	20.7	19.0	18.2	19.9	17.5	18.6
	Engine OV length, in.	28.5	28.5	28.5	28.5	28.5	28.5	28.5
($\Delta P/P$) = 10%	Bundle ID, in.	14.0[4]	17.0[8]	15.2[12]	15.5[16]	15.5[20]	14.75[24]	14.5[28]
	Bundle OD, in.	20.7	22.4	19.7	20.2	19.3	17.2	18.4
	Tube length, in.	12.0	9.0	9.8	8.6	8.0	8.0	5.6
	Tube diameter, in.	.10	.10	.10	.125	.10	.125	.15
	Tube weight, lb	56.0	37.0	26.0	20.0	15.0	9.7	6.0
	Recuperator weight, lb	77.6	58.2	45.0	39.1	32.4	25.3	21.5
	Engine weight, lb	203.8	186.4	171.2	165.3	158.6	151.5	147.7
	Engine OD, in.	20.9	22.6	19.9	20.4	19.5	17.4	19.6
	Engine OV length, in.	28.5	28.5	28.5	28.5	28.5	28.5	28.5

* Reference engine conditions.

① Unit numbers referred to in Figure 60.

recuperator and engine cost over a range of effectiveness and pressure loss, and these are shown in the sensitivity curve arrays. A comparison of heat transfer and weight data for the four configurations at the reference engine conditions is given in Table XVII.

In comparing the two external installations, it can be seen from the tables that configuration A-1 is more attractive from the standpoint of minimum engine weight and also has a slightly smaller package envelope. Similarly, for the internal installations, configuration B-2 has the smallest weight and package size. This trend for both these configurations exists over the range of effectiveness and pressure loss examined. The weight scalars, established from a detailed weight analysis at the reference engine conditions, were used to generate the curves for recuperator and engine weight shown in the sensitivity study.

From the thermal, weight, and cost analyses, it is concluded that arrangements A-1 and B-2 are the most attractive from the standpoints of minimum weight and cost. The effects of small changes in any one of the design variables for these two flow configurations have been analyzed in the sensitivity study.

All of the tube weights quoted in the recuperator parametric study are based on a tube wall thickness of 0.004 in. since this represents the minimum value being used in current high performance lightweight tubular recuperators. The work outlined in Reference 4 indicates that tube walls as thin as 0.0035 in. can withstand the severe hot corrosive environment associated with the gas turbine exhaust. The effects of recuperator tube wall thickness on overall engine weight are shown on Figures 61 and 62 for engine configurations A-1 and B-2, respectively. At the reference engine conditions, the utilization of the thinner tube wall results in an overall engine weight savings of only 3 pounds. The cost of the recuperator would increase by 3 percent, showing up as a less than 1 percent increase in overall engine cost. There is little incentive in using wall thicknesses greater than 0.004 in. since this results in a weight penalty without a decrease in cost. From the tube material cost curves on Figure 57, it can be seen that for diameters of less than 0.15 in. (most of the minimum weight solutions were for diameters smaller than this value), the tube cost for the 0.005 and 0.006 in. walls is the same as that for the 0.004 in. walls.

In the analysis and designs discussed so far, no reference has been made to the engine final exhaust system. None of the engine weight figures includes the weight of the final exhaust ducting, since the exact shape and size, etc., is very much dependent on the engine installation for a particular application. A curve relating exhaust duct size with exhaust gas velocity and velocity head for a range of recuperator effectiveness is shown in Figure 63. Because of the low gas side pressure loss allowable, there is a big incentive in the recuperative gas turbine to keep the exhaust gas velocities as low as possible. For the 5 lb/sec mass flow recuperative engine under consideration, a final exhaust duct diameter

TABLE XVII. COMPARISON OF FOUR RECUPERATIVE ENGINE CONFIGURATIONS AT THE REFERENCE ENGINE CONDITIONS

Installation Type	External		Internal	
Configuration	A-1	A-2	B-1	B-2
Tube bundle ID, in.	15.83	17.18	18.15	14.36
Tube bundle OD, in.	20.83	22.50	22.15	18.86
Tube length, in.	16.20	16.18	15.45	12.22
Number of tubes	4800	6656	4690	5004
Tube diameter, in.	.10	.10	.10	.125
Dimple parameter, Ψ	0.04	0.06	0.04	0.02
Outside surface geometry	SB300100	IB200125	SB270100	SB150100
Surface compactness, ft^2/ft^2	241.0	289.0	268.0	389.0
G inside tubes, $lb/sec\text{-}ft^2$	21.65	15.46	21.89	25.43
Reynolds number inside	6808.0	4964.0	6867.0	9955.0
hA inside, Btu/hr-^{0}F	21,495	31,363	20,815	17,790
G outside tubes, $lb/sec\text{-}ft^2$	2.91	4.284	2.92	3.39
Reynolds number outside	2108.0	2461.0	1787.0	936.0
hA outside, Btu/hr-^{0}F	12,729	10,472	13,138	14,395
hA_I/hA_o	1.69	2.99	1.59	1.24
Core volume, ft^3	1.35	1.55	1.13	0.83
Tube weight, lb	27.14	37.59	25.29	26.90
Recuperator weight, lb	76.63	91.76	69.70	47.40
Engine weight, lb	202.8	217.96	195.9	173.6
Engine overall diameter, in.	23.45	25.00	25.50	19.04
Engine overall length, in.	29.90	30.18	30.95	28.50
Recuperator cost, percent	136.0	186.0	115.0	100.0
Engine cost, percent	108.0	119.5	103.5	100.0

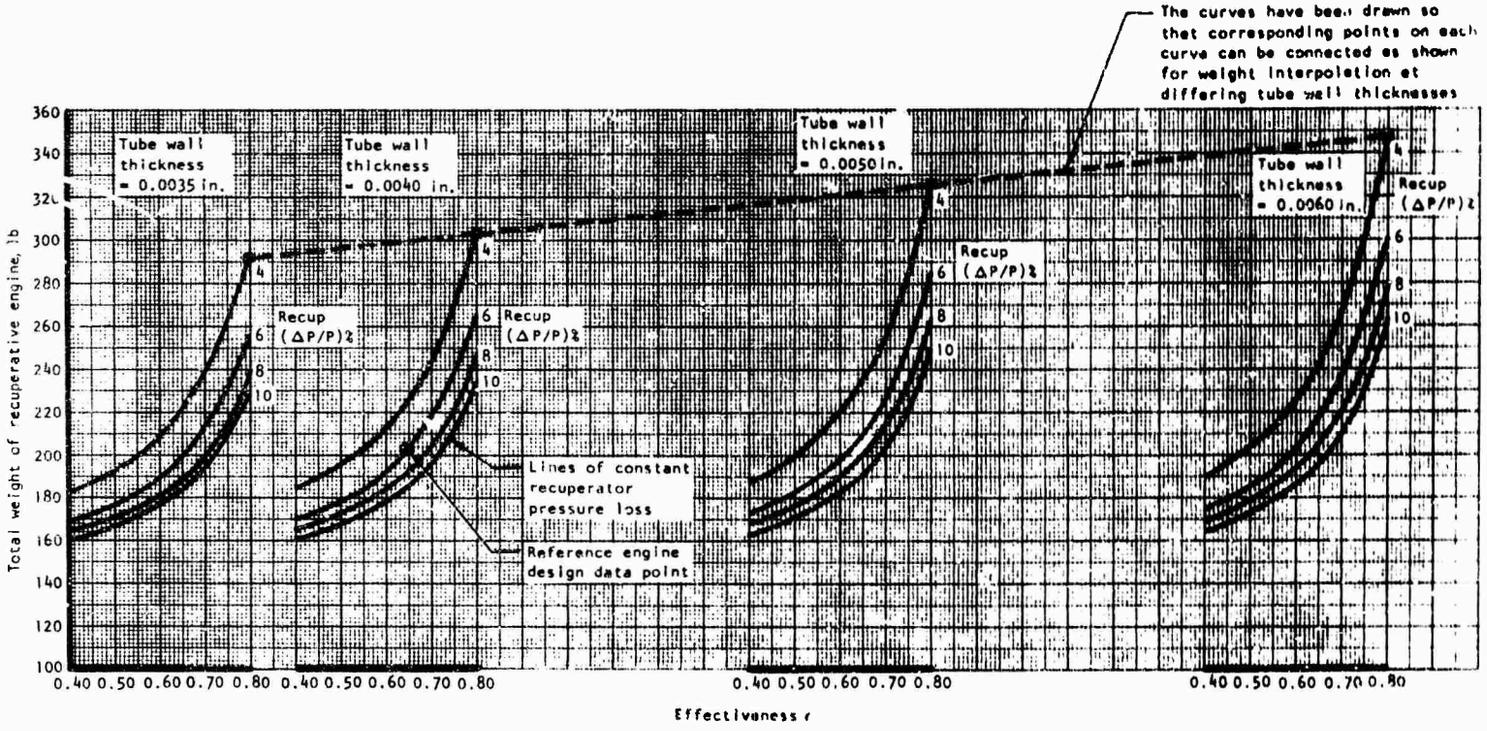

Figure 61. Effect of Recuperator Tube Wall Thickness on Overall Weight of Engine Configuration A-1.

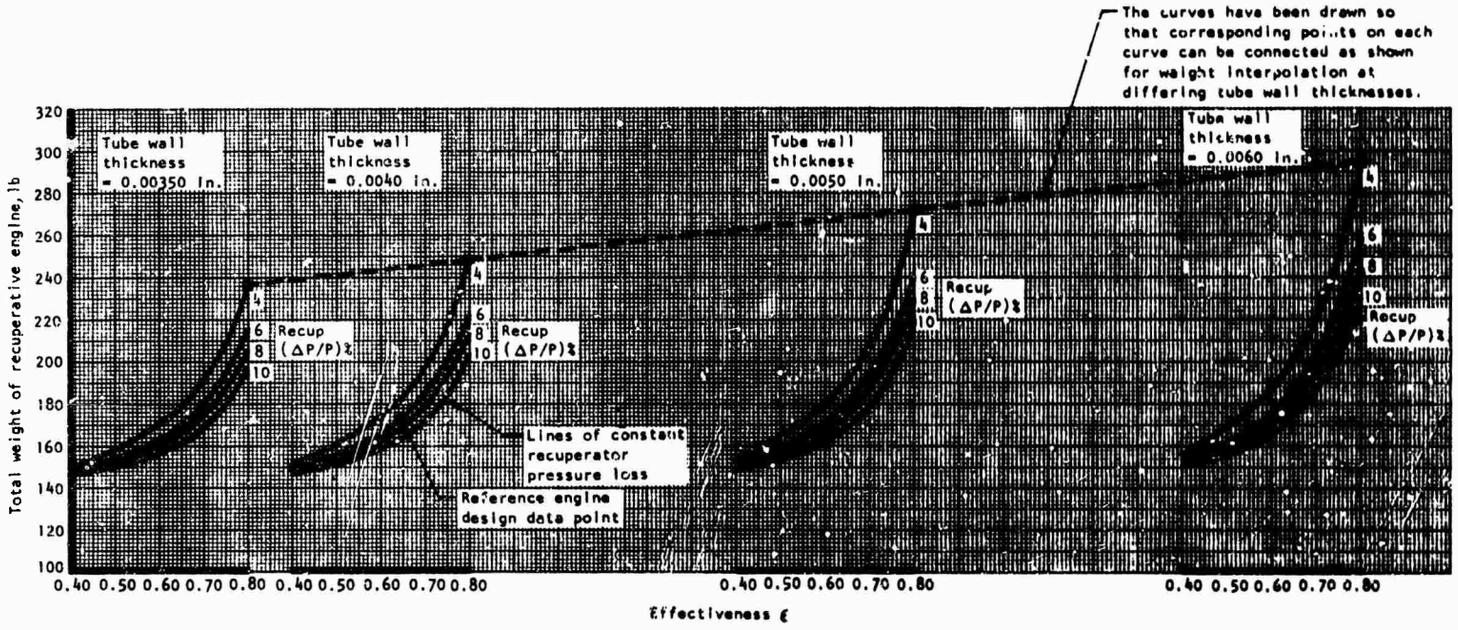

Figure 62. Effect of Recuperator Tube Wall Thickness on Overall Weight of Engine Configuration B-2.

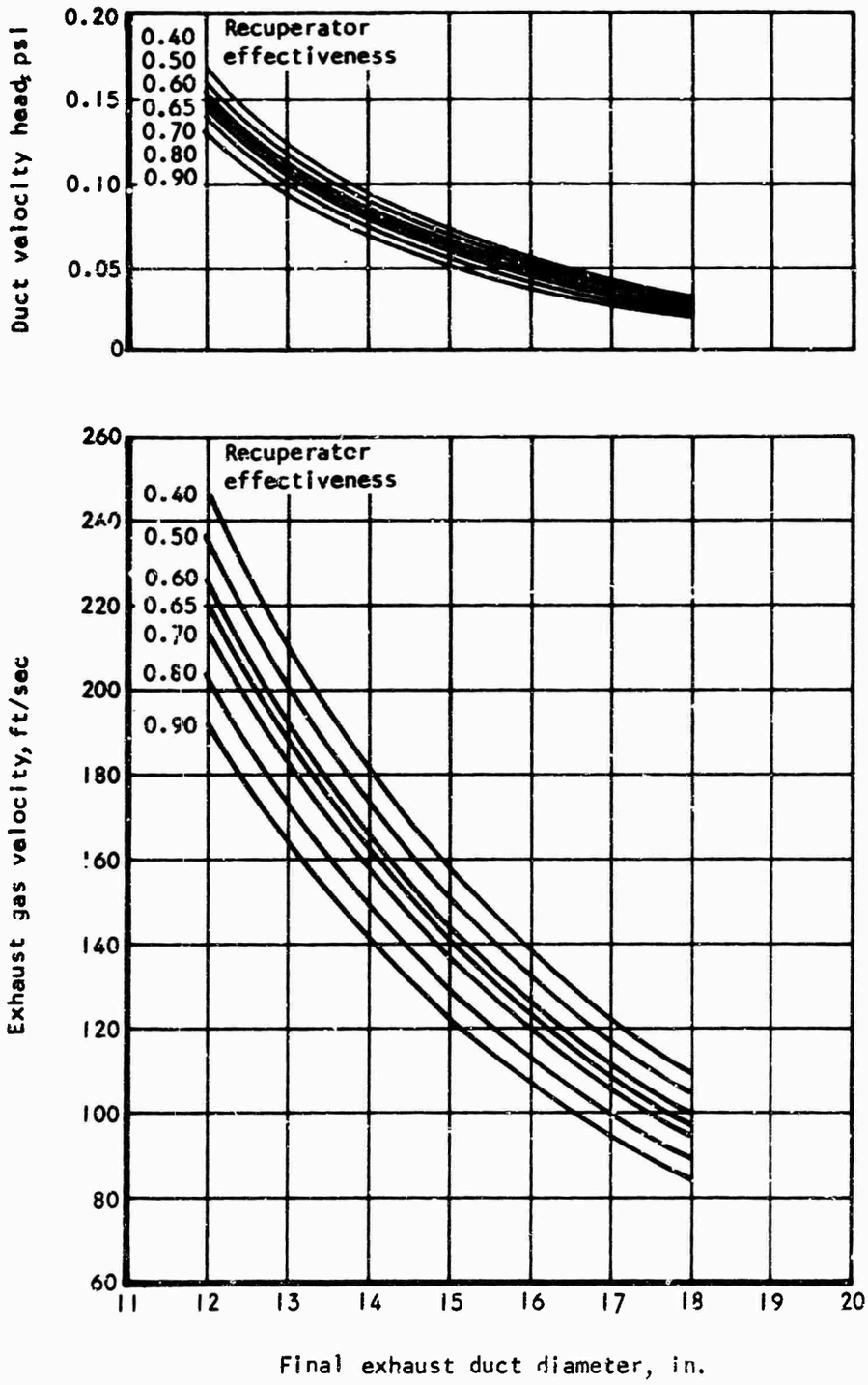

Figure 63. Effect of Exhaust Duct Size and Recuperator Effectiveness of Final Gas Leaving Velocity.

in the order of 15 to 16 in. would result in exhaust gas velocities of 140-120 ft/sec at the reference engine conditions. Equivalent flow areas could be used to give exhaust duct geometries that are compatible with the engine and installation. An exhaust duct system considered for the A-1 engine is shown in Figure 64. In this system, the gas leaving the annulus at the recuperator exit is collected in a type of volute and directed to the final exit plane which is shown as a simple rectangular duct. An isometric view of the A-1 configuration showing the simplicity of the overall engine and exhaust system is shown in Figure 65. For the internal installation, the exhaust geometry is much dependent on the engine location within the airframe. Essentially, the exhaust gas must be collected in an annular scroll from the recuperator exit and ducted to the final exhaust plane. An exhaust duct system considered for the B-2 engine is shown in Figure 66. An isometric view of the B-2 configuration showing the simplicity of the overall engine and exhaust system is shown in Figure 67. With a nonrecuperated engine, there is no exhaust back pressure from the heat exchanger, and much higher exhaust gas velocities are in order; by careful design of the exhaust system, additional benefits in thrust and hence overall fuel consumption can be realized. To complete the picture, a very simple exhaust system is shown for the nonrecuperative engine in Figure 68.

In the design of the recuperative engines, considerable thought was given to the complete integration of the heat exchanger and the turbomachinery structures to give a compact, lightweight design. The A-1 and B-2 engines are of essentially modular construction and can be disassembled very quickly for routine inspection or maintenance. The basic modular concept for engines A-1 and B-2 is illustrated in the exploded views shown in Figures 69 and 70 respectively. By removal of the bolts from flange A, the engine is split into the two basic gas-generator and power turbine modules. Using the same tool, the bolts can be removed from flange B, and after removing the end cap from the bearing housing at C, the complete recuperator assembly can be removed from the power turbine section, this giving the three basic assemblies shown in the figures. Using one simple double-ended tool, the engine can be disassembled into the three basic elements in just a few minutes.

A

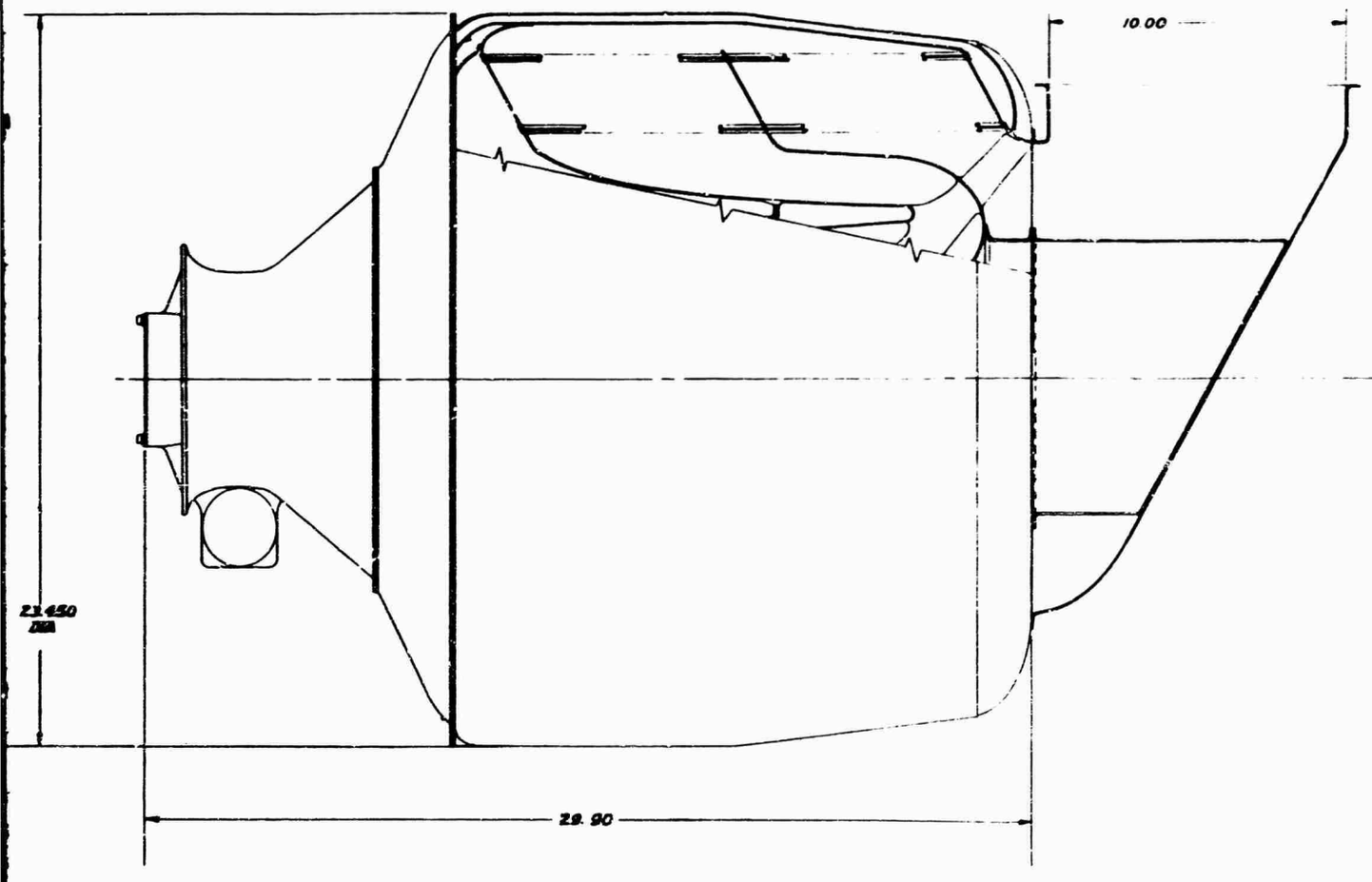

Figure 64. View of Engine Configuration A-1 Showing Exhaust Duct System.

15

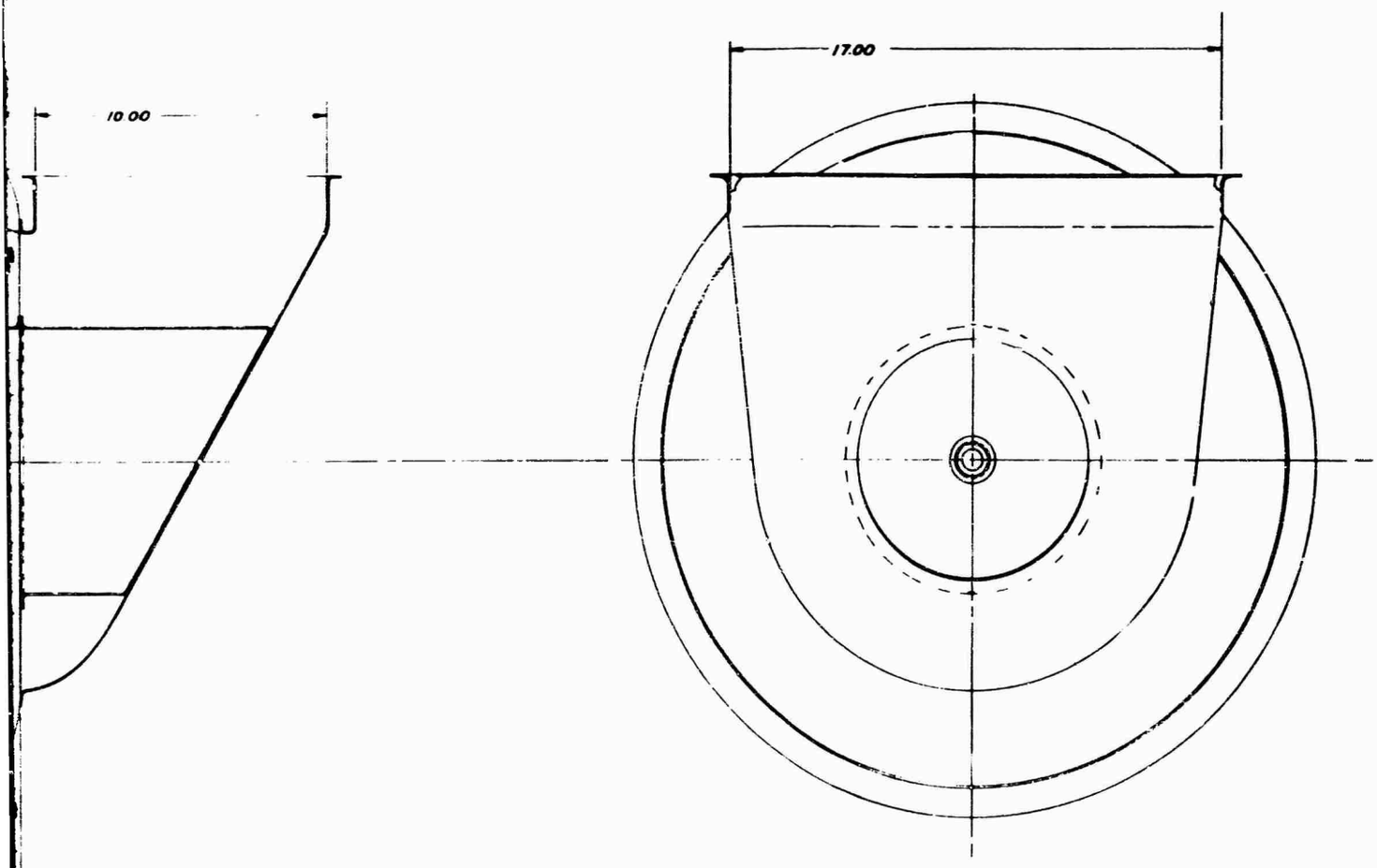

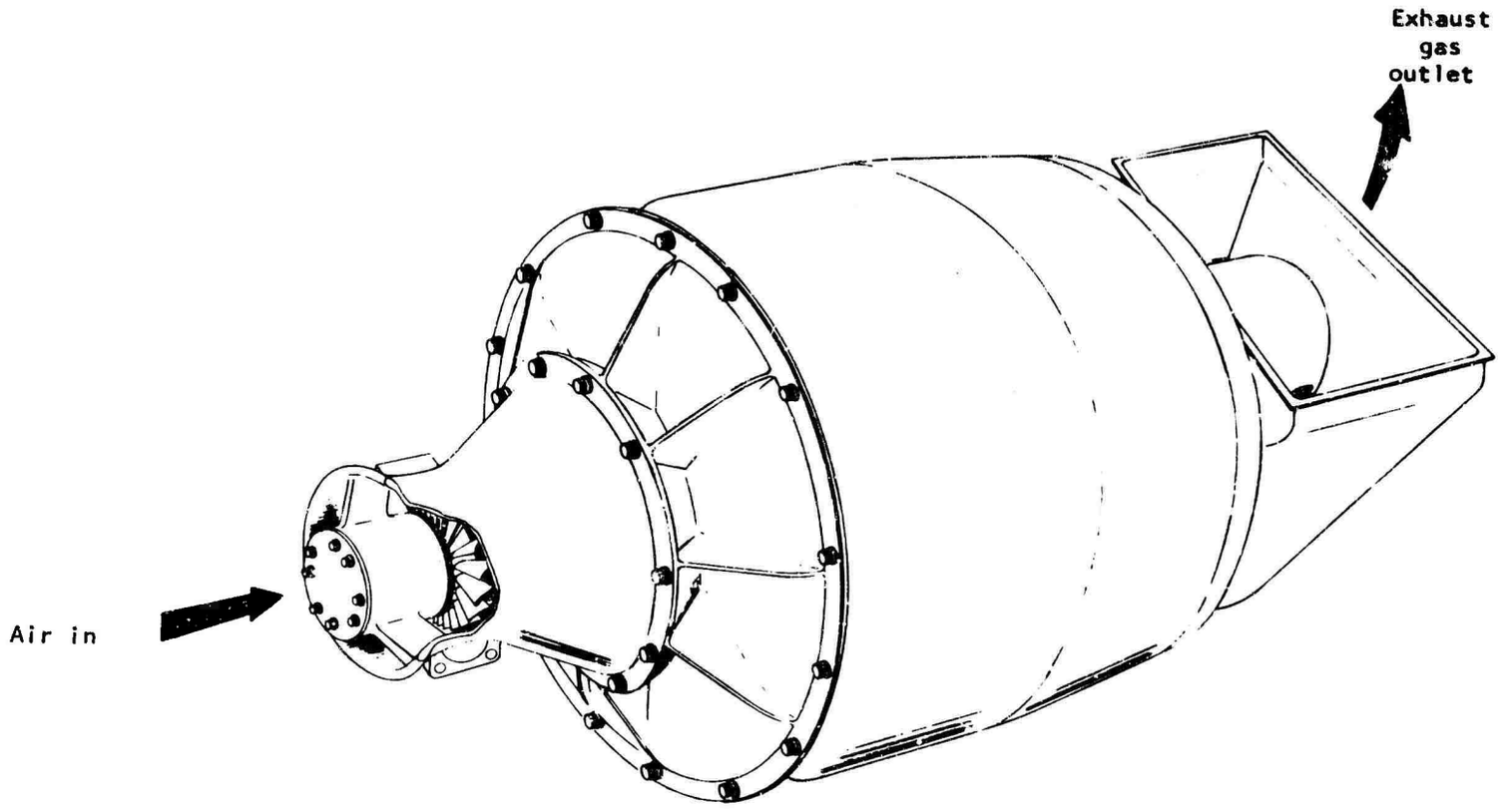

Figure 65. Overall View of Engine Configuration A-1.

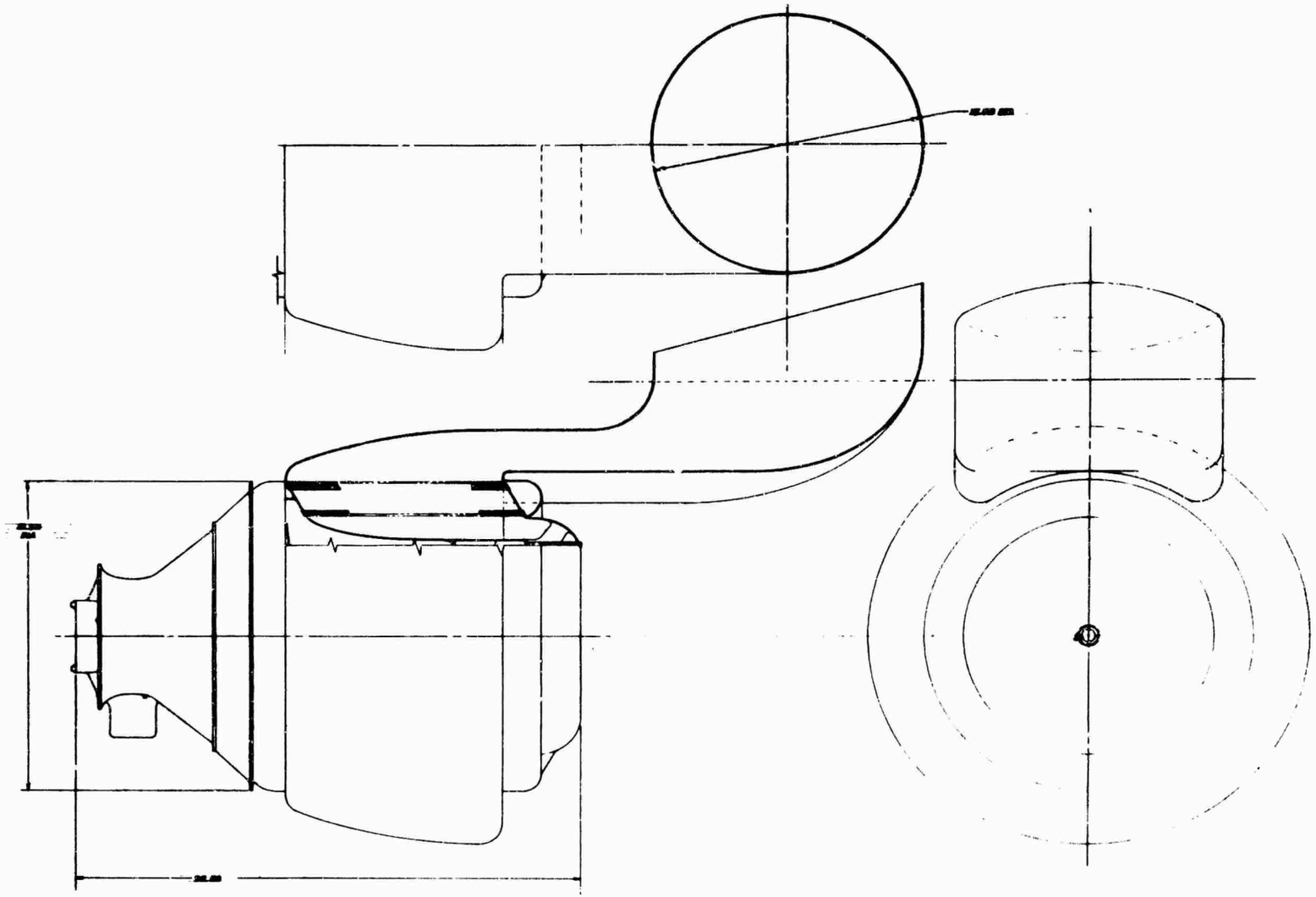

Figure 66. View of Engine Configuration B-2 Showing Exhaust Duct System.

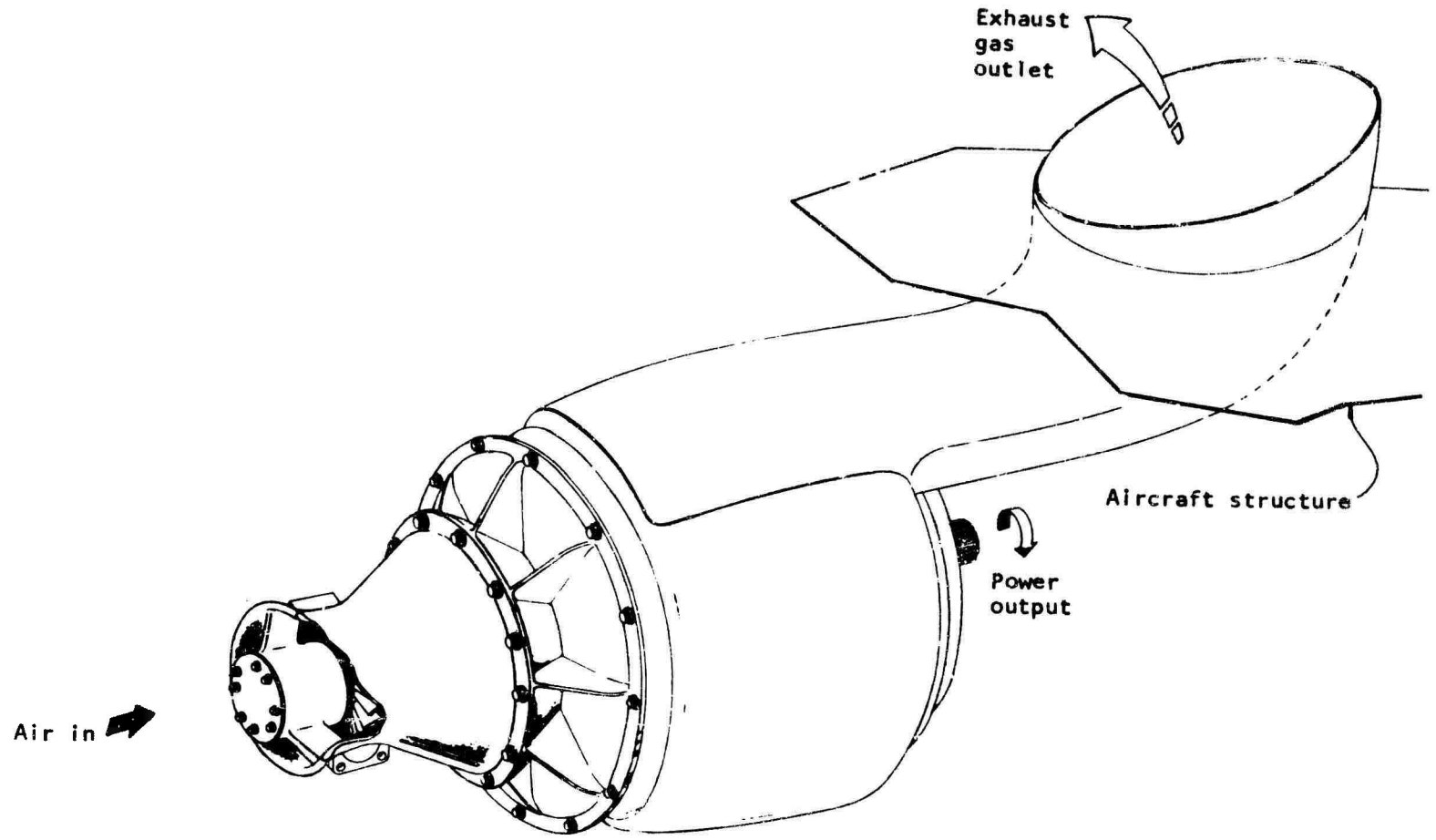

Figure 67. Overall View of Engine Configuration B-2.

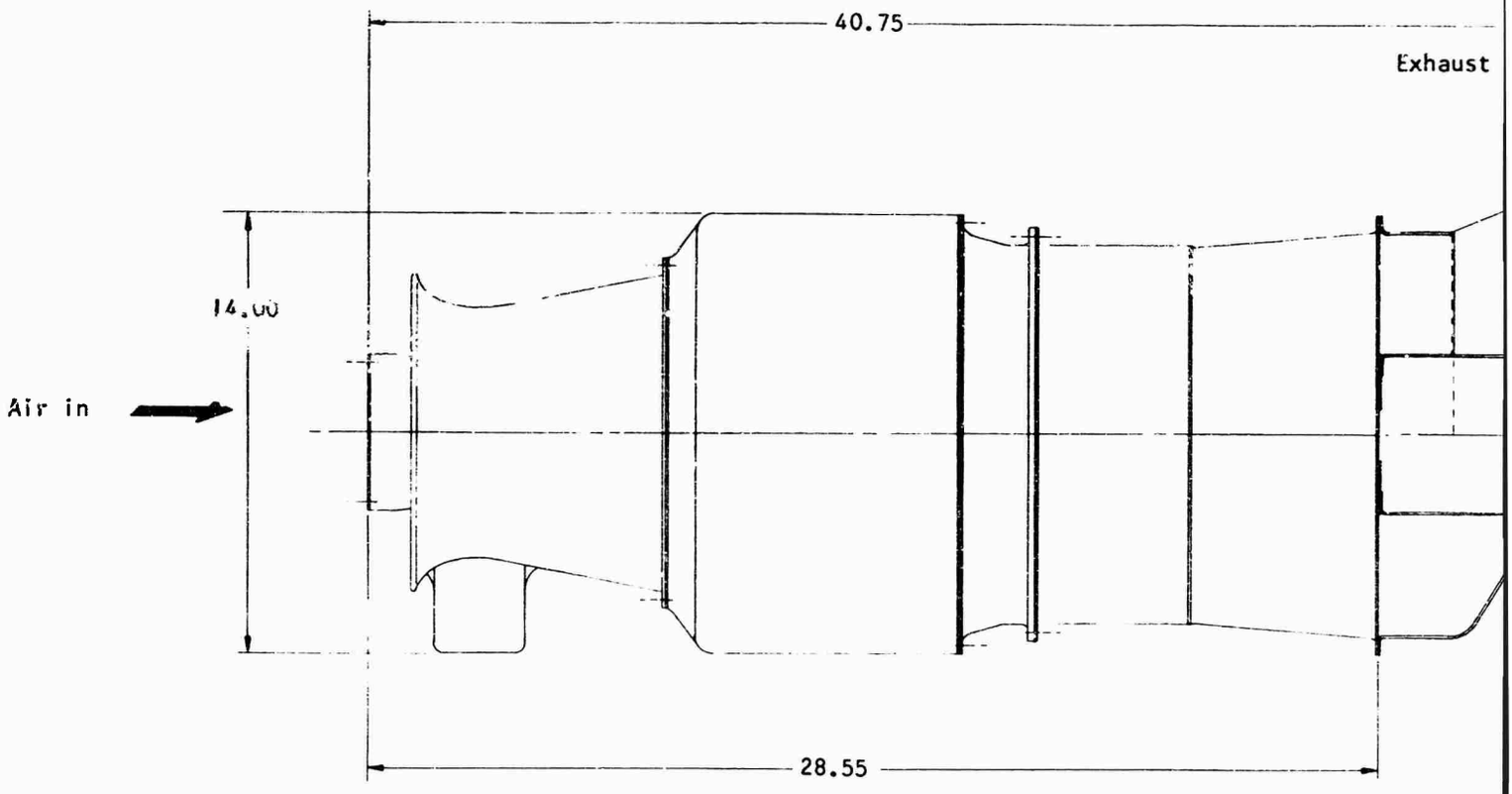

Figure 68. View of Nonrecuperative Engine Showing Exhaust Duct System.

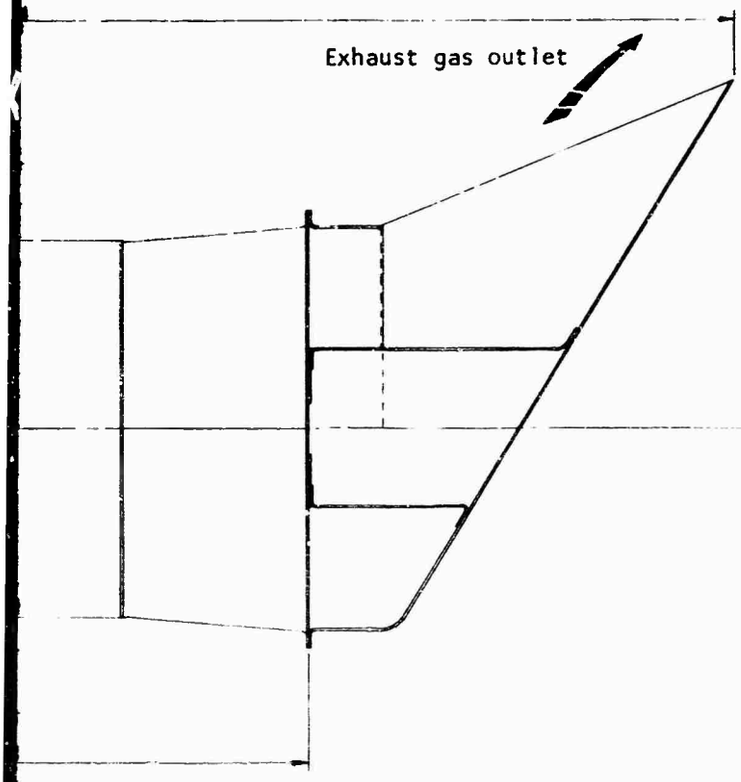
Exhaust gas outlet

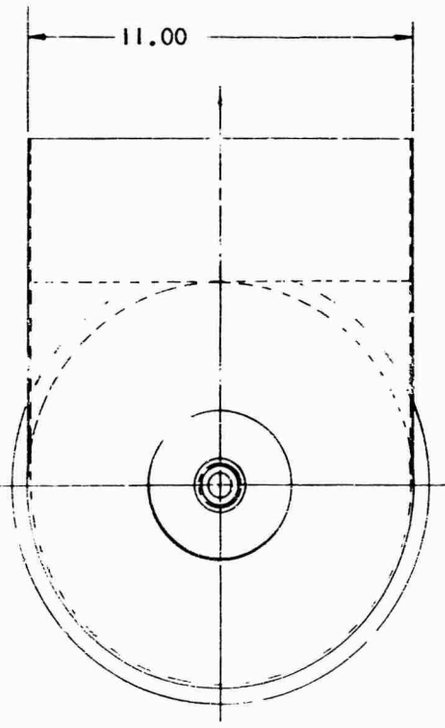
11.00

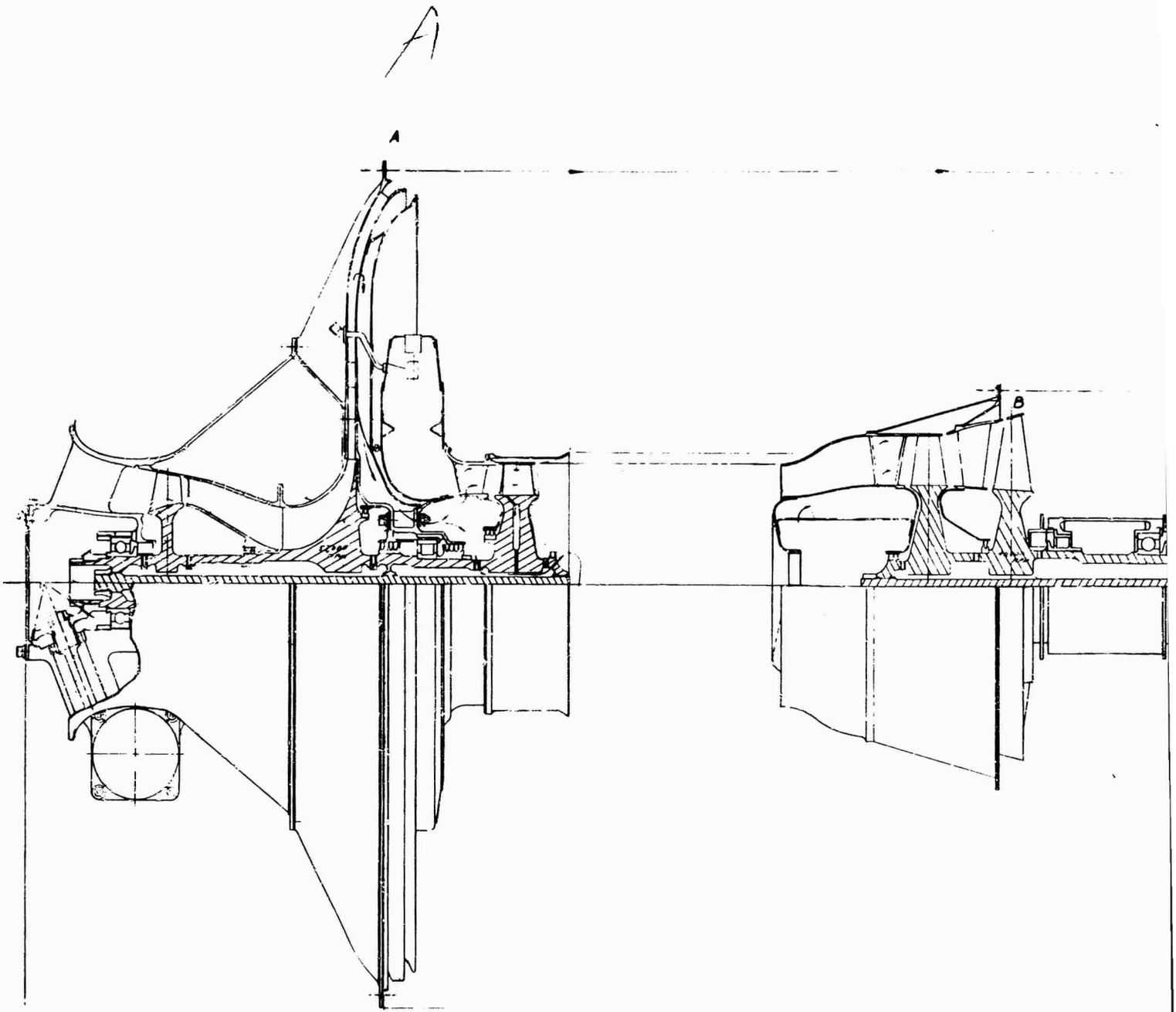

Gas generator section

Power turbine section

Figure 69. View Showing Modular Construction of Engine Configuration A-1.

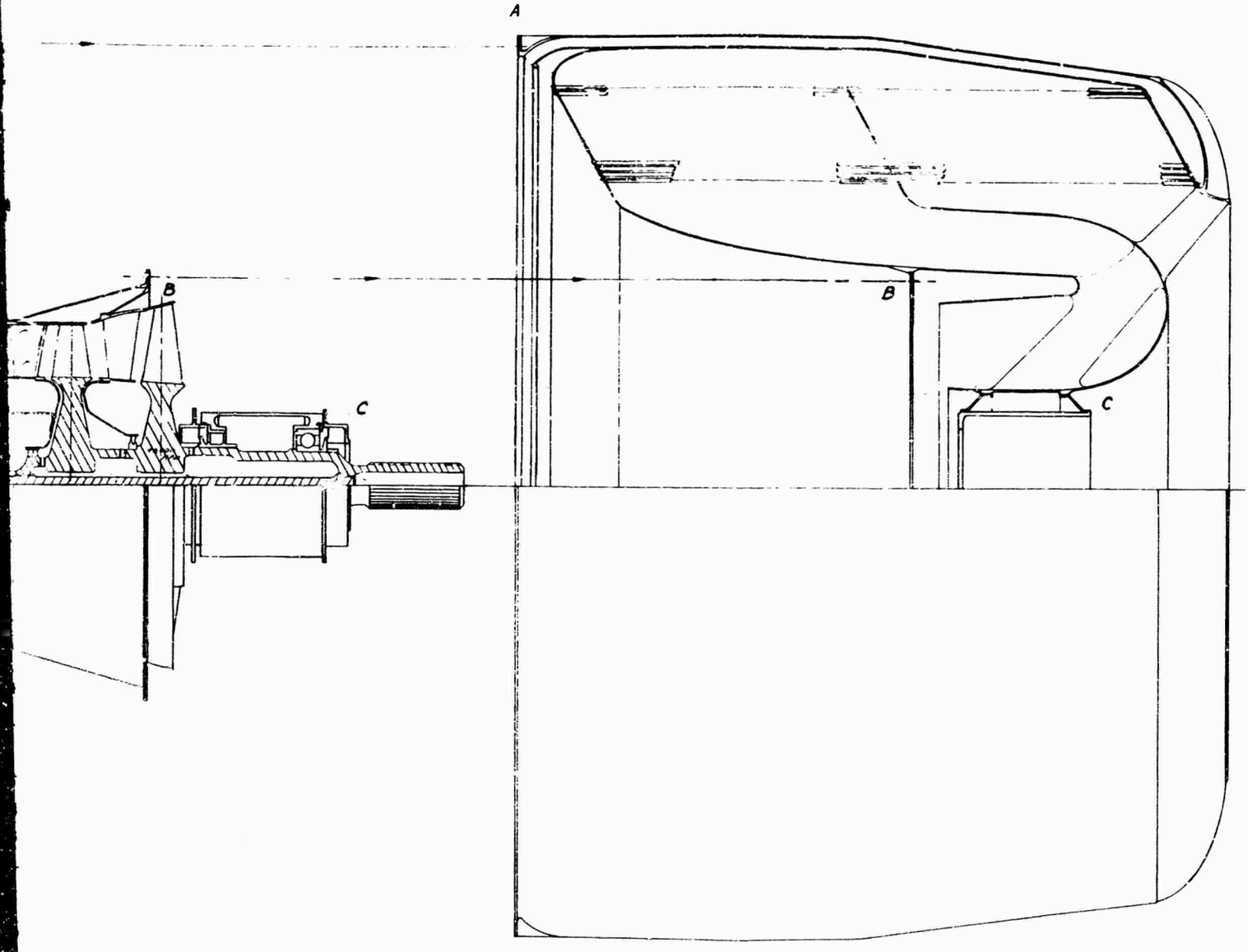

turbine section

Recuperator assembly

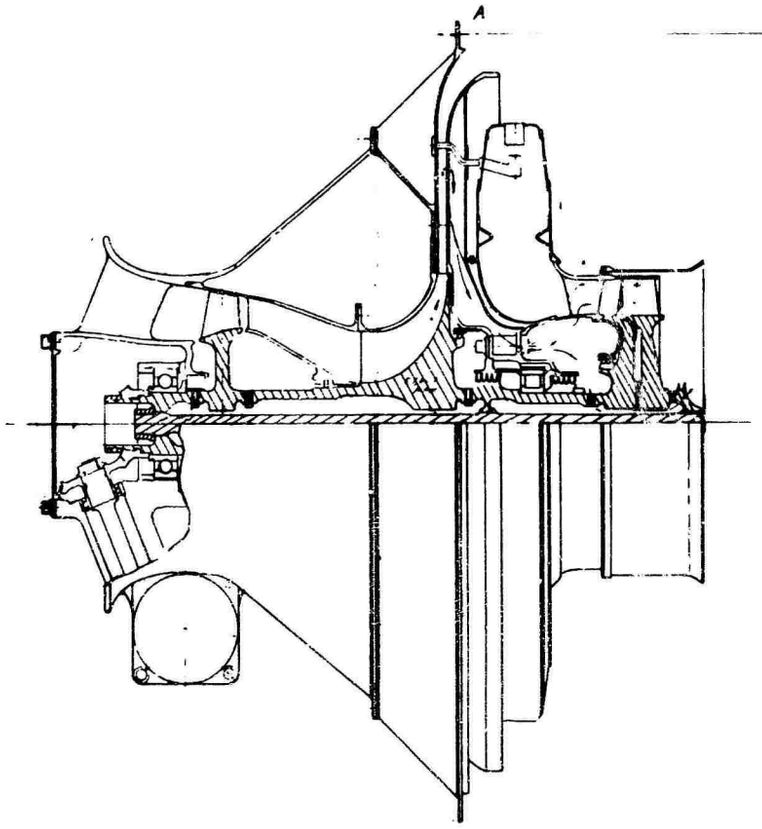

Gas generator section

Power turbine se

Figure 70. View Showing Modular Construction of Engine Configuration B-2.

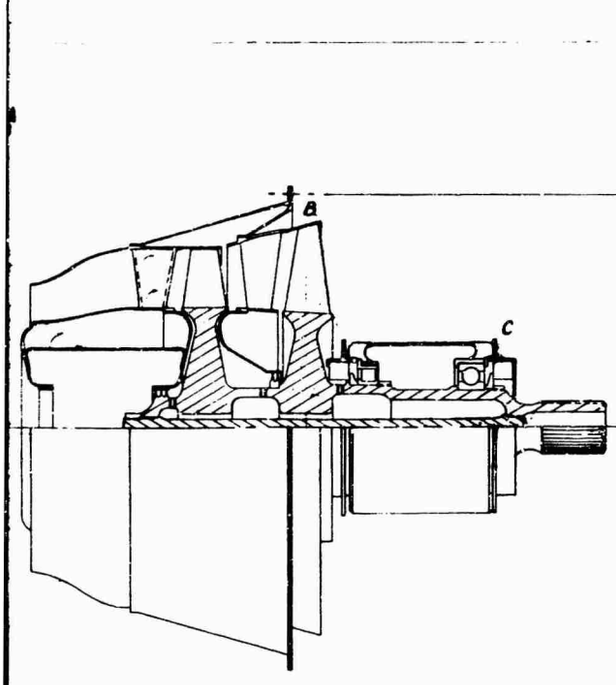

Power turbine section

Recuperator assembly

SENSITIVITY STUDY

VARIABLES CONSIDERED

In the previous section, it was established that engine configurations A-1 and B-2 were the most attractive from the standpoints of minimum weight and cost for the external and internal installations, respectively.

The sensitivity study is aimed at establishing a series of curve arrays for engine configurations A-1 and B-2 in which the following variables will be shown in a related manner:

- Recuperator effectiveness
- Recuperator pressure loss
- Recuperator weight
- Recuperator cost
- Specific fuel consumption
- Specific power
- Engine weight
- Engine cost
- Fuel savings compared with nonrecuperative engine
- Mission time

The curve arrays are presented in such a manner that the effect of a small change in any one of the variables on the overall system can be readily seen and evaluated.

To enable a meaningful performance and weight comparison to be made between the nonrecuperated and recuperated engines, simple scaling factors were generated. Both cycles initially had the same air through-flow and component performance. However, the power produced by the recuperated engine was approximately 6 percent less than that of the nonrecuperated engine cycle because of the pressure loss in the recuperator. A series of influence coefficients was generated, such that the through-flow and component performance of the nonrecuperated engine cycle could be adjusted so that the output power of the nonrecuperated engine would correspond to the output power of the referenced recuperated engine. The weight and SFC of the scaled engine were also determined, and the results are shown in Table XVIII.

TABLE XVIII. COMPARISON OF NONRECUPERATIVE AND RECUPERATIVE ENGINE DATA

Engine Configuration	Reference Recuperated Cycle ϵ = .65, ($\Delta P/P$) = 6% A-1	B-2	Nonrecuperated Cycle Initial	Scaled
Airflow, lb/sec	5.0	5.0	5.0	4.71
Shaft horsepower	962.7	962.7	1028.3	962.7
SFC, lb/hp hr	0.365	0.365	0.464	0.4663
Specific power, hp/lb/sec	192.54	192.54	205.66	204.39
Engine weight, lb	202.8	113.6	114.8	110.0

SENSITIVITY CURVES FOR EXTERNAL INSTALLATION (A-1)

The recuperator and engine weight and cost data plotted are for the optimum units selected in the previous section and outlined in Table XIII. The two curve sheets necessary for the sensitivity plots are shown in Figures 71 and 72. With recuperator effectiveness and pressure loss as the two main parameters, the curves shown on Figure 71 can be summarized as follows:

a. Effectiveness - SFC relationship for lines of constant recuperator pressure loss.

b. Effectiveness - Recuperator weight for lines of constant recuperator pressure loss.

c. Effectiveness - Relative recuperator cost for lines of constant recuperator pressure loss. In these curves a recuperator cost factor is shown with a datum value of unity for the reference engine conditions.

d. Effectiveness - Difference in engine weights between recuperative and nonrecuperative variants at the same power level for lines of constant recuperator pressure loss.

e. Effectiveness - Engine weight for lines of constant recuperator pressure loss.

f. Effectiveness - Relative engine cost for lines of constant recuperator pressure loss. In these curves, an engine cost factor is shown with a datum of unity at the reference engine conditions (recuperator effectiveness of 0.65 and pressure loss of 6 percent).

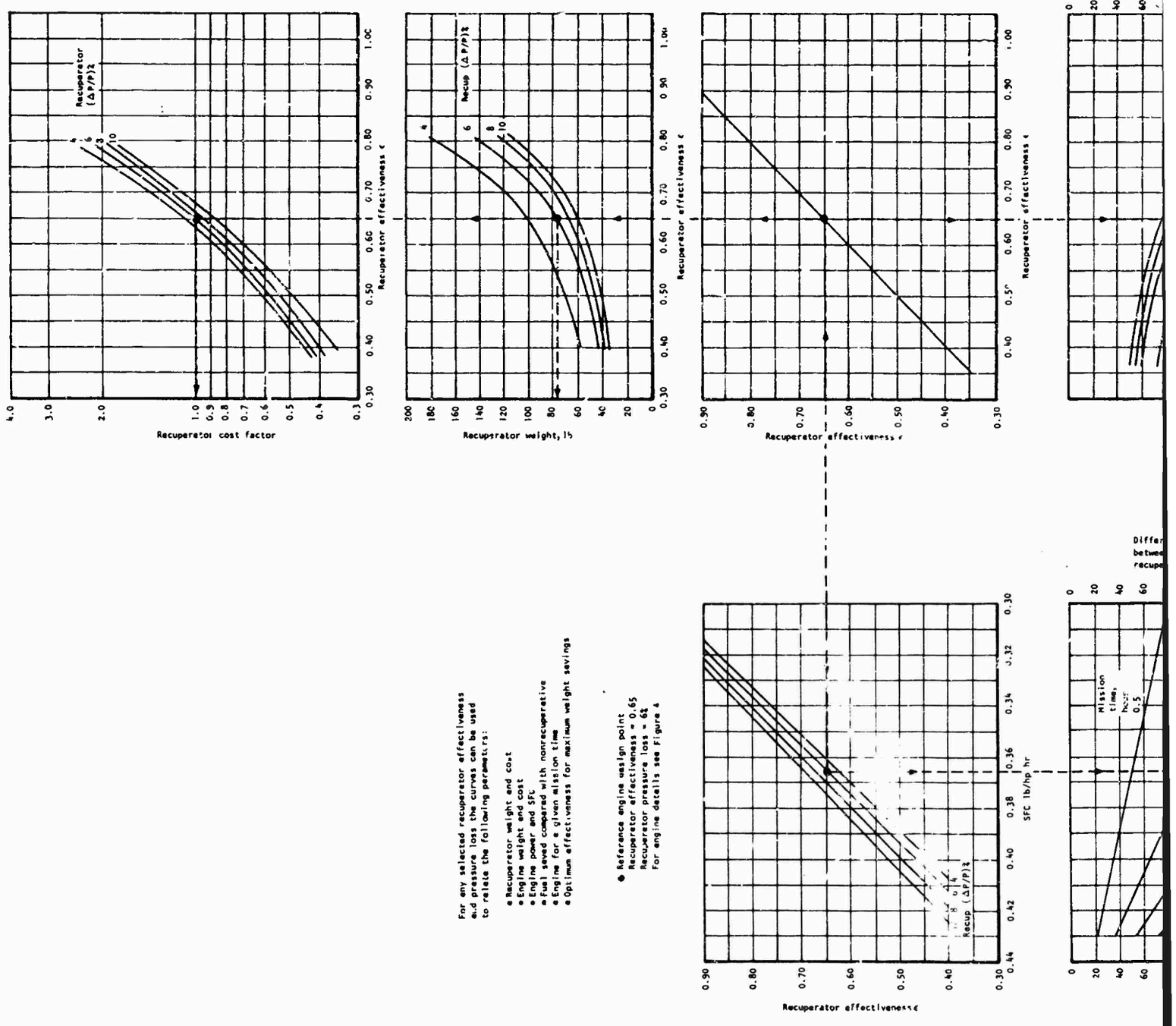

Figure 71. Sensitivity Curves for Engine Configuration A-1.

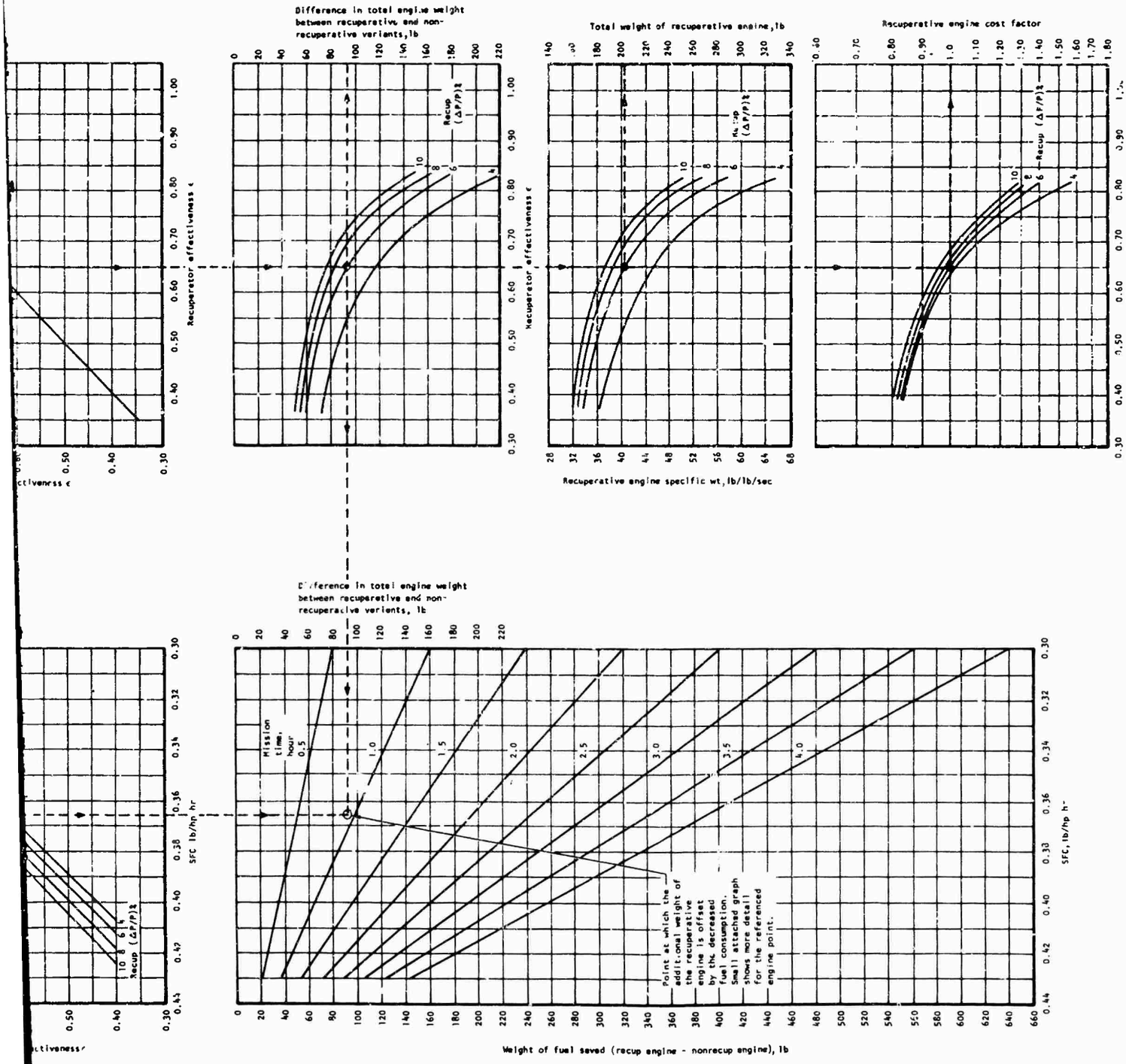
Difference in total engine weight between recuperative and non-recuperative variants, lb
Total weight of recuperative engine, lb
Recuperative engine cost factor
Recuperator effectiveness ε
Recuperative engine specific wt, lb/lb/sec
Recup (ΔP/P)%
10
8
6
4

Difference in total engine weight between recuperative and non-recuperative variants, lb
Mission time, hour
0.5
1.0
1.5
2.0
2.5
3.0
3.5
4.0
Point at which the additional weight of the recuperative engine is offset by the decreased fuel consumption. Small attached graph shows more detail for the referenced engine point.
SFC lb/hp hr
Recup (ΔP/P)%
Weight of fuel saved (recup engine - nonrecup engine), lb

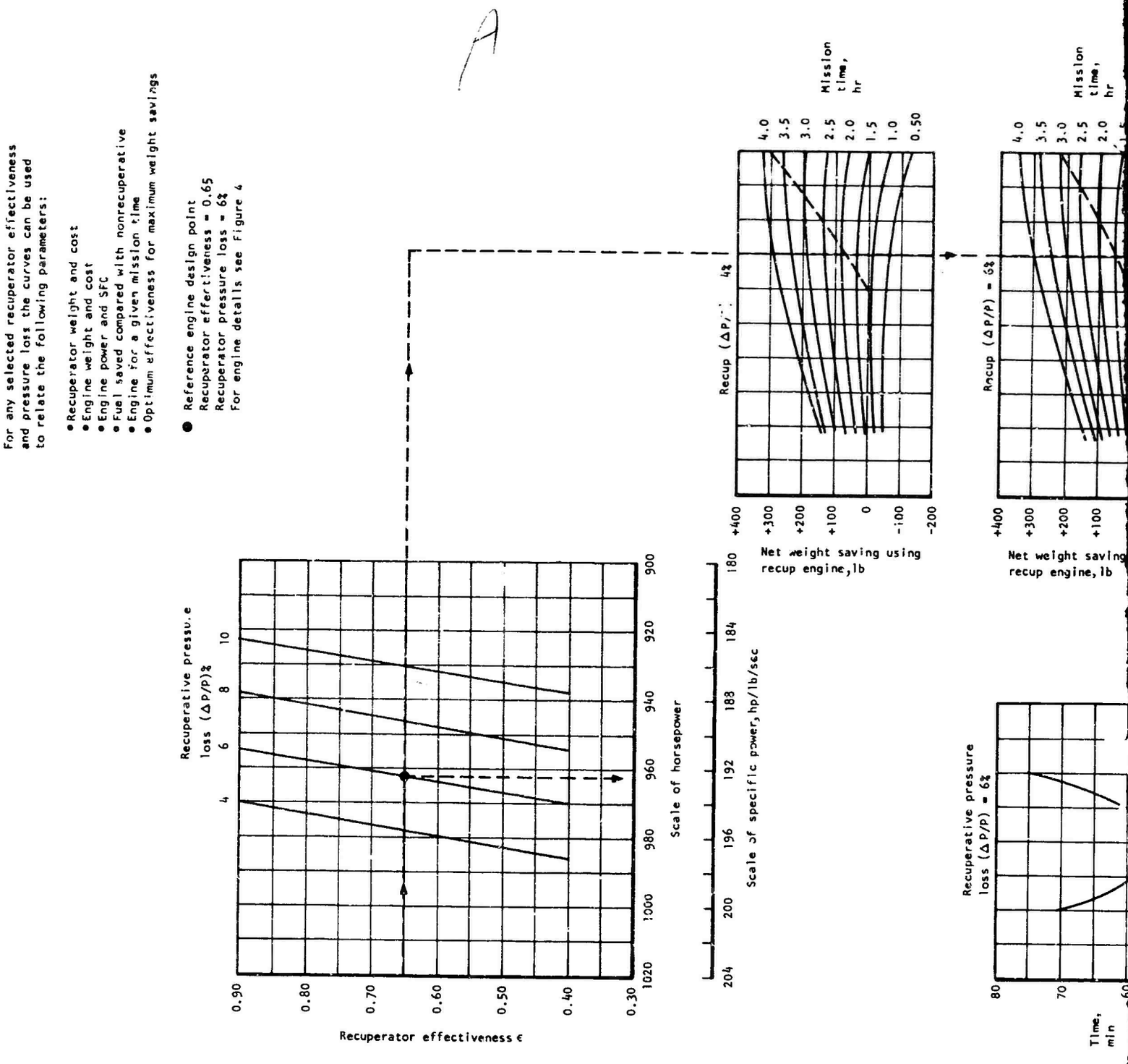

Figure 72. Sensitivity Curves for Engine Configuration A-1.

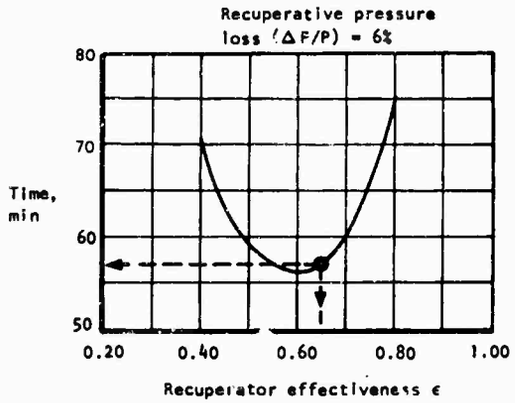

Curve to show minimum flight time at which the fuel saving equals the additional weight of the recuperator

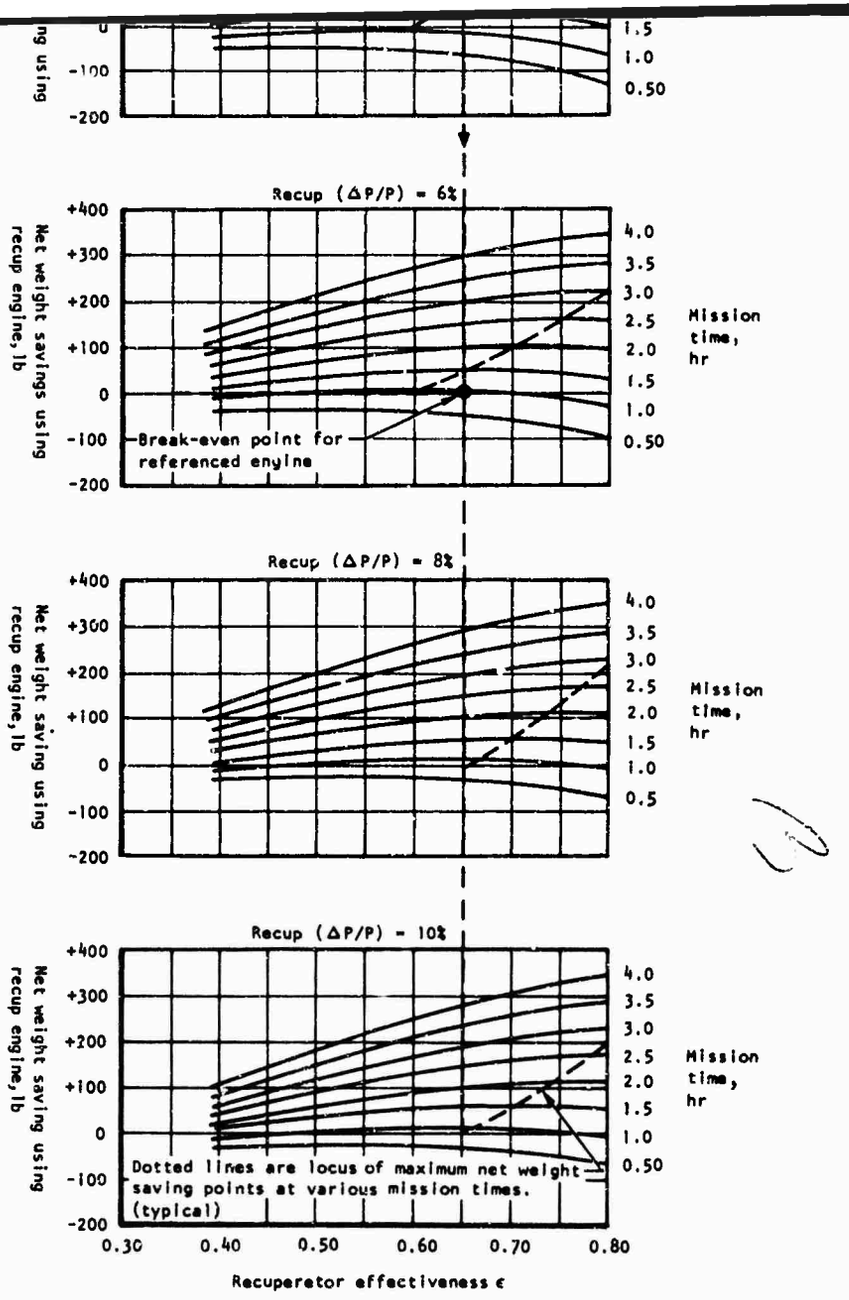

Curves showing optimum effectiveness values at various mission times for maximum net weight savings by using a recuperative engine compared with a simple cycle engine

g. SFC - Weight of fuel saved between recuperative and non-recuperative variants at the same power level for lines of constant mission time.

The other family of curves shown on Figure 72 can be summarized as follows:

h. Effectiveness - Engine power, for lines of constant recuperator pressure loss.

i. Four basic plots of effectiveness - Net weight saving by using recuperative engine for lines of constant mission time. The four basic plots are for recuperator pressure loss values of 4, 6, 8 and 10 percent.

j. Effectiveness - Minimum flight time at which the fuel saving, by using the recuperative variant, equals the additional weight of the recuperator for a recuperator pressure loss of 6 percent.

On each of these two curve sheets, the various curve arrays outlined above are essentially related by common basic recuperator parameters. On these figures, a dotted line is shown relating the various curve arrays at the reference engine conditions. Use of the curves is illustrated in an example for engine configuration A-1 given in Table XIX.

SENSITIVITY CURVES FOR INTERNAL INSTALLATION (B-2)

The recuperator and engine weight and cost data plotted are for the optimum units selected in a previous section and outlined in Table XVI. The two curve sheets necessary for the sensitivity plots are shown in Figures 73 and 74. The graphical format is the same as that used for the external type of installation described above. Use of the curves is illustrated in an example for engine configuration B-2 given in Table XX.

PERFORMANCE OF EXTERNAL ENGINE INSTALLATION (A-1)

For a continuous-duty industrial gas turbine, where minimization of overall engine weight and package size are not the influencing features in the engine design, there is naturally a big incentive in selecting a high effectiveness recuperator to realize the maximum possible fuel savings. For such units, with life requirements often in excess of 50,000 hr, the fuel cost represents a high percentage of the overall operating cost over the life of the machine. To minimize overall operating costs of such machines, low specific fuel consumptions can be achieved by high degrees of recuperation.

For aircraft gas turbines there is also a requirement for low fuel consumptions. However, for machines of this type, designed for relatively short life requirements and short-duration continuous-duty periods, the ground rules for heat exchanger selection are different. For short-duration

TABLE XIX. EXAMPLE ON USE OF SENSITIVITY CURVES FOR ENGINE CONFIGURATION A-I

Recuperator Effectiveness			0.65	0.70
Recuperator Pressure Loss ($\Delta P/P$), %			6.0	6.0
Figure 71	a)	SFC, lb/hp hr	0.365	0.356
	b)	Recuperator weight, lb	76.6	90.0
	c)	Recuperator cost factor	1.0	1.27
	d)	Difference in engine weight, lb	92.8	106.2
	e)	Engine weight, lb	202.8	216.2
	f)	Engine cost factor	1.0	1.077
	g)	Fuel saved, lb*	97.5	106.2
Figure 72	h)	Engine power	962.7	961.0
	i)	Net weight savings, lb	**	**
	j)	Break-even time, minutes***	57.0	60.0

*Fuel saved given in lb/hr (i.e., for a 1-hr mission time)

**Net weight savings is defined as the difference in fuel consumption minus the difference in engine weights, for the recuperative and non-recuperative variants. From Figure 72, it can be seen that the net weight savings is dependent on mission time. For example, at a mission time of 2 hours, the net weight savings would be 102.2 lb and 106.2 lb for the above effectiveness values of 0.65 and 0.70, respectively.

***Break-even time is defined as the time in which the additional weight of the recuperative engine is offset by the decreased fuel consumption.

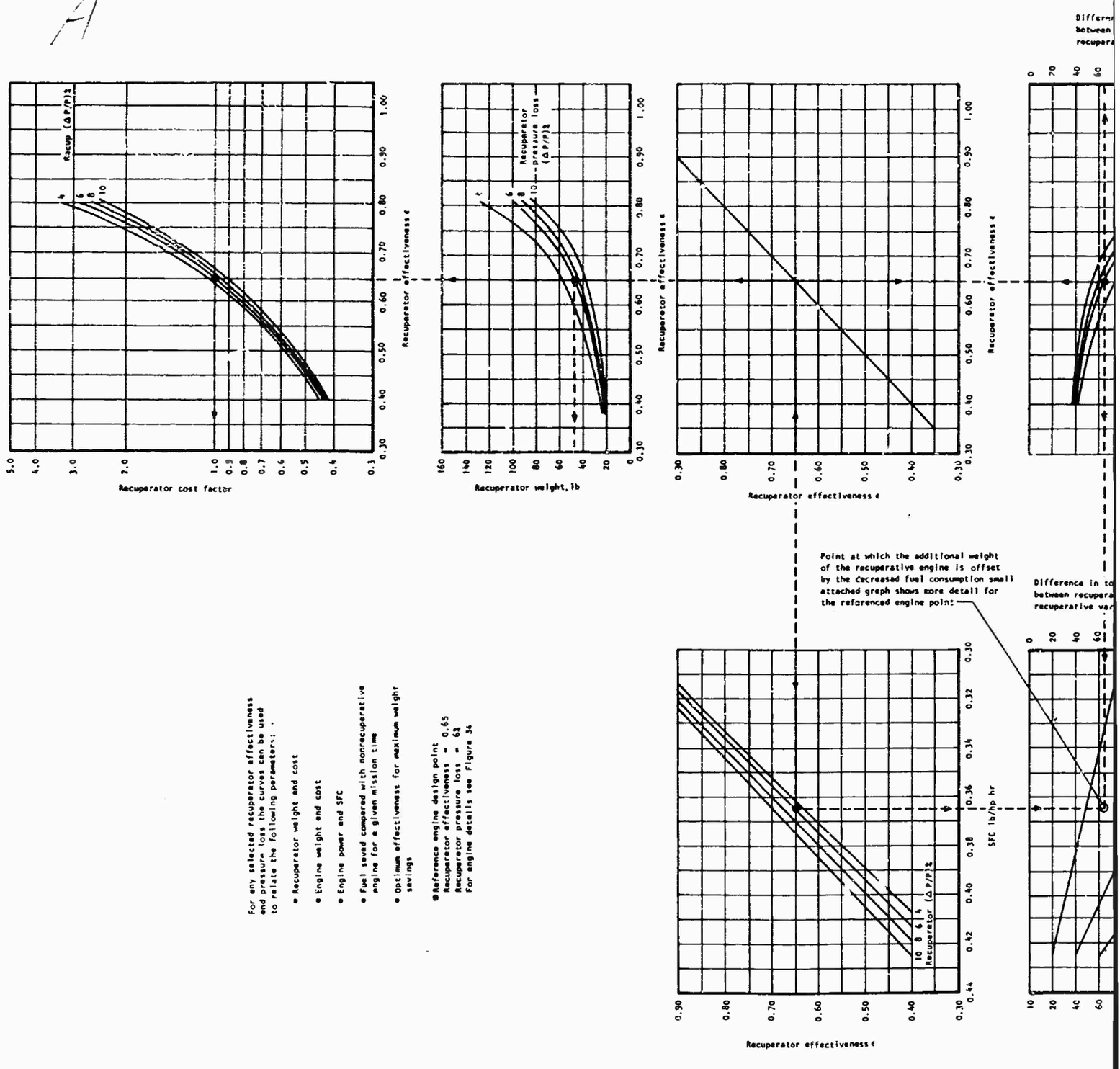

Figure 73. Sensitivity Curves for Engine Configuration B-2.

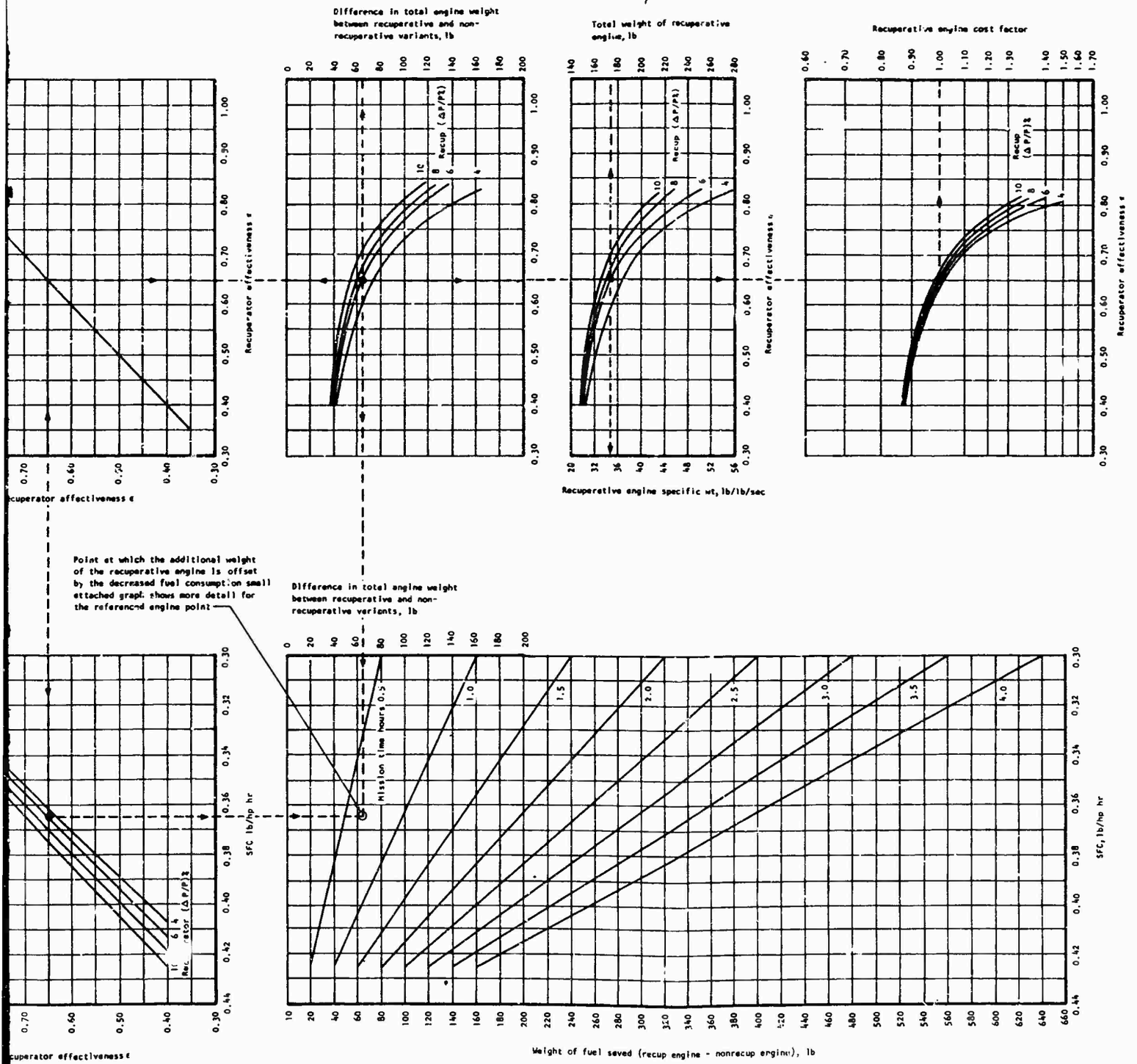
Difference in total engine weight between recuperative and non-recuperative variants, lb
Total weight of recuperative engine, lb
Recuperative engine cost factor
Recuperator effectiveness ε
Recup (ΔP/P)%
Recuperative engine specific wt, lb/lb/sec
Point at which the additional weight of the recuperative engine is offset by the decreased fuel consumption small attached graph shows more detail for the referenced engine point
Mission time hours
SFC lb/hp hr
Weight of fuel saved (recup engine - nonrecup engine), lb

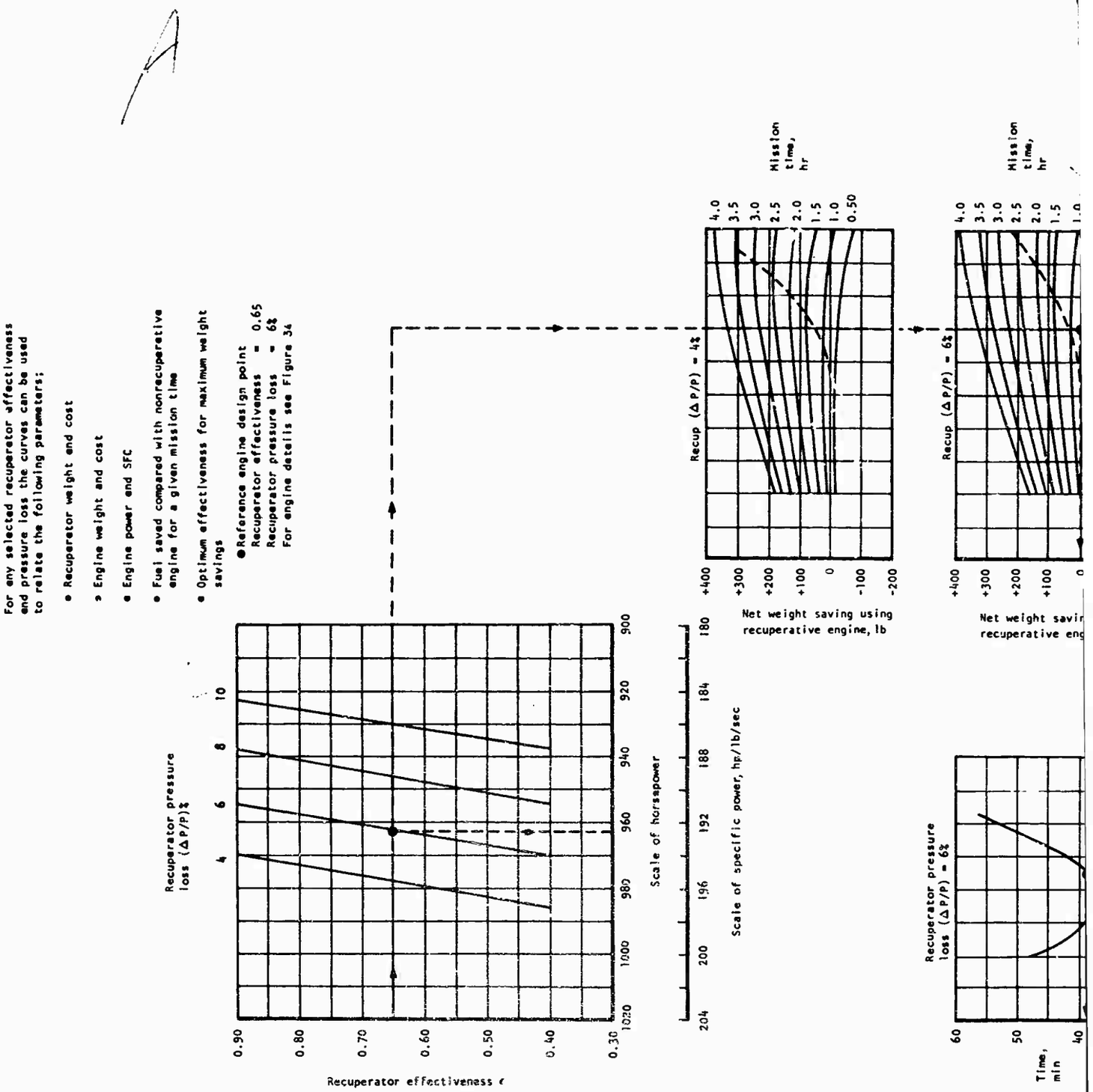

Figure 74. Sensitivity Curves for Engine Configuration B-2.

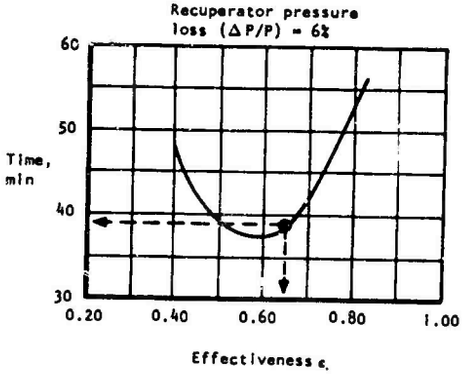

Curve to show minimum flight time at which the fuel savings equals the additional weight of the recuperator

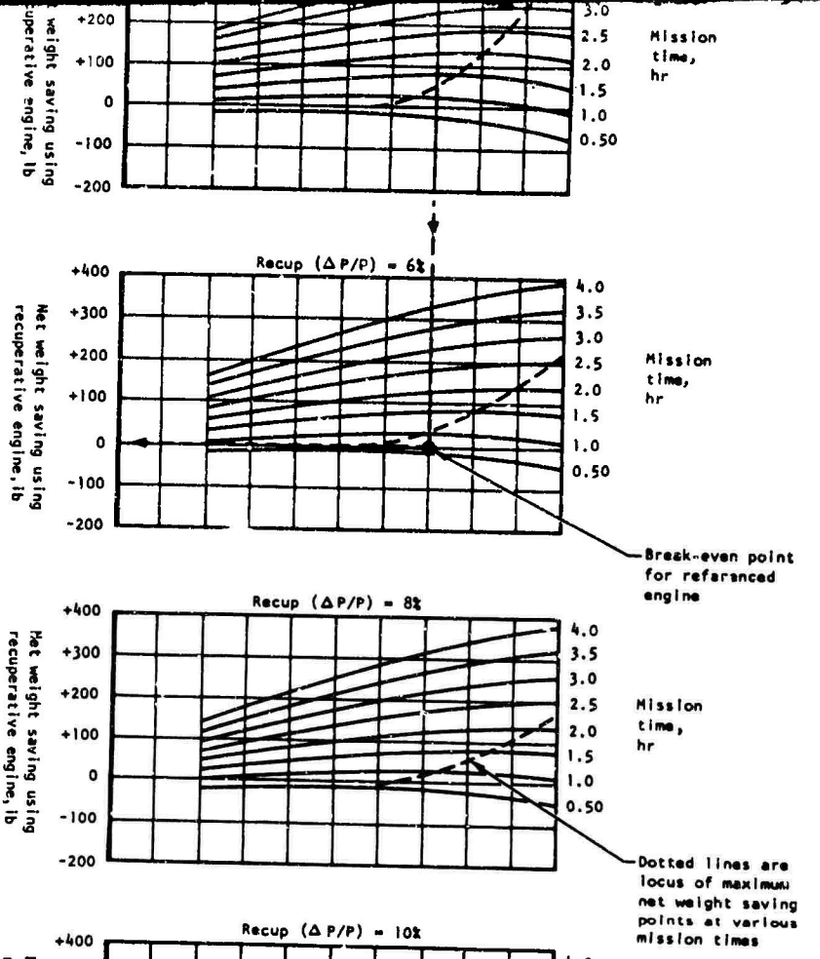

Curves showing optimum effectiveness values at various mission times for maximum net weight savings by using a recuperative engine compared with a simple cycle engine

TABLE XX. EXAMPLE ON USE OF SENSITIVITY CURVES FOR ENGINE CONFIGURATION B-2

Recuperator Effectiveness			0.65	0.70
Recuperator Pressure Loss (ΔP/P), %			6.0	6.0
Figure 73	a)	SFC, lb/hp hr	0.365	0.356
	b)	Recuperator weight, lb	47.4	58.0
	c)	Recuperator cost factor	1.0	1.32
	d)	Difference in engine weight, lb	63.6	74.2
	e)	Engine weight, lb	173.6	184.2
	f)	Engine cost factor	1.0	1.072
	g)	Fuel saved, lb*	97.5	106.2
Figure 74	h)	Engine power	962.7	961.0
	i)	Net weight savings, lb	**	**
	j)	Break-even time, minutes***	39.2	41.9

*Fuel saved given in lb/hr (i.e., for a 1-hr mission time)

**Net weight savings is defined as the difference in fuel consumption minus the difference in engine weights for the recuperative and non-recuperative variants. From Figure 74, it can be seen that the net weight savings is dependent on mission time. For example, at a mission time of 2 hours, the net weight savings would be 131.4 lb and 138.2 lb for the above effectiveness values of 0.65 and 0.70, respectively.

***Break-even time is defined as the time in which the additional weight of the recuperative engine is offset by the decreased fuel consumption.

flights, only a small fuel weight saving would be achieved using a recuperative engine compared with a non-heat-exchanged version. For such flights, the utilization of a high effectiveness recuperator will result in a parasitic weight penalty, since fuel weight saving is less than the additional weight of the recuperator.

For a given pressure loss, it can be seen from Figure 72 that an effectiveness can be selected to give the maximum net weight savings for a given mission time. Typically, for the 6-percent pressure loss recuperator, it can be seen that a minimum break-even time of 56 min corresponds to an effectiveness of 60 percent. Recuperator effectiveness for maximum net weight savings for different mission times is given below:

Mission time, hours	1	1.5	2.0	2.5	3.0
Recuperator effectiveness for maximum net weight savings	0.61	0.657	0.706	0.752	0.80

A curve array summarizing the performance of the A-1 engine configuration is shown in Figure 75. The basic carpet plot relates recuperator effectiveness and pressure loss with engine weight. Superimposed on this map are lines of constant specific fuel consumption and lines of engine cost factor. This figure supplements the main sensitivity curves and provides a simple means of rapidly determining the effect of small changes in any one of the basic parameters.

PERFORMANCE OF INTERNAL ENGINE INSTALLATION (B-2)

The comments given above for the external installation equally apply here, and for a given pressure loss, it can be seen from Figure 74 that an optimum effectiveness can be selected to give the maximum net weight savings for a given mission time. Typically, for the 6-percent pressure loss recuperator, it can be seen that a minimum break-even time of 37.5 minutes corresponds to an effectiveness of 58 percent. Recuperator effectiveness for maximum net weight savings for different mission times is given below:

Mission time, hours	1	1.5	2	2.5
Recuperator effectiveness for maximum net weight savings	0.645	0.704	0.747	0.787

A curve array summarizing the performance of the B-2 engine configuration is shown in Figure 76. This figure supplements the main sensitivity curves and provides a simple means of rapidly determining the effect of small changes in any one of the basic parameters.

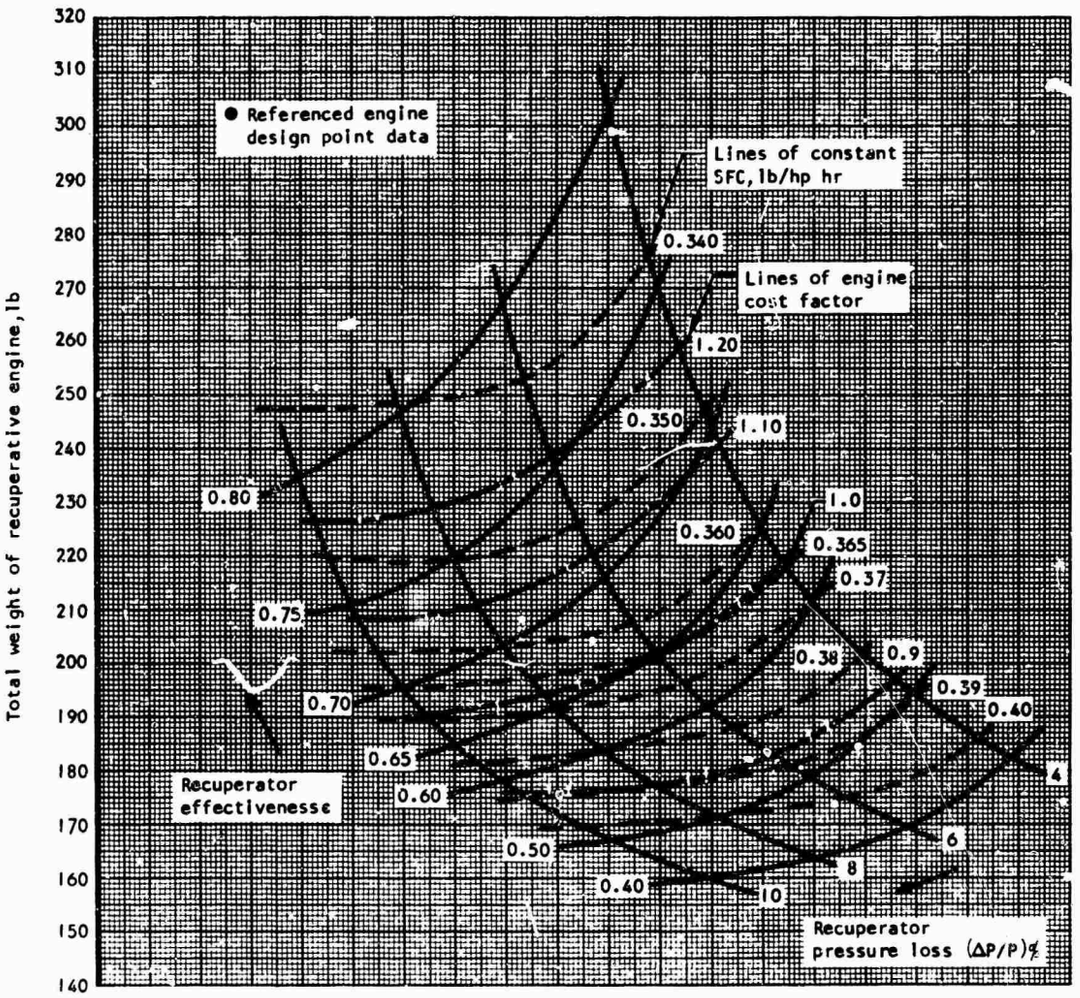

Figure 75. Curves Showing Relationships Between Recuperator Parameters and Engine Weight, Fuel Consumption, and Relative Cost for Configuration A-1.

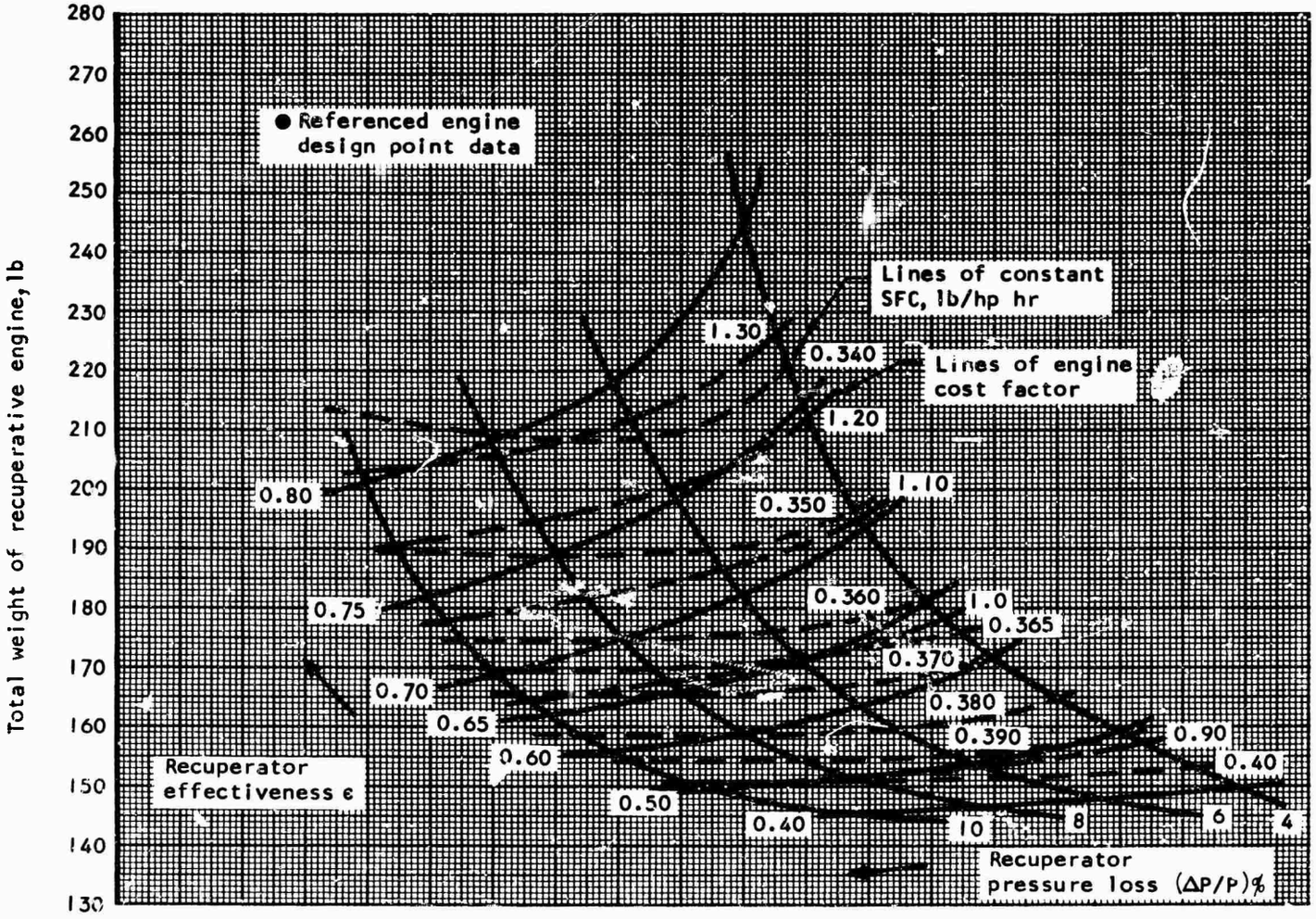

Figure 76. Curves Showing Relationships Between Recuperator Parameters and Engine Weight, Fuel Consumption, and Relative Cost for Configuration B-2.

SENSITIVITY STUDY SUMMARY

The curve arrays have been presented in such a manner that the effect of a small change in one of the salient variables on the overall system can be readily seen and evaluated. The additional curve in Figure 77 shows the fuel savings in gallons per hour by using a recuperative engine. At the reference engine conditions, in the order of 14.5 gallons/hour are saved by using a recuperative engine. Additional curves are included which show the fuel cost savings using the recuperative engine for a range of fuel costs.

The question of what the fuel will cost the user in remote areas has not been examined in this study. As long as aircraft fuel will be required in remote areas where this fuel will have to be transported by aircraft, the cost of fuel will be considerably higher than 10 cents/gallon dockside cost. From the curves in Reference 6, the cost of fuel delivered by helicopters for a radius of 100 nautical miles is estimated to be in the order of $1 per gallon. For the engine considered in this study, with a life requirement of 1000 hours, the added cost of the recuperative variant could be offset with a fuel cost of less than $1 per gallon.

A summary of the two recuperative engines (at the reference engine conditions) and the nonrecuperated engine is outlined in Table XXI.

To compare the estimated performance of the recuperative engine with cycle data from previous engine studies, the design values of specific fuel consumption and specific power (at the reference engine conditions) are shown plotted on Figures 78 and 79; the basic curves shown on these plots are taken from Reference 7.

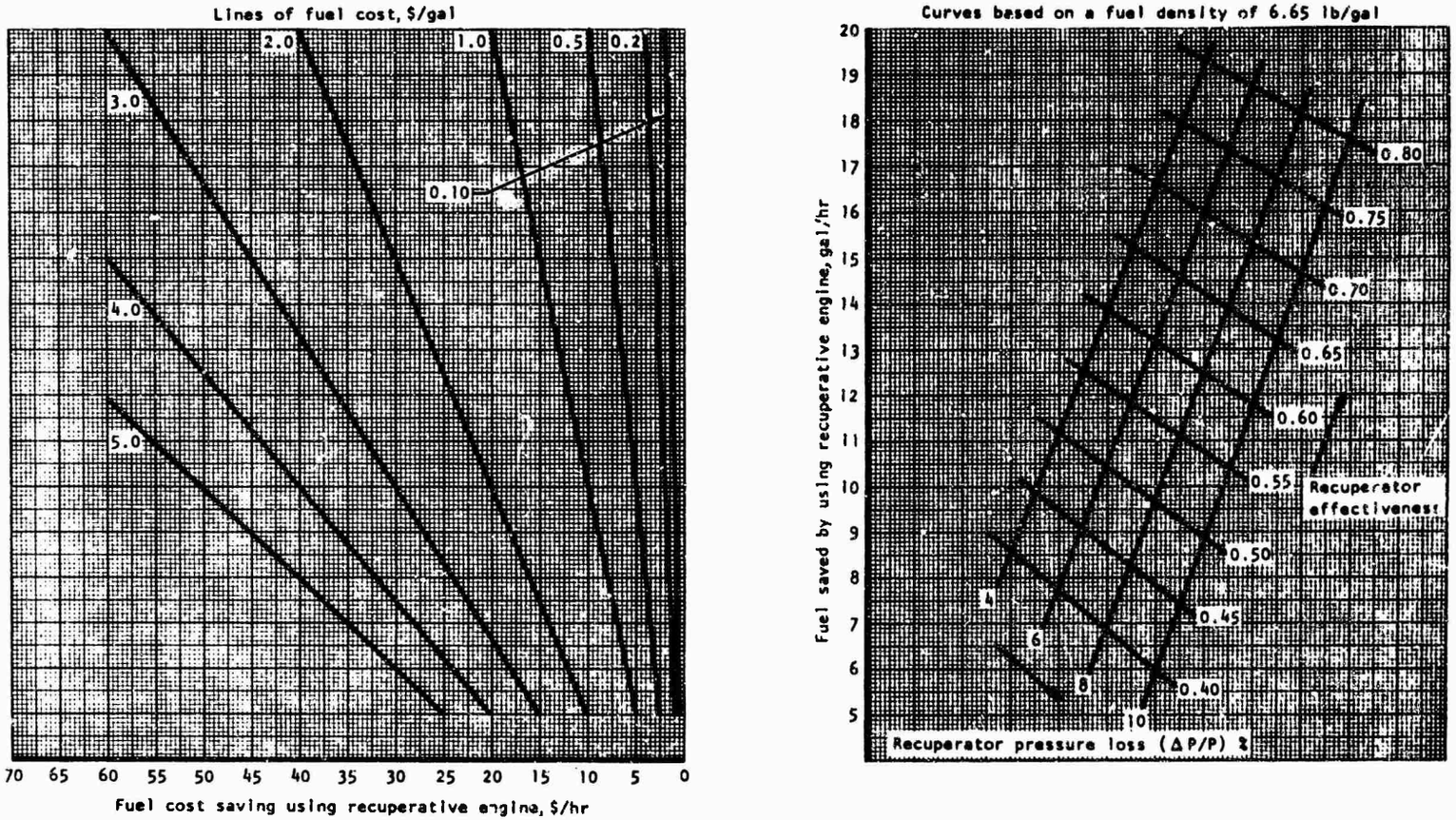

Figure 77. Relationships Between Recuperator Parameters and Fuel Savings by Using a Heat-Exchanged Engine.

TABLE XXI. PERFORMANCE, WEIGHT, AND COST SUMMARY FOR NONRECUPERATIVE AND RECUPERATIVE ENGINES AT THE REFERENCE ENGINE CONDITIONS

Engine Configuration	A-1	B-2	Non-recuperative
Installation Type	External	Internal	Not defined
Figure Number	4	34	5
Airflow, lb/sec	5.0	5.0	4.71
Recuperator Effectiveness	0.65	0.65	-
Recuperator Press Loss	6.0	6.0	-
Specific Power, hp/lb/sec	192.54	192.54	204.39
Horsepower	962.7	962.7	962.7
Specific Fuel Consumption, lb/hp/hr	0.365	0.365	0.4663
Recuperator Weight, lb	76.6	47.4	-
Specific Recuperator Weight, lb/lb/sec	15.32	9.48	-
Engine Weight, lb	202.8	173.6	110.0
Specific Engine Weight, lb/lb/sec	40.56	34.72	23.35
Horsepower/Engine Weight	4.75	5.55	8.75
Engine Overall Diameter, in.	23.45	19.04	14.00
Engine Overall Length, in.	29.90	28.50	28.55
Engine Cost, $/hp	46.40	42.90	33.24

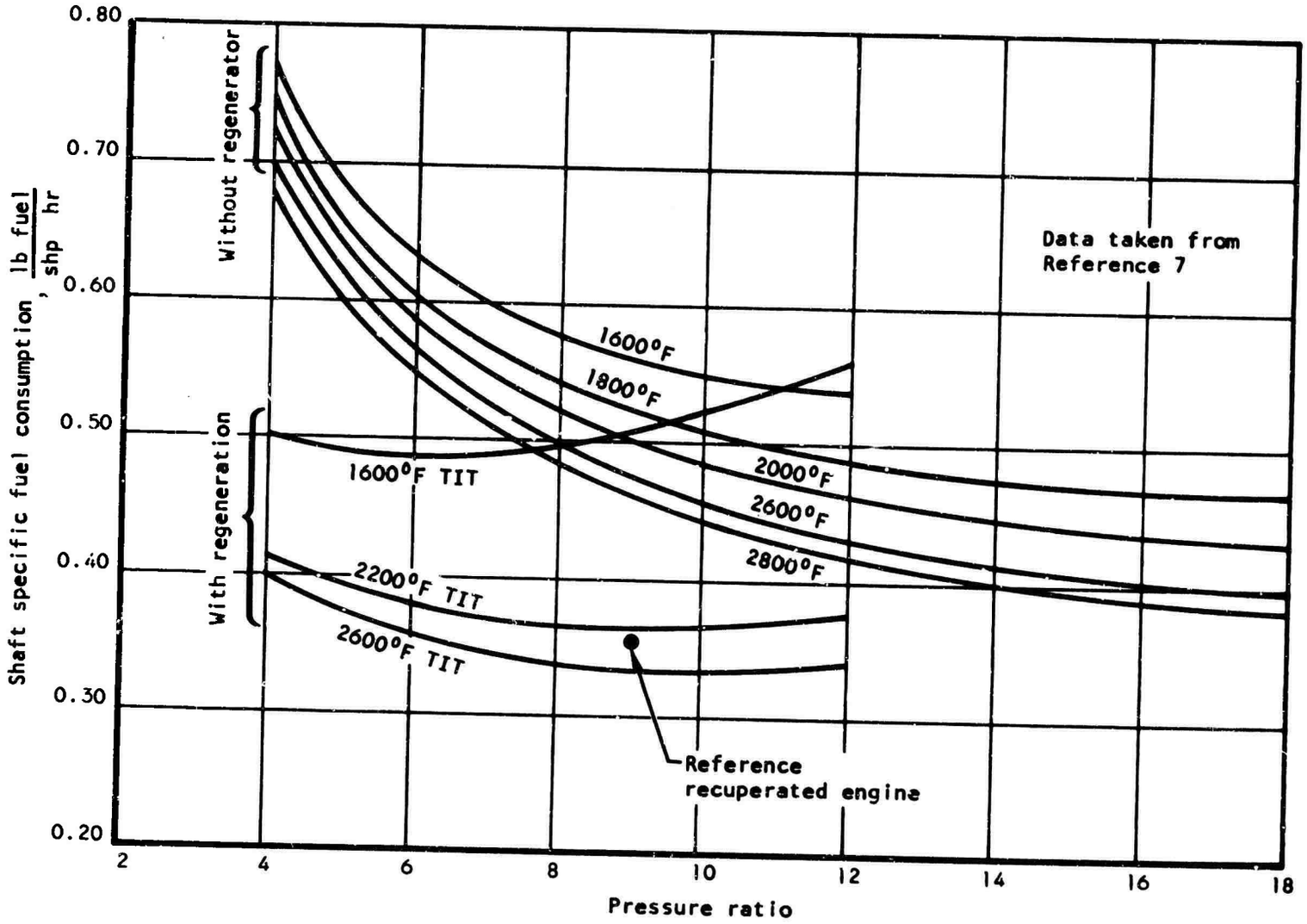

Figure 78. Specific Fuel Consumption Versus Pressure Ratio.

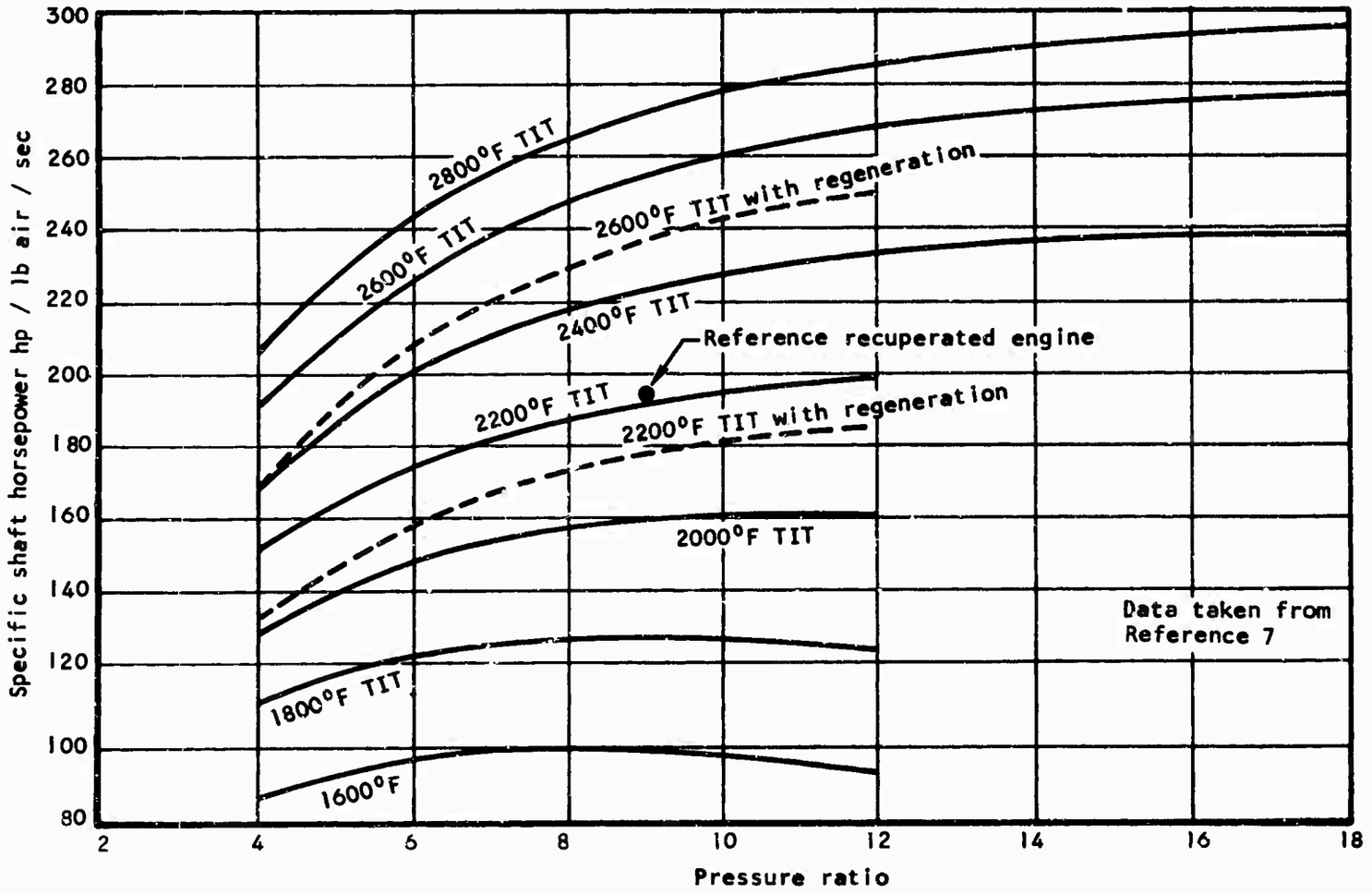

Figure 79. Specific Power Versus Pressure Ratio.

RESULTS

In this study, analytical and design approaches have been presented for two integrated engine designs. In both configurations, the recuperator is considered to be the prime element and forms the structural backbone of the turbomachinery assembly. Using the same cycle conditions and component efficiencies, a simple cycle engine design has been presented to enable a comparison of performance, weight, and cost to be made between a nonrecuperative and a recuperative engine, at the same power level.

All the variants presented have a simple two-shaft turbomachinery layout. A power turbine consisting of two axial stages is used, and the output shaft is located at the rear of the engine to obtain a simplified shafting and bearing system. A single-stage axial gas generator turbine is used to drive the compressor, which embodies a single axial and centrifugal stage. All turbomachinery designs have a fixed geometry, and for the turbine inlet temperature of 2300°F, a total bleed airflow of 3-1/2 percent is appropriated for the cooling of the first- and second-stage nozzles and the first-stage blade. No final reduction gearbox design has been proposed, and a power turbine shaft output rotational speed of 40,000 rpm has been assumed.

For both internal and external engine installations, the recuperator configurations proposed are annular designs, wrapped around the turbomachinery to give a fully integrated, lightweight, compact engine package. This annular concept is structurally desirable, in that the heat exchanger and rotating components are concentric, and the need for additional ducting to take the air and gas to and from the recuperator is eliminated.

In comparing several types of heat exchanger surface geometries, it was concluded that lightweight, compact recuperators could be realized using dimpled plain tube surface geometries. It was also found that minimum weight, two-pass cross-counterflow designs could be achieved by having the high-pressure compressure discharge air flowing inside the dimpled tubes and by having the low-pressure turbine exhaust gas flowing across the tube bundle.

Data presented in the parametric study showed that unrealistic recuperator sizes, as regards compatibility with the aircraft turbomachinery, resulted for effectiveness values much greater than 80 percent and for pressure loss values less than 4 percent. From the tables of selected optimum designs, it has been shown that for the high effectiveness cases, very small hydraulic diameter surfaces must be used to give units that have inner and outer diameters that are compatible with the turbomachinery. In this study, the smallest tube diameter considered practical for compact, low-cost, tubular gas turbine application was 0.075 in. Where detailed drawings were available, detailed cost analyses were carried out at the reference engine conditions, enabling realistic estimates to be made for the detail parts. Knowing the exact cost breakdown for the reference engine designs, a series of equations was developed such that costs of units over a wide range of effectiveness and pressure loss could be estimated with a high degree of

confidence. From the cost curves presented in the sensitivity study, it has been shown that the recuperator and engine costs are a strong function of heat exchanger effectiveness.

In comparing the selected A-1 and B-2 designs at the reference engine conditions, it is apparent that the added structure associated with the external type of installation results in a considerable weight penalty. The difference in weight between the two designs is 29.2 lb, which reflects almost a 17-percent increase in engine weight for the A-1 design compared with the much simpler B-2 configuration. The recuperator specific weights at the reference engine conditions are 15.32 lb/lb/sec and 9.48 lb/lb/sec for configurations A-1 and B-2, respectively. The ratios of tube weight to total recuperator weight for configurations A-1 and B-2, at the reference engine conditions, are 35.5 percent and 56.8 percent, respectively. This additional weight clearly shows up in the break-even time, which is defined as the flight time in which the additional weight of the recuperative engine is offset by the decreased fuel consumption. At the reference engine conditions, the break-even times for the A-1 and B-2 configurations are 57.0 min and 39.2 min, respectively.

To date, most of the research conducted in the area of recuperative aircraft gas turbines has been aimed at advancing heat exchanger technology and applying the units to existing engines, which have to be modified to incorporate the recuperator. The maintenance and operating costs of these engines, with essentially bolt-on recuperators, are virtually unknown since experience gained in actual aircraft installations is minimal. For the types of advanced designs presented in this study, in which the recuperator and its associated structure are considered during the design phase of the engine, there is no reason to doubt that with development, the recuperator reliability will be made equal to that of the other major engine components. If this is the case, the maintenance costs of the recuperative engine should essentially be the same as the nonrecuperative engine.

At the extremes of the range of recuperator variables considered, the lowest SFC engine corresponds to a recuperator effectiveness and pressure loss of 0.80 and 4 percent, respectively. The highest SFC engine corresponds to a recuperator effectiveness and pressure loss of 0.40 and 10 percent, respectively. A comparison of these engines with the reference engine and the nonrecuperative engine is outlined in Table XXII.

In the sensitivity study, curves have been presented that show the selection of optimum recuperator effectiveness, for maximum net weight savings, to be dependent on mission time. The fact that the net weight savings curves have a maximum point shows that for short-duration flights, the quest for low SFC by utilizing a high effectiveness recuperator is not justified. Beyond the maximum point on the curve, the fuel weight saving benefit from using a high effectiveness value becomes offset because of the associated increase in recuperator weight. Since the positive slope of the curve toward the maximum point is small, low-effectiveness recuperators can be used with only a very small penalty in net weight savings. This of course results in an engine of considerably reduced cost. This effect is best illustrated by

TABLE XXII. ENGINE DESIGN SUMMARY FOR RANGE OF SFC COVERED IN ANALYSIS

Engine Configuration	Low SFC Engine		Reference Engine		High SFC Engine		Nonrecuperated engine
	A-1	B-2	A-1	B-2	A-1	B-2	
Recuperator Effectiveness	0.80	0.80	0.65	0.65	0.40	0.40	-
Recuperator Pressure Loss, %	4.0	4.0	6.0	6.0	10.0	10.0	-
SFC, lb/hp hr	0.333	0.333	0.365	0.365	0.425	0.425	0.4663
Specific Power, hp/lb/sec	194.70	194.70	192.54	192.54	187.5	187.5	204.39
Engine Weight, lb	303.7	248.3	202.8	173.6	161.1	147.7	110.0
Power/Weight, hp/lb	3.20	3.92	4.75	5.55	5.82	6.35	8.75
Engine OD, in.	26.3	23.18	23.45	19.04	19.60	19.58	14.0
Engine Length, in.	40.5	33.0	29.90	28.50	28.7	28.5	28.55
Engine Cost Factor	2.06	1.94	1.40	1.29	1.14	1.12	1.00*

*Nonrecuperative engine cost as datum for comparison

examples for both the A-1 and B-2 engine configurations. Assuming that recuperator pressure loss of 6 percent is selected, and a design is being considered for a vehicle with a mission time of 2 hours, then the following data can be taken from the sensitivity curves for the A-1 engine configuration:

Effectiveness	0.50	0.55	0.60	0.65	0.706	0.75	0.80
New weight savings, lb	70.7	83.4	93.4	102.2	106.5	102.2	94.0
Engine cost factor	0.879	0.910	0.947	1.00	1.09	1.185	1.342

From the above data taken from the sensitivity curves, it can be seen that the maximum weight savings corresponds to an effectiveness of 0.706. Assuming that an effectiveness of 0.55 is selected, then a reduction in net weight saving of 23.1 lb results, but the actual cost of the engine is decreased by almost 20 percent.

Similarly for the B-2 engine configuration, the following data can be taken from the sensitivity curves:

Effectiveness	0.50	0.55	0.60	0.65	0.70	0.747	0.80
Net weight savings, lb	93.5	108.4	120.6	131.4	138.[illegible]	140.0	136.4
Engine cost factor	0.90	0.926	0.955	1.00	1.072	1.18	1.395

From the above data and the sensitivity curves, it can be seen that the maximum net weight savings corresponds to an effectiveness of 0.747. Assuming that an effectiveness of 0.55 is selected, then a reduction in net weight savings of 31.6 lb results, but the actual cost of the engine is decreased by almost 28 percent.

The actual tradeoff between net weight saving and engine cost, etc., is dependent on the mission time and particular application; however, effects of small changes in any one of the basic parameters can be rapidly examined using the sensitivity curve arrays presented.

CONCLUSIONS

This study has shown that for mission times of less than half an hour, there is no net weight advantage in using a recuperative engine. The optimum effectiveness and pressure loss for maximum net weight savings are dependent on mission time. High effectiveness units are only beneficial for flight times in excess of 3 hours. For mission times in the order of 2 hours, maximum net weight savings are realized with recuperator effectiveness values in the range 0.60 to 0.70.

Economic justification of the recuperative engine, from the standpoint of fuel cost savings, is very much dependent on the mission profile and the actual cost of the fuel. The total engine cost is a strong function of recuperator effectiveness. A direct recuperator cost comparison with units already in existence would not be meaningful, since for the integrated design, part of the recuperator cost is associated engine prime structure. At the reference engine value of effectiveness of 0.65, the cost ratios of recuperative to nonrecuperative engines were 1.29 and 1.39 for the internal and external types of installation respectively.

Well integrated designs were achieved by utilizing an annular recuperator, of tubular construction, wrapped around the turbomachinery to give a compact lightweight engine package. Having such an arrangement, with the recuperator and turbomachinery concentric, minimizes any distortion, temperature differentials, and pressure losses, and having all the ducts integral with the engine structure contributes to lower overall engine cost. With the annular recuperator wrapped around the turbomachinery to give a compact, integral unit, additional secondary benefits can be realized. In combat areas, one bullet could severely damage a nonrecuperative engine, but the heat exchanged variant, although bigger in exposed area, is less vulnerable because the recuperator protects the rotating components, and even with local damage in the matrix, resulting in loss of performance, the helicopter or aircraft could still fly back to base. In addition, the recuperator will provide turbine self-containment, and should result in a reduced engine noise level compared with existing designs.

Ease of routine inspection and maintenance is emphasized for the integral type of design concept. With a single tool, the engine assembly can be split into the three basic modules, namely, the gas generator power section, the power turbine, and the recuperator, in just a few minutes.

The axial-centrifugal compressor performance estimates were based on advanced technology projections considered to be achievable within a 3-year development period. With a turbine inlet temperature of 2300°F, and only 3-1/2 percent of the compressor air flow available for cooling, highly sophisticated vane and blade cooling techniques must be developed, in combination with advanced materials, which would allow metal temperature in excess of 1800°F. The small volume radial combustor is an advanced design and should have starting capability up to 33,000 ft when developed, and

will maintain a high level of efficiency over a wide operating range. The tubular recuperator performance estimates and proposed manufacturing techniques are based on state-of-the-art technology.

Unclassifled

Security Classification

DOCUMENT CONTROL DATA - R & D

(Security classification of title, body of abstract and indexing annotation must be entered when the overall report is classified)

1. ORIGINATING ACTIVITY (Corporate author) AlResearch Manufacturing Company 9851-9951 Sepulveda Blvd. Los Angeles, California 90009	2a. REPORT SECURITY CLASSIFICATION Unclassified 2b. GROUP

3. REPORT TITLE

Lightweight Integral Regenerative Gas Turbines for High Performance

4. DESCRIPTIVE NOTES (Type of report and inclusive dates)

5. AUTHOR(S) (First name, middle initial, last name)

Colin F. McDonald

6. REPORT DATE	7a. TOTAL NO. OF PAGES	7b. NO. OF REFS
August 1970	234	7

8a. CONTRACT OR GRANT NO. DAAJ02-69-C-0087	9a. ORIGINATOR'S REPORT NUMBER(S) USAAVLABS Technical Report 70-39
b. PROJECT NO. 1G162203D14417	
c. d.	9b. OTHER REPORT NO(S) (Any other numbers that may be assigned this report) 70-6179

10. DISTRIBUTION STATEMENT

This document is subject to special export controls, and each transmittal to foreign governments or foreign nationals may be made only with prior approval of U. S. Army Aviation Materiel Laboratories, Fort Eustis, Virginia 23604.

11. SUPPLEMENTARY NOTES	12. SPONSORING MILITARY ACTIVITY
	U.S. Army Aviation Materiel Laboratories Fort Eustis, Virginia

13. ABSTRACT

Two integrated engine concepts have been designed by utilizing an annular recuperator of tubular construction wrapped around the turbomachinery to give compact, lightweight engine packages. In both designs, the recuperator is considered to be prime structure and acts as the structural backbone of the engine assembly.

For the cycle conditions, with an airflow of 5 lb/sec, pressure ratio of 9:1, and a turbine inlet temperature of 2300°F, a family of lightweight engine designs has been established over a range of recuperator effectiveness from 0.40 to 0.80 and a range of pressure loss from 4 percent to 10 percent. At the extreme end of the ranges of variables, an engine design is included with a specific fuel consumption of 0.333 lb/hp hr, the corresponding specific power being 194.70 hp/lb/sec. This performance is achieved within an engine envelope of 23.18 in. diameter by 33.0 in. length; the specific weight of the unit is 49.66 lb/lb/sec.

In the analysis, a reference engine design was established with a recuperator effectiveness and pressure loss of 0.65 and 6 percent respectively. With an SFC and specific power of 0.365 and 192.54 respectively, the specific weight of the lightest design was 34.72. This performance is achieved within an engine envelope of 19.04 in. diameter by 28.5 in. length and at an estimated cost of $42.9/horsepower.

DD FORM 1 NOV 68 1473 REPLACES DD FORM 1473, 1 JAN 64, WHICH IS OBSOLETE FOR ARMY USE.

Unclassified

Security Classification

14. KEY WORDS	LINK A		LINK B		LINK C	
	ROLE	WT	ROLE	WT	ROLE	WT
Gas turbine						
Recuperator						
Turbomachinery						
Integrated engine structure						
Heat exchanger						
Tubular construction						